NBS TECHNICAL NOTE 672

U.S. DEPARTMENT OF COMMERCE / National Bureau of Standards

Time Domain Automatic Network Analyzer for Measurement of RF and Microwave Components

NATIONAL BUREAU OF STANDARDS

The National Bureau of Standards [1] was established by an act of Congress March 3, 1901. The Bureau's overall goal is to strengthen and advance the Nation's science and technology and facilitate their effective application for public benefit. To this end, the Bureau conducts research and provides: (1) a basis for the Nation's physical measurement system, (2) scientific and technological services for industry and government, (3) a technical basis for equity in trade, and (4) technical services to promote public safety. The Bureau consists of the Institute for Basic Standards, the Institute for Materials Research, the Institute for Applied Technology, the Institute for Computer Sciences and Technology, and the Office for Information Programs.

THE INSTITUTE FOR BASIC STANDARDS provides the central basis within the United States of a complete and consistent system of physical measurement; coordinates that system with measurement systems of other nations; and furnishes essential services leading to accurate and uniform physical measurements throughout the Nation's scientific community, industry, and commerce. The Institute consists of a Center for Radiation Research, an Office of Measurement Services and the following divisions:

Applied Mathematics — Electricity — Mechanics — Heat — Optical Physics — Nuclear Sciences [2] — Applied Radiation [2] — Quantum Electronics [3] — Electromagnetics [3] — Time and Frequency [3] — Laboratory Astrophysics [3] — Cryogenics [3].

THE INSTITUTE FOR MATERIALS RESEARCH conducts materials research leading to improved methods of measurement, standards, and data on the properties of well-characterized materials needed by industry, commerce, educational institutions, and Government; provides advisory and research services to other Government agencies; and develops, produces, and distributes standard reference materials. The Institute consists of the Office of Standard Reference Materials and the following divisions:

Analytical Chemistry — Polymers — Metallurgy — Inorganic Materials — Reactor Radiation — Physical Chemistry.

THE INSTITUTE FOR APPLIED TECHNOLOGY provides technical services to promote the use of available technology and to facilitate technological innovation in industry and Government; cooperates with public and private organizations leading to the development of technological standards (including mandatory safety standards), codes and methods of test; and provides technical advice and services to Government agencies upon request. The Institute consists of a Center for Building Technology and the following divisions and offices:

Engineering and Product Standards — Weights and Measures — Invention and Innovation — Product Evaluation Technology — Electronic Technology — Technical Analysis — Measurement Engineering — Structures, Materials, and Life Safety [4] — Building Environment [4] — Technical Evaluation and Application [4] — Fire Technology.

THE INSTITUTE FOR COMPUTER SCIENCES AND TECHNOLOGY conducts research and provides technical services designed to aid Government agencies in improving cost effectiveness in the conduct of their programs through the selection, acquisition, and effective utilization of automatic data processing equipment; and serves as the principal focus within the executive branch for the development of Federal standards for automatic data processing equipment, techniques, and computer languages. The Institute consists of the following divisions:

Computer Services — Systems and Software — Computer Systems Engineering — Information Technology.

THE OFFICE FOR INFORMATION PROGRAMS promotes optimum dissemination and accessibility of scientific information generated within NBS and other agencies of the Federal Government; promotes the development of the National Standard Reference Data System and a system of information analysis centers dealing with the broader aspects of the National Measurement System; provides appropriate services to ensure that the NBS staff has optimum accessibility to the scientific information of the world. The Office consists of the following organizational units:

Office of Standard Reference Data — Office of Information Activities — Office of Technical Publications — Library — Office of International Relations.

---

[1] Headquarters and Laboratories at Gaithersburg, Maryland, unless otherwise noted; mailing address Washington, D.C. 20234.
[2] Part of the Center for Radiation Research.
[3] Located at Boulder, Colorado 80302.
[4] Part of the Center for Building Technology.

Time Domain Automatic Network Analyzer for Measurement of RF and Microwave Components

Technical note, no 672

William L. Gans

James R. Andrews

Electromagnetics Division
Institute for Basic Standards
National Bureau of Standards
Boulder, Colorado 80302

U.S. DEPARTMENT OF COMMERCE, Rogers C. B. Morton, Secretary
John K. Tabor, Under Secretary
Dr. Betsy Ancker-Johnson, Assistant Secretary for Science and Technology

NATIONAL BUREAU OF STANDARDS, Ernest Ambler, Acting Director

Issued September 1975

NATIONAL BUREAU OF STANDARDS TECHNICAL NOTE 672
Nat. Bur. Stand. (U.S.), Tech Note 672, 176 pages (Sept. 1975)

CODEN: NBTNAE

For sale by the Superintendent of Documents, U.S. Government Printing Office , Washington, D.C. 20402
(Order by SD Catalog No. C13.46:672) $2.40

CONTENTS

CONTENTS (Continued)

LIST OF FIGURES

LIST OF FIGURES (Continued)

LIST OF FIGURES (Continued)

LIST OF FIGURES (continued)

LIST OF TABLES

FOREWORD

This technical note is the result of several years of effort at NBS to automate time domain measurements and apply them to the determination of frequency domain parameters. The efforts began in 1968 under the able leadership of Dr. Norris S. Nahman. Many people have contributed to the eventual success of this effort. Those individuals directly involved with the earlier phases of the project included Dr. William D. McCaa, Jr., Mr. John F. Shafer, and Mr. Terrance R. Whittemore. More recently the assistance is acknowledged of Mr. Bill Hall for software assistance, Dr. John LeBrecque statistician, Mr. Dick Bailer for the fixed frequency attenuator calibrations, and Miss Sharon Foote and Mrs. Janet Jasa for the typing of the manuscript. In addition, the assistance and support of many other personnel in the Electromagnetics Division is gratefully acknowledged.

The financial support of the tri-services Calibration Coordination Group (CCG) is acknowledged. The members of the CCG Time-Domain Working Group were: Mr. W.R. Carter (Army), Mr. J.C. Santo (Air Force), Mr. F. Flynn (Air Force), and Mr. P. Strucker (Navy). Their support beginning in FY 70 got the concept of a Time Domain Automatic Network Analyzer (TDANA) at NBS moving from just an idea into a practical measurement instrument. Without the support of the CCG supplementing NBS funds the development of the NBS TDANA could have been delayed by several years.

This technical note serves as a final report to the CCG for project CCG 72-68 entitled "Pulse Testing of RF and Microwave Devices." The objective of the CCG with this project was to decrease the measurement uncertainty to 1% or less for calibration of coaxial 1-40 dB attenuators over the frequency range of 400 MHz to 12.4 GHz using time domain measurement techniques.

TIME DOMAIN AUTOMATIC NETWORK ANALYZER FOR MEASUREMENT OF RF AND MICROWAVE COMPONENTS

by

William L. Gans and James R. Andrews

This technical note describes in detail a new NBS instrument for the measurement of the scattering parameters (S_{ij}) of RF and microwave components. The instrument is the Time Domain Automatic Network Analyzer (TDANA). It utilizes time domain pulse measurements to obtain frequency domain parameters. The frequency range is dc to 18 GHz with a lower upper limit for large values of attenuation. The instrument consists of three major components: an ultra-fast pulse generator, a broadband sampling oscilloscope, and a digital minicomputer.

Key words: Attenuation; discrete Fourier transform; fast Fourier transform; insertion loss; jitter; microwave measurement; mismatch; network analyzer; noise; pulse generator; pulse measurement; sampling oscilloscope; scattering parameters; spectral analysis; time domain analysis.

1. INTRODUCTION

1.1 TDANA

This technical note introduces a new NBS instrument for the measurement of the scattering parameters (S_{ij}) of RF and microwave components. The instrument is the Time Domain Automatic Network Analyzer hereafter abbreviated as TDANA. It utilizes time domain measurements and the fast Fourier transform (FFT) to obtain frequency domain parameters. This is a radical departure from classical CW techniques for measuring these parameters.

The NBS TDANA measures the scattering parameters in both magnitude and phase over the frequency range of dc to 18 GHz. The upper frequency limit is less for large values of attenuation ($\sim$ 4 GHz for 60 dB). The accuracy and precision of the system have been evaluated by comparing insertion loss measurements of three wideband coaxial attenuators (10 dB, 20 dB, and 40 dB) with those made on the NBS 30 MHz IF piston attenuator working standard. Measurements were made at selected frequencies from 0.5 GHz to 12.5 GHz. The results agreed within 1.5%. The standard deviations were functions of insertion loss and frequency. Work is continuing on evaluation of the system for measurements of phase and return loss. The results of these evaluations will be reported in later publications.

The NBS TDANA has been used for measuring the scattering parameters of a wide assortment of components. They have included: low-pass, band-pass, and high pass filters; wide-band transistor amplifiers; directional couplers; and broad-band antennas.

The practicality of a TDANA is dependent upon three major components. The first is a pulse generator with sufficient spectrum amplitude in the frequency range of interest. The second is an oscilloscope, i.e., a time domain receiver, with a broad bandwidth to cover the frequency range of interest. The third major component is a digital computer. The computer is necessary to perform the mathematical shift from the time domain to the frequency domain via the Fourier transformation.

For many years researchers have been converting time data to frequency data and vice versa. However, the process has been very laborious and time consuming. It involved photographing an oscilloscope CRT display, reading the data point by point from the photograph, typing the data onto paper tape or computer cards, and then analyzing the data on a time share or large central computer. The entire process easily consumed an entire eight hour working day for a single simple waveform.

With the advent of inexpensive (< $10K) minicomputers this has all changed. The cost of computing capability is now comparable to that of a high performance oscilloscope. It is now cost-effective to dedicate a minicomputer to be hardwired to an oscilloscope. The interface between the two consists of sample and hold (S/H) circuits, analog to digital (A/D) converters of the oscillocope analog data, and digital to analog (D/A) converters for computer control of oscilloscope functions.

1.2 TDANA vs. ANA

The major competitor to the TDANA is a commercial automatic network analyzer system (ANA).* The ANA consists of an ensemble of programmable swept frequency generators, a complex amplitude/phase measuring microwave network analyzer, and a minicomputer.

Both systems have advantages and disadvantages. For the TDANA one of its major advantages is lower cost. In general both systems will have comparable minicomputers, associated computer peripherals, and software programming costs. The TDANA's cost advantage is in lower cost for the source and receiver. For measurements from dc to 18 GHz the TDANA requires a single ultrafast tunnel diode pulse generator costing approximately $500. The ANA covers the frequency range 0.1 to 18 GHz and requires several sweep

*It is NBS policy not to mention manufacturers nor commercial products in their publications. This is done to avoid giving unfair economic advantage to any manufacturer which might occur through a real, implied, or imagined NBS endorsement.

generators for a total source cost of $15,000 or more. Likewise the cost of the receiver for the TDANA is lower than the ANA. The TDANA receiver is a sampling oscilloscope costing approximately $8,000. For the ANA the receiver is a microwave network analyzer costing $20,000. A complete commercial ANA system costs upwards from $175,000. Discussions with an oscilloscope manufacturer indicated that a commercial TDANA would probably cost in the neighborhood of $60,000 to $80,000.

There are also other considerations. One is frequency coverage. The commercial ANA consists of separate test sets for 0.1 to 2 GHz and 2 to 18 GHz. The TDANA will make measurements from dc to 18 GHz. The ANA will make measurements at any programmed frequency. The TDANA, due to the use of the FFT, gives results only at frequencies that are harmonics of the reciprocal of its observation time window. For example if a 10 ns window is used, results are given at 100 MHz, 200 MHz, 300 MHz, etc. The TDANA is better suited to the measurement of broadband devices. Problems arise with the TDANA in the measurement of high Q, narrowband devices.

Another advantage of the TDANA is that it can also be used for purely time domain measurements. Examples are measurements of pulse risetime, delay, duration, distortion, amplitude, etc. When used as a time domain reflectometer (TDR) in conjunction with the computing and signal averaging, it can be used to resolve extremely small impedance discontinuities as small as a fraction of a femtofarad ($< 10^{-15}$F) [1]. One should also acknowledge that an ANA can be used as a TDR. This is accomplished by making network analyzer amplitude and phase measurements at many harmonically related frequencies and then synthesizing time domain pulses using the inverse Fourier transform, IFT, [2].

Another advantage of the TDANA is that the sampling oscilloscope and minicomputer can be used as a spectrum analyzer for calibration of impulse generators [3,4]. This appears to be particularly promising at frequencies above 1 GHz.

1.3 TDANA History

A.M. Nicolson developed the first really usable TDANA in 1968. At CPEM in 1968 he presented the system and results of measurements of microwave components [5]. Nicolson, Ross, Cronson, Lamensdorf, Susman, and other coworkers have continued their pioneering work in TDANA's. References [6-10] detail some of the important advances they have made in this field. Their system was developed for use within their corporate laboratories and also on contract for the Army and Air Force.

Several other companies and institutions have built or used automated oscilloscopes and TDANA's of various degrees of sophistication. In 1969 P. Stuckert developed CAOS which stood for Computer Augmented Oscilloscope System [11]. Also in 1969 a time domain data acquisition system was developed for the AEC [12]. Bancroft and Johnston of the University of Calgary reported a TDANA in 1973 [13].

The major oscilloscope manufacturers were not ignorant of the trend toward automated time domain measurements. They have responded by developing suitable automated oscilloscopes. Most of the information regarding these oscilloscopes and systems is given in advertising circulars, etc., and as such cannot be referenced here. One manufacturer is very close to possibly announcing a commercially available TDANA. This system was described by D. Hannaford at the 1974 Joint Measurement Conference [14].

1.4 Development of the NBS TDANA

During this flurry of TDANA activity in the late 60s and early 70s, the NBS Pulse and Time Domain Section was not idle. Dr. William D. McCaa, Jr. assembled the first NBS time domain data system. He called it RUDA for Rudimentary Data Acquisition. It consisted of simply a digital voltmeter (3-1/2 digit) connected to the Y recorder output of a sampling oscilloscope. The parallel BCD output of the digital voltmeter was converted to serial ASC II data. This was routed to a paper tape punch. At the completion of the conversion of one data point the oscilloscope was triggered again to acquire a new sampled data point. Once a paper tape was prepared the data was then transferred by a teleprinter to a time-share computer for processing. The entire process was agonizingly slow. Typically a half hour was required for the acquisition of a single waveform. The results were not very satisfactory. Very substantial drifts in the horizontal and vertical data occurred during the long acquisition time of a single waveform. Also due to the long time required to obtain a single waveform, computer averaging of many waveforms was not feasible. RUDA did serve the purpose of demonstrating the principle of interconnecting an oscilloscope to a computer.

Meanwhile during the late 60s the military standards and calibration laboratories began to experience a need for subnanosecond domain pulse calibrations. Thus research and development funds began to flow into NBS through the tri-services Calibration Coordination Group (CCG). Starting in 1969 some of this money along with NBS funds was used to develop an improved time domain data acquisition system.

The improved system was called the Time Domain Waveform Measurement System. It was developed by Dr. W.D. McCaa, Dr. J.R. Andrews, and Mr. J.F. Shafer. The improved system was described at the 1970 ISA conference. The new system replaced the RUDA digital voltmeter with a commercial analog-digital recorder/generator. This instrument was essentially a high speed (100 kHz), 3 digit, analog to digital converter and a 1000 word magnetic core memory. With the new system a single 1000 point waveform could be acquired in 10 ms. This was much faster than RUDA and thus eliminated the problem of long term vertical and horizontal drifts. The major disadvantage of this system was still the computer connection. The system still required a parallel BCD to ASC II conversion, paper tape punching and teleprinter transmission over a telephone line to a time-share computer. Fifteen minutes were required to transmit a single 1000 point waveform.

The time-share arrangement was not very satisfactory. Operating problems included many computer "outages" with loss of data and sometimes programs and imperfect transmission of data with random data dropouts. This system was used by Mr. W.L. Gans, Dr. W.D. McCaa, Jr., and Dr. N.S. Nahman for their experiments with the fast Fourier transform (FFT) [15] and pulse testing of microwave components in 1971 and 1972.

By 1972, sufficient funds from CCG and NBS allowed the purchase of a minicomputer and the peripheral equipment. The NBS TDANA was then developed around this minicomputer and an 18 GHz bandwidth sampling oscilloscope.

1.5 Technical Note Organization

This technical note describes in full detail the NBS APMS and its use as a TDANA. This note is divided into ten chapters. Chapter two develops the concept of pulse testing theory as applied to the determination of frequency domain parameters. Chapter three discusses the relationship between the time domain and the frequency domain through the Fourier transformation, Laplace transformation, Fourier series, discrete Fourier transformation, and the fast Fourier transformation. Chapter four deals with a set of experiments performed on the fast Fourier transformation to highlight potential problem areas when doing TDANA calculations. Chapter five is a description of the various instruments contained in the NBS TDANA. It also demonstrates the use of the APMS portion as an extremely wideband spectrum analyzer. Chapter six deals with the actual circuit details of the sampling oscilloscope/minicomputer interface. Chapter 7 describes the system software. Chapter eight discusses experimental results of comparison measurements of coaxial attenuators using the TDANA, a commercial automatic network analyzer, and the NBS 30 MHz IF piston attenuator working standard. Chapter nine is a partial error analysis of the TDANA. Chapter ten is the summary chapter and contains recommendations for future work. Chapters 1, 2, 3, 5, and 6 were the responsibility of Dr. Andrews. Mr. Gans was the author of Chapters 4, 7, 8, 9, and 10.

2. PULSE TESTING THEORY

The objective of this project was to apply time domain measurements to the determination of scattering parameters as functions of frequency. This chapter will discuss the interchangability of time and frequency, and develop the theory of time domain insertion loss measurements.

2.1 Time Domain/Frequency Domain Representations of Physical Signals

Every physical signal can in principle be represented mathematically in both the time domain and the frequency domain. In the time domain a signal waveform is described by an algebraic equation v(t). The connection between the time domain and the frequency domain is the Fourier transformation [16]. It is defined by the following transform pair [17]

$$V(f) = \int_{-\infty}^{\infty} v(t)e^{-j2\pi ft}\,dt \tag{2-1}$$

$$v(t) = \int_{-\infty}^{\infty} V(f)e^{+j2\pi ft}\,df \tag{2-2}$$

V(f) is the frequency domain representation of the same physical signal v(t). Both v(t) and V(f) are valid representations of the same physical signal. v(t) is always a real function, while V(f) is a complex function.

For this report the physical signal to be considered is an electrical voltage having units of volts. V(f) is an integration of v(t) over time; thus V(f) is an area with units of volt-second. Arthur [17] gives an excellent discussion and visual illustrations of V(f).

As an example consider a single rectangular baseband pulse $v_{rp}(t)$, figure 2-1(a). $v_{rp}(t)$ is defined as

$$v_{rp}(t) = v_o u(t) - v_o u(t-t_o) \tag{2-3}$$

where u(t) is the unit step function. Applying the Fourier transform, eq. (2-1), to this pulse one obtains

$$V_{rp}(f) = |V_{rp}(f)|e^{\phi_{rp}(f)} \tag{2-4}$$

where

$$|V_{rp}(f)| = v_o t_o \left|\frac{\sin(\pi f t_o)}{(\pi f t_o)}\right| \tag{2-5}$$

and

$$\phi_{rp}(f) = -\pi f t_o \tag{2-6}$$

The magnitude of $V_p(f)$ is plotted in figure 2-1(b). It is a continuous function for all frequencies from $-\infty$ to $+\infty$. Thus a single baseband pulse is a source of a continuous frequency spectrum. This is one advantage of pulse testing over single frequency measurements.

The magnitude of V(f) is a quantity of engineering importance. It is called the Spectrum Amplitude* S(f). It is defined [18] as

$$S(f) = 2|V(f)| \tag{2-7}$$

Arthur [19] has noted that the IEEE dictionary has an error in its mathematical definition of S(f). It uses a constant of $1/\pi$ instead of 2 in the definition. In this report the constant 2 of eq. (2-7) is used.

The unit of S(f) is the same as for V(f), namely volt-second. Many times the unit volt/hertz is found in the literature. These two units are dimensionally the same. In this report S(f) is sometimes expressed in dB above 1 volt-picosecond in which case it is defined as

$$X \text{ in dB V - ps} = 20 \log_{10}\left\{\frac{X \text{ in V - s}}{1 \times 10^{-12} \text{ V - s}}\right\} \tag{2-8}$$

A volt-picosecond (V-ps) is equivalent to a microvolt per megahertz (μV/MHz).

Chapter 3 will discuss in greater detail the Fourier Transformation and its relatives the Laplace Transformation, Fourier Series, Discrete Fourier Transformation, and the Fast Fourier Transformation.

2.2 Time Isolation Property of Delay Lines

Figure 2-2 is the basic pulse measurement system. The measuring instrument is almost always an oscilloscope. A connection must be made between the pulse generator and the oscilloscope. For slow pulses (t_r > 100 ns) and low frequencies an oscilloscope probe is used to connect the two instruments. For high frequencies and fast pulses (t_r < 1 ns), probes are no longer useful [20,21]. The connection is then made with a piece of transmission line such as a coaxial cable. The transmission line is capable of relatively faithfully transmitting the generator waveform to the oscilloscope or some other circuit where it is to be utilized. The use of a coaxial cable is not limited to fast pulses and high frequencies but is equally useful with slower pulses and low frequencies. The coaxial cable also has the advantage that it presents a relatively constant load impedance to the pulse generator. In reality no transmission line is perfect. Various things such as skin effect will cause the impedance Z_o and the propagation function γ to be functions of frequency [22]. These effects do cause distortion in the transmission of

*Many other names are found in the literature for this same quantity. They include: Spectral Intensity, Impulse Spectral Intensity, Impulse Strength, Spectral Density, Voltage Spectrum, and Interference Intensity.

pulses. For the purposes of this discussion these effects will be considered negligible. To a first order, the coaxial cable can be characterized as not being frequency dependent and simply having a real characteristic impedance $Z_o = R_o$, a propagation velocity v_p, a length ℓ, and a time delay TD.

An understanding of the effect of the cable in the measurement system is fundamental to proper interpretation of the results of time domain measurements. Figure 2-3 is an example of a mismatched system that will be used for illustrative purposes. Both the generator and oscilloscope are mismatched to the transmission line.

Consider a 1 volt pulse departing the generator at t = 0. This pulse enters the left end of the line at t = 0. Initially the line simply appears as a 50 ohm resistor across the generator terminals. The initial incident voltage wave v_i that enters the line is simply

$$v_i(t) = \frac{R_o}{R_o + R_g} v_g(t) \tag{2-9}$$

Due to the finite propagation velocity v_p the leading edge of the incident pulse v_i arrives at the oscilloscope later in time, namely at

$$t_1 = TD = \ell/v_p. \tag{2-10}$$

At the oscilloscope a portion, v_t, will be transmitted into the internal load, R_L, and a portion, v_r, will be reflected back toward the generator.

$$v_t = v_i + v_r \tag{2-11}$$

$$v_t = \tau\, v_i \tag{2-12}$$

$$v_r = \rho\, v_i \tag{2-13}$$

τ is the transmission coefficient, and ρ is the reflection coefficient.

$$\tau = \frac{2\, R_L}{R_L + R_o} \tag{2-14}$$

$$\rho = \frac{R_L - R_o}{R_L + R_o} \tag{2-15}$$

The above equations are also valid in the frequency domain with an appropriate change in notation. All of the parameters (Z_g, Z_L, Z_o, V_i, V_t, V_r, τ, and ρ) are complex and functions of frequency. In the frequency domain the various resistances, R, become impedances, Z, and the reflection coefficient is commonly denoted by Γ. The initial waveform transmitted into the oscilloscope

is seen to be an identical replica of the generated waveform $v_g(t)$ with the exception of amplitude scaling due to the line input voltage divider, eq. (2-9), and the load mismatch, eqs. (2-12) and (2-14). If the system were matched, $R_g = R_L = R_o$, then $v_2(t) = 1/2\ v_g(t)$.

The reflected pulse, v_r, travels back to the left and arrives at the generator at $t_2 = 2TD$. If the generator and the line are not perfectly matched (i.e., if $R_g \neq R_o$) then a new reflection of the pulse will result. Equations (2-11) through (2-15) are also valid for the generator terminal if R_g is substituted for R_L. The new reflection now propagates back to the right through the line. It arrives at the oscilloscope at $t_3 = 3TD$. This new reflection as it is transmitted to the oscilloscope is in addition to the initial incident waveform. The voltage at the oscilloscope, $v_2(t)$, is no longer an identical replica of the generated waveform $v_g(t)$. $v_2(t)$ is

$$v_2(t) = K\ v_g(t-TD), \quad t < 3TD \tag{2-16}$$

$$v_2(t) = K\ v_g(t-TD) + v_{reflections}(t), \quad t > 3TD \tag{2-17}$$

where K is a constant. The above example used a rectangular pulse for clarity. The analysis is equally valid for other transients such as a step function.

For purposes of clarity and precision the words "initial" and "incident" should be defined further. Words such as "initial" and "final" refer to time related properties. As used above the word "initial" refers to the waveform present at the load only during the time interval 0 to 3TD. The word "incident" refers to a direction of wave propagation. In this case it is the wave traveling forward from left to right on the transmission line and striking the load. No time element is involved as the word applies for all time ($-\infty$ to $+\infty$). "Incident" refers to a spatial vector. The words "reflected" and "transmitted" likewise refer to spatial vectors. By using two different terms, a clearer distinction is made between the generator waveform over all time, and that part of the generator waveform delivered to the oscilloscope undistorted by reflections from either the source or the oscilloscope impedance discontinuities within the time window. Furthermore, the term "initial" can be used to describe waves arriving at, or departing from, a given port.

Advantage can be taken of the transmission line time delay property in a practical measurement set-up in which the generator and/or load are not matched to the line. As seen above, the output waveform is distorted after $t = 3TD$. The actual time window, T_w, available for observation of an undistorted waveform is 2TD. Thus one may widen the undistorted window simply by increasing the transmission line length between the generator and the

oscilloscope. A practical limitation is reached, however, when the actual line response starts to introduce distortion on the generator waveform.

2.3 Theory of Time Domain Insertion Loss Measurements

The measurements made are actually time domain insertion loss measurements for the purpose of computing the transfer insertion scattering parameter, $S_{21}(j\omega)$,* where ω is the angular frequency variable [23]. A circuit model analysis of the measurement technique has been derived by Gans and Nahman and is presented here.

The circuit used to obtain the incident voltage waveform at the plane of insertion is shown in figure 2-4. $V_g(s)$ and $Z_g(s)$ represent the pulse generator. s is the complex frequency variable. Two sections of precision 50 ohm coaxial airline are represented by ℓ_1 and ℓ_2. The box labeled T(s) represents the sampling oscilloscope sampling gate with an input impedance of $Z_s(s)$ and a transfer function T(s) between the sampling gate and the CRT display. The oscilloscope is also terminated in a 50 ohm load, R_o. $v_{d1}(t)$ is an observable voltage; it is the insertion plane waveform as seen through the transfer properties of ℓ_2 and the oscilloscope. For this analysis, it is assumed that all connectors are ideal.

Since the generator impedance, $Z_g(s)$, may not be equal to R_o, and since the presence of the sampling oscilloscope at the end of line ℓ_2 certainly changes the total load impedance as seen by line ℓ_2 to some value other than R_o, the reflections caused by these two discontinuities will invalidate this analysis after some time. The available time window, T_w, in which this measurement is valid is determined by the lengths of the two lines, ℓ_1 and ℓ_2. The time delays for reflections from the generator and oscilloscope, respectively, are

$$2TD_1 = 2\ell_1/v_p \qquad (2\text{-}18)$$

$$2TD_2 = 2\ell_2/v_p \qquad (2\text{-}19)$$

where v_p is the propagation velocity in the medium ($v_p \cong 3 \times 10^8$ m/s for coaxial air lines). Thus T_w, the available time window, will be either $2TD_1$ or $2TD_2$, whichever is smaller. For example, a 30 cm airline thus provides a 2 ns time window.

The displayed initial input transition voltage waveform, $v_{d1}(t)$, figure 2-4, may be expressed as

$$v_{d1}(t) = \mathcal{L}^{-1}\{V_{d1}(s)\} \quad 0<t<TD_1+TD_2+T_w \qquad (2\text{-}20)$$

---

*$S_{ij}(j\omega)$ is the commonly accepted notation for the scattering parameters of microwave networks. It is not be confused with S(f) which is commonly used for spectrum amplitude.

where $\mathcal{L}^{-1}$ denotes the inverse Laplace transformation operator, and where $V_{d1}(s)$ is given in terms of the complex frequency variable s as

$$V_{d1}(s) = V_g(s) \left[\frac{R_o}{Z_g(s)+R_o}\right] e^{-s(TD_1+TD_2)} \tau_s(s)\ T(s) \tag{2-21}$$

where τ is the transmission coefficient at the oscilloscope input

$$\tau_s(s) = \frac{2\ Z_{CRT}(s)}{R_o + Z_{CRT}(s)} \tag{2-22}$$

and Z_{CRT} is the input impedance of the oscilloscope

$$Z_{CRT}(s) = \frac{Z_s(s)\ R_o}{Z_s(s) + R_o} \tag{2-23}$$

The initial incident waveform onto the reference plane is given by

$$V_{1i}(s) = V_g(s)\left[\frac{R_o}{Z_g(s) + R_o}\right] e^{-s\ TD_1} \tag{2-24}$$

Writing eq. (2-21) in terms of $V_{1i}(s)$

$$V_{d1}(s) = V_{1i}(s) e^{-s\ TD_2}\ \tau_s(s)\ T(s). \tag{2-25}$$

Referring to figure 2-5, with the addition of the device under test inserted in the 50 ohm system, the initial transmitted voltage waveform $V_{2t}(s)$ may be expressed in the complex frequency plane in terms of the transfer insertion scattering parameter as

$$V_{2t}(s) = V_{1i}(s)\ S_{21}(s). \tag{2-26}$$

The displayed initial transmitted voltage waveform $v_{d2}(t)$ is

$$v_{d2}(t) = \mathcal{L}^{-1}\{V_{d2}(s)\} \qquad 0<t<TD_1+TD_2+T_w+T_d. \tag{2-27}$$

where

$$V_{d2}(s) = V_{2t}(s) e^{-s\ TD_2} \tau_s(s)\ T(s) \tag{2-28}$$

T_d is the additional time delay introduced by the device under test. From eqs. (2-26) and (2-28) $V_{d2}(s)$ is given by

$$V_{d2}(s) = V_{1i}(s)\ S_{21}(s) e^{-s\ TD_2} \tau_s(s)\ T(s) \tag{2-29}$$

The ratio of $V_{d2}(s)$ and $V_{d1}(s)$, eqs. (2-29) and (2-21), will yield the following result:

$$\frac{V_{d2}(s)}{V_{d1}(s)} = S_{21}(s). \tag{2-30}$$

Thus, for the two time domain waveforms actually observed, in terms of Laplace transforms,

$$S_{21}(s) = \frac{\mathcal{L}\{v_{d2}(t)\}}{\mathcal{L}\{v_{d1}(t)\}} \tag{2-31}$$

or, replacing s by $j\omega$, we arrive at the final Fourier transform equation

$$S_{21}(j\omega) = \frac{\mathcal{F}\{v_{d2}(t)\}}{\mathcal{F}\{v_{d1}(t)\}} \tag{2-32}$$

Thus, for insertion loss measurements we have obtained the important result that the frequency response of the sampling oscilloscope does not affect the final result. The circuit loading due to $Z_s(s)$ and the transfer function T(s) were seen to cancel out. Likewise the actual generator waveform and source impedance effects cancel out.

The above comments should not be construed to mean that any arbitrary low frequency pulse generator and oscilloscope can be used to make microwave measurements of attenuators. Other factors must be considered that were not included in the above derivation. The most important is the signal to noise ratio at the frequency of interest. The generator spectral amplitude S(f) must be above the system noise level. In addition, the frequency response $|T(f)|$ of the oscilloscope must be such that the detected level $|T(f)|S(f)$ is above the noise level. This problem will be discussed in more detail in later chapters.

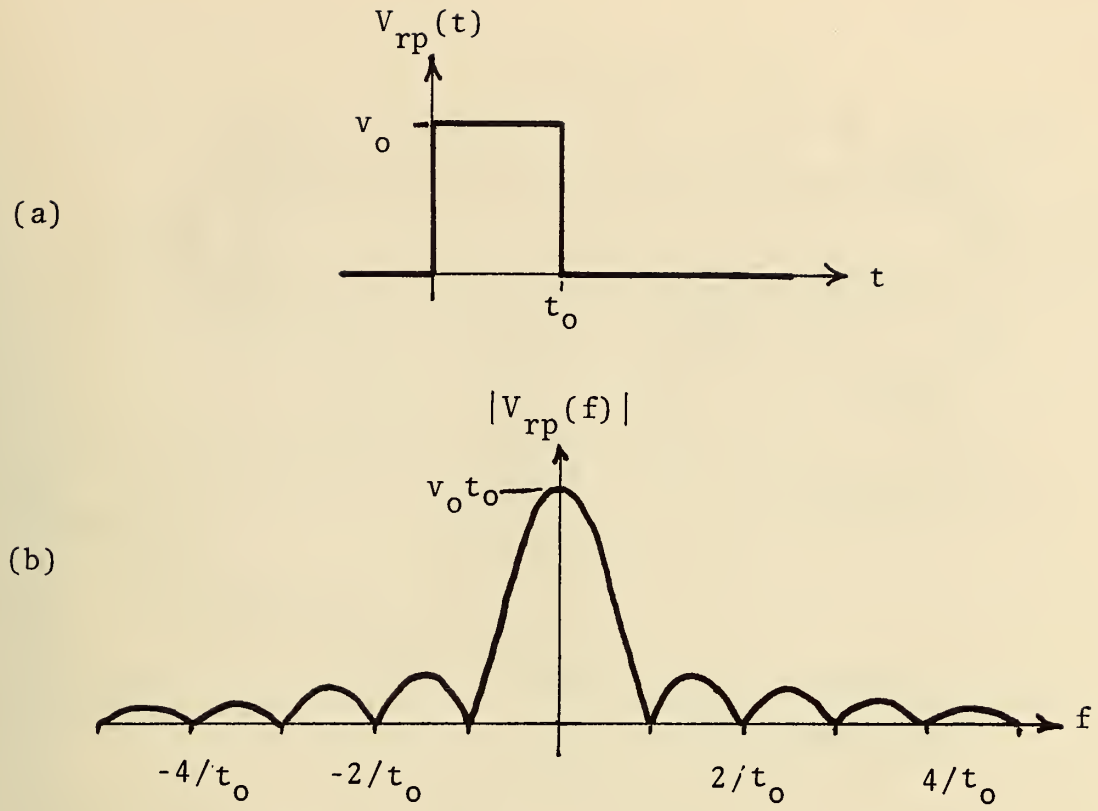

Figure 2-1. Time Domain (a) and Frequency Domain (b) Representations of a Single Rectangular Baseband Pulse.

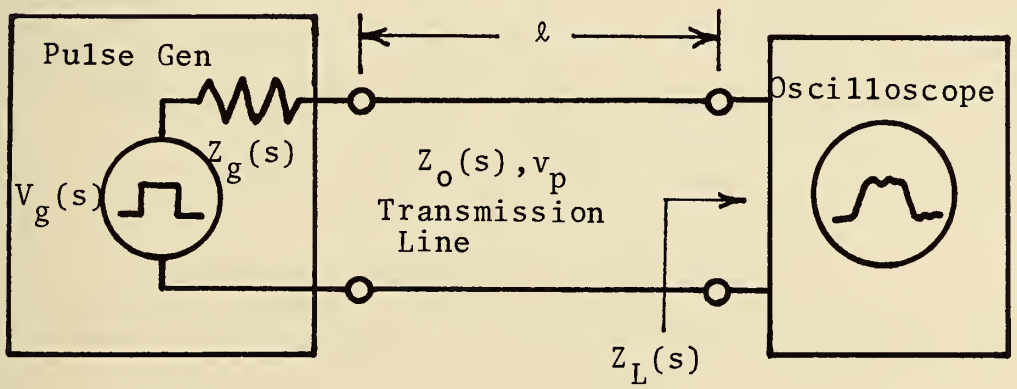

Figure 2-2. Basic Pulse Measurement System.

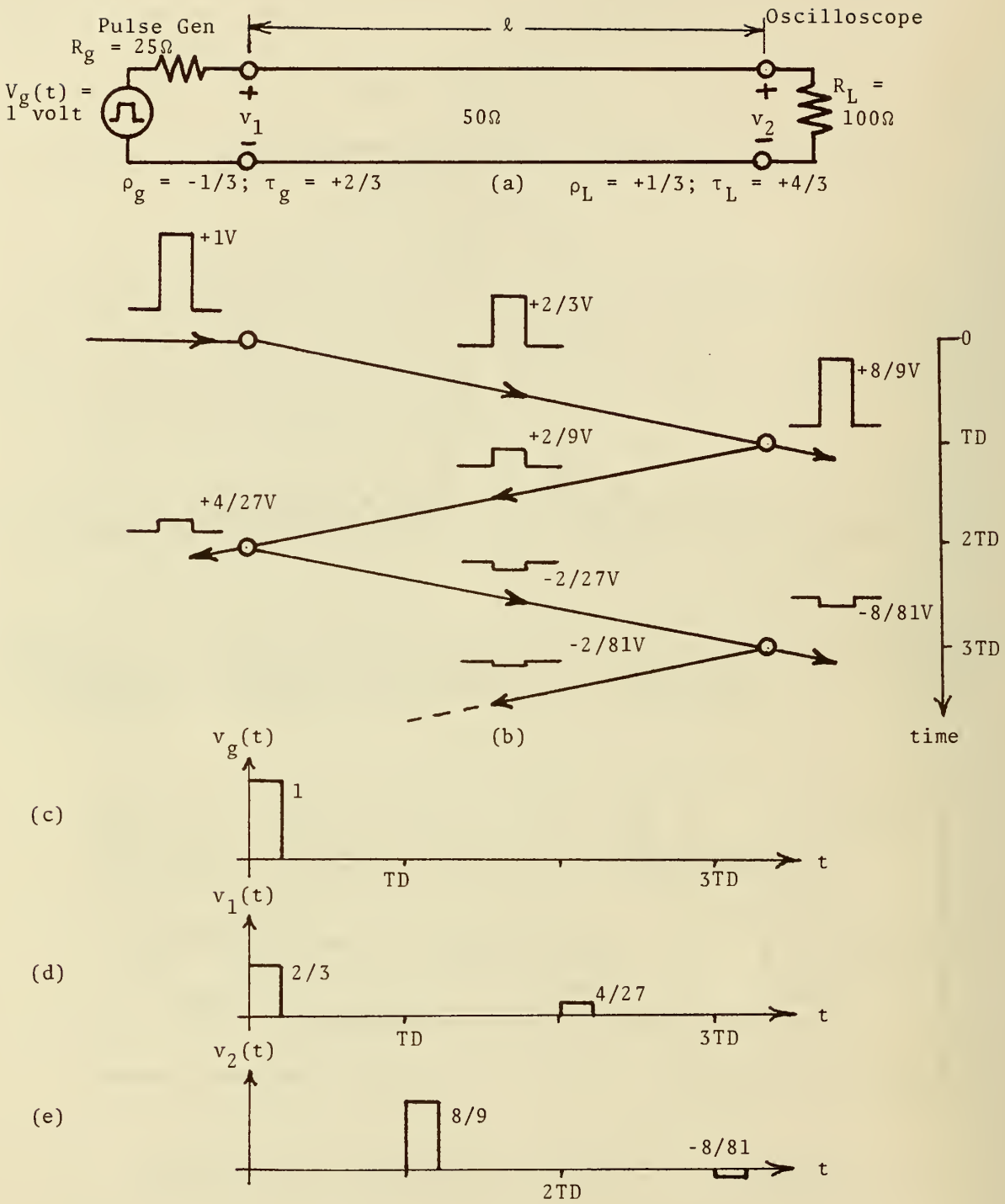

Figure 2-3. Pulse Response of Mismatched Basic Pulse Measurement System. (a) Circuit. (b) Zig-Zag Diagram. (c) Generator Source Voltage. (d) Generator Terminal Voltage, (e) Load Terminal Voltage.

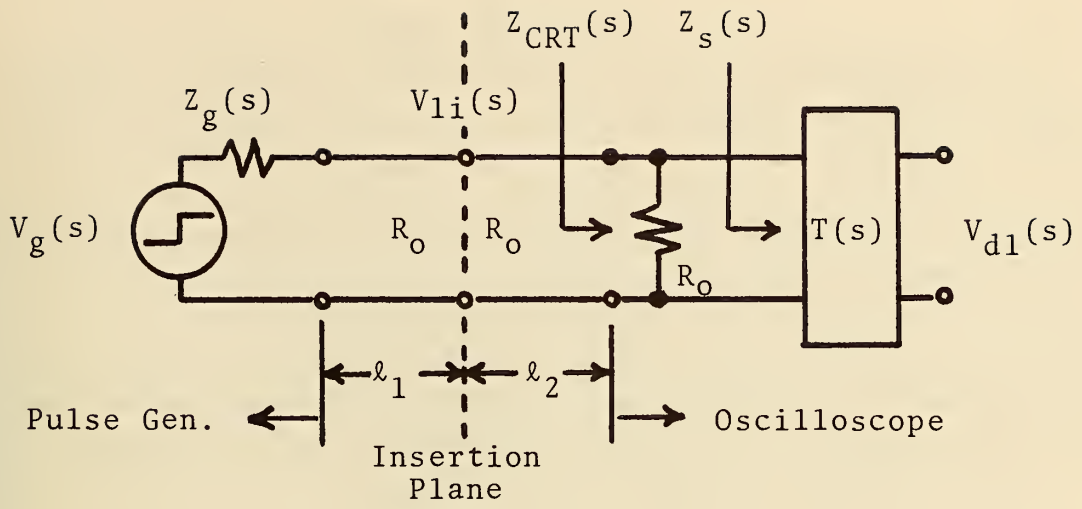

Figure 2-4. Diagram of Circuit Used to Obtain $V_{d1}(s)$.

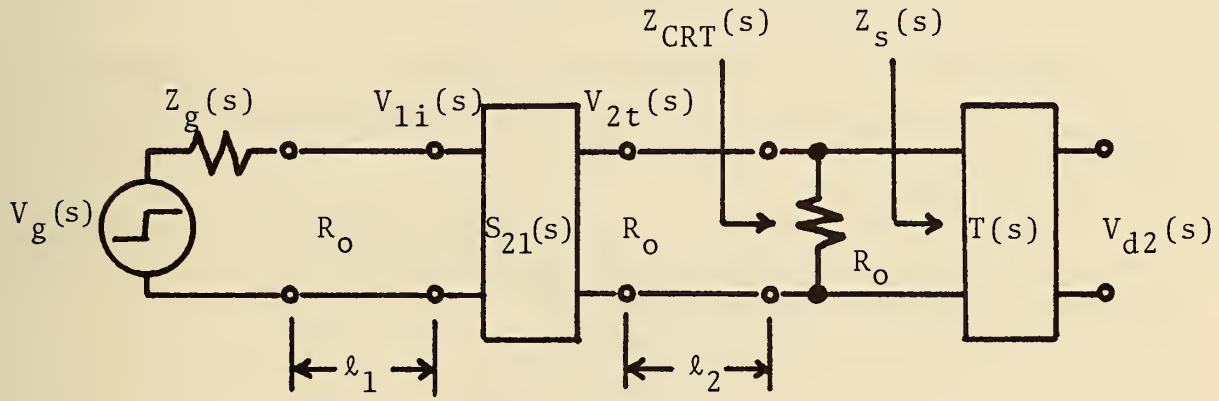

Figure 2-5. Diagram of Circuit Used to Obtain $V_{d2}(s)$.

3. THE FOURIER FAMILY

This chapter will discuss in greater detail than Chapter 2 the time domain/frequency domain interrelationship. The basic connection between the two domains is the Fourier transformation (FT). The other relatives in the Fourier family are also discussed. They are the Laplace transformation (LT), Fourier series (FS), discrete Fourier transformation (DFT), and the fast Fourier transformation (FFT).

3.1 Fourier Transformation

As briefly mentioned in Chapter 2, the connection between the time and frequency domain is the Fourier transform (FT) pair defined as

$$V(f) = \int_{-\infty}^{\infty} v(t)e^{-j2\pi ft}\,dt \tag{3-1}$$

$$v(t) = \int_{-\infty}^{\infty} V(f)e^{+j2\pi ft}\,df \tag{3-2}$$

or in operator notation

$$V(f) = \mathcal{F}[v(t)] \tag{3-3}$$

$$v(t) = \mathcal{F}^{-1}[V(f)] \tag{3-4}$$

v(t) and V(f) are the time domain and frequency domain representations of the same physical signal. When the signal is an electrical voltage, the units are volts for v(t) and volt-seconds for V(f). Tables of transform pairs have been tabulated [24].

For a given v(t) to possess a FT, V(f) the integral (3-1) must converge; a set of conditions which insures that the integration will converge is the Dirichlet conditions which are as follows:

1. v(t) must be absolutely integrable

$$\int_{-\infty}^{\infty} |v(t)|dt < \infty$$

2. v(t) may only have a finite number of maxima or minima in a finite interval.
3. v(t) may only have a finite number of discontinuities in a finite interval.

These conditions restrict the FT to energy signals, that is, to signals which contain a finite energy,

$$\int_{-\infty}^{\infty} [v(t)]^2\,dt < \infty$$

On the other hand they exclude power signals, that is, signals which contain a finite power,

$$\lim_{T\to\infty} \frac{1}{2T} \int_{-T}^{T} [v(t)]^2 \, dt < \infty$$

Important power signals are periodic signals and the unit step. It is possible to include these important signals in the FT by allowing the FT to include delta functions, $\delta(f)$; however, their inclusion only provides a formal method for a unified treatment of energy and power signals [51]. In the discussion presented here, the unified treatment is not used and is replaced by four separate methods defined as the Fourier family:

1. The Fourier Transformation for energy signals.
2. The Laplace Transformation for causal transient signals.
3. The Fourier Series for periodic signals.
4. The Discrete Fourier Transformation for discrete (sampled) data signals.

3.2 Laplace Transformation

For transient (causal) signals the Laplace transformation (LT) provides the link between time and frequency [25]. The word transient (causal) implies that the signal did not exist prior to some time, say $t = 0$; furthermore, initial conditions are included at $t = 0$.

$$v(t) = 0, \quad t < 0 \tag{3-5}$$

The Laplace transform pair is defined as

$$V(s) = \int_{0}^{\infty} v(t)e^{-st} \, dt \tag{3-6}$$

$$v(t) = \frac{1}{2\pi j} \int_{c-j\infty}^{c+j\infty} V(s)e^{+st} \, ds \tag{3-7}$$

for $t \geq 0$.

c is a constant of integration. s is the complex frequency variable.

$$s = \sigma + j\omega \tag{3-8}$$

where

$$\omega = 2\pi f \tag{3-9}$$

In operator notation the LT pair is

$$V(s) = \mathcal{L}[v(t)] \tag{3-10}$$

$$v(t) = \mathcal{L}^{-1}[V(s)] \tag{3-11}$$

Although eqs. (3-6) and (3-7) appear to be more formidable than those of the FT, they also are more powerful. Many real signals that could not be handled by the FT due to integration convergence problems do have solutions in the LT. The introduction of the damping term $e^{-\sigma t}$ in addition to the reactive term $e^{-j\omega t}$ found in the FT is what allows the integration (3-6) to converge. The inverse LT, $\mathcal{L}^{-1}$, is accomplished with the powerful tool of contour integration in the complex frequency (s) plane. A complete discussion of the FT and LT is quite lengthy and the reader is referred to the many books that are written on the subject.

For an electrical voltage the units in the LT are the same as for the FT. Namely, v(t) is in volts and V(s) is in volt-seconds.

3.3 Fourier Series

The Fourier Series (FS) provides the link between the time and frequency domain for periodic signals. Such signals must necessarily exist for all time from $-\infty$ to $+\infty$. The periodic property is defined as

$$v(t) = v(t \pm kT) \qquad k = 1,2,3,\ldots,\infty \tag{3-12}$$

T is the fundamental period. The fundamental frequency f_o of the periodic waveform is

$$f_o = 1/T \tag{3-13}$$

A periodic signal may be written in a Fourier series expansion as an infinite sum of sines and cosines.

$$v(t) = \frac{A_o}{2} + \sum_{n=1}^{+\infty} A_n \cos(2\pi n f_o t) + B_n \sin(2\pi n f_o t) \tag{3-14}$$

n is an integer $\quad n = 1,2,3,\ldots$

The frequency coefficients A_n and B_n are given by

$$A_n = \frac{2}{T}\int_o^T v(t)\cos(2\pi n f_o t)dt \tag{3-15}$$

$$B_n = \frac{2}{T}\int_o^T v(t)\sin(2\pi n f_o t)dt \tag{3-16}$$

The FS may also be written in a complex exponential form.

$$D_n(nf_o) = \frac{1}{T}\int_o^T v(t)e^{-j2\pi n f_o t}\,dt \tag{3-17}$$

$$v(t) = \sum_{n=-\infty}^{+\infty} D_n(nf_o)e^{+j2\pi n f_o t} \tag{3-18}$$

The FS expansion shows that if a signal is periodic in the time domain for all time, it only exists in the frequency domain at integer multiples of the fundamental frequency f_o; i.e.,

$$\begin{aligned} D(f) &\neq 0 \quad , \quad f = \pm nf_o \\ D(f) &\equiv 0 \quad , \quad f \neq \pm nf_o \end{aligned} \tag{3-19}$$

Attention is called to the fact that the exponential form of the FS, eqs. (3-17) and (3-18), closely resembles the FT, eqs. (3-1) and (3-2), and the LT, eqs. (3-6) and (3-7). For the integrals (3-15) through (3-17) to converge the Dirichlet conditions discussed in section 3.1 have to be satisfied but only over the interval defined by the period T.

The units of A_n, B_n, and D_n are the same as those of v(t). The integration of eq. (3-17) results in an area (volt-second) that is then normalized by 1/T (per second) to give volts. Thus, a sine wave, for example, in the time domain has the units of volts and when it is expressed in the frequency domain, it still has units of volts but at a single frequency.

3.4 Discrete Fourier Transformation

In actual practice a finite amount of discrete sampled data, v_{sd}, is many times used to represent a physical signal. The actual signal, v(t), is unknown for all other values of time.

$$\begin{aligned} v_{sd}(t=i\Delta t) &= v(t) \qquad \text{for } i = 0,1,2,\ldots N-1 \\ v_{sd}(t) &= v_{sd}(t=i\Delta t) \quad \text{for } i\Delta t \leq t < (i+1)\Delta t \end{aligned} \tag{3-20}$$

This type of data is obtained directly from sampling oscilloscopes and is the natural state of numbers in a digital computer. The FT, LT, and FS all assume that v(t) is a continuous function. For discrete data the integrations of the FT, LT, or FS must be approximated by the finite summation technique.

$$\int_0^{T_o} v(t)dt \simeq \sum_{i=0}^{N-1} v_{sd}(t=i\Delta t)\Delta t \tag{3-21}$$

where

$$T_o = N\Delta t \tag{3-22}$$

The sampling rate, f_{sr}, is simply

$$f_{sr} = 1/\Delta t \tag{3-23}$$

If one has a finite amount (N points) of data taken at a fixed sampling interval Δt, this data can be applied to the Fourier Series. Using the finite

summation method as in eq. (3-21), eq. (3-17) can be transformed to

$$U_n(nf_o) = \frac{1}{N\Delta t} \sum_{i=0}^{N-1} v_{sd}(i\Delta t) e^{-j2\pi n f_o (i\Delta t)} \Delta t \qquad (3\text{-}24)$$

U_n replaces D_n to distinguish between the FS and the DFT. The Δt within the summation cancels the Δt in the denominator. The exponential argument may also be rewritten with eqs. (3-13) and (3-22).

$$U_n(nf_o) = \frac{1}{N} \sum_{i=0}^{N-1} v_{sd}(i\Delta t) e^{-ji2\pi n/N} \qquad (3\text{-}25)$$

This is the normal form given in the literature for the discrete Fourier transformation (DFT) [26]. This form is preferred when programming a digital computer. Equation (3-24) is more useful for obtaining insight and understanding of the properties of the DFT.

For an electrical voltage, the units of v(t) are volts. Equation (3-24) is from the Fourier series and the result of the summation is an area in units of volt-second. The final result $U_n(nf_o)$ is the summation normalized by the time interval of summation, T_o. Thus the units of $U_n(nf_o)$ are volts.

As with FT, LT, and FS there exists an inverse Discrete Fourier Transform. It is normally written in the literature [27] as

$$v_{sd}(i\Delta t) = \sum_{n=0}^{N-1} U_n(nf_o) e^{+ji2\pi n/N} \qquad (3\text{-}26)$$

Using eq. (3-22), eq. (3-26) can be rewritten to demonstate its similarity to the FS expansion eq. (3-18).

$$v_{sd}(i\Delta t) = \sum_{n=0}^{N-1} U_n(nf_o) e^{+j2\pi n f_o (i\Delta t)} \qquad (3\text{-}27)$$

Equation (3-26) is different from the FS equation (3-18) in that it is a summation over a finite number of frequencies while eq. (3-18) is an infinite summation. The reason for this is the discrete nature of $v_{sd}(t)$ due to the sampling process. A complete derivation will not be shown here as it has already been covered adequately in the literature. Brigham [28] gives a good description of the DFT along with appropriate illustrations.

In a report of this nature it is useful to summarize the important properties and limitations of the DFT.

1. The actual time domain waveform v(t) extends from t = $-\infty$ to $+\infty$, figure 3-1(a).
2. The waveform is sampled N times at the sampling rate, f_{sr}, with a uniform sampling interval Δt, figure 3-1(b), to give $v_{sd}(t)$. $f_{sr} = \frac{1}{\Delta t}$.

3. A finite time segment of length T_o of the waveform is sampled, figure 3-1(b). $T_o = N\Delta t$.
4. The DFT is in reality a discrete Fourier series.
5. The DFT gives the transform of a periodic waveform $v_p(t)$, figure 3-1(c).
6. $v_p(t)$ and $v_{sd}(t)$ are related.

$$v_p(t) = \sum_{\ell=-\infty}^{+\infty} v_{sd}(t+\ell T_o) \tag{3-28}$$

7. $v_p(i\Delta t) = v(i\Delta t)$ only in the interval $0 \leq t < T_o$.
8. $v_p(t)$ is periodic with period T_o and a fundamental repetition frequency $f_o = 1/T_o$.
9. The FT of v(t) is a continuous function V(f) for all frequencies, figure 3-2(a).
10. The DFT gives frequency coefficients $U_n(nf_o)$ only at discrete frequencies that are integer multiples of the fundamental frequency, nf_o, figure 3-2(b).
11. As a result of the sampling process the bandwidth of the frequency coefficients is limited.
12. The sampling process and the DFT produce a periodic spectrum $U_n(nf_o)$ in the frequency domain of period f_{sr}, figure 3-2(c).

$$U_n(nf_o) = U_n(nf_o - f_{sr}) \tag{3-29}$$

n is an integer with allowable values from $-\infty$ to $+\infty$.
13. $U_n(nf_o)$ is obtained by an infinite summation of the shifted spectrum of the original signal V(f).
14. V(f) is a bandlimited function if its tails are zero above a cutoff frequency, f_{co}, figure 3-2(a).
15. If the tails of V(f) are zero above the folding frequency, f_f, where $f_f = f_{sr}/2$, then $U_n(nf_o)$ is an accurate representation of V(f) for $|f| < f_f$.
16. If the tails of V(f) extend above f_f, i.e., $f_{co} > f_f$, then aliasing results which distorts $U_n(nf_o)$.
17. The Nyquist sampling rate, f_{N_y}, is the special case when $f_{sr} = 2\, f_{co}$. It is the lowest sampling rate which will accurately sample V(f) without aliasing.
18. U_n for negative frequencies is the complex conjugate of U_n for positive frequencies.

$$U_n(-f) = U_n^*(f) \tag{3-30}$$

19. In normal computer processing of the DFT pair, eqs. (3-24) and (3-26), the frequency span from f = 0 to $f = (N-1)f_o$ is used. The

frequency domain coefficients $U_n(nf_o)$ in the range 0 to f_f contain the normally anticipated values. The coefficients $U_n(nf_o)$ in the range f_f to $(N-1)f_o$ are in reality the negative frequency coefficients of $f = -f_f$ to $-f_o$. They are shifted in frequency due to the periodic property of the DFT.

20. For frequencies above the folding frequency, f_f, $U_n(nf_o)$ is not the same as V(f).

3.5 Fast Fourier Transformation

The Fast Fourier Transformation (FFT) is not really a different transform from those already discussed. The FFT is in fact the DFT. All of the comments made in the previous section on the DFT apply to the FFT. The FFT is simply a computer algorithm for the rapid and efficient computation of the DFT. The FFT dates back to the early 1900's but it was given its push to prominence in 1965 by Cooley and Tukey [29].

The common FFT is a DFT with the restriction that the number of sample points, N, be an integer power of 2.

$$N = 2^{\gamma} \tag{3-31}$$

where $\gamma = 1,2,3,....$

The value of the FFT is in the reduction of computer time required to evaluate a DFT [30]. An arbitrary N-point DFT requires approximately N^2 operations while the FFT requires $2N \log_2(N)$ arithmetic operations.

Gans and Nahman [31] give a good description of the inner mechanisms of the FFT.

3.6 Relationship Between FT and DFT for an Impulsive Waveform

In actual measurements one is never able to obtain data over a time interval of infinite extent. One is always constrained to obtaining a finite amount (N) of data in a limited time window (T_w). Thus one always obtains data that is more suitable for the DFT rather than the FT. The question often arises, "What is the relationship between the FT and the DFT?" This section will deal with this question for an impulsive waveform.

An impulsive waveform is one that suddenly departs from zero amplitude, rises to a peak value, and then rapidly relaxes back to zero. If the observation time window is sufficiently wide, figure 3-3(a), to include the beginning zero departure and the final return to zero then the waveform, $v_i(t)$, may be completely described as

$$v_i(t) = \begin{cases} f(t), & 0 \le t \le T_w \\ 0, & t < 0, \quad \text{and} \quad t > T_w \end{cases} \tag{3-32}$$

where f(t) is finite and continuous in the time window $0 \leq t \leq T_w$. Because the signal is zero outside of the time window, the FT reduces to

$$V_i(f) = \int_0^{T_w} v_i(t) e^{-j2\pi ft}\, dt \tag{3-33}$$

An artificial periodic signal $v_{pi}(t)$, figure 3-3(b), is assumed to be related to $v_i(t)$ by eq. (3-12).

$$v_{pi}(t) = \sum_{n=-\infty}^{\infty} v_i(t \pm nT_w) \tag{3-34}$$

The FS of $v_{pi}(t)$ exists with frequency coefficients given by

$$D_{ni}(nf_o) = \frac{1}{T_w} \int_0^{T_w} v_i(t) e^{-j2\pi nf_o t}\, dt \tag{3-35}$$

Section 3.4 demonstrated that the DFT was approximately the same as the FS.

$$U_{ni}(nf_o) \simeq D_{ni}(nf_o) \tag{3-36}$$

Note that the integral in eq. (3-35) is in fact simply $V_i(f)$, eq. (3-33), evaluated at nf_o. Thus the relationship between the FT and the DFT for an impulsive waveform is

$$V_i(nf_o) \simeq T_w U_{ni}(nf_o)$$
$$n = 0,1,2,.... \tag{3-37}$$

where

$$f_o = 1/T_w. \tag{3-38}$$

It should be noted that V_i is obtained only at discrete harmonically related frequencies. Values at other discrete frequencies may be obtained by numerically integrating eq. (3-33) directly.

3.7 Relationship Between FT and DFT for a Step-Like Waveform

In pulse measurements one normally encounters impulsive or step-like waveforms. The impulse was discussed in the preceding section. The step-like waveform poses a bit more difficulty in determining the relationship between the DFT and the FT. Once again the discussion will deal with the actual measurement problem of a finite amount (N) of data in a limited time window (T_w).

A step-like waveform $V_{s\ell}(t)$, figure 3-4(b), is one that suddenly departs from zero amplitude (or a fixed baseline), rises to a new amplitude value and remains there until $t = +\infty$. If the observation time window T_w is sufficiently wide to include the beginning zero departure and the final steady state value, v_o, then the waveform may be completely described.

The step-like waveform can be considered to be the step response of some linear system. The excitation $v_s(t)$, figure 3-4(a), is a unit step function.

$$v_s(t) = u(t) \tag{3-39}$$

The LT of $v_s(t)$ is

$$[v_s(t)] = V_s(s) = \frac{1}{s} \tag{3-40}$$

The linear system step response in the complex frequency s domain is

$$V_{s\ell}(s) = V_s(s)\ H(s) = \frac{H(s)}{s} \tag{3-41}$$

where H(s) is the system transfer function. In the time domain the system step response is

$$v_{s\ell}(t) = \mathcal{L}^{-1}[\frac{H(s)}{s}] \tag{3-42}$$

Now consider the effect of using a unit rectangular pulse $v_{rp}(t)$ of duration T_w, figure 3-4(c), as an excitation.

$$v_{rp}(t) = u(t) - u(t-T_w) \tag{3-43}$$

The LT of $v_{rp}(t)$ is

$$\mathcal{L}[v_{rp}(t)] = V_{rp}(s) = (1-e^{-sT_w})/s \tag{3-44}$$

The response, $v_{rpr}(t)$, of the linear system to this rectangular pulse excitation is

$$v_{rpr}(t) = \mathcal{L}^{-1}[V_{rp}(s)\ H(s)] \tag{3-45}$$

$v_{rpr}(t)$ would appear as shown in figure 3-4(d). With the pulse duration T_w chosen such that $v_{s\ell}(T_w)$ has attained its final value v_o, then the pulse response $v_{rpr}(t)$ is simply

$$v_{rpr}(t) = \begin{cases} v_{s\ell}(t), & t < T_w \\ v_o - v_{s\ell}(t-T_w), & t \geq T_w \end{cases} \tag{3-46}$$

Now consider making the single rectangular pulse into a periodic square wave, $v_p(t)$, of duration T_w and period $2T_w$, figure 3-4(e). The response, $v_{s\ell p}(t)$, of the linear system to this excitation would appear as shown in figure 3-4(f) and as given by the following equations.

$$v_{s\ell p}(t) = v_{s\ell p}(t \pm n2T_w), \quad n = 0,1,2,.... \tag{3-47}$$

$$v_{s\ell p}(t) = \begin{cases} v_{s\ell}(t), & 0 \leq t < T_w \\ v_o - v_{s\ell}(t-T_w), & T_w \leq t < 2T_w \end{cases} \tag{3-48}$$

This periodic square wave response waveform is now in the form that can be handled easily by the FS or the DFT. The fundamental frequency is

$$f_o = 1/2T_w \tag{3-49}$$

The FS coefficients of this quasi-square wave $v_{s\ell p}(t)$ are

$$\begin{aligned} D_{ns\ell}(nf_o) = {} & \frac{1}{2T_w}\int_o^{T_w} v_{s\ell}(t)e^{-jn\pi t/T_w}\,dt \\ & - \frac{1}{2T_w}\int_{T_w}^{2T_w} v_{s\ell}(t-T_w)e^{-jn\pi t/T_w}\,dt \\ & + \frac{V_o}{2T_w}\int_{T_w}^{2T_w} e^{-jn\pi t/T_w}\,dt \end{aligned} \tag{3-50}$$

The integrations in eq. (3-50) are straightforward and give the result

$$D_{ns\ell}(nf_o) \begin{cases} = \dfrac{1}{T_w}\displaystyle\int_o^{T_w} v_{s\ell}(t)e^{-jn\pi t/T_w}\,dt + j\left[\frac{V_o}{n\pi}\right] \\ \qquad \text{for } n = 1,3,5,\ldots \\ = 0, \text{ for } n = 2,4,6,\ldots \end{cases} \tag{3-51}$$

The fact that $D_{ns\ell} = 0$ for even n is consistent with the property that no even harmonics exist for a symmetrical waveform. Section 3.4 demonstrated earlier that the DFT was approximately the FS.

$$U_{ns\ell}(nf_o) \simeq D_{ns\ell}(nf_o) \tag{3-52}$$

Substituting eqs. (3-52) and (3-51) into eq. (3-47) gives the result

$$V_{s\ell}(nf_o) \simeq U_{ns\ell}(nf_o)T_w \qquad \text{for } n = 1,3,5,\ldots \tag{3-53}$$

This is the same result as obtained for the impulsive waveform except that now the fundamental frequency is $1/2T_w$ and only the odd harmonics are obtained. $V_{s\ell}$ is obtained only at discrete harmonically related frequencies. $V_{s\ell}(f)$ may be evaluated at any other frequency by numerically integrating eq. (3-47) directly.

3.8 Amplitude Spectrum of Common Waveforms

In time domain pulse testing, a limited number of waveforms are commonly encountered. They are the step, truncated ramp, impulse, rectangular pulse, triangular pulse, sine squared pulse, and the RF burst. These waveforms are important because they can be described mathematically and their spectra can be readily calculated. Actual generators are capable of closely approximating these idealized waveforms.

Table 3-1 lists the various waveforms, their mathematical equations in the time domain, and the equations for their amplitude spectrum, S(f). Figures 3-5 through 3-10 show the waveforms and their respective S(f).

The unit step, figure 3-5, and the truncated ramp, figure 3-6, are power signals and as such do not possess FT's as defined earlier. The spectral equations given in table 3-1 were obtained from the more general unified FT by deleting the delta functions. For example, the unified FT gives for the unit step

$$\mathfrak{F}[u(t)] = \frac{1}{j\omega} + \pi\delta(\omega) \tag{3-54}$$

$$|\mathfrak{F}[u(t)]| = \frac{1}{\omega}, \qquad \omega > 0 \tag{3-55}$$

The spectrum of the ideal step, figure 3-5, is inversely proportional to frequency. It is thus characterized by a constant slope of -20 dB/decade. The truncated ramp's spectrum, figure 3-6, is identical to that of the ideal step for low frequencies. However as the frequency increases and approaches $1/t_o$, S(f) departs from the -20 dB/decade slope and assumes more the characteristic of the triangular pulse, figure 3-8.

The rectangular pulse, figure 3-7, is seen to have a sin(x)/x variation (see also Chapter 2). A distinguishing feature of this pulse and most other impulsive shaped pulses, such as the triangular pulse, figure 3-8, and the sine squared pulse, figure 3-9, is the fact that the spectrum amplitude approaches a constant value $2\ v_o t_o$ at low frequencies. $v_o t_o$ is simply the area under the v(t) curve. The shape of the spectrum for the triangular pulse, figure 3-8, is identical to that of the rectangular pulse except that S(f) drops faster with frequency. Note that the vertical scale is 20 dB/div. instead of 10 dB/div. The sine squared pulse, figure 3-9, has its first spectrum zero at $1/t_o$ like earlier pulses. Its higher order zeros occur twice as often.

A special case of the rectangular pulse is the true impulse or as it is called in mathematics, the Dirac delta function, $\delta(t)$. It is defined as

$$\delta(t) = \lim_{a \to 0} \frac{u(t) - u(t-a)}{a} \tag{3-56}$$

$$\int_{-\infty}^{\infty} \delta(t) = 1 \tag{3-57}$$

This is seen to be a rectangular pulse of width a and height 1/a with a constant unit area. Its spectrum is like that of the rectangular pulse except that its first sin(x)/x zero occurs at infinity. In other words its spectrum is constant for all frequencies.

In normal laboratory practice a narrow rectangular pulse is often times referred to as an impulse. This is done with the implicit understanding that its spectrum amplitude is essentially constant for all frequencies of interest.

The spectrum of the rectangular RF burst, figure 3-10, is seen to be simply that of the rectangular pulse transposed in frequency by the carrier frequency, f_c. However, the sidebands are not symmetrical. The dissymmetry is caused by the second term involving $(2f_c + \Delta f)$. This second term accounts for the aliasing caused by the transposition of the rectangular pulse spectrum to both $+f_c$ and $-f_c$. When the RF burst contains an integer number of cycles, i.e., $t_o = N/f_c$, then the number of zeros of s(f) between zero and f_c are equal to N. For frequencies near f_c (i.e., $\Delta f \simeq 0$), S(f) is essentially flat and approximately equal to $v_o t_o$.

Table 3-1. Amplitude Spectrum of Common Waveforms

Waveform	V(t)	S(f)
Step	$V_o u(t)$	$V_o/(\pi f)$
Truncated Ramp	$\frac{V_o}{t_o}[t\,u(t) - (t-t_o)u(t-t_o)]$	$\left(\frac{V_o t_o}{\sqrt{2}\,\pi}\right)\frac{[1-\cos(2\pi f t_o)]^{1/2}}{(t_o f)^2}$
Rectangular Pulse	$V_o[u(t) - u(t-t_o)]$	$2V_o t_o\left\lvert\frac{\sin(\pi f t_o)}{(\pi f t_o)}\right\rvert$
Triangular Pulse	$\frac{V_o}{t_o}[t\,u(t) - 2(t-t_o)u(t-t_o) + (t-2t_o)u(t-2t_o)]$	$2V_o t_o\left\lvert\frac{\sin(\pi f t_o)}{(\pi f t_o)}\right\rvert^2$
Sine Squared Pulse	$V_o\left[\sin^2\left(\frac{\pi t}{2t_o}\right)u(t) - \sin^2\left(\frac{\pi t}{2t_o}\right)u(t-t_o)\right]$	$2V_o t_o\left\lvert\frac{\sin(2\pi f t_o)}{(2\pi f t_o)[1-(2f t_o)^2]}\right\rvert$
RF Burst	$V_o[\sin(2\pi f_c t)u(t+t_o/2) - \sin(2\pi f_c t)u(t-t_o/2)]$	$V_o t_o\left\lvert\frac{\sin(\pi\Delta f t_o)}{(\pi\Delta f t_o)} - \frac{\sin[\pi(2f_c+\Delta f)t_o]}{[\pi(2f_c+\Delta f)t_o]}\right\rvert$ where $\Delta f = f - f_c$

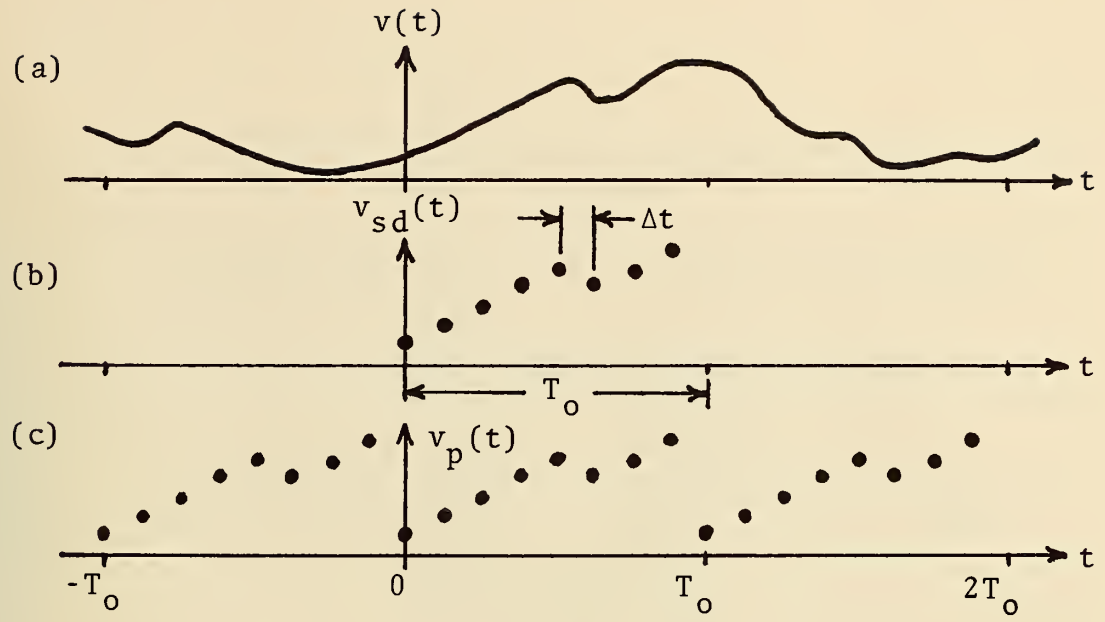

Figure 3-1. (a) Actual Time Domain Waveform. (b) Sampled Data Obtained in a Finite Time Window. (c) Periodic Waveform Used in DFT.

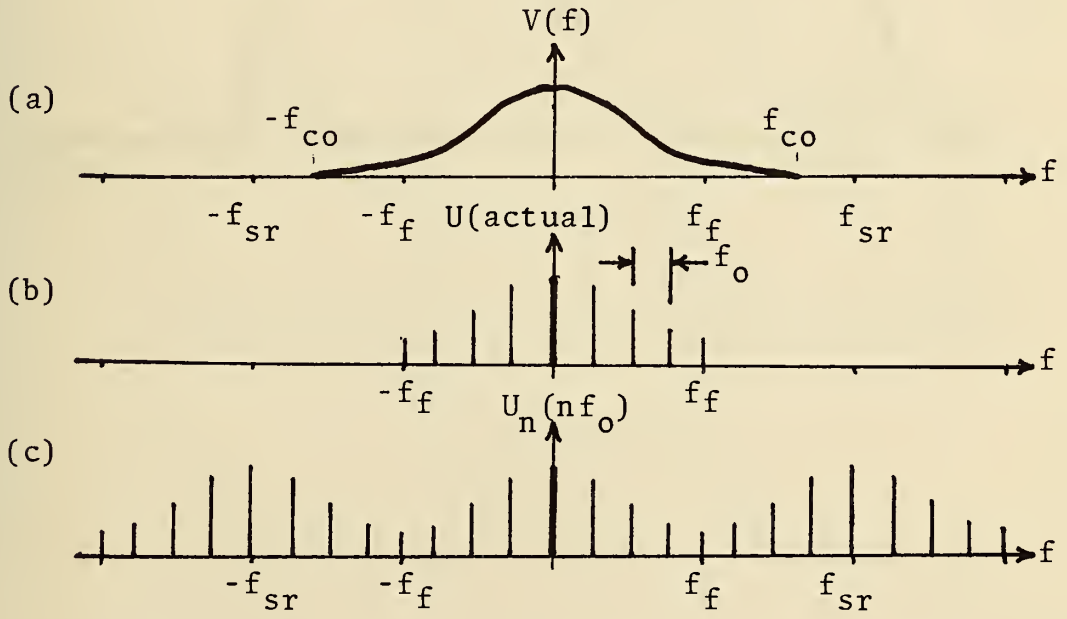

Figure 3-2. (a) FT of Actual Time Domain Waveform. (b) Actual Frequencies Present in DFT of Sampled Data. (c) Periodic Spectra U_n Produced in the Frequency Domain by the DFT.

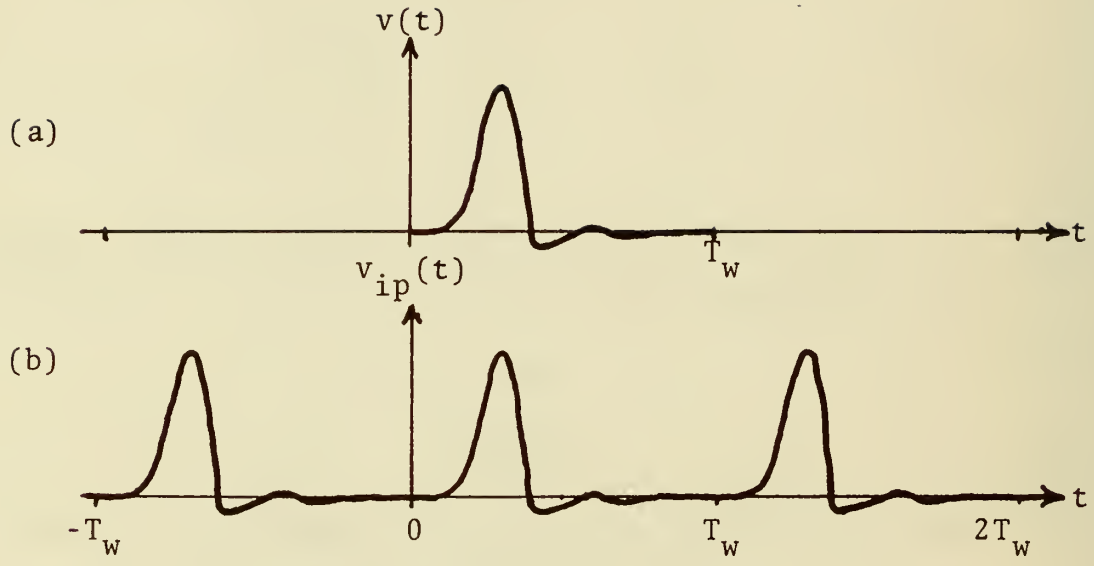

Figure 3-3. Impulsive Waveform Made Periodic.

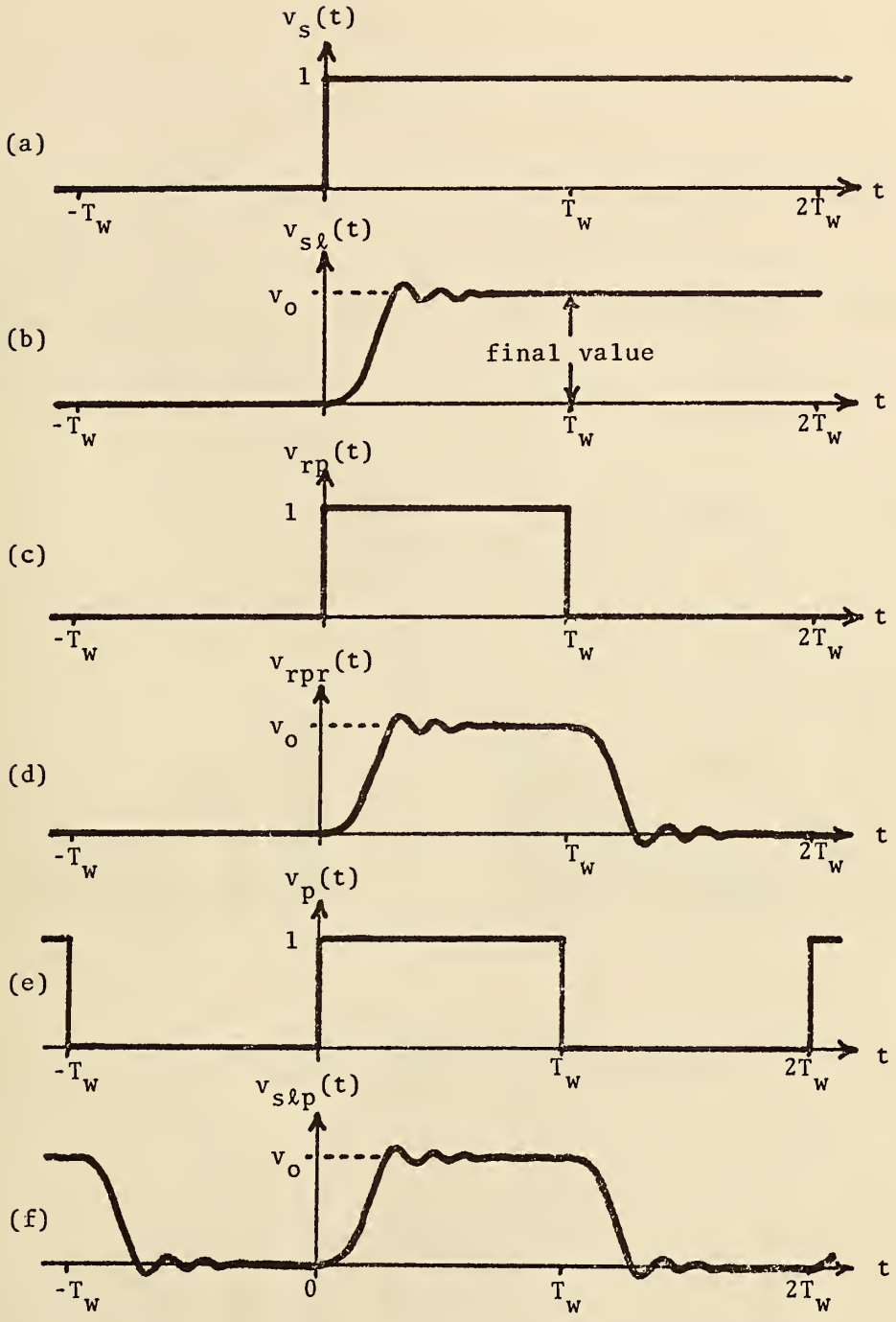

Figure 3-4. A Step-Like Waveform and Various Related Waveforms.

Fig. 3-5. Step.

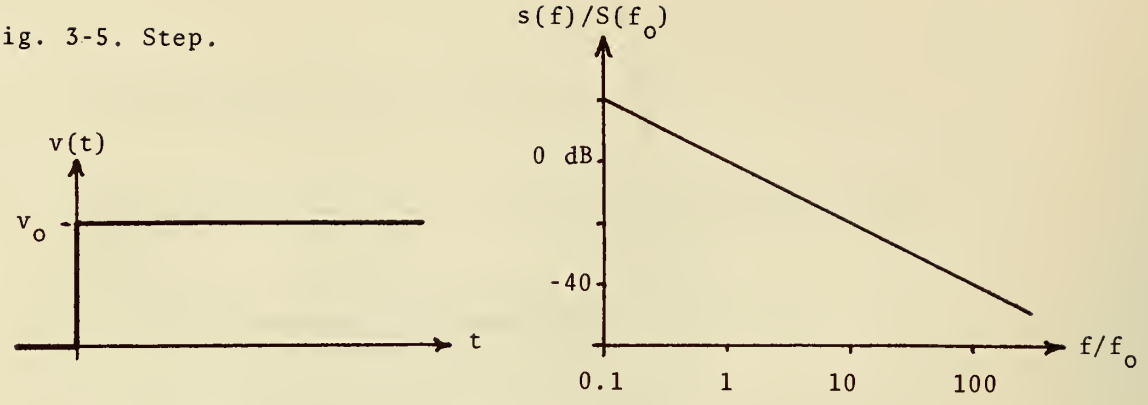

Figure 3-6. Truncated Ramp.

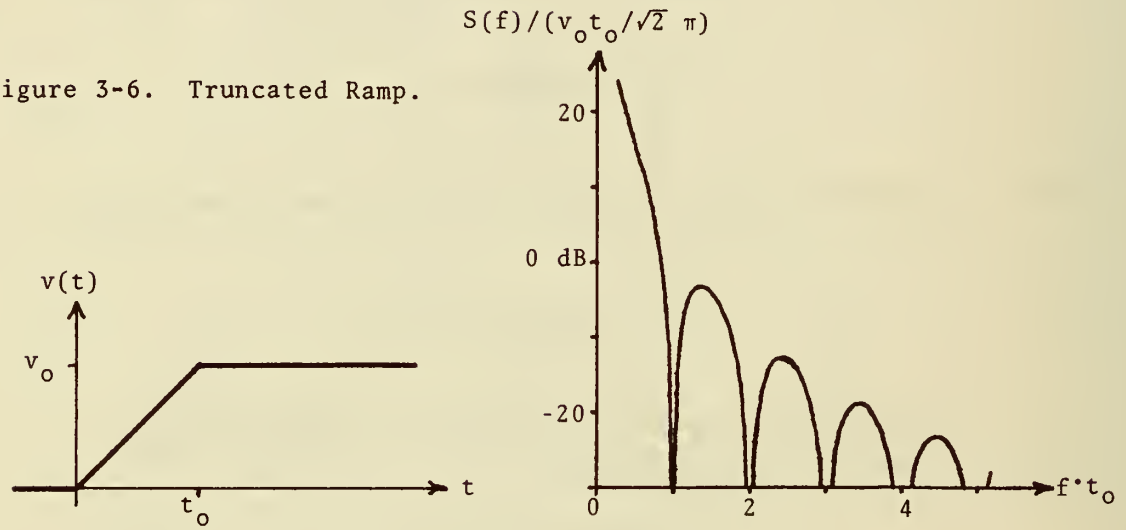

Figure 3-7. Rectangular Pulse.

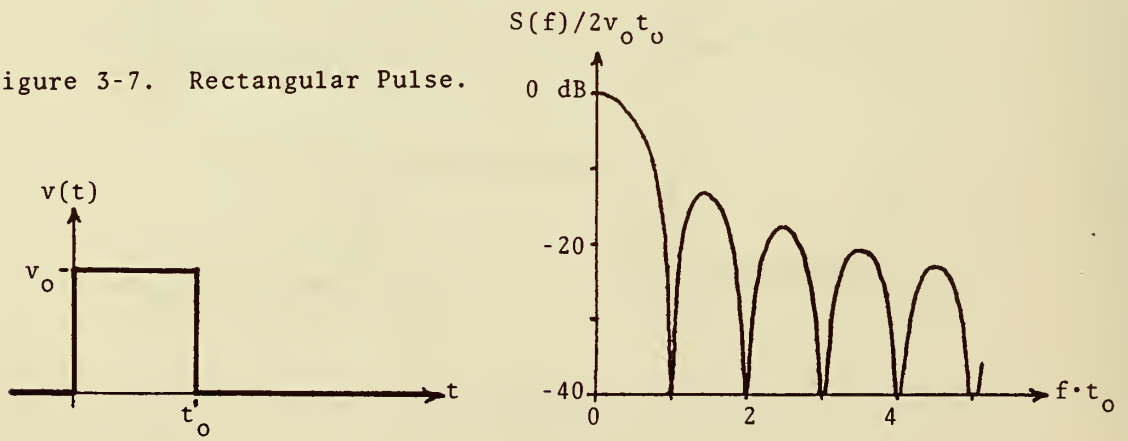

Figure 3-8. Triangular Pulse.

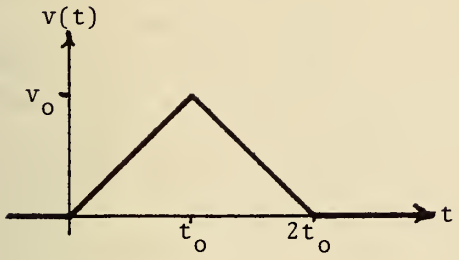

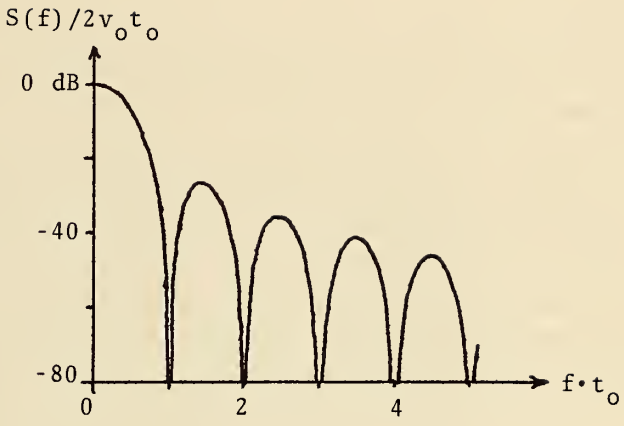

Figure 3-9. Sine Squared Pulse..

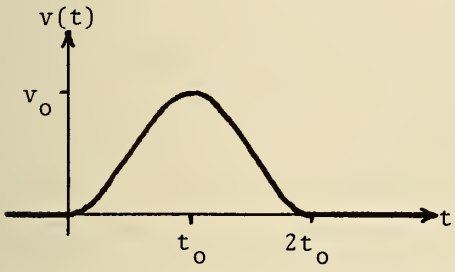

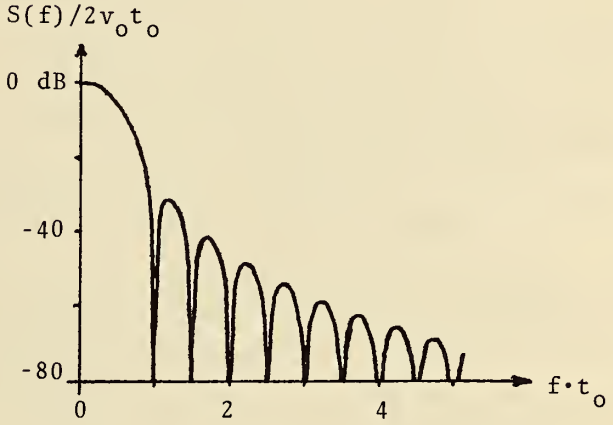

Figure 3-10. RF Burst.

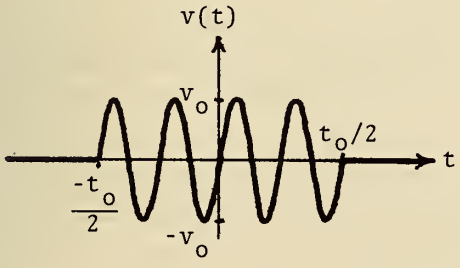

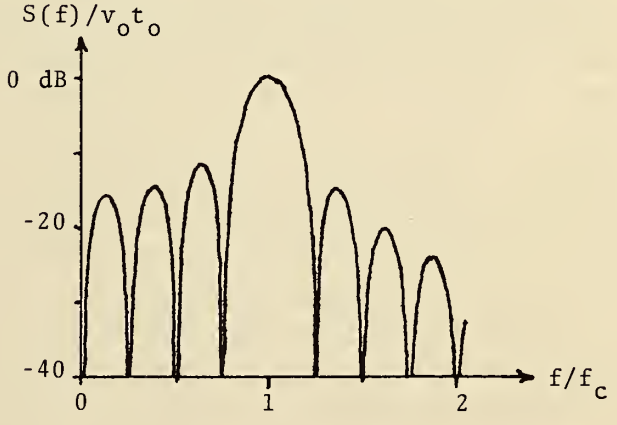

4. EXPERIMENTAL FFT'S OF SOME IDEAL WAVEFORMS

4.1 Background

In the course of software development for the TDANA it was found necessary to conduct a set of experiments in order to understand more fully the mechanisms of the FFT. (A number of rather odd spectrum amplitude observations were made when certain time domain waveforms were transformed.) Also, a clearer understanding of the relationship between pulse shape and spectrum amplitude was desired for certain pulses typically encountered in time domain studies. What follows, then, are descriptions and results of the various experiments performed. These are broken down into two major types of waveforms; rectangular pulses and repetitive rectangular pulses.

4.2 Single Rectangular Pulses

For this experiment, as well as for those that follow, idealized 128-point time domain waveforms were transformed on the system computer using a moderately fast and accurate FFT routine written in BASIC. An example of one of these time domain waveforms appears in figure 4-1. Photographs were then taken of the resulting spectrum amplitudes as observed on the system monitor oscilloscope. For the DFT

$$U_n(nf_o) = \frac{1}{N} \sum_{i=0}^{N-1} v_{sd}(i\Delta t)e^{-ji2\pi n/N}, \qquad i = 0,1,2,\cdots,127 \qquad (4\text{-}1)$$

The observed output was of the form $|U_n(nf_o)|$ where

$$|U_n(nf_o)| = [a_n^2 + b_n^2]^{1/2}. \qquad (4\text{-}2)$$

a_n and b_n are the real and imaginary parts, respectively, of the n^{th} complex frequency coefficient.

The set of spectral points produced by this N-point transform in order of ascending frequency, consists of a DC term, N/2-1 equally spaced harmonic terms, a folding frequency term, and N/2-1 additional equally spaced harmonic terms. The latter set of N/2-1 harmonic terms are merely complex conjugates or mirror images of the first set of N/2-1 harmonic terms and are thus redundant. Consequently, the photographs appearing in this chapter are displays of only the DC term and the first 63 harmonic terms. In the figures $|U_n(nf_o)|$ is plotted on a vertical uncalibrated linear scale. The horizontal axis is a linear frequency scale.

Figure 4-2 is a photograph of the displayed spectrum amplitude for an "impulsive" time domain waveform. That is, the first point of the 128-point waveform was assigned a positive value and the remaining 127 points were set to zero. The lower trace of points in the photo is a baseline reference only and not part of the spectrum. As one would expect, the spectrum amplitude for this waveform has a constant value.

By making the pulse width two points wide rather than one, the photo in figure 4-3 results. Note that for a two-point rectangular pulse, the spectrum amplitude decays to a zero value at the folding frequency (f_f). This will be true for any length FFT as long as the total number of points in the time domain waveform is 2^γ, γ a positive integer.

The photo in figure 4-4 is a spectrum amplitude display of a three-point rectangular pulse. The only zero now occurs at two-thirds f_f. After this zero the spectral density rises again arriving at a peak value at f_f.

Figure 4-5 is the spectrum amplitude for a four-point rectangular pulse. Two zeros are now present, one at one half f_f and one at f_f. A number of inferences may now be made. First of all, it appears that the number of zeros occurring between DC and f_f in the spectrum amplitude of a rectangular pulse is equal to half the number of points in the pulse. This is indeed true, not only for a 128-point transform but for a transform of any length 2^γ, γ an integer. Expressing this mathematically,

$$N_o = \frac{n_p}{2}, \qquad n_p \leq \frac{N}{2} \tag{4-3}$$

where N_o is the number of spectral zeros, n_p is the number of points in the rectangular pulse, and N is the number of points in the time waveform. The restriction that the pulse width cannot be wider than half the time window will be explained and modified below.

By simply looking at figure 4-6, now, since there are six spectral zeros between DC and f_f one could apply eq. (4-3) to show that the number of points in the pulse is twelve. Likewise, since the photo in figure 4-7 contains 16 zeros there must have been 32 points in the rectangular pulse generating that spectrum.

Now to carry this inference a step further, one may imply that the number of zeros present between DC and f_f for a rectangular pulse spectrum amplitude is really a function of the ratio of the pulse width, τ, and the width of the time window, T. That is,

$$N_o = \frac{N\tau}{2T}, \qquad \frac{T}{N} < \tau \leq \frac{T}{2} \tag{4-4}$$

where N_o is again the number of zeros occuring between DC and f_f. The lower limit on τ (i.e. T/N) indicates that the spectrum for a single-point pulse contains no zeros. The upper limit of T/2 can best be explained by comparing the spectra shown in figures 4-7 and 4-8. The spectrum in figure 4-7 corresponds to a 32-point rectangular pulse while a 96-point rectangular pulse generated the spectrum in figure 4-8. Note that, aside from the difference in DC terms, both spectra are identical. (The spectrum in figure 4-8 was scaled down vertically to allow display of the large DC term.) The time domain rectangular pulse that generated the spectrum in figure 4-7 (32 points)

corresponds to a pulse width of $\frac{32}{128}$ = 1/4 the total time window. That of figure 4-8 corresponds to a width of $\frac{96}{128}$ = 3/4 the total time window. Since the pulse causing the spectrum in figure 4-8 is really a negative pulse with a width of 1/4 the total time window, and since the spectrum amplitudes for both positive and negative pulses of equal width are the same (disregarding the DC terms), it follows that the two spectra should be the same. Equation (4-4) may now be expanded to cover all possible pulse widths as follows.

$$N_o = \begin{cases} \frac{N\tau}{2T} & \frac{T}{N} < \tau \leq \frac{T}{2} \\ \frac{N(T-\tau)}{2T} & \frac{T}{2} \leq \tau < T - \frac{T}{N}. \end{cases} \qquad (4\text{-}5)$$

This equation is a very helpful rule of thumb for quickly determining the relationship between a time domain rectangular pulse and its spectrum amplitude. If one knows the folding frequency and the number of zeros, N_o, in the spectrum, he may quickly determine both the pulse width and the width of the time window. It should be noted, however, that eq. (4-5) does not provide the pulse polarity, thus allowing a possibility of two answers. In practice this ambiguity is usually avoided by prior knowledge of the approximate pulse width, i.e., greater or less than T/2.

Another interesting observation was made concerning rectangular pulses of widths close to but not equal to T/2. Figure 4-9 is a photo of the spectrum amplitude for a 40-point rectangular pulse. Substitution of 40 for n_p in eq. (4-3) yields a value of 20 for N_o. Careful scrutiny of figure 4-8 indicates that there are 20 zeros in the spectrum but this count is difficult to make due to the lack of symmetry of the spectral points. The spectrum amplitude of the Fourier transform for a rectangular pulse is of the form $K|\sin(x)/x|$ where K is a function of both pulse width and pulse amplitude, and x is a function of pulse width (see eq. 2-5). For the FFT of the same rectangular pulse the location of the observed spectral points with respect to the continuous integral transform curve is a function of both pulse width and time window width. There is a lack of symmetry in figure 4-9 because the ratio of time window width to pulse width is not an integer power of 2.

Between DC and the folding frequency the spectrum amplitude points for the FFT of a rectangular pulse may be expressed as

$$|U_n(nf_o)| = K\left|\frac{\sin\left(\frac{n\pi\tau}{T}\right)}{n}\right| \qquad n = 0,1,2\cdots \frac{N}{2} \qquad (4\text{-}6)$$

where spectrum aliasing has been neglected. n is the harmonic number, $|U_n|$

is the spectrum amplitude point for the nth harmonic, τ is the pulse width, T is the time window width, K is a magnitude constant, and N is the total number of points in the transform. For the example of a 40-point pulse in a 128-point time window, eq. (4-6) becomes

$$|U_n| = K\left|\frac{\sin(\frac{5n\pi}{16})}{n}\right| \qquad n = 0,1,2\cdots 64. \tag{4-7}$$

Because of the 5/16 fraction in the argument of the sine term, the values of $|U_n|$ as n goes from 0 to 64 will be out of synchronization with the peaks and zeros of the sine function.

If we now examine the case of a 32-point pulse in a 128-point time window, eq. (4-6) becomes,

$$|U_n| = K\left|\frac{\sin(\frac{n\pi}{4})}{n}\right| \qquad n = 0,1,2\cdots 64. \tag{4-8}$$

The values of $|U_n|$ will now be synchronized with the sine function, i.e., the values of the sine term will repeat as 0, $\pi/4$, $\pi/2$, $3\pi/4$.

Parenthetically, if one wishes to express τ and T in units of time rather than simple integers, eq. (4-6) becomes,

$$|U_n| = K\left|\frac{\sin(\pi f_n \tau)}{f_n T}\right| \qquad n = 0,1,2\cdots \frac{N}{2}. \tag{4-9}$$

where, from the definition of the DFT,

$$f_n = \frac{n}{T} \qquad n = 0,1,2\cdots \frac{N}{2}. \tag{4-10}$$

The important point to notice in eq. (4-6) or (4-9) is that the ratio τ/T must evaluate to a fraction of the form 1/n, n an integer, in order for the peak and zeros of the sine function to be synchronized to the values of $|U_n|$. Because the FFT requires time window widths that contain 2^γ points, the fractional form of 1/n will only occur if the pulse width also contains a number of points equal to a power of 2.

The constant K is a function of both pulse width and pulse amplitude. Figure 4-10 is the spectrum amplitude for a 4-point rectangular pulse with an amplitude of 3200 arbitrary units in a 128-point window. The spectrum amplitude for an 8-point pulse of amplitude 1600 is shown in figure 4-11. Figure 4-12 is the spectrum for a 16-point pulse of amplitude 800. In each case the areas under the pulses (amplitude times width) are the same. These three figures graphically illustrate the fact that while K is a function of the area under the pulse, the number of spectral zeros or peaks obtained will be a function of τ/T.

The last experiment of interest performed on rectangular pulses was concerned with pulses of width T/2 or very close to T/2. Figure 4-13 is a photo of the spectrum amplitude for a rectangular pulse of width T/2. Note that, from eq. (4-6), the magnitude of the harmonic terms alternate between zero and a decreasing positive value as the frequency goes from DC to f_f. This is the DFT equivalent of the Fourier series representation of a symmetrical square wave where the even harmonics are all zero and the odd harmonics decrease monotonically as a function of frequency. As described elsewhere in this report, one may take advantage of this property of a pulse of width T/2 to eliminate unwanted zeros in the spectrum amplitude.

For pulses with widths very close to T/2 an interesting rectangular spectrum amplitude results. Figure 4-14 is the spectrum for a 511-point rectangular pulse. The total time window, or equivalently, the transform length, was 1024 points. For this figure, as for the two that follow, a 1024-point transform was used rather than a 128-point transform for purposes of clarity. Also, the displays are logarithmic in amplitude and because of certain system memory limitations, only the first 500 of the 512 useful spectral points are displayed. It may be seen, however, that the even harmonics appear to be constant while the odd harmonics decay in amplitude to a zero at f_f.

Figure 4-15 is a spectrum amplitude display for a 508-point rectangular pulse. A trend may now be noticed that the odd and even harmonic spectral amplitudes vary up and down alternately. Equation (4-5) may be used to show that, for figure 4-14, there must be 255-1/2 actual zeros in the spectrum amplitude while the spectrum amplitude for figure 4-15 must contain 254 actual zeros. From eq. (4-6) it may be shown that the sine term variations are just slightly out of synchronization with the values of $|U_n|$. In addition, eqs. (4-50 and (4-6) may be used to show that the number of points missing from or added to a pulse of width T/2 is equal to the number of zeros observed in the display for pulses with widths close to T/2. For example, the single zero in figure 4-14 indicates that the time domain pulse must have contained either 511 or 513 points. Similarly, the pulse producing the display in figure 4-15 must have contained either 508 or 516 points. Figure 4-16, studied closely, contains 19 zeros (or approaches toward zero) indicating that the pulse must have contained 512 ± 19 points, i.e., 493 or 531 points.

The major practical utility of this phenomenon is that a pulse width of exactly T/2 should be used to avoid the beat phenomena. An algorithm that transforms a step-like time domain waveform into a waveform of T/2 width is described in section 4.4.

4.3 Repetitive Rectangular Pulses

Armed with a practical knowledge of the spectrum amplitudes of single rectangular pulses, one could logically ask how the spectra of two or more rectangular pulses in the time window would appear. Several combinations of rectangular pulse transforms are described in this section. As was the case with the single rectangular pulse transforms, 128-point time domain waveforms were generated and transformed using the system minicomputer. The resulting 64-point spectrum amplitudes were again displayed on the system monitor oscilloscope.

Figures 4-17 through 4-20 are photographs of the spectrum amplitudes of an "impulse" pair. Referring to eq. (4-1), the time domain waveform, $v_{sd}(i\Delta t)$, consists of a 128-point array; two of the points are assigned a positive value and the other 126 points are set to zero. Thus, the FFT "sees" a pair of impulsive signals in the time window.

Figure 4-17 is a display of the spectrum amplitude for the impulse pair $v_{sd}(\Delta t)$ and $v_{sd}(3\Delta t) = 1$. Comparison with the spectrum amplitude for a single impulse (fig. 4-1) shows that a zero has been introduced into the previously constant spectrum. Figure 4-18 is the displayed spectrum for the impulse pair $v_{sd}(\Delta t)$ and $v_{sd}(4\Delta t) = 1$, and figure 4-19 shows the spectrum for the pair $v_{sd}(\Delta t)$ and $v_{sd}(13\Delta t) = 1$. Observation of these three figures indicates that as the impulses are spaced farther apart more zeros appear in the spectrum. Figure 4-20 is a display of the spectrum amplitude resulting from an impulse pair separated by half the time window, i.e., $v_{sd}(\Delta t)$ and $v_{sd}(65\Delta t) = 1$. For this case, all of the even harmonics have been forced to zero.

In the last section it was shown that the maximum amount of useful spectral information for a single rectangular pulse was obtained by choosing the pulse width to be exactly half the time window. Similarly, the results of this impulse pair experiment appear to indicate that maximum spectral information is obtained when only one impulse is present in the time window. Additional pulses generate unnecessary zeros in the resulting spectra and, to further complicate matters, the number of zeros generated is a function of the spacing between impulses. The next set of experiments discussed reinforces this notion.

Figures 4-21 through 4-23 are all spectrum amplitudes of four-point rectangular pulse trains. Figure 4-21 is the spectrum of two four-point rectangular pulses spaced half the time window apart. Comparison with figure 4-5, the spectrum for a single four-point rectangular pulse, shows an agreement in spectral envelope shape. Figure 4-21 differs only by the fact that all even harmonics are zero. This also agrees with the impulsive pair transform for a pulse separation of half the time window, i.e., two

equally spaced pulses in the time window yield a transform similar in shape to that of a single pulse, the only difference being the zeroing of the even harmonics.

Figure 4-22 is a photograph of the spectrum amplitude for a train of four equally spaced four-point rectangular pulses. Note now that only every fourth spectral point is non-zero. The spectrum for a train of eight equally spaced four point rectangular pulses is shown in figure 4-23. In this case, only every eighth spectral point is non-zero. As was indicated by the impulse pair transforms, the amount of useful spectral information is inversely proportional to the number of identical rectangular pulses in the time window. In general, it may be shown that the amount of useful spectral information is inversely proportional to the number of cycles of any periodic waveform present in the time window. The more cycles present in the time window, the more spectral points become zero or nearly zero. Ultimately, for a periodic waveform at the folding frequency, all spectral points become zero except the DC term. Thus, a periodic waveform at exactly the folding frequency will be "invisible" to the DFT and any frequencies higher than f_f will be aliased back down and will erroneously appear as non-zero spectral values below f_f.

Figures 4-24 through 4-26 have been included to show the effects of disturbing the symmetry within a rectangular pulse train. Figure 4-24 is a display of the spectrum amplitude of two four-point rectangular pulses spaced almost half the time window apart. The two pulses were placed at Δt through $4\Delta t$ and $64\Delta t$ through $67\Delta t$. The distortion is most evident in the even harmonics when compared to figure 4-21. Figure 4-25 is a photograph of the spectrum amplitude for the same two four-point pulses but this time placed at Δt through $4\Delta t$ and $63\Delta t$ through $66\Delta t$. Thus, as was noticed for the impulse pair transforms, the spacing between pulses strongly affects the shape of the resulting spectrum.

Figure 4-26 shows the effect of varying the width of one rectangular pulse with respect to the other in a pulse pair. In this case a four-point pulse was placed at Δt through $4\Delta t$ and a two-point pulse was placed at $65\Delta t$ and $66\Delta t$. Note the similarity to figures 4-3 and 4-5.

The last waveform transforms examined in this section are those for pulse doublets, that is, a positive pulse followed by a negative pulse. Figure 4-27 is the spectrum amplitude of a positive pulse at Δt through $8\Delta t$ and an equal magnitude negative pulse at $9\Delta t$ through $16\Delta t$. Figure 4-28 is the transform of a positive pulse at Δt through $16\Delta t$ and an equal magnitude negative pulse at $17\Delta t$ through $32\Delta t$. As the width of the two pulses is increased the first spectral peak will shift to the left and the number of spectral zeros will increase. Finally, for pulse widths of half the time window, the spectrum of figure 4-13 will be generated.

4.4 Practical Application of the DFT to Waveform Spectral Analysis

In this section some practical guidelines and algorithms are presented for the application of the DFT to actual pulse and step waveforms acquired with the TDANA system. These guidelines and algorithms are based in part on interpretation of the ideal pulse experiments of the previous section.

In practical applications of the DFT to spectral analysis of time domain waveforms, the two major problems encountered are commonly referred to as "aliasing" and "leakage" [32]. Based upon knowledge gleaned from the ideal pulse experiments described in the last section (4.2), methods have been developed that minimize errors caused by these two DFT problems.

Aliasing, first, is a term used to describe errors arising in the computed spectrum of a time domain waveform that is not band-limited. Shannon's Sampling Theorem [33] states that if a function of time, f(t) contains no frequencies higher than f_o hertz, then it is completely determined by giving the value of the function at a series of equispaced points $\frac{1}{2f_o}$ seconds apart. From a DFT spectral point of view, this means that there will be no overlapping of spectra, and therefore no aliasing errors if the time domain waveform contains no frequency components above the folding frequency, f_f. Recalling that the folding frequency is related to the sampling period by

$$f_f = \frac{1}{2\Delta t} \tag{4-11}$$

where Δt is the time spacing between samples, it becomes apparent that aliasing errors can be avoided by increasing f_f, or equivalently, by decreasing the sampling period, Δt. An equally effective method of eliminating aliasing errors is to band-limit the time domain waveform to contain no spectral energy at frequencies above the chosen f_f.

In practice, both methods are used to avoid aliasing errors. The time window and transform length, which together will dictate the sampling period, are judiciously chosen to yield a value of f_f considerably higher than the highest frequency in the measurement band of interest. To be safe, f_f is usually chosen to be at least twice the highest frequency of interest. Additionally, low-pass filters are often used on the output of the pulse generator to band-limit the reference waveform to the measurement band of interest.

The elimination of leakage errors is not quite as simple. Leakage errors are the result of discontinuities in the time domain waveform caused by the fact that the DFT assumes that the waveform in the time window is periodic over all time. Thus, for example, if a waveform in the time window starts at 0 V and ends at 2 V, the DFT of this waveform will contain leakage errors. One way to visualize this is to mentally draw the waveform to be

transformed around a cylinder whose circular perimeter is equal to the length of the displayed time window. If the beginning and end part of the waveform do not exactly meet with the same slope, leakage errors will occur. Stated another way, the periodic function over all time is constructed by repeating the waveform in the time window over all time, i.e.

$$f(t) = \begin{cases} \vdots & \vdots \\ f_T(t+2T) & -2T \leq t \leq -T \\ f_T(t+T) & -T \leq t < 0 \\ f_T(t) & 0 \leq t < T \\ f_T(t-T) & T \leq t < 2T \\ f_T(t-2T) & 2T \leq t < 3T \\ \vdots & \vdots \end{cases} \qquad (4\text{-}12)$$

where f_T is the waveform in the time window and T is the time window. This function must be continous and have a finite first derivative at the points $t = kT$ for $k = 0, \pm 1, \pm 2, \ldots \pm\infty$. Otherwise, leakage errors will result in the DFT spectrum.

The usual approach [34] is to minimize leakage errors by multiplying the time domain waveform data by some weighting function. In effect, whenever a waveform is transformed using the DFT, the waveform is multiplied by the time window, represented by a unity amplitude rectangular pulse. In the frequency domain the waveform spectrum is convolved with the spectrum of the unity amplitude rectangular pulse. As long as the waveform meets the criteria stated above (continuous with a finite first derivative at $t = kT$), then no leakage errors will occur. Whenever there is a discontinuity at kT, however, the resulting spectrum will be the correct one convolved with the spectrum of the "artificial" step waveform caused by the rectangular time window. This usual method, then, involves multiplying the waveform data by some weighting function other than the rectangular pulse implicit in the DFT operation. The reader is directed to Reference [34] for a description of a few of the more commonly used weighting functions as well as a fairly comprehensive list of additional references on the subject. The main point to be made here is that no matter what weighting function is chosen to force the waveform data to meet the no-leakage criteria, the resulting spectrum must be in error to the extent that the weighting function distorted the original waveform data.

A very simple algorithm has been developed by Gans which, for certain classes of waveforms and for certain applications, completely eliminates the effects of leakage errors. This "windowing algorithm" involves inverting

the original time domain waveform, shifting DC levels, and attaching this new waveform to the end of the original waveform. The effect is to create a new waveform, twice as long in time as the original, which is mathematically described as,

$$f_{WA}(t) = \begin{cases} f(t) & 0 \leq t < T \\ -f(t-T) + f(0) + f(T) & T \leq t < 2T \end{cases} \quad (4\text{-}13)$$

where f(t) is the original waveform, $f_{WA}(t)$ is the new waveform obtained from the windowing algorithm, and T is the original time window.

Figure 4-29(a) is a photograph of a typical step-like waveform obtained on the TDANA. Transforming the waveform would lead to disastrous leakage errors due to the fact that the initial and final voltage levels of the waveform differ substantially. Figure 4-29(b) is a photograph of the same waveform after being modified by the windowing algorithm. Notice that the time window becomes 2T and that the new waveform closely resembles a rectangular pulse of width T. As long as the slope of the original waveform is zero at t = 0 and t = T, this algorithm will yield a new waveform that fulfills the no-leakage criteria.

Furthermore, experiments have shown that this new waveform, created from a step-like original waveform, will have a spectrum amplitude very similar to that shown in figure 4-13. That is, the spectrum amplitude will be essentially that of a rectangular pulse whose width is half the time window. (Recall that, for this special case, all of the even harmonics of the spectrum are zero and all the odd harmonics decay monotonically as 1/f.)

Indeed, experiments on a variety of step-like waveforms have shown that the spectrum amplitude of figure 4-13 always results from step-like waveforms modified by the windowing algorithm. The only deviations in the spectrum of actual step-like waveforms, in comparison to the spectrum of figure 4-13, are those caused by the deviations of the actual waveform from the ideal rectangular pulse shape.

An heuristic proof of the validity of this algorithm may be made simply by considering the actual step-like waveform acquired and modified by the windowing algorithm to be the output waveform of some linear circuit driven by an ideal rectangular pulse source. One would expect, then, that the spectrum amplitude of the output waveform would be the magnitude of the product of the input spectrum and the transfer function of the linear circuit.

Another way of justifying the use of the windowing algorithm is to consider that the step response of a linear system will have the same form, regardless of the input step polarity. A linear system must "go up" and "come down" along the same but inverted curve if the input differs only in polarity. The windowing algorithm may be thought of as the response of the

linear system to a rectangular pulse whose duration is great enough for the system response to reach essentially its final value before the pulse turns-off. This algorithm, then, synthesizes a rectangular pulse response waveform from the original step response waveform and assumes that the system is linear. The characteristics of, and restrictions governing the use of this windowing algorithm may be summarized as follows.

To obtain leakage error-free results, the original time domain waveform only must have a zero slope at the beginning and end points of the time window. The price paid to eliminate leakage errors with this algorithm is the requirement of performing a double-length FFT on the waveform data. If a 512-point step-like waveform is acquired, for example, then the waveform resulting from the algorithm will consist of 1024 points. Just as was the case for the spectrum amplitude of an ideal rectangular pulse whose width is half the time window, all of the even harmonics resulting from the FFT of the 1024-point waveform will be zero. As one would expect, no new information is introduced into the spectrum by the fact that the transform length has been doubled.

The output spectrum amplitude of the DFT, operating on a waveform modified by the windowing algorithm will consist of a DC term, and amplitude coefficients at frequencies

$$f_r = \frac{1}{2T}, \quad \frac{2}{2T}, \quad \frac{3}{2T}, \quad \cdots, \quad \frac{2N}{2T}. \tag{4-14}$$

where T is the original time window and N is the original number of points in the acquired waveform. Of these amplitude coefficients, the ones at frequencies higher than the folding frequency, i.e.,

$$f_f = \frac{N}{2T} \tag{4-15}$$

are redundant. Also, the amplitude coefficients of all the even harmonics will be zero due the the symmetry of the modified waveform. The remaining odd harmonic amplitude coefficients, i.e.,

$$f_r = \frac{r}{2T} \qquad r = 1,3,5,\cdots, \frac{N-1}{2T} \tag{4-16}$$

will be correct and useful.

Finally, it should be mentioned that applying the windowing algorithm to waveforms that already meet the no-leakage criteria is valid but wasteful. Since half of the useful spectral coefficients will be zero, then no new information is gained by performing a double-length transform on the original waveform data. All of the useful spectral information available is obtained by transforming the original waveform.

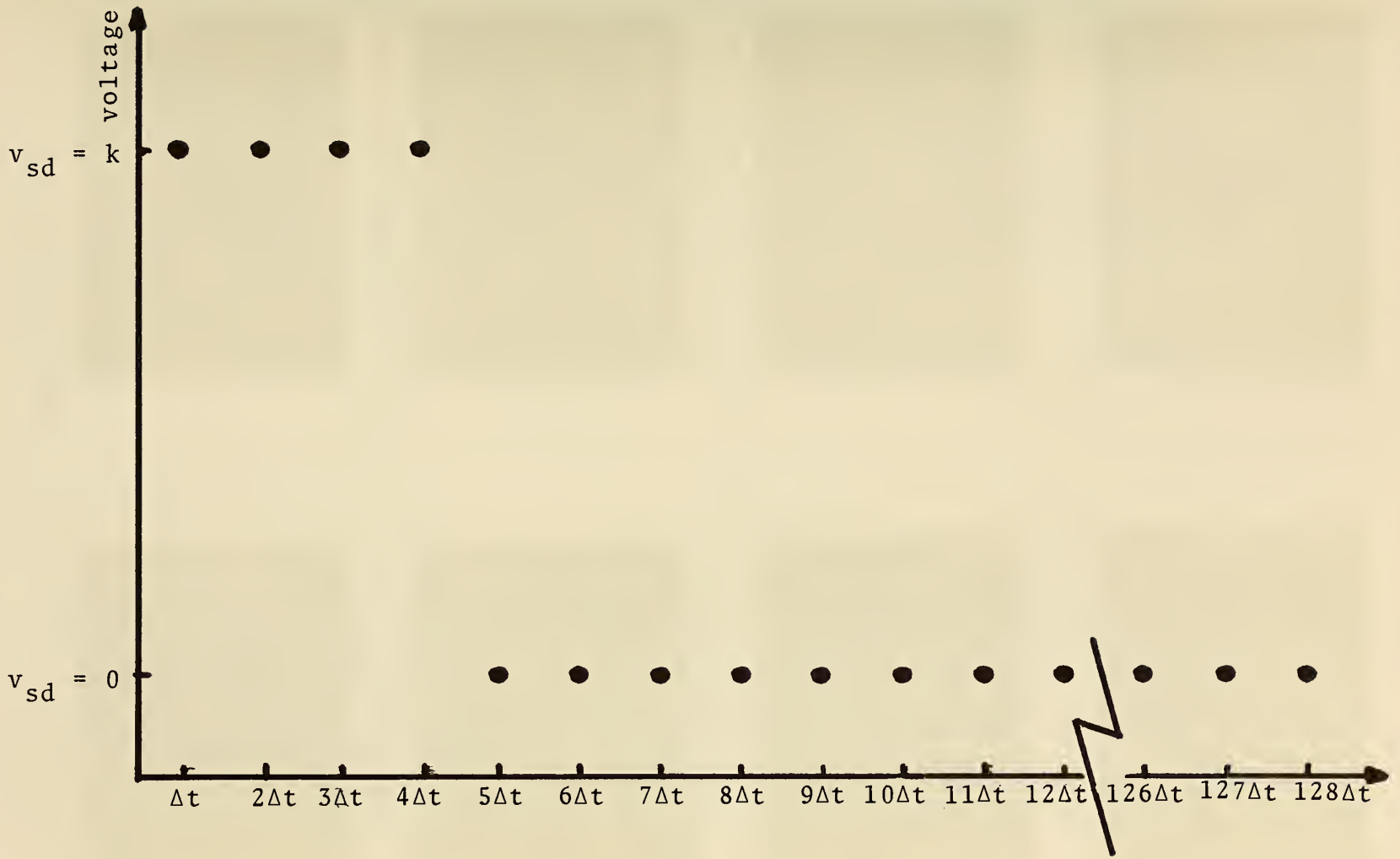

Figure 4-1. Example of a 128-Point Idealized Time Domain Waveform. This 4-Point Rectangular Pulse Generated the Spectrum Amplitude Shown in Figure 4-5.

Figure 4-2. Spectrum Amplitude of an "Impulsive" Time Domain Waveform.

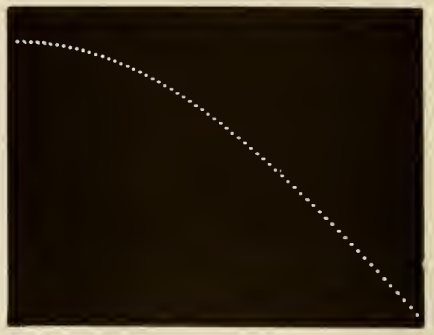

Figure 4-3. Spectrum Amplitude of a 2-Point Rectangular Pulse.

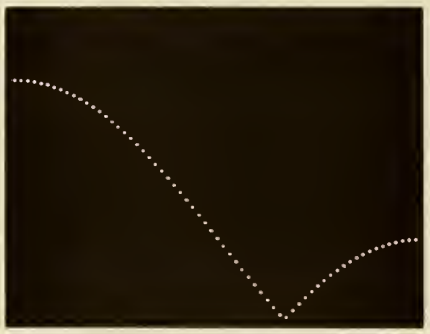

Figure 4-4. Spectrum Amplitude of a 3-Point Rectangular Pulse.

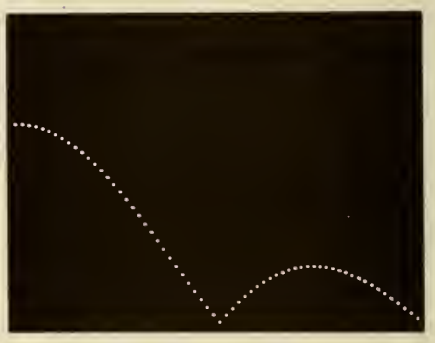

Figure 4-5. Spectrum Amplitude of a 4-Point Rectangular Pulse.

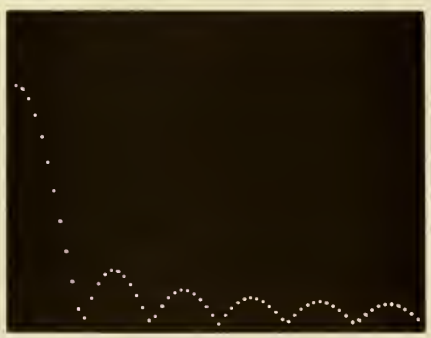

Figure 4-6. Spectrum Amplitude of a 12-Point Rectangular Pulse.

Figure 4-7. Spectrum Amplitude of a 32-Point Rectangular Pulse.

Figure 4-8. Spectrum Amplitude of a 96-Point Rectangular Pulse.

Figure 4-9. Spectrum Amplitude of a 40-Point Rectangular Pulse.

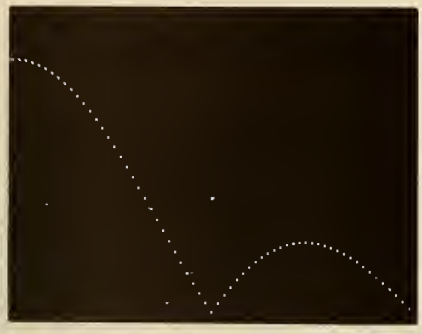

Figure 4-10. Spectrum Amplitude of a 4-Point Rectangular Pulse of Amplitude 3200 Units.

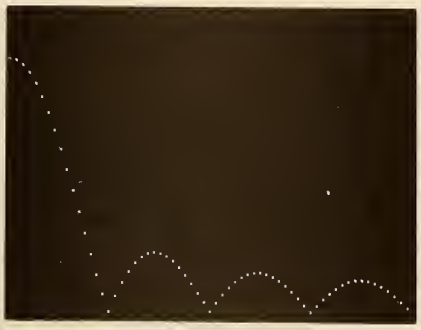

Figure 4-11. Spectrum Amplitude of an 8-Point Rectangular Pulse of Amplitude 1600 Units.

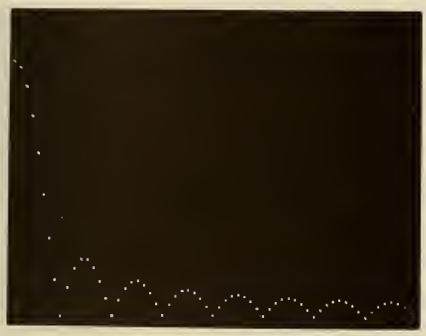

Figure 4-12. Spectrum Amplitude of a 16-Point Rectangular Pulse of Amplitude 800 Units.

Figure 4-13. Spectrum Amplitude of a 64-Point Rectangular Pulse.

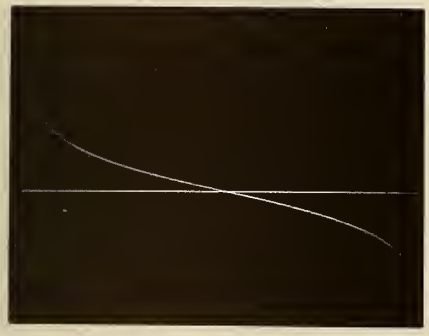

Figure 4-14. 512-Point Spectrum Amplitude of a 511-Point Rectangular Pulse in a 1024-Point Time Window.

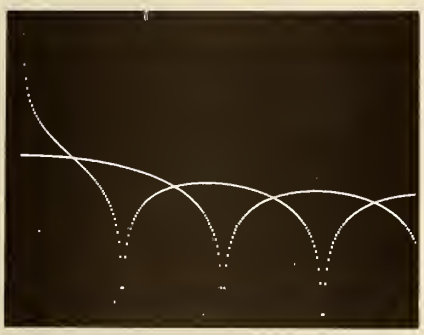

Figure 4-15. 512-Point Spectrum Amplitude of a 508-Point Rectangular Pulse in a 1024-Point Time Window.

Figure 4-16. 512-Point Spectrum Amplitude of a 493- or 531-Point Rectangular Pulse in a 1024-Point Time Window.

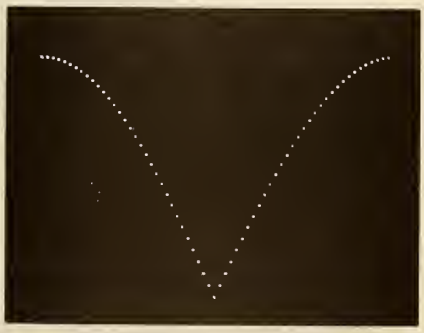

Figure 4-17. Spectrum Amplitude of an "Impulse" Pair. $V_{SD}(\Delta t) = V_{SD}(3\Delta t) = 1$.

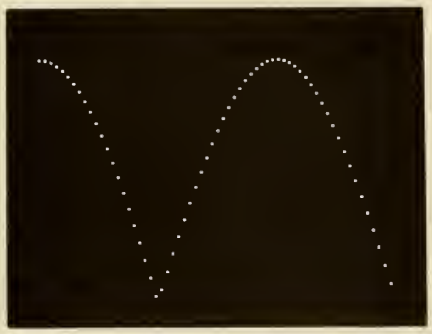

Figure 4-18. Spectrum Amplitude of an "Impulse" Pair. $V_{SD}(\Delta t) = V_{SD}(4\Delta t) = 1$.

Figure 4-20. Spectrum Amplitude of an "Impulse" Pair. $V_{SD}(\Delta t) = V_{SD}(65\Delta t) = 1$.

Figure 4-22. Spectrum Amplitude of Four 4-Point Rectangular Pulses Each Separated by $\tau/4$.

Figure 4-24. Spectrum Amplitude of Two 4-Point Rectangular Pulses Spaced by $\frac{63}{128}\tau$.

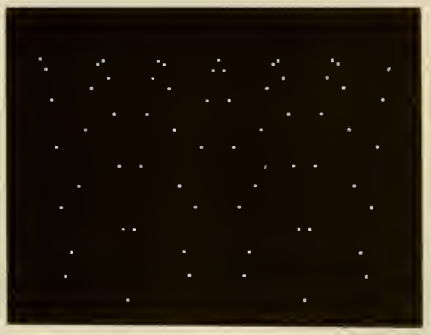

Figure 4-19. Spectrum Amplitude of an "Impulse" Pair. $V_{SD}(\Delta t) = V_{SD}(13\Delta t) = 1$.

Figure 4-21. Spectrum Amplitude of Two 4-Point Rectangular Pulses Separated by $\tau/2$.

Figure 4-23. Spectrum Amplitude of Eight 4-Point Rectangular Pulses Each Separated by $\tau/8$.

Figure 4-25. Spectrum Amplitude of Two 4-Point Rectangular Pulses Spaced by $\frac{62}{128}\tau$.

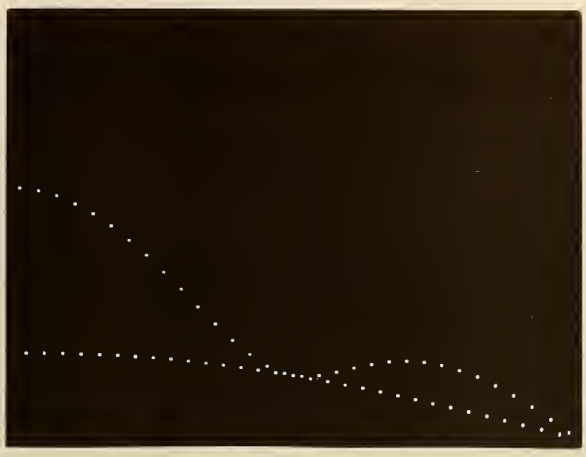

Figure 4-26. Spectrum Amplitude of a 4-Point and a 2-Point Rectangular Pulse Separated by $\tau/2$.

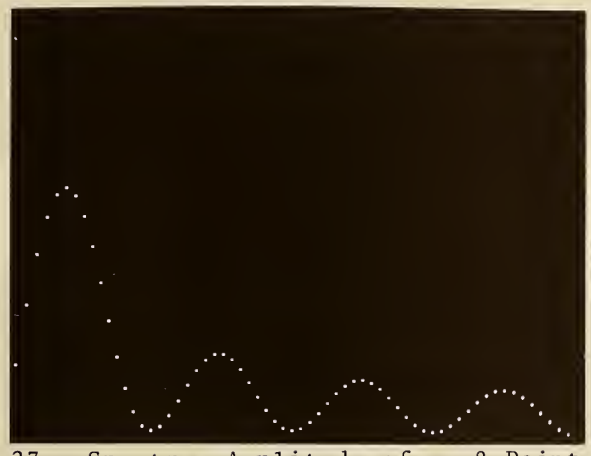

Figure 4-27. Spectrum Amplitude of an 8-Point Positive Rectangular Pulse Immediately Followed by an 8-Point Negative Rectangular Pulse of Equal Amplitude Magnitude.

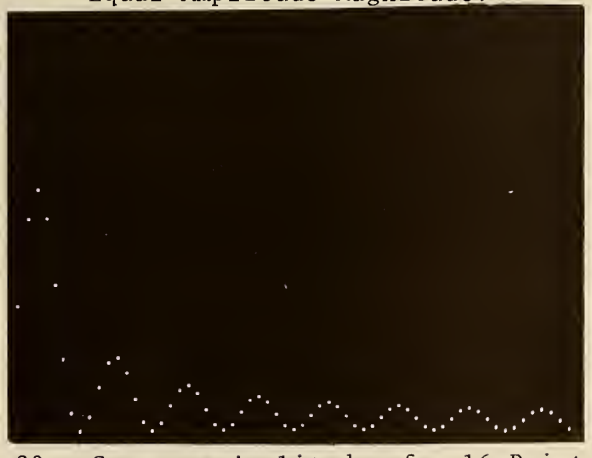

Figure 4-28. Spectrum Amplitude of a 16-Point Positive Rectangular Pulse Immediately Followed by a 16-Point Negative Rectangular Pulse of Equal Amplitude Magnitude.

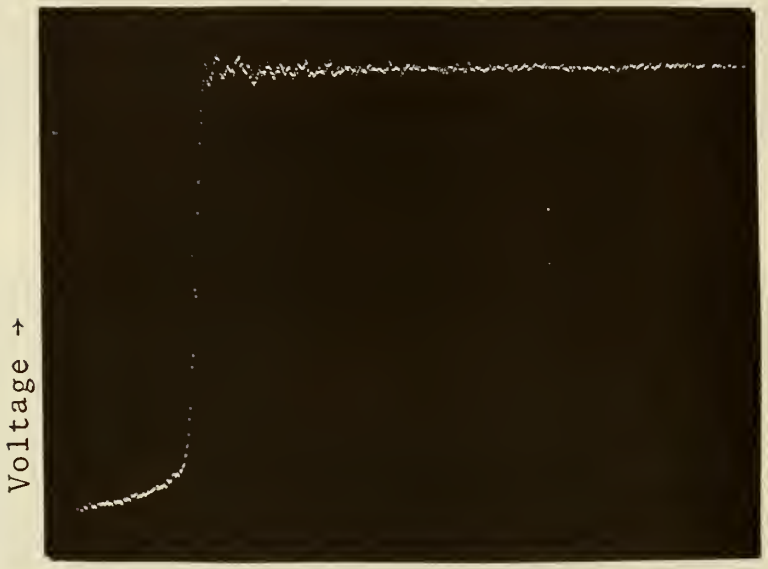

(a) Original Time Domain Waveform

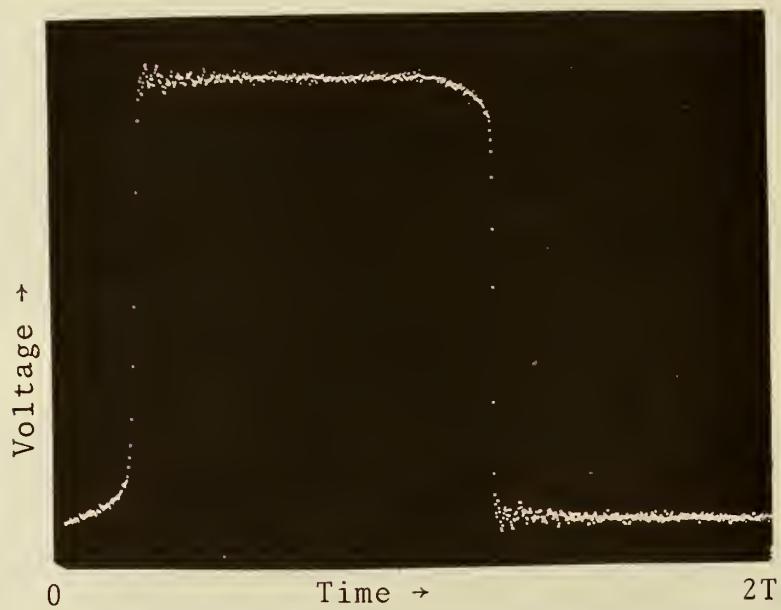

(b) Waveform After Application of Windowing Algorithm

Figure 4-29. Example of Windowing Algorithm Applied to a Step-Like Waveform.

5. TIME DOMAIN AUTOMATIC NETWORK ANALYZER

We have given the acronym, Time Domain Automatic Network Analyzer (TDANA), to the particular system that we have assembled to perform the pulse testing of RF and microwave components. The basic TDANA system, figure 5-1, consists of a fast transition time pulse generator, a wideband sampling oscilloscope, and a minicomputer. Figure 5-2 is a photograph of the actual system. The pulse generator is the exciting source that supplies spectral amplitude from dc to the microwave (GHz) region. The sampling oscilloscope is the receiver capable of operation over the same frequency range. The minicomputer performs two important functions. The first is data averaging to improve the system signal to noise (S/N) ratio. The second function is to transform the averaged time domain measurement data to the desired computed frequency domain data via the fast Fourier transform (FFT).

5.1 Pulse Generator

The pulse generator serves as the exciting source. In classical measurement methods frequency data is obtained on a point-by-point basis by stepping the frequency of a sine wave oscillator. A pulse generator, on the other hand, is theoretically capable of exciting an infinite series of frequencies simultaneously. All the frequencies generated are harmonically related to the fundamental repetition rate (f_o) of the generator. In actuality a practical upper frequency limit is always reached when the spectrum amplitude decreases below the system noise level.

For the TDANA some practical limitations are imposed upon the parameters of the input waveform. The sampler used in the TDANA has a specified dynamic range of ± 1 volt and a burnout level of ± 3 volts. Actually some compression of signals occurs at levels somewhat below the specified range of ± 1 volt [35]. Thus, to avoid compression, we have imposed an upper limit of ± 500 mV on signals applied to the sampler. The noise level of the sampler is typically 10 mV p.t.p., and thus for an adequate S/N ratio the pulse generator amplitude should lie in the range of 100 mV to 500 mV.

The pulse generator must also generate a stable pretrigger for the oscilloscope (∿ 75 ns in advance of the main pulse) or be capable of being triggered electronically with picosecond precision. Any time jitter between the trigger and main pulse serves to degrade the TDANA system performance [36].

The choice of a pulse generator depends upon the particular measurement to be undertaken. The major choices concern the 10%-90% transition time and waveshape. The transition time is inversely proportional to the upper frequency of interest. Thus MHz range measurements require ns transition times and GHz measurements call for ps transition times. The waveshape

choice usually boils down to (1) a step-like square wave pulse, (2) an impulsive signal, or (3) an RF burst. The RF burst is used when measurements are wanted only in a band of frequencies. The square wave carries considerable low frequency spectral amplitude and has a 1/f frequency roll-off. The impulsive signal has a flatter spectrum, but its spectral amplitude at low frequencies is less than for a square wave of equal amplitude.

Chapters 2, 3, and 4 discussed and showed examples of various pulse spectra. The guidelines discussed should be followed in the selection of the actual transition time and pulse duration used. The best TDANA measurement results are obtained when the pulse generator used has a "clean" waveform free from a lot of fine structure on the waveform. The pulse spectra should be band limited, i.e. the transition time should be just fast enough so that its spectra covers the band of interest. The transition time, t_r, should be $t_r > 4\Delta t$ where Δt is the sampling interval. This is necessary to reduce aliasing in the DFT and to obtain accurate repeatable measurements.

For transition times and durations greater than 1 ns, commercial generators are available which allow these parameters to be adjusted easily. For faster pulses, the available generators tend to have fixed-pulse parameters.

The very fastest generator used was a tunnel diode with a transition time on the order of 15 ps. This generator produces a step-like output of 250 mV amplitude into 50 ohms with a 50 ohm source impedance. Attempts to differentiate this step into an impulsive waveform usually result in a loss in amplitude and a slowing of the transition time. Thus for measurements into the X band region we are constrained to using a step-like signal. The tunnel diode generator was used for the attenuator measurements reported in Chapter 8.

Larger amplitude (several volts) step and impulsive signals in the 70 ps region can be generated using snap-off diodes. In the 500 ps region avalanche transistors are useful for generating 50 V pulses. Figure 5-3 through 5-6 show the measured pulses and calculated spectra of several different pulse generators.

Figure 5-3(a) is the leading edge transition of a commercial pulse generator. It produces a positive or negative pulse of adjustable amplitude up to ± 10 volts into 50 ohms. The 10%-90% transition time is 0.75 ns. The pulse duration is continuously adjustable from 1 ns to 100 ns. The pulse repetition rate is variable up to 1 MHz. This generator is typical of 1 ns generators in which the waveform can be adjusted. With the pulse duration set at 100 ns and a waveform time window of 10 ns, the waveform is step-like: Thus the square wave FFT program was used to calculate the spectral intensity, figure 5-3(b). The fundamental frequency is $f_o = 1/2T_w = 50$ MHz. The even harmonics are eliminated due to the square

wave symmetry. Harmonics at 150, 250, 350 MHz, etc. are plotted. The parameter plotted versus frequency is the spectral amplitude S(f) in volts-sec. S(f) follows closely that of the ideal truncated ramp, table 3-1, with useful spectral content up to 1 GHz.

Figure 5-4(a) is the leading edge transition of an NBS built snap-off diode pulse generator. The maximum pulse amplitude is +18 volts. The transition time is approximately 50 ps with 25% overshoot. The pulse duration is fixed at 20 ns. The repetition rate is crystal controlled from 200 Hz to 100 kHz in a 1-2-5 sequence. This waveform is also step-like. Its spectral amplitude S(f) is shown in figure 5-4(b). It is useful up to 10 GHz.

Figure 5-5(a) is the leading edge transition of the 15 ps tunnel diode pulse generator discussed earlier. Figure 5-5(b) shows that S(f) has a useful spectrum to above 30 GHz.

A very fast impulsive waveform may be obtained by differentiating the step transition from a snap-off diode. Figure 5-6(a) shows the resultant time domain waveform. The impulse amplitude is 4 volts, and the full width half amplitude (50%-50%) duration is 74 ps. Figure 5-6(b) is the calculated spectral amplitude. S(f) is essentially flat out to 6 GHz, and it is down by -20 dB at 10 GHz.

To directly compare the various pulse generators the spectra from figure 5-3 to 5-6 are plotted in dB v-ps versus log frequency on figure 5-7. The tunnel diode is seen to provide the smoothest S(f) over the frequency range of interest up to 12 GHz. It however also gives the lowest level spectral amplitude. An equalizing factor, however, is the ± 1 volt dynamic range of the TDANA sampler. The peak voltage of all the generators except the tunnel diode exceeds the 1 volt limit. Their outputs must be attenuated which shifts their spectra down as shown on figure 5-7.

5.2 Sampling Oscilloscope

An NBS modified commercial sampling oscilloscope is used in the TDANA. The oscilloscope consists of four modules. They are (1) a variable persistence storage CRT mainframe, (2) sequential sampling time base plug-in, (3) sampling vertical amplifier plug-in, and (4) remote sampling head.

The CRT mainframe furnishes power to the sampling plug-ins and houses a variable persistence storage CRT. Its dimensions are 22.1 cm x 42.5 cm x 46.7 cm, and it fits into a standard 48.3 cm (19 inch) rack panel.

The sequential sampling time base features equivalent sweep time ranges of 10 ps/cm to 500 μs/cm in a 1, 2, 5 sequence. It has two trigger inputs ($f < 1$ GHz, 1 GHz $< f <$ 4 GHz). For pulse triggering, its time jitter is specified at less than 10 ps on the 1 ns/cm range.

The sampling vertical amplifier plug-in is designed to operate with a remote sampling head. It features dual channel operation and deflection factors of 1 mV/cm to 200 mV/cm in a 1, 2, 5 sequence.

The remote sampling head contains two samplers. It has a risetime of 20 ps and a bandwidth of dc to 18 GHz. It is a 50 ohm feed-through coaxial sampler with APC-7 precision 7 mm connectors on the input and output. The dynamic range is ± 1 volt. The unsmoothed noise of the sampler is of the order of 10 mV p.t.p.

An NBS modification of this commercial sampling oscilloscope was necessary to interface it with the minicomputer. Analog amplifiers were added to provide Ch A, Ch B, and X output voltages to the minicomputer analog to digital (A/D) converter. An amplifier was also necessary to allow the minicomputer digital to analog (D/A) converter to drive the X axis in the time base. Considerable digital logic circuitry was also necessary to allow the computer and oscilloscope to communicate back and forth. Chapter 6 will describe in full detail the interface and oscilloscope modifications.

5.3 Minicomputer

The computational portions of the TDANA are shown in the block diagram, figure 5-8. It consists of a minicomputer and several peripherals. They include teleprinter, high speed paper tape punch and reader, floppy disc memory, an A/D with multiplexer, 3 D/A's, and a storage display CRT monitor.

The minicomputer is a general purpose computer system with a 16 bit word length. The machine is organized around four accumulators, two of which can be used as index registers. It is equipped with a programmer's console. Its maximum memory capacity is 32K words while our unit presently has 28K words. The full memory cycle time is 2.6 μs and it executes arithmetic and logical instructions in 1.35 μs. It mounts in a standard 48.3 cm (19 inches) rack. Its height is 26.7 cm (10.5 inches) and has sixteen plug-in slots available for memory and I/O interfaces. Not all slots are presently being used.

A standard electromechanical teleprinter is used. It operates at ten characters per second. Eight channel fanfold perforated paper tape is used with the high speed paper tape reader and punch. The reader operates photoelectrically at 300 characters per second. The punch can output at 63.3 characters per second.

The flexible disc memory greatly enhances the memory capacity of the TDANA. It features a direct access, removable disc. The disc is round, flat, and appears similar to a 45 rpm record. It is coated with a gray magnetic iron oxide material. The discs are inexpensive (< $10). The disc rotates at 375 rpm. Data may be retrieved at a rate of 250 kilobits/sec. The disc has a memory capacity of 2.2 megabits or 131K, 16 bit words.

The multiplexer, A/D, and D/A's are all housed in a separate unit called the data conversion system. They provide the analog connection with the outside world. The multiplexer allows up to eight analog input channels to be routed to the A/D converter.

The analog to digital (A/D) converter provides 14 bits or resolution (i.e. 1 part in 16,384). The nominal conversion time is 84 μs. This corresponds to a maximum conversion rate of 11.9 kHz. The sampling oscilloscope is capable of sampling at rates up to 100 kHz (higher input frequencies are counted down below 100 kHz). The maximum conversion rate of this A/D thus sets the maximum data acquisition rate of the TDANA. A faster (and more expensive) A/D would allow TDANA measurements to be performed in a shorter time, particularly when signal averaging of large numbers of waveforms is required.

The X sweep voltage for the sampling time base is furnished by a 14 bit digital to analog (D/A) converter. The D/A settling time to 1/2 least significant bit (LSB) is 5 μs. Two inexpensive NBS built D/A's are used to drive the CRT monitor. They have 10 bit resolution (1 part in 1024).

The display monitor features a bistable storage CRT. The screen is 8 cm x 10 cm. It is simply an X-Y monitor and must be supplied with X and Y voltages and Z unblanking and has a bandwidth of dc to 100 kHz. Problems have been encountered in this instrument with gain and position drift as functions of operating time and temperature. It is not recommended that this particular monitor be used in future TDANA's.

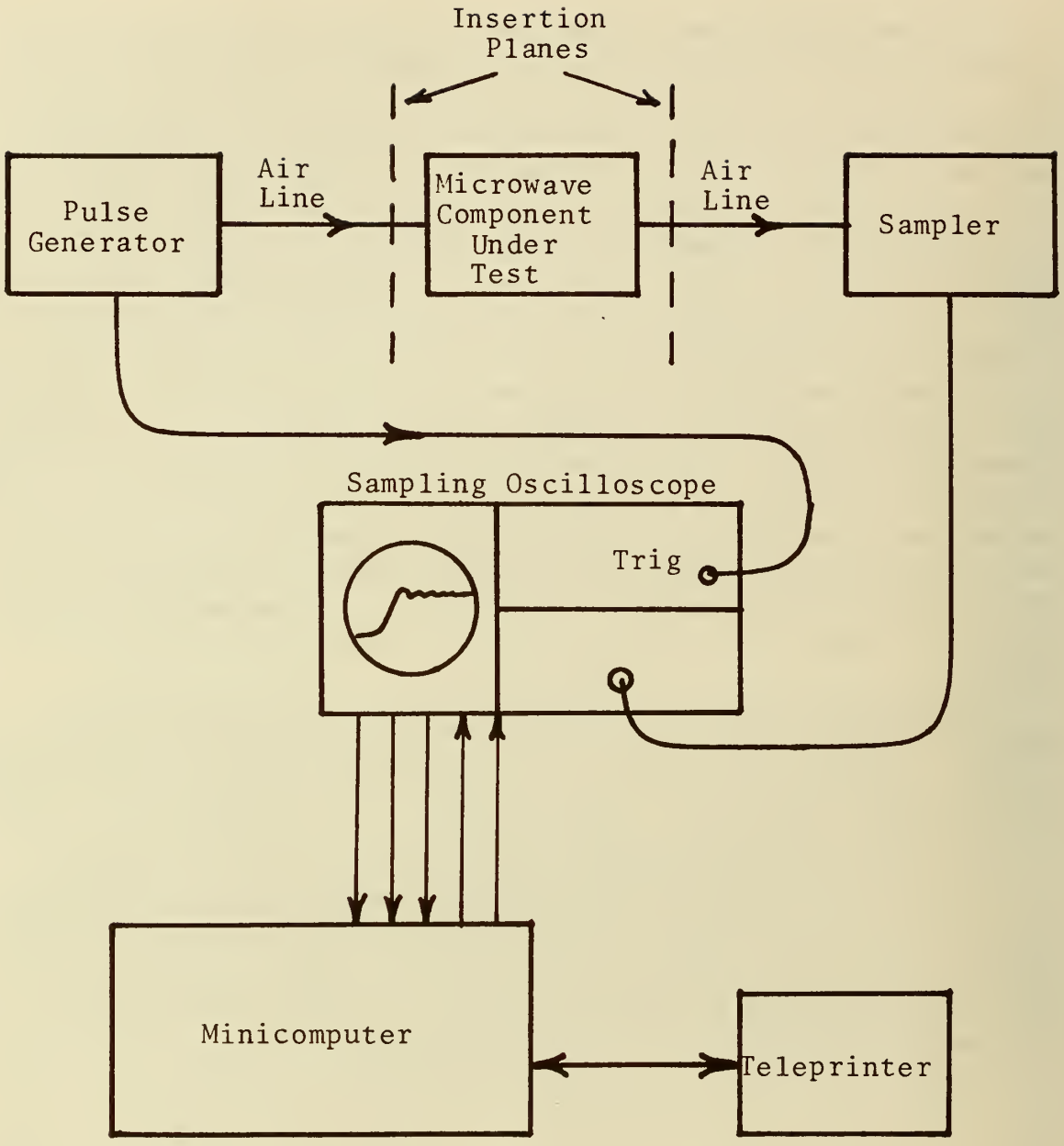

Figure 5-1. Time Domain Automatic Network Analyzer (TDANA) Basic Block Diagram.

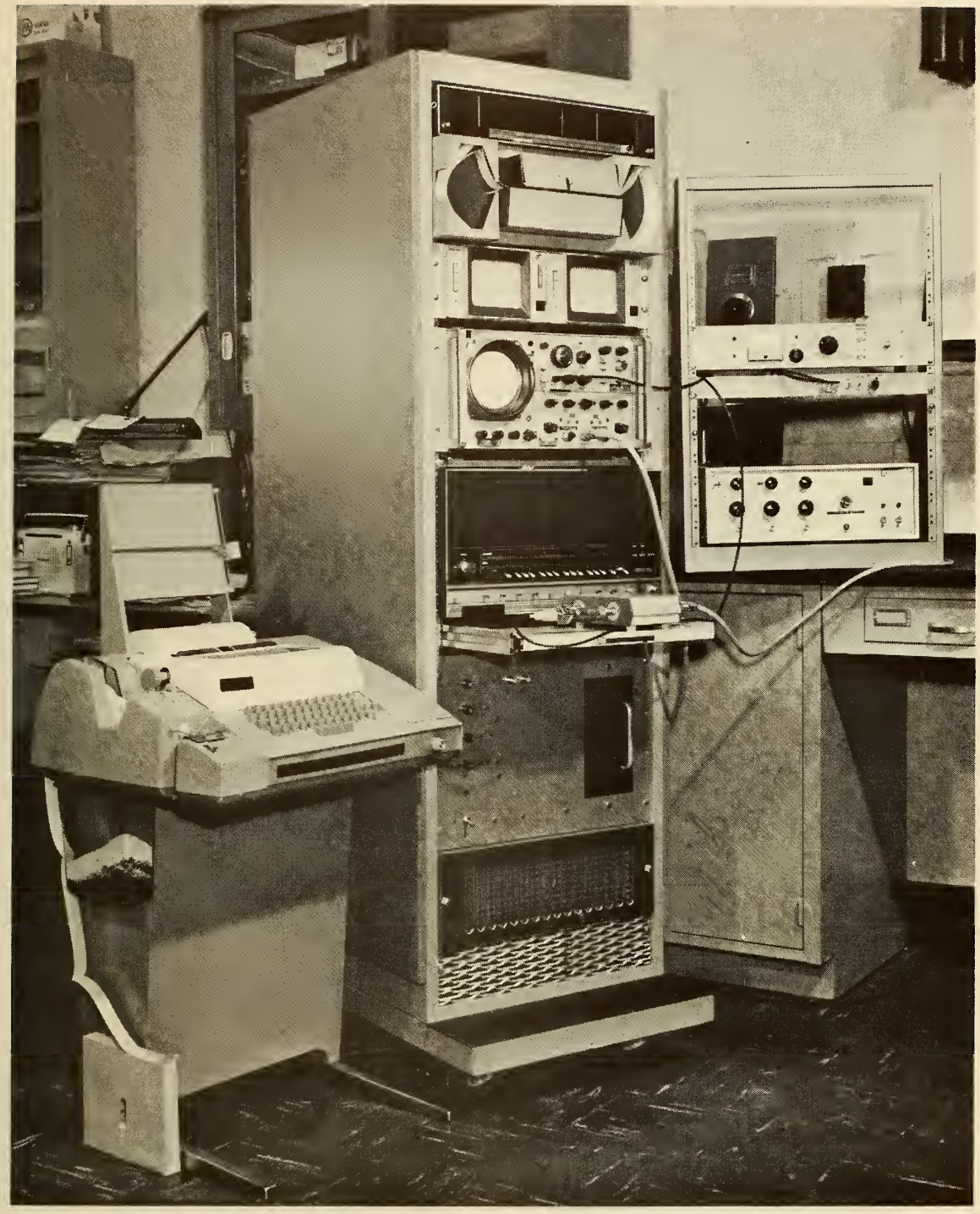

Figure 5-2. Photograph of Time Domain Automatic Network Analyzer (TDANA).

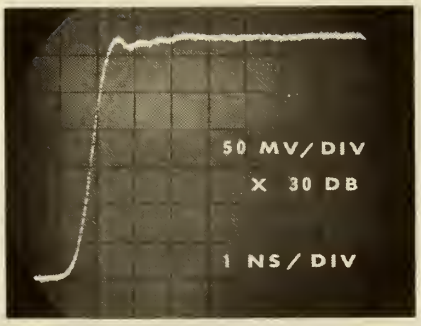

(a)

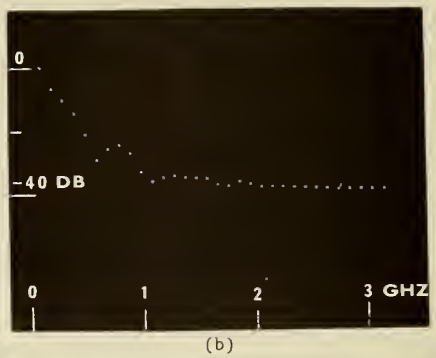

(b)

Figure 5-3. Commercial 1 ns Transition Time Pulse Generator Leading Edge Transition and Spectral Amplitude.

(a)

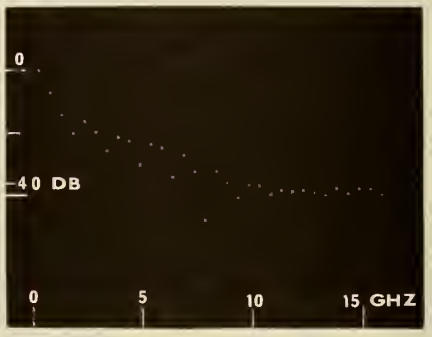

(b)

Figure 5-4. NBS Snap-Off Diode Pulse Generator Leading Edge Transition and Spectral Amplitude.

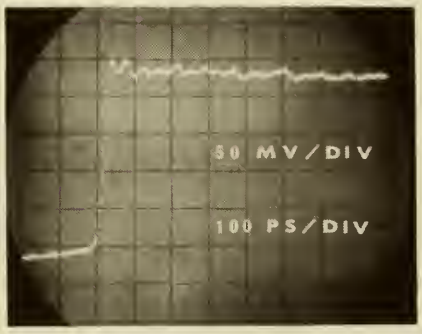

(a)

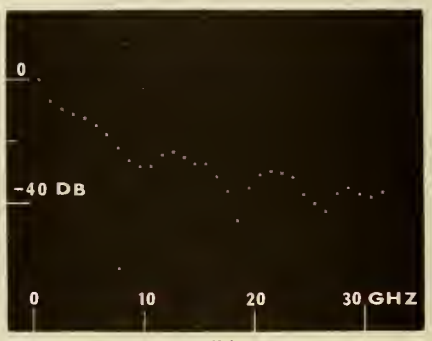

(b)

Figure 5-5. Ultrafast Tunnel Diode Pulse Generator Leading Edge Transition and Spectral Amplitude.

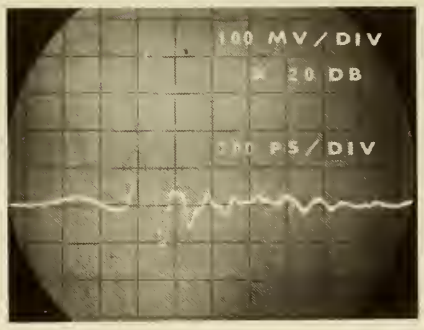

(a)

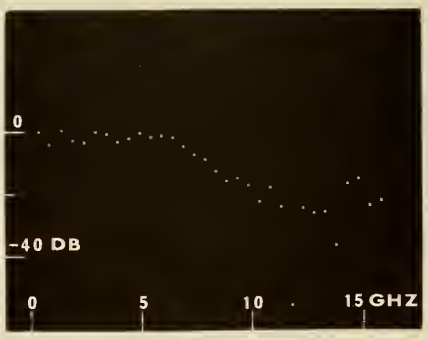

(b)

Figure 5-6. NBS Snap-Off Diode Impulse Generator Waveform and Spectral Amplitude.

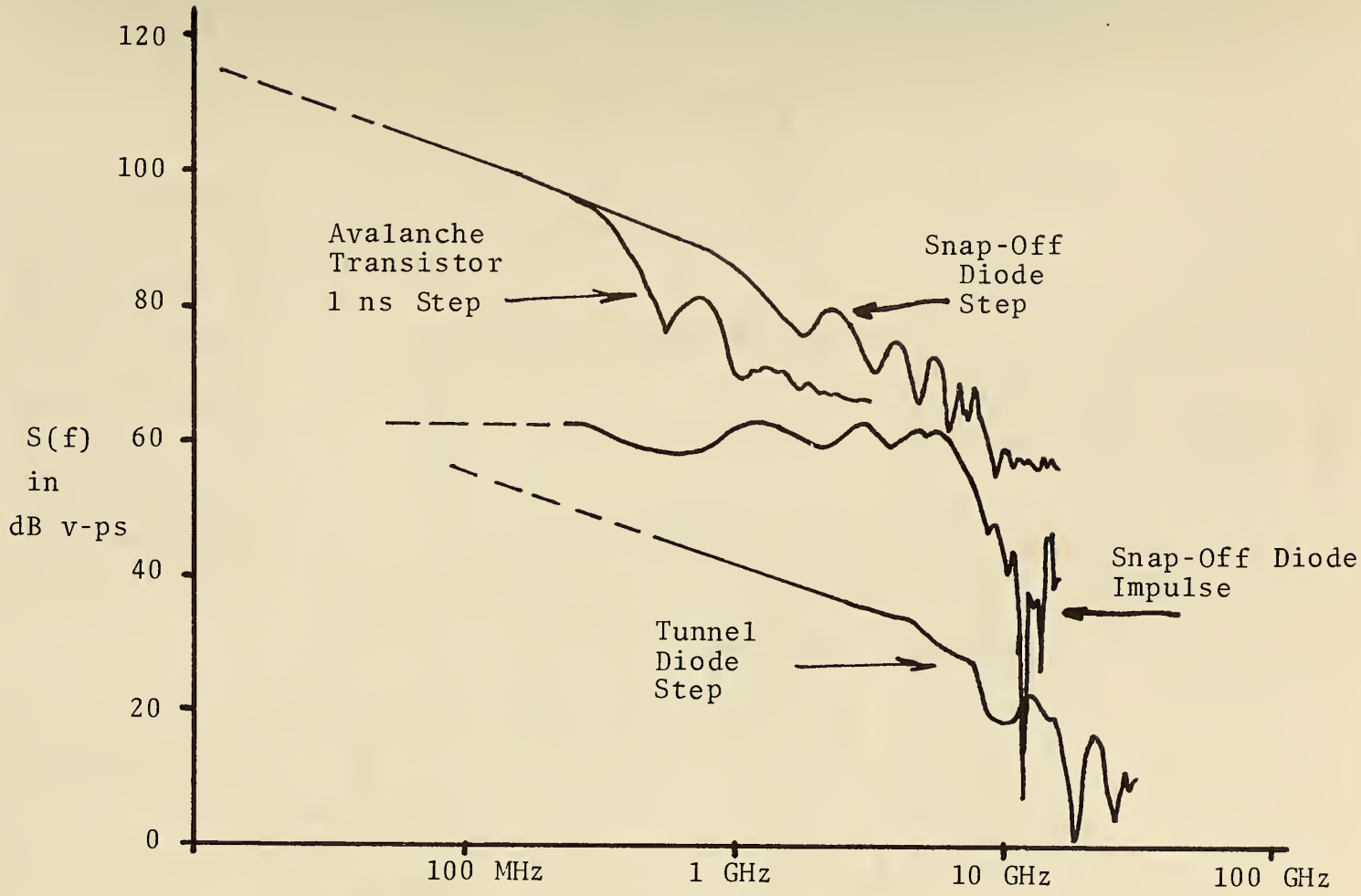

Figure 5-7. Spectral Amplitude S(f) for Various Pulse Generators as Measured on the TDANA.

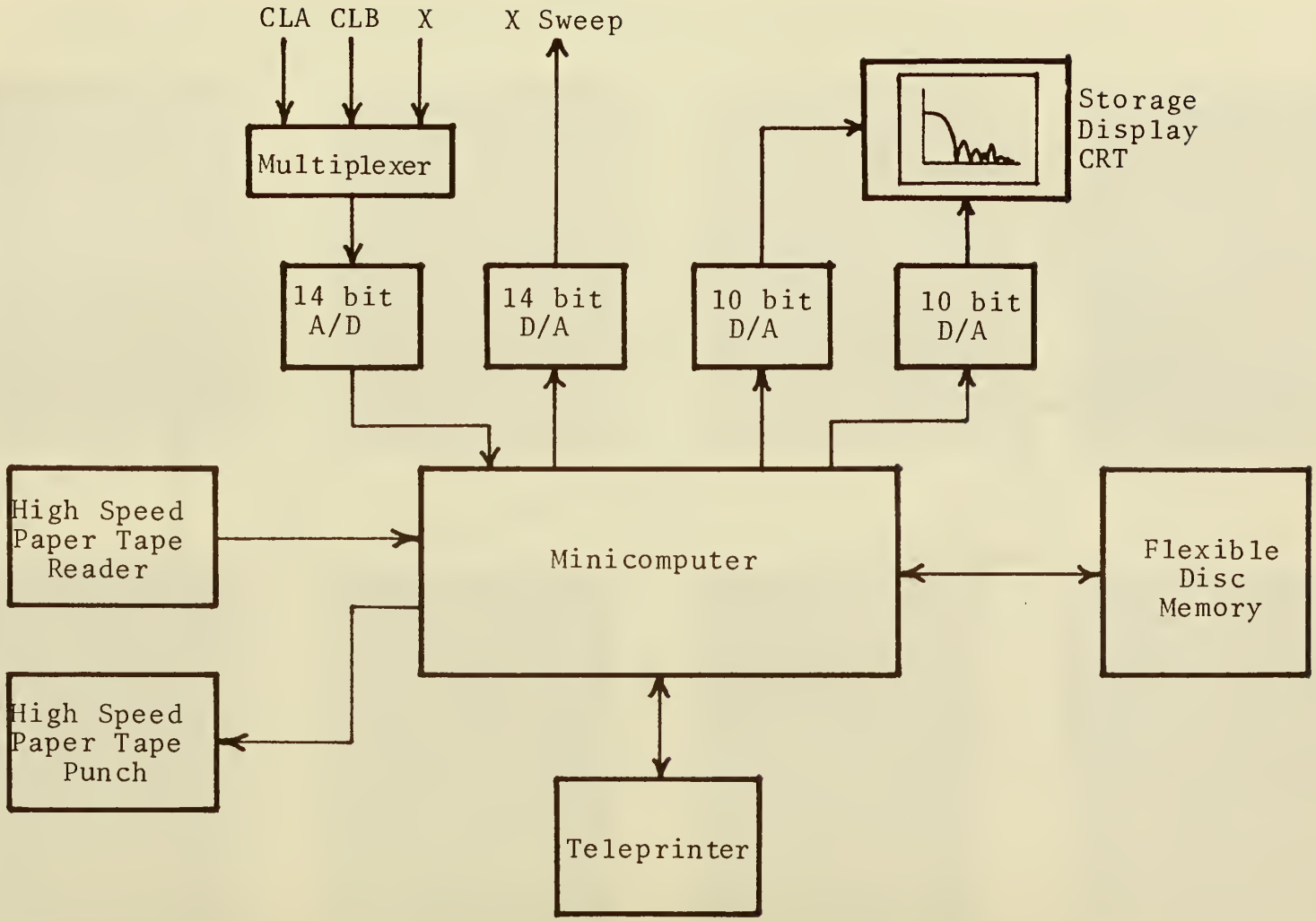

Figure 5-8. Block Diagram of TDANA Computer and Peripherals.

6. SAMPLING OSCILLOSCOPE/MINICOMPUTER INTERFACE

This chapter will describe in detail the NBS modifications and additional circuits added to the commercial sampling oscilloscope to interface it with the minicomputer. They include analog treatment of Ch A, Ch B, and X voltages along with external voltage control of the time base X position. Digital logic is also included for oscilloscope/computer communication.

6.1 Analog Interface

The major analog interface requirements are the voltage range of 0 V to +5 V for the A/D input and the D/A output, corresponding to 10 cm deflection vertically and horizontally, respectively. These voltage ranges do not exist in the oscilloscope exactly. Thus amplifiers are needed. The amplifiers must not affect the operation of the existing circuits to which they are connected.

Figures 6-1 and 6-2 are the schematics of the analog interface. There are four nearly identical circuits for the Ch A data out, Ch B data out, X data out, and the X sweep in. Only Ch A is discussed as an example.

The desired Ch A sampled data voltage is found in the sampling vertical amplifier plug-in at the dc amplifier output of the channel A stretcher loop. The voltage at this point varies from -1.8 V to +1.8 V corresponding to deflection at the bottom or top of the CRT screen (0.36 V/cm). To obtain 0 V to +5.0 V a gain of +1.38 and a dc shift of 2.5 V is required. The 531 fast slew rate, operational amplifier provides the necessary gain. The gain is fixed by the resistor ratio $(R_1+R_2)/R_1$. The dc shift, V_{os}, is obtained by lifting the bottom leg of R_1 by a fixed dc potential V_{dc}. V_{os} is fixed by the resistor ratio, $V_{os} = -(R_2/R_1)V_{dc}$. V_{dc} is provided by the 741 operational amplifier. DC power is obtained from the supply voltages already present in the plug-in.

The analog interface components are mounted on a single circuit board, figure 6-3, that is mounted in unused space in the top half of the sampling vertical amplifier, figure 6-4. The analog signals to and from the minicomputer's A/D and D/A are transmitted over twisted pair cables. A single 14 pin connector, J10, is installed on the back panel of the oscilloscope mainframe. All analog and digital signals to and from the computer pass through J10, figure 6-5, and the plug-in connectors J1 and J2, figure 6-6. The analog signals from J10 to the analog interface are passed through unused pins on the mainframe/vertical plug-in interconnect J1/P1, figure 6-7. The X analog voltages to and from the analog interface and the sampling time base are passed through the sampling vertical/horizontal plug-in interconnect P3/J3, figures 6-7 and 6-8. The digital control signals are routed from J10 through J2 and P2 to the time base plug-in, figure 6-8. The digital interface is described in the next section.

6.2 Sampling Oscilloscope/Minicomputer Digital Interface Controller

A digital interface controller is required between the sampling oscilloscope and the minicomputer to assure proper operation of both units and to eliminate the possibility of computer acquisition of invalid data. This is necessary due to the asynchronous nature of the operation of the two instruments.

In normal operation the sampling oscilloscope is triggered externally by the pulse generator in use. The oscilloscope can be triggered and will take a sample at each trigger at rates up to 100 kHz. For higher trigger repetition rates, the trigger circuitry locks out many trigger pulses and only admits one every 10 μs or greater (i.e., $f_{sample} \leq 100$ kHz). For trigger frequencies at VHF or higher, the trigger circuitry divides (or counts down) the input to a lower phase-locked frequency.

The computer has its own internal clock. As the computer cycles through its program listing, it will from time to time request data input from the analog to digital converter (A/D). In addition, under program control it will change the X sweep voltage output of the digital to analog converter (D/A). These data requests and sweep voltage changes are governed only by the computer clock and the program. Triggering and sampling events in the sampling oscilloscope occur completely independently.

The digital interface controller is designed with the following features:

1. Permit asynchronous or synchronous operation.
2. Oscilloscope mode of operation is determined by the setting of the SCANNING switch on the time base front panel. In EXT position the oscilloscope is operated under computer control with the X axis swept by the 14 bit D/A. In NORMAL or SINGLE (sweep) the oscilloscope operates normally with all computer functions locked out.
3. In EXT (computer controlled) operation, the oscilloscope CRT displays only the valid data acquired by the computer.
4. If the computer intertie cable is disconnected from the oscilloscope (J10 open), the oscilloscope functions normally.
5. All possible error conditions are guarded against. If an error is detected, the sampled data is discarded and not sent to the A/D nor the CRT.

The controller is required to furnish one digital control signal to the computer; namely, Y DATA CONVERT. When this control signal goes high to the "one" state the 14 bit A/D starts the conversion of the analog voltage on its input if it has previously been armed by the computer (DOA = 1). The computer supplies two digital control signals to the controller. The first is EOC. EOC goes high to a "one" when the A/D is triggered by the Y DATA.

CONVERT pulse. It remains high during the conversion and resets to "zero" at the end of the conversion. The other control signal is the X DATA XFER. It is a negative going pulse (1 to 0 to 1) that is a command from the computer to the 14 bit D/A storage register to load the new X data present on the digital data bus. This causes a change in the X sweep voltage supplied to the time base.

The error conditions that must be guarded against are many. They are:

1. The oscilloscope functions as a sample and hold circuit for the A/D. Thus, the Y sampled data output cannot be changed during the A/D conversion cycle (i.e. when EOC = 1).
2. Adequate time must be given for a new sampled data value to settle to its final value before the A/D is triggered.
3. Adequate time must be given for the X sweep voltage to settle to its final value after an X DATA XFER pulse. The oscilloscope should be prevented from sampling during this time interval.
4. The oscilloscope should not be reenabled during the timing ramp run-up portion of the trigger cycle.
5. Sampled data taken immediately (< 3 μs) after the reenabling of the oscilloscope is subject to timing errors.
6. Slivering must be avoided. Slivering is the unintentional generation of narrow (< 20 ns) digital pulses due to transition crossings of asynchronous signals. Sliver pulses could cause the controller to pass invalid sampled data.
7. If the X sweep voltage changes during a timing ramp run-up invalid sampled data will result.

Figure 6-9 is the schematic diagram for the digital interface controller. Fourteen TTL integrated circuits are used. They are mounted on a single plug-in circuit card, figure 6-10, positioned vertically in the rear of the sampling time base plug-in, figure 6-11.

The basic function of the controller is to furnish a Y DATA CONVERT pulse when the sampling head has taken a new piece of data that is valid. A 1.5 μs monostable, IC 208 (lower right -- figure 6-9) produces this pulse. A pulse labeled SAMPLED is derived from the time base circuitry at the instant the sampling head is strobed. The SAMPLED pulse is routed (bottom horizontal wire -- figure 6-9) through several control and delay IC's (IC 209-2,* IC 205-1, IC 206-12, and IC 207-6) to IC 208. The leading edge is differentiated and inverted by IC 209-2. This pulse is then delayed

*The nomenclature used for IC identication is the first three digits refer to the particular IC package while the last digit is the particular output pin number.

150 ns by monostable IC 205. This delay is necessary to prevent slivering when the pulse is passed through the alternate gated path of IC 211-6, IC 211-8, and IC 204-8. IC 206-12 is another control gate. Monostable IC 207 provides 3.5 μs delay to compensate for the Y sampled data settling time.

The EOC signal (upper left -- figure 6-9) is used as the CRT BLANKING signal (upper horizontal wire -- figure 6-9). EOC is routed through several buffers and control gates IC 202-3, IC 203-2, IC 202-6, IC 202-8, and IC 203-6. Only during A/D conversion (EOC = 1) is the CRT unblanked (BLANKING = 0). Flip-flop IC 201-5 is set by the leading edge of EOC. The X DATA XFER pulse resets this flip-flop. If the X sweep voltage is changed during the A/D conversion then the resetting of the flip-flop blanks the CRT via blanking control AND gate IC 202-6.

Once an A/D conversion has commenced the sampling oscilloscope must be disabled to prevent it from taking a new sample. This is accomplished by clamping the timing ramp with the LOCKOUT (=1) signal (upper right -- figure 6-9). LOCKOUT is obtained from EOC via IC 202-3, IC 213-12, IC 202-11, and IC 213-6.

The LOCKOUT function is enabled also when other error conditions are present. When the X sweep voltage is changing LOCKOUT is set to a "1" with the X DATA XFER via IC 203-12, IC 211-3, IC 212-1, and into the OR gate IC 213-12. Monostable IC 212 provides a 5 μs pulse to allow for the X sweep voltage settling time.

Flip-flop IC 201-8 is included in the LOCKOUT circuitry to prevent multiple sampling at the same time position. The flip-flop is set by the leading edge of EOC. It is cleared 5 μs after the occurence of the X DATA XFER pulse. When the flip-flop is set ($\overline{Q}$ = 0) the LOCKOUT signal is held in the "1" state via OR gate IC 213-12. If the programmer desires several samples at the same X location, he must reload that X location after each A/D conversion. This feature eliminates the accidental acquisition of several data points without updating the X position. It also eliminates LOCKOUT slivering that might occur if the X DATA XFER pulse occurs near the end of EOC.

Flip-flop IC 204-6 is included to extend the length of the LOCKOUT if the above described circuitry attempts to reenable (set LOCKOUT to "0") the timing ramp during the portion of the trigger cycle when the timing ramp is triggered (allowed to run-up). A signal, called TRG'D, is derived from the time base that is high during the first half of the trigger cycle when the timing ramp is triggered. As long as TRG'D is high, the timing ramp would start its run-up whenever it is unclamped (LOCKOUT = "0"). IC 204-6 is a D-type edge-triggered flip-flop. The data (D input) is the

state of the TRG'D signal. This data is toggled into the flip-flop by the positive going edge of the output of IC 202-11. If TRG'D is a "1" then $\overline{Q}$ is set to a "0" thus holding the LOCKOUT in the "1" state via OR gate IC 213-6. The flip-flop is cleared on the trailing edge transition of TRG'D, thus setting LOCKOUT to "0."

Timing errors can occur if the oscilloscope is triggered immediately after the LOCKOUT resets to "0." This is due to charge storage effects in the timing ramp clamp transistor Q14, figure 6-12. The timing ramp is not clamped during this time and thus the sampling head can be strobed to take new data. This new data will be invalid. To prevent an A/D conversion of invalid data the AND gate IC 206-12 is used to prevent the generation of a Y DATA CONVERT pulse. To allow for complete charge depletion in Q14, a 3 μs interval after LOCKOUT reset is declared the invalid data interval. A signal called LOCKOUT + 3 μs is generated to cover this interval. The LOCKOUT signal is stretched 3 μs by monostable IC 214 and the OR gate IC 213-8. $\overline{\text{LOCKOUT + 3 μs}}$ is applied to AND gate IC 206-12. In addition, flip-flop IC 204-8, OR gate IC 211-6, and the AND gate IC 211-8 are used to determine if the oscilloscope has been triggered (TRG'D goes high) or a sample has been taken (SAMPLED goes high) during the time interval of LOCKOUT + 3 μs. If either condition occurs, flip-flop IC 204-8 is set ($\overline{Q}$ = "0") thus disabling AND gate IC 206-12. The flip-flop is reset on the trailing edge transition of TRG'D.

Differentiator IC 210-4 and buffer IC 210-6 are used to generate an internal trigger pulse for the time base at the end of the LOCKOUT + 3 μs interval. This pulse is used when the operator desires synchronous operation of the sampling oscilloscope and the minicomputer. The time base SYNC pulse output is then used to trigger an external pulse generator.

The SCANNING switch input (upper right -- figure 6-9) is used to disable the BLANKING, LOCKOUT, and Y DATA CONVERT pulses in normal or single sweep operation. This is accomplished by the gates IC 202-8, IC 202-11, and IC 207-5.

The digital interface controller requires regulated +5 V dc power. This is not available in the oscilloscope. To obtain this an additional supply was installed. A 6.3 V ac filament transformer was installed in the mainframe. The 6.3 V ac voltage was routed to the horizontal plug-in through two pins on J2 designated for that purpose. A bridge rectifier, filter capacitor, and voltage regulator were mounted on the bottom plate of the time base plug-in.

It was necessary to modify some of the circuitry in the horizontal plug-in. The major modifications were on the time base circuit board A4, figure 6-12. These provided the TRG'D and SAMPLED signals and the timing ramp LOCKOUT function.

The timing ramp, TP4, is generated by a capacitor on the time/cm switch being charged by a current source. The current source is the +250 V supply and the 24 KΩ resistor A9R9. The timing capacitor is initially clamped to ground by the RAMP GATE transistor Q3. When the time base is triggered, tunnel diode CR2 turns off Q3 thus allowing the timing ramp, TP4, to start its run-up.

A transistor, Q13, is added to the circuit by connecting it to the base of Q3. When Q3 is turned off, Q13 is turned off simultaneously. The positive going TRG'D pulse is generated at the collector of Q13. Halfway through the trigger cycle CR2 is reset thus turning Q3 on and resetting the timing ramp to zero volts. This also turns on Q13 thus setting TRG'D back to "0."

The ramp lockout function is added by simply connecting an additional ramp gate transistor Q14 to TP4. Q14 is driven by the LOCKOUT signal. When LOCKOUT is a "1," Q14 is turned on clamping the timing ramp to zero volts regardless of the state of Q3.

Q4 is the COMPARATOR. It compares the timing ramp voltage to a dc voltage. The dc voltage is the staircase generator output in NORMAL operation or the X sweep voltage from the D/A in EXT operation. When the ramp voltage exceeds the dc voltage, the SAMPLING TRIGGER GENERATOR, Q5-Q6, is activated producing the SAMPLING COMMAND TRIGGER that is sent to the sampling head via the vertical amplifier plug-in. This positive going pulse is also used as the SAMPLED pulse. It is obtained simply by adding a 1.5 KΩ resistor. The resistor attenuates the large pulse and reduces the loading on the existing circuit.

Figure 6-13 shows the modifications made to the wiring of the SCANNER switch. Figure 6-14 is the simple modification to the horizontal amplifier circuit board A7 to obtain an X voltage for the X data out amplifier in the analog interface.

Figure 6-15 is the modification to the marker, magnifier and blanking circuit board A6 to provide blanking from the digital interface controller. The BLANKING AMPLIFIER, Q11, functions as an RTL OR gate. It normally has three inputs, pins J, H, and E. If any one of these is high, then Q11 is turned on blanking the CRT. An additional input, pin B, has been added for the controller BLANKING signal.

An additional modification of the sampling time base plug-in has been made for operator convenience. The SYNC PULSE DELAY is normally an internal adjustment. In experimental measurement setups, many times one needs to adjust this control. Therefore it was moved to the front panel according to figure 6-16. The control occupies the hole formerly used by the BNC EXT SWEEP INPUT that was removed (see figure 6-14).

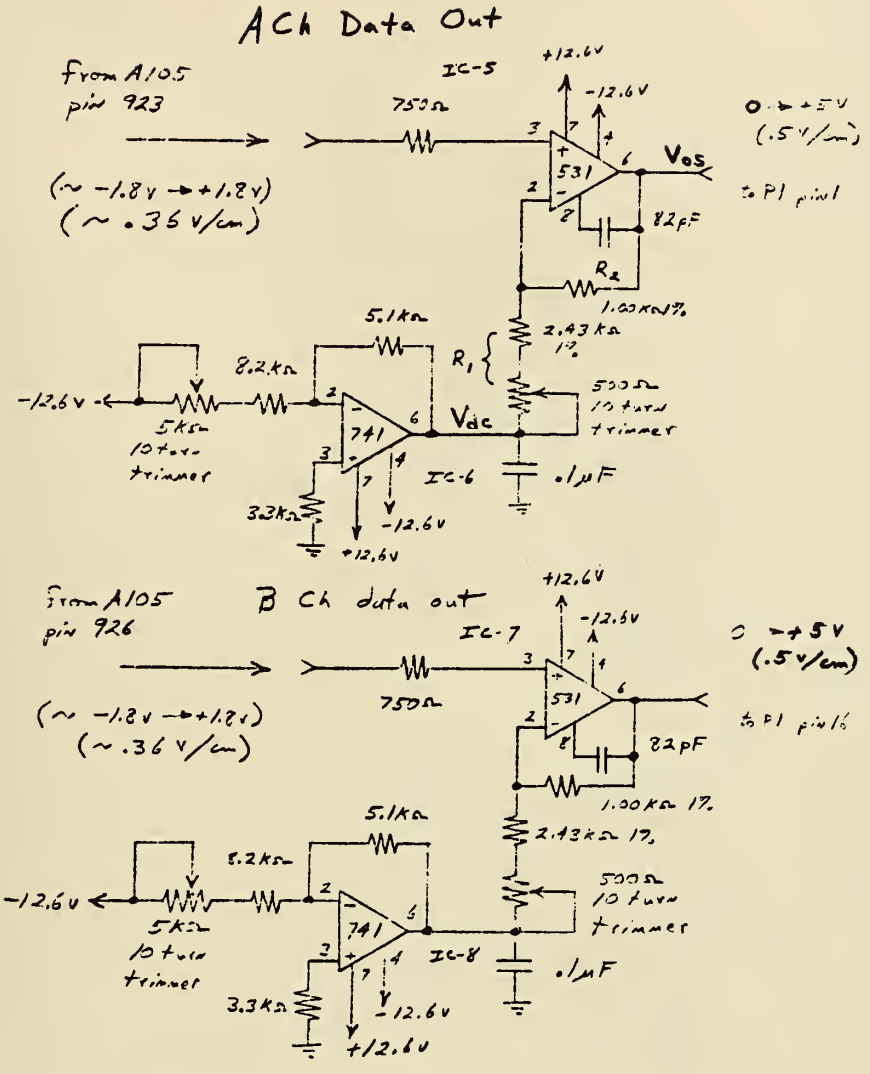

Figure 6-1. Analog Interface Amplifiers for CLA and CLB Sampled Data Output.

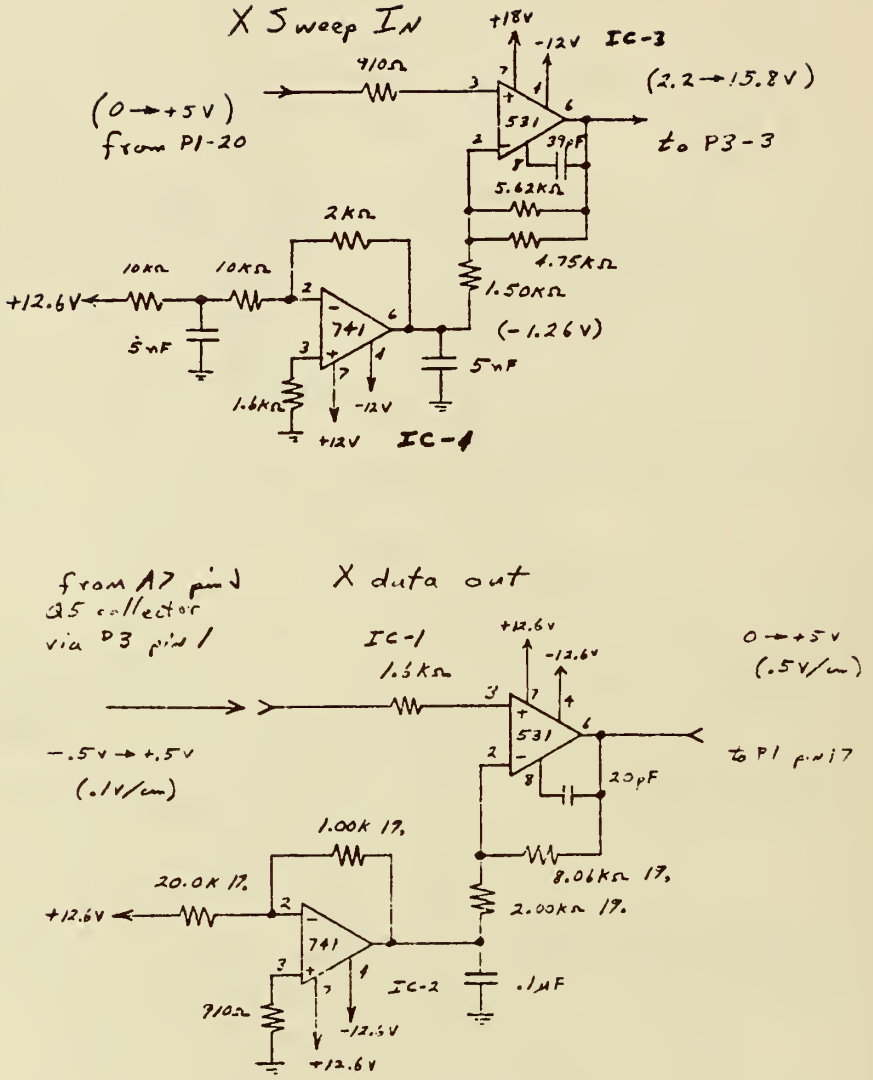

Figure 6-2. Analog Interface Amplifiers for X Data Output and X Sweep Input.

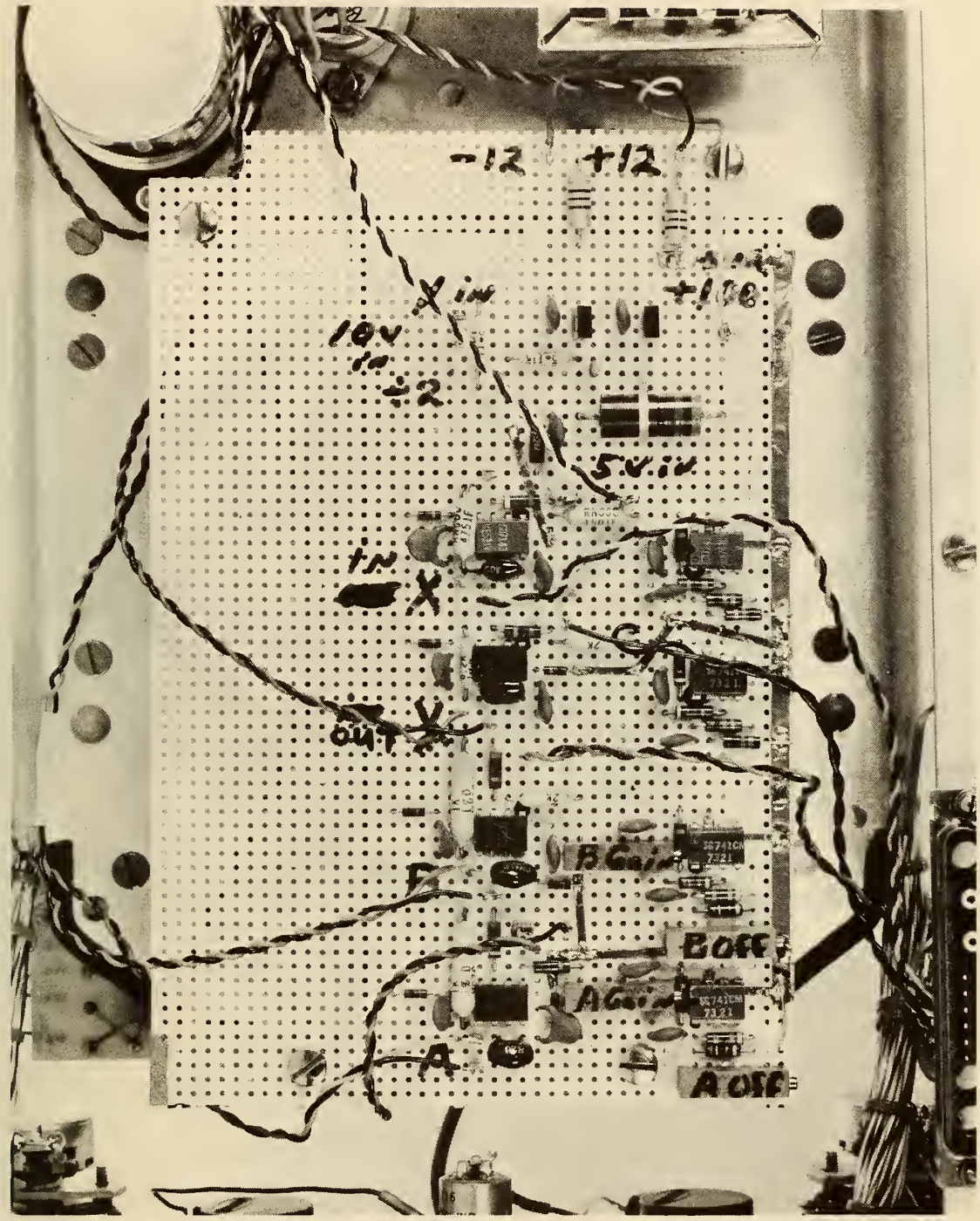

Figure 6-3. Analog Interface Circuit Card Mounted in Sampling Vertical Amplifier Plug-In Unit.

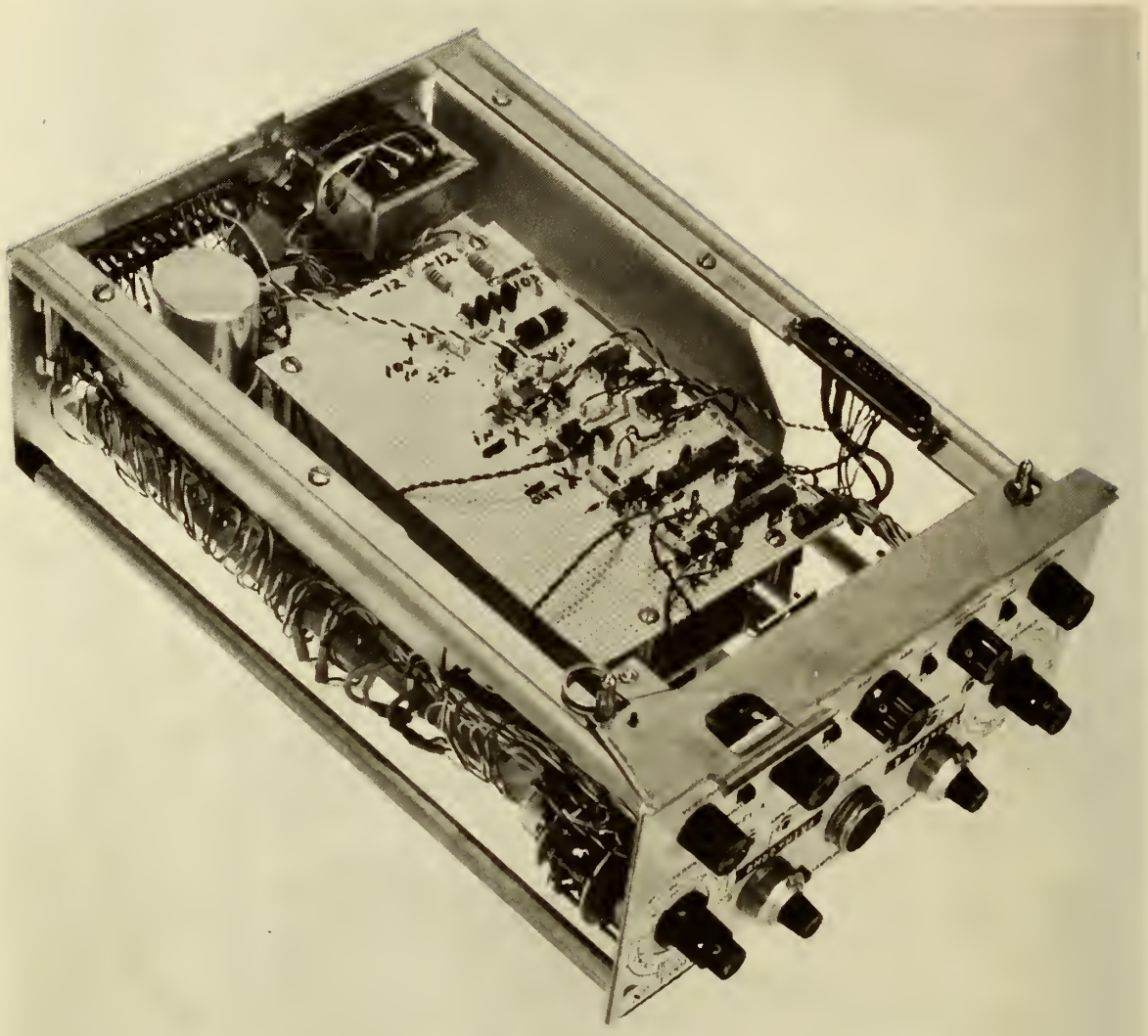

Figure 6-4. Sampling Vertical Amplifier Plug-In Unit Showing Position of Analog Interface Circuit Card.

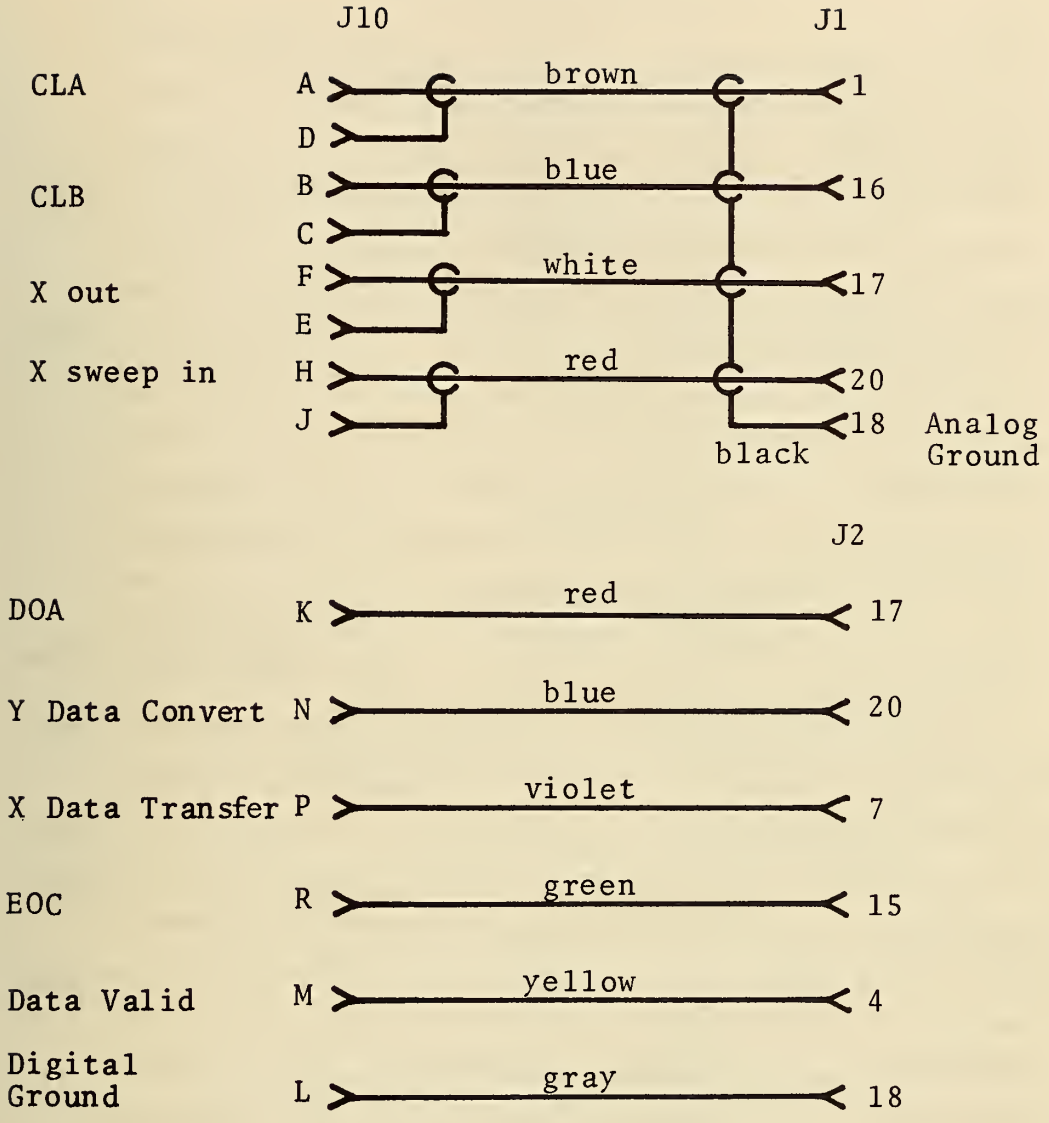

Figure 6-5. Oscilloscope Rear Panel Interface Connector J10.

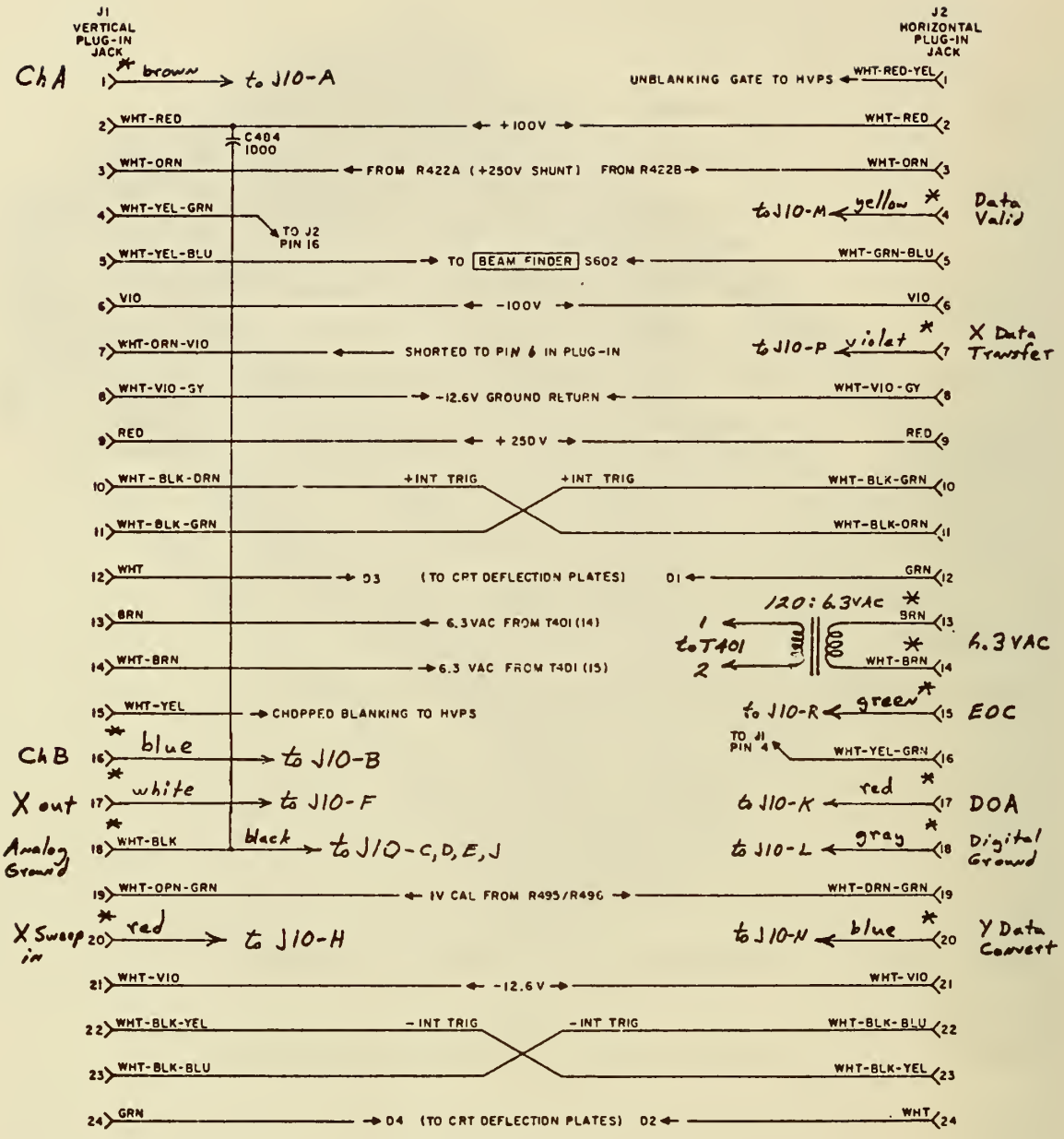

Figure 6-6. Oscilloscope Main Frame/Plug-In Jack Connections. Starred Pin Numbers Have Modified Connections from the Original Factory Wiring.

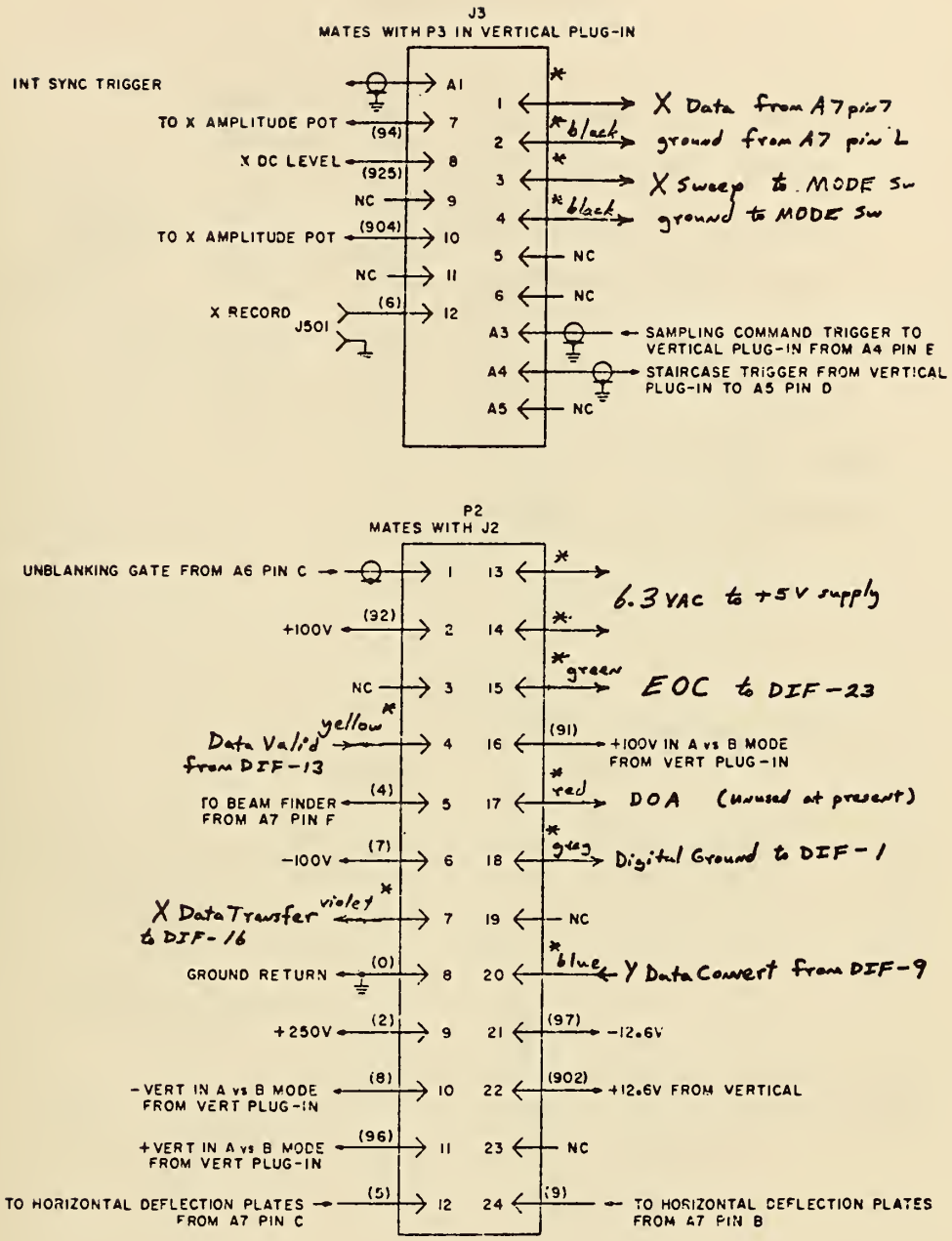

Figure 6-7. Sampling Vertical Amplifier Plug-In Plug P2 and Jack J3 Connections.

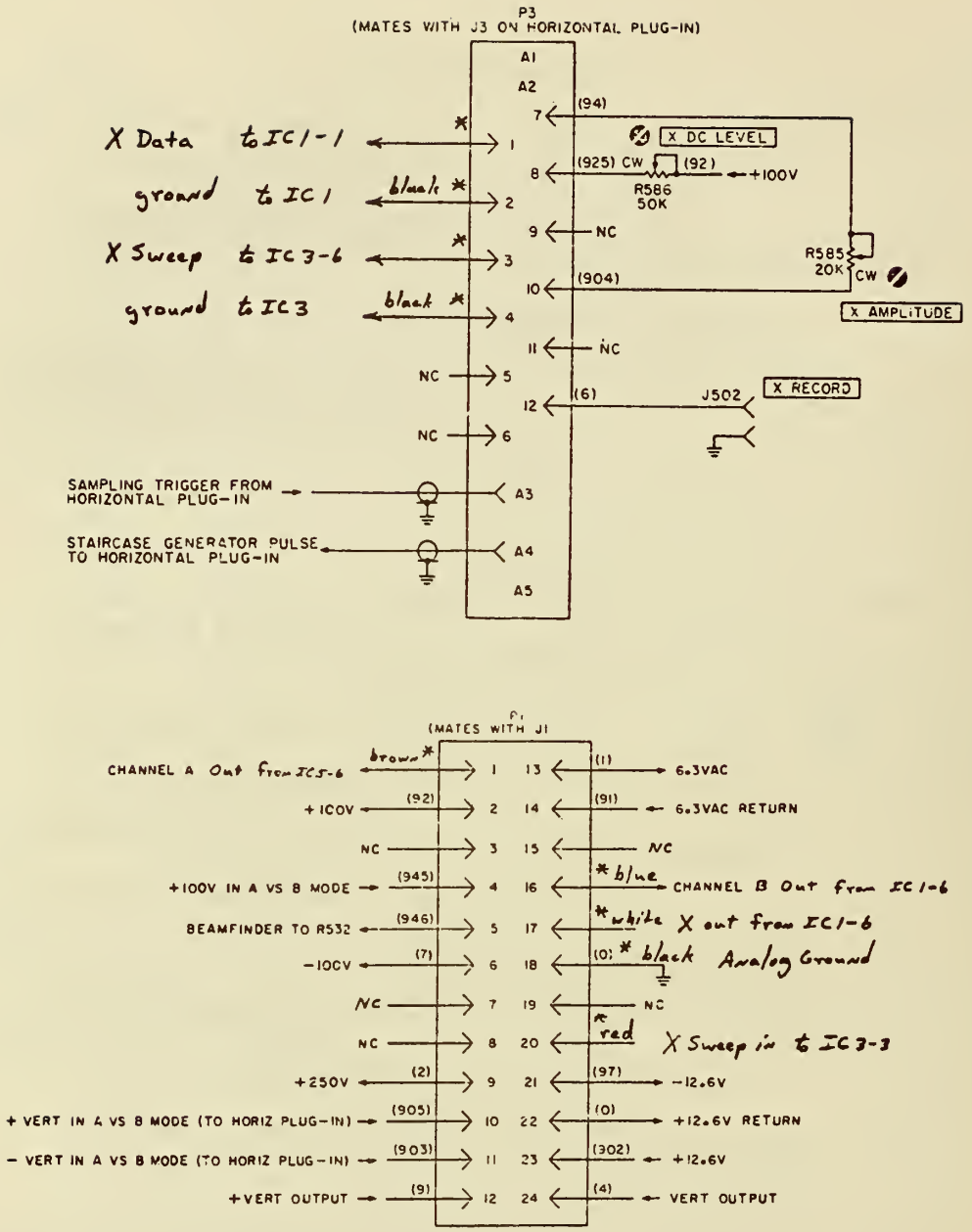

Figure 6-8. Sequential Sampling Time Base Plug-In Plugs P1 and P3 Connections.

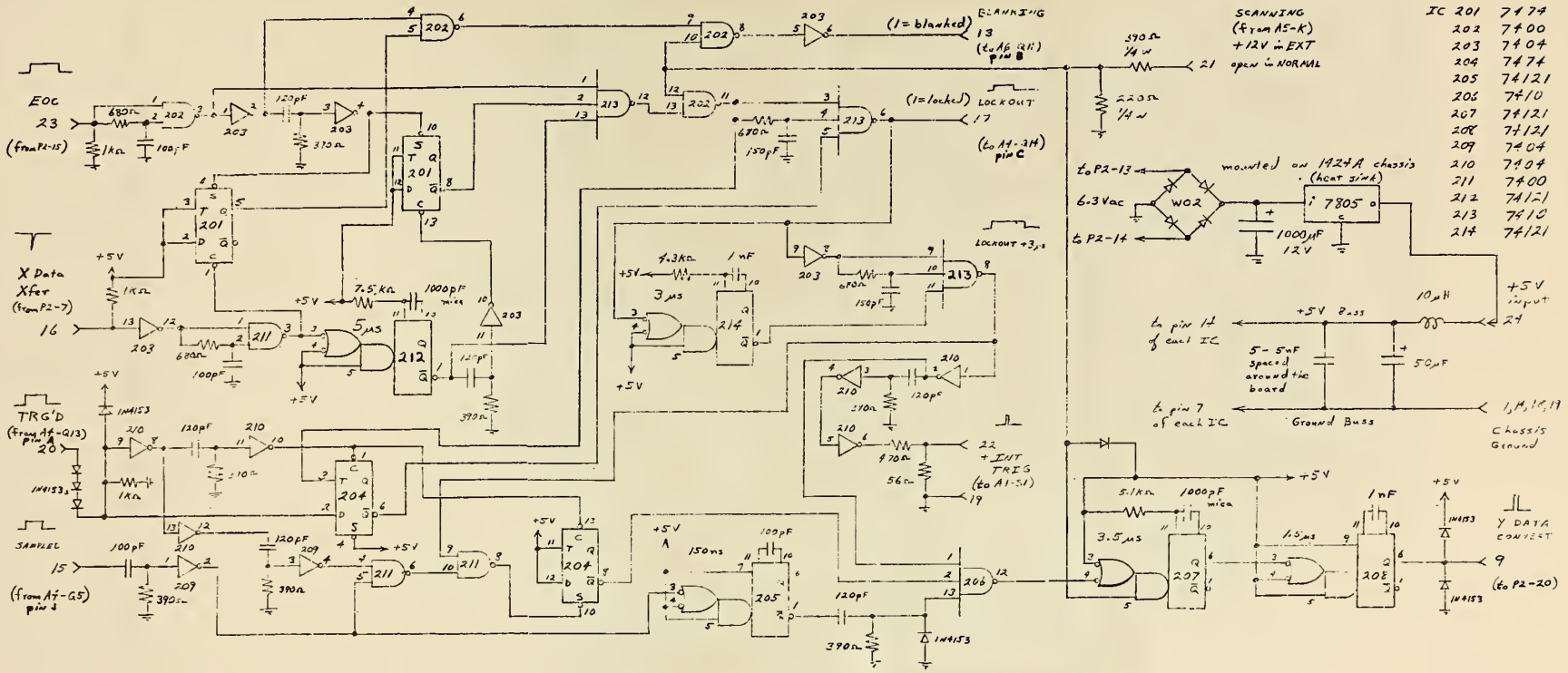

Figure 6-9. Sampling Oscilloscope/Minicomputer Digital Interface (DIF) Schematic Diagram.

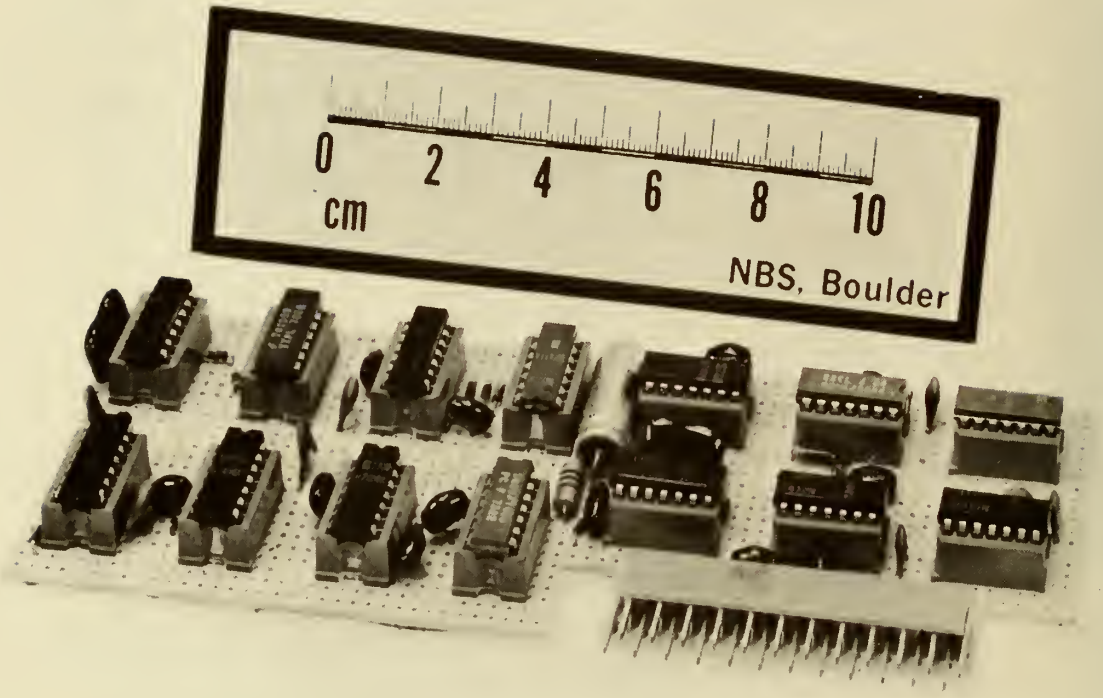

Figure 6-10. Digital Interface Circuit Card.

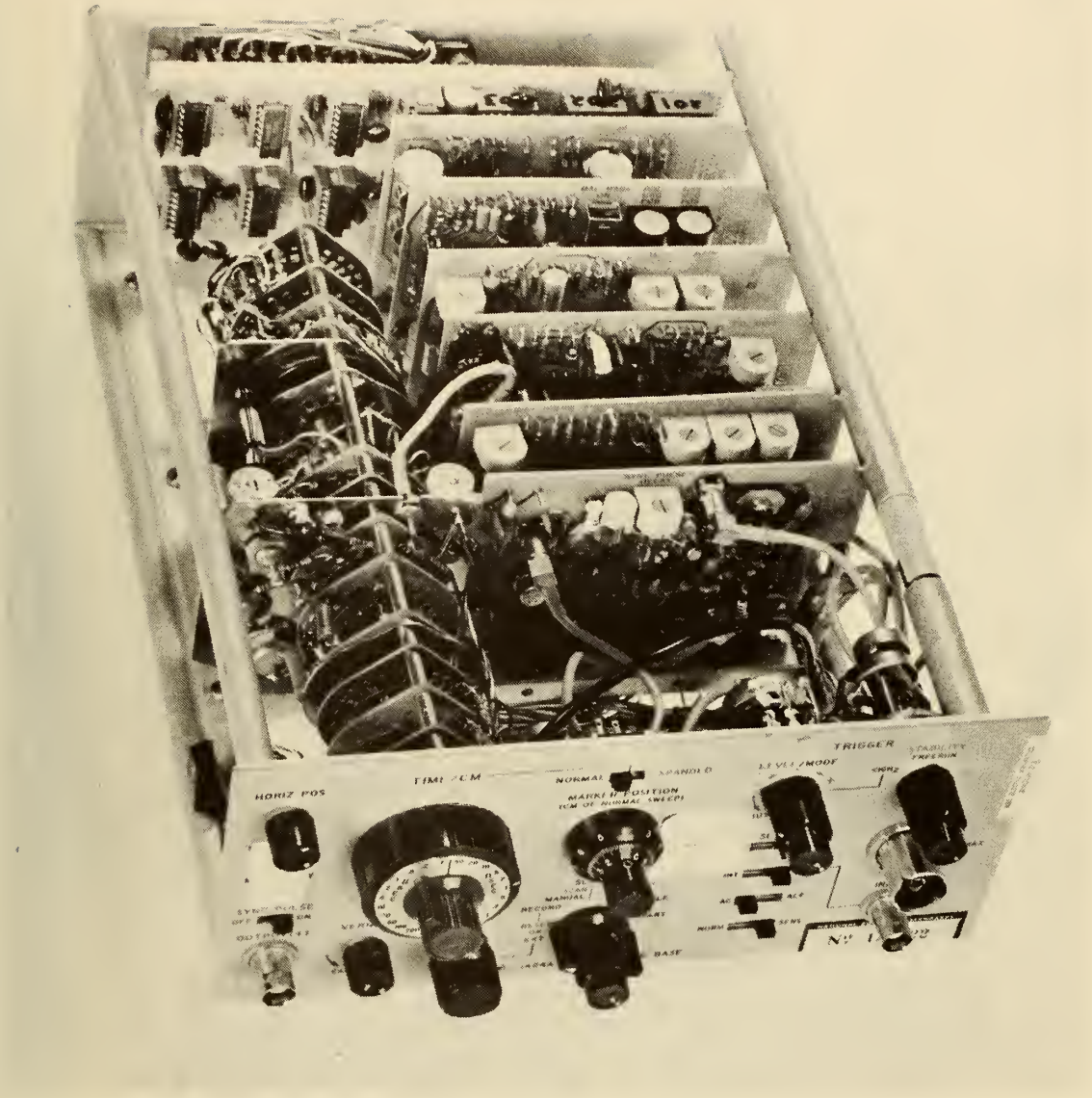

Figure 6-11. Sampling Time Base Plug-In Showing Position of Digital Interface Circuit Card.

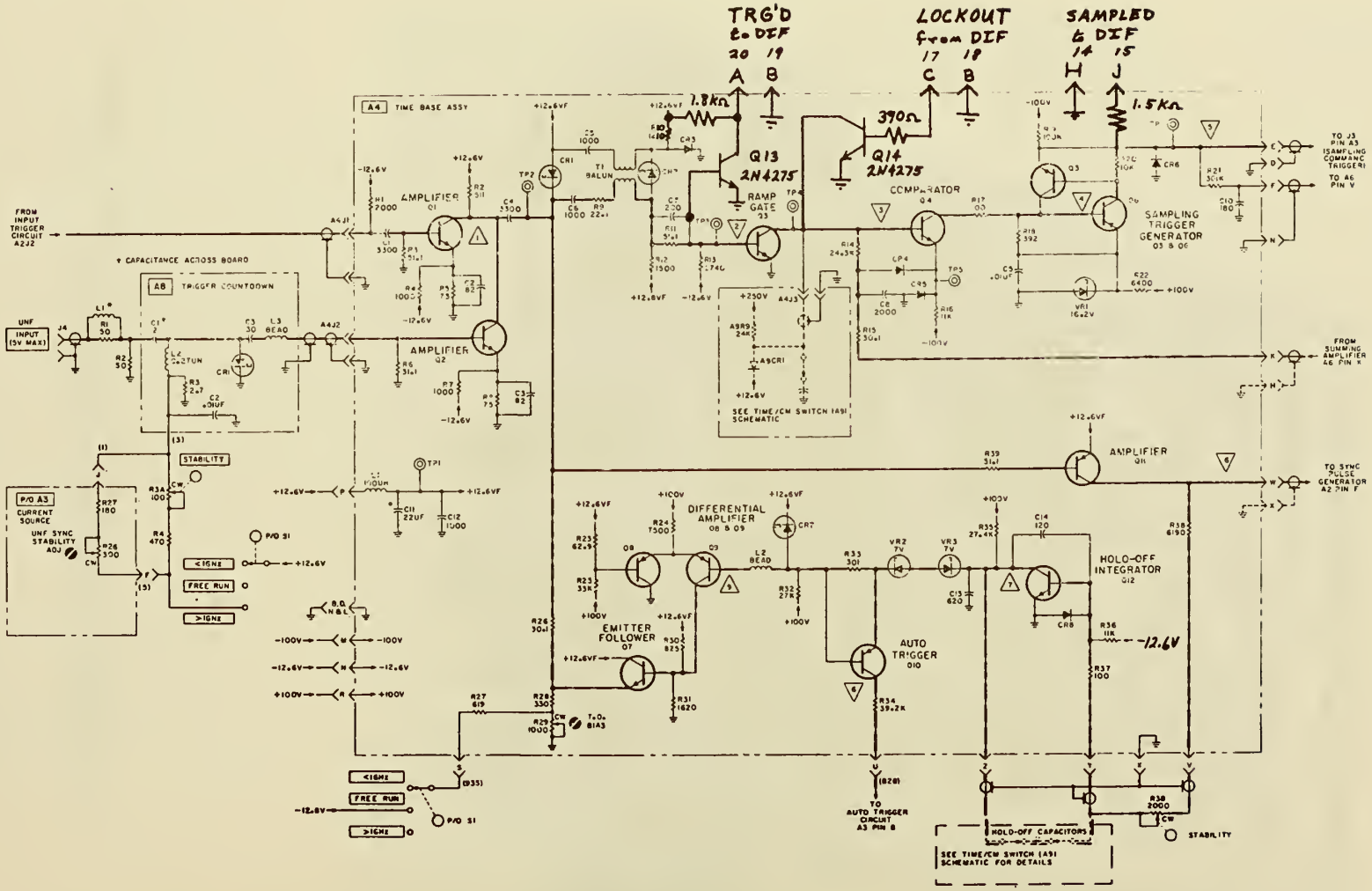

Figure 6-12. A4 Time Base Card Modifications.

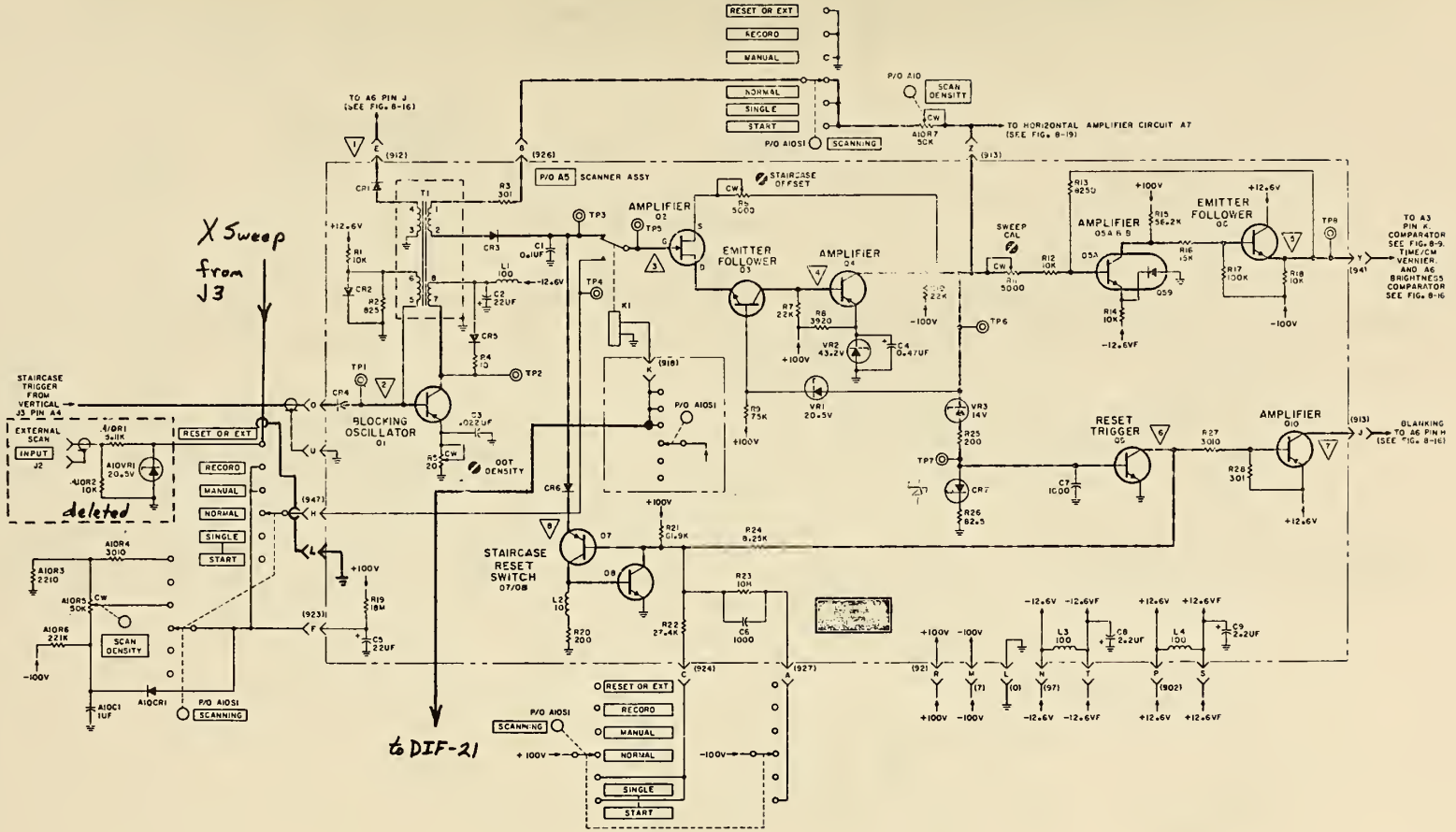

Figure 6-13. Scanner Switch Modifications.

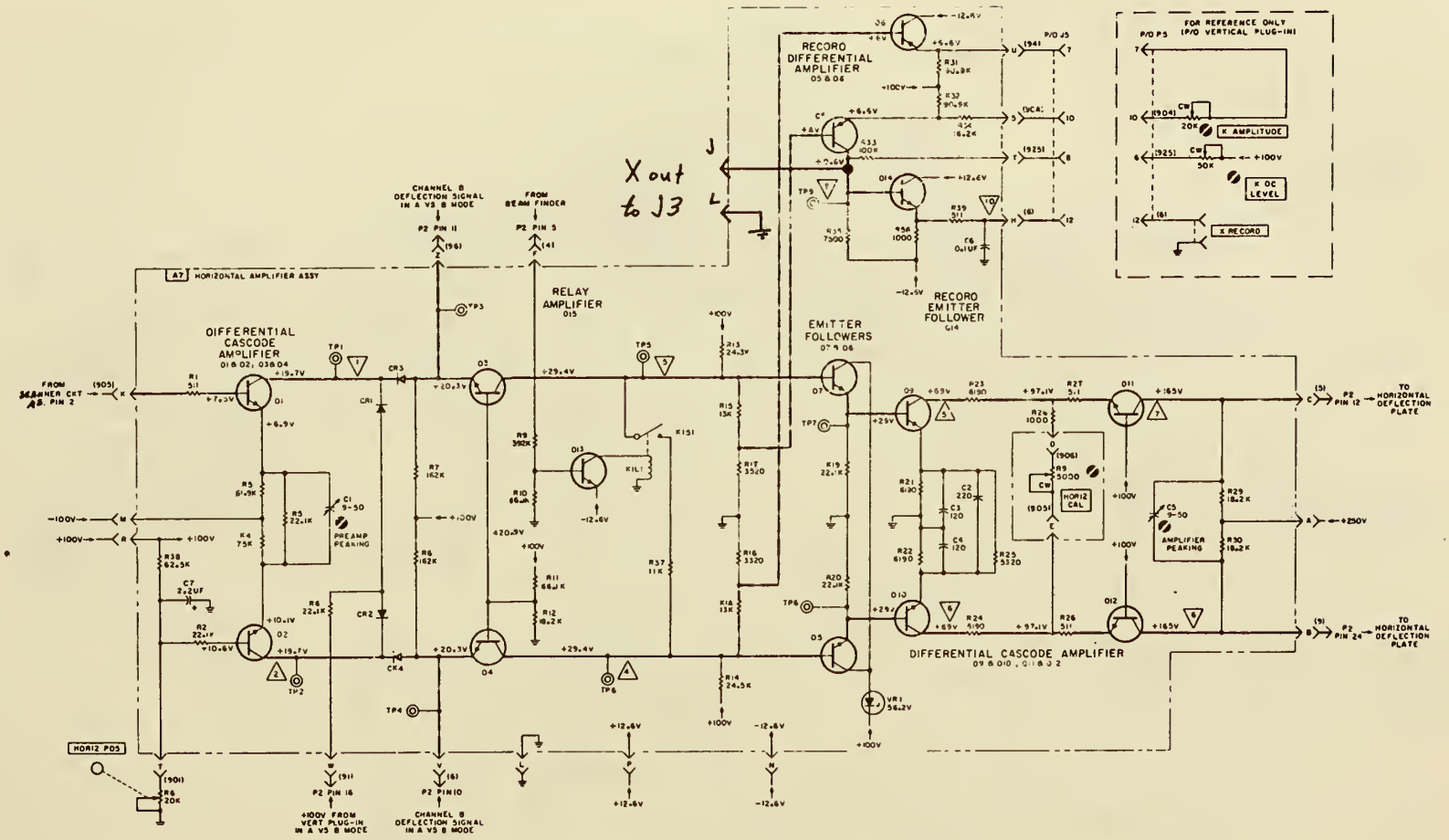

Figure 6-14. Horizontal Amplifier Card A7 Modification.

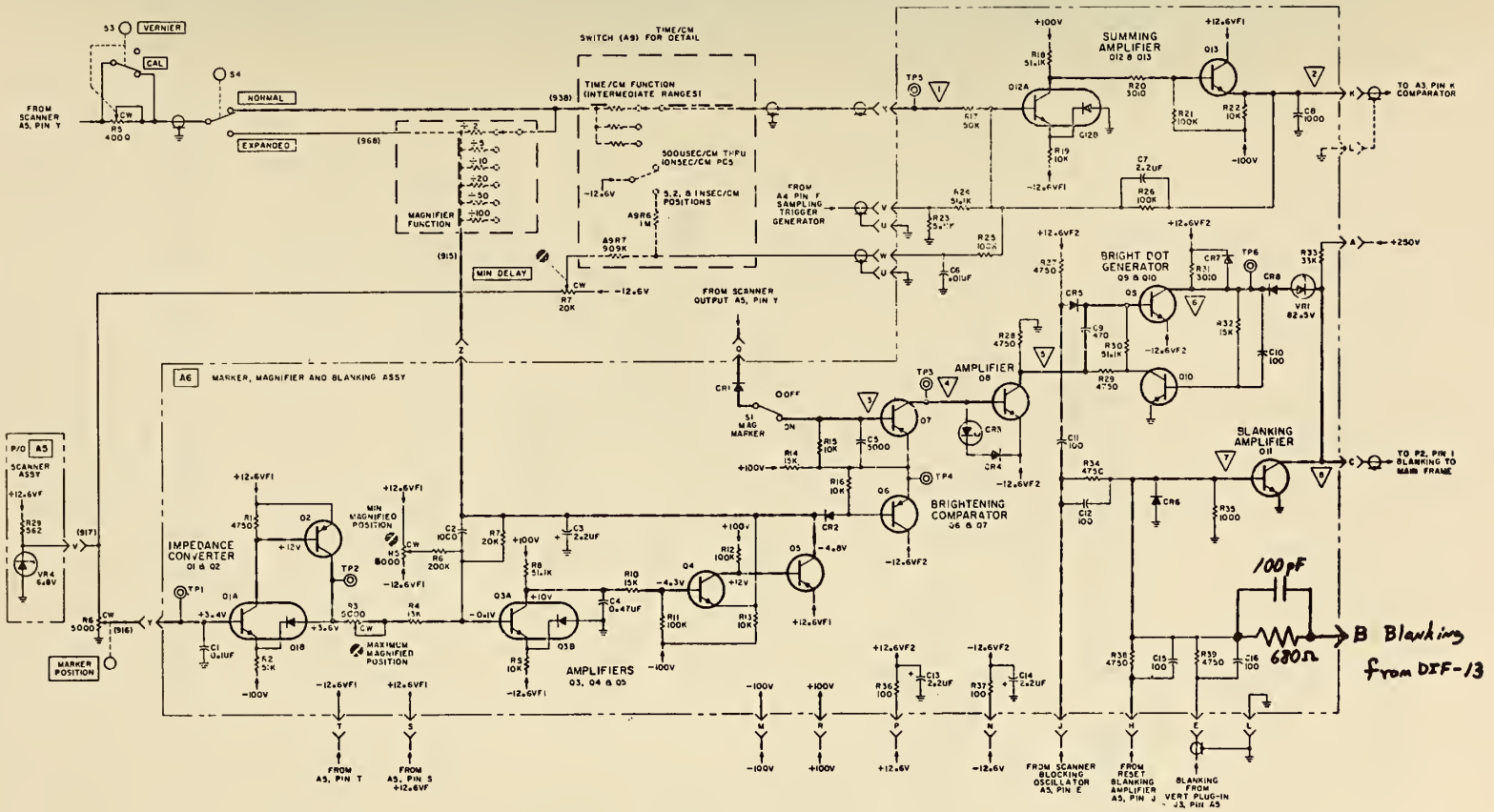

Figure 6-15. Blanking Card A6 Modification.

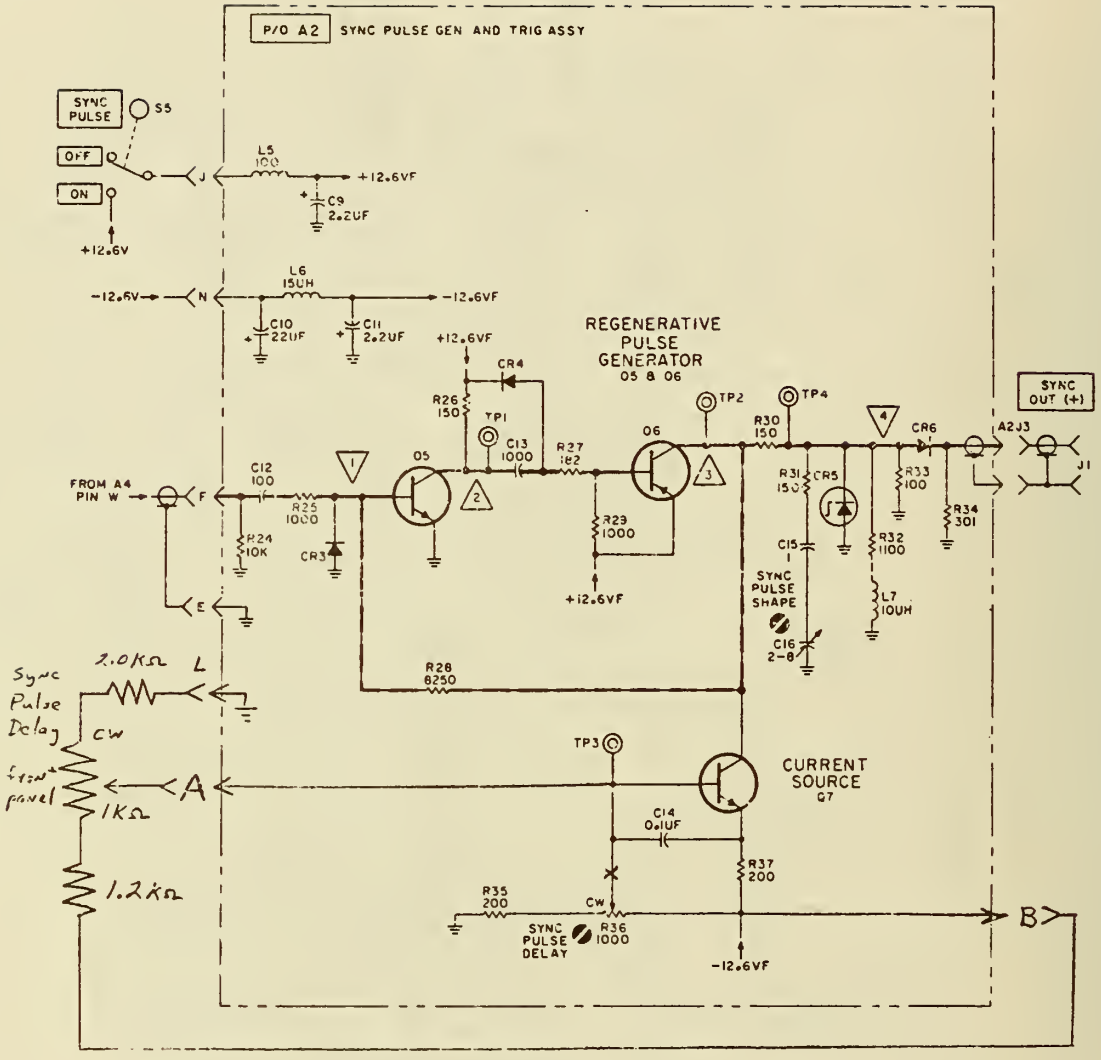

Figure 6-16. Sync Pulse Generator Card A2 Modification.

7. SYSTEM SOFTWARE

7.1 Introduction

This chapter is concerned with the computer programs used for system operation. The overall system software configuration is discussed first, followed by a description of both the BASIC language and assembly language programs used in the system. The actual program listings are contained in the appendices.

7.2 System Software Configuration

The primary task of the system minicomputer and peripherals is to digitize, store and process sampled time domain waveforms acquired from a broadband sampling oscilloscope. Starting from scratch it quickly became evident that no single programming language was suitable for the entire task. Higher level languages such as BASIC or FORTRAN are ideal for performing numerical or mathematical operations. They are also relatively easy languages to learn and use and thus are desirable from the computer operator's standpoint. On the other hand, it is difficult if not impossible to use higher level languages to program the control of external devices such as A/D converters and tape readers. Hardware device handling is best done using either machine language or assembly language. Of the two, assembly language is by far the easier to use. Mathematical calculations, however, are difficult and time consuming to program in either machine or assembly language.

Therefore, in order to satisfy all the system criteria, a software package was written consisting of both BASIC and assembly language programs. BASIC was chosen over FORTRAN only because FORTRAN program compilation on the system minicomputer is very time consuming and must be repeated every time the program is changed.

The particular version of BASIC employed in the system is one provided by the minicomputer manufacturer. It occupies the lower 5K of memory, approximately, and allows calls to external subroutines in upper memory. In order to use this version of BASIC with called subroutines, the programmer must provide an external interrupt routine and a special subroutine table.

There are three other restrictions of interest built into this version of BASIC. First, the system will only recognize a teletypewriter as an I/O device. All other hardware must be controlled by assembly language subroutines called from BASIC. Second, this version has no capability for string manipulation or matrix operations. Third, the maximum allowable number of elements in a single-dimension array variable is 256. Other more subtle restrictions will be described in the next two sections.

The division of tasks between BASIC and assembly language may be listed in more detail as follows.

BASIC

1. Hardware Control -- teletypewriter.
2. Mathematical Operations -- most.
3. User/System Interface (via keyboard).

ASSEMBLY LANGUAGE

1. Hardware Control -- A/D - D/A converters, high speed paper tape reader and punch, monitor oscilloscope, x-y recorder, sampling oscilloscope.
2. Data Acquisition.
3. Data to/from BASIC Control.
4. Mathematical Operations -- optional high-speed FFT and binary data averaging.

In terms of core memory allocation, a core memory map is shown in figure 7-1. Roughly 16K of memory is dedicated to BASIC and 12K to assembly language programs and binary data storage. Spare capacity exists for software expansion at a later date.

7.3 BASIC Program Descriptions

7.3.1 128-Point Fast Fourier Transform

Appendix A-1 contains a listing for this BASIC program. It is designed to transform a 128-point complex time domain waveform into a 64-point array of complex frequency domain coefficients. The input waveform must be programmed into arrays A and B (real and imaginary, respectively) starting with statement number 250.

This program was used primarily for study of the FFT algorithm. The 128-point waveforms discussed in Chapter 4 were all generated and transformed using this program. The output of this routine consists of a listing of the first 32 unnormalized spectrum amplitude points along with a monitor oscilloscope display of all 64 of those points. At run time the program will ask the user for the time scale in nsec/cm of the time-domain waveform to be transformed. The output listing will then automatically include a frequency in MHz associated with each spectral point.

There are three unusual facets of this program that may not be obvious. First, the called subroutines in statement 120 and 130 may seem unnecessary. They have been included in order to disable the A/D converter interrupt. Were they not present, the program would halt upon reception of an interrupt signal from the A/D converter. The second anomaly exists in statements 480, 500 and 970. In these statements integer values are computed for use in FOR-NEXT loops and IF statements. A factor of +.001 was found to be necessary

in order to assure a proper result of these computations. In statement 480, for example, the integer function 2 ↑ (G-L-1) may yield, for G = 5 and L = 1, a result of 7.99999 instead of 8.0. Then, the FOR-NEXT loop starting at statement 560 would do one less iteration than required. By adding +.001 to the result of 2 ↑ (G-L-1) a result greater than or equal to the integer result required is assured. The employment of this "fudge factor" is often necessary in systems, such as this one, that use floating point arithmetic processing.

The third oddity is contained in statements 800 through 850. In order to avoid a number overflow error in subsequent computations of the spectrum amplitude, it was necessary to force numbers very close to zero to be identically equal to zero.

Otherwise, this program is quite straightforward. Run time is approximately 1.5 minutes, excluding the time required for listing results on the teletypewriter. Descriptions of the CALL subroutines used in this program are located in section 7.4.

7.3.2 128-Point Transfer Function

Based on the discrete Fourier transform theory discussed in Chapter 3, this program is designed to compute a discrete frequency-domain transfer function from two time-domain waveforms. A listing of this BASIC program is contained in Appendix A-2. A listing of the salient features of the program follows:

1. Generally, this program is designed to acquire two 64-point time domain waveforms, compute the FFT of each waveform after modification, compute the quotient of the two resulting spectra (output/input) and output the results via teletypewriter and monitor oscilloscope.
2. The first waveform acquisition is done in BASIC statements 100 through 410. The operator signals the system that he is ready (type ϕ), inputs the desired number of time and frequency domain averages, and inputs the waveform time scale in nsec/cm. The BASIC program, along with appropriate assembly language subroutines, then causes the acquisition of the number of 64-point waveforms specified by the user (number of time-domain averages). These waveforms are acquired additively and stored in upper memory. The sum of the waveforms is then returned to BASIC where each point is divided by N1, the number of waveforms acquired, to yield one scaled, time-averaged waveform.

   For example, if N1 = 100, the system will acquire 100 64-point sequential waveforms from the sampling oscilloscope. Each time a new waveform is acquired it will be added point-by-point to the sum of the previously acquired waveforms. Upon completion of the 100th waveform acquisition, the sum total of all 100 waveforms will be converted, point-by-point from binary form to floating point and returned into the

BASIC array, A. Each point in this array will then be divided by 100 to yield a single averaged time domain waveform.

The minimum upper limit for the maximum number of time domain waveforms that may be acquired and averaged is governed by the largest binary number that may be stored in upper memory. For this system, based upon the use of 14 bit A/D conversion and 31 bit (plus sign bit) maximum binary number size, the minimum upper limit is 2^{18} or a maximum of 262,144 time domain waveforms per averaged waveform.

3. Once the first time-averaged waveform is acquired and stored in the BASIC array A, program statements 420 through 670 are executed to prepare the waveform for Fourier transformation. Statements 420 through 480 reset the values of A(0) and A(1) to be linear extensions of the next four points. Resetting A(0) and A(1) in this fashion eliminates any errors in these points caused by sampling oscilloscope instabilities in sampling efficiency. In addition, the value of A(0) is critical to the windowing algorithm used in statements 540 through 610.

Statements 490 through 530 are used to produce a display of the acquired time-averaged waveform on the monitor oscilloscope. This allows the operator to verify the proper operation of the waveform acquisition system on each run.

The windowing algorithm is encountered next in statements 540 through 610. Since the FFT assumes that the time domain waveform to be transformed is periodic then the beginning and end points of the acquired waveform must have the same value of amplitude. If these values are different, such as in the case of a tunnel diode step waveform, then the FFT will treat that difference as an abrupt step-like change in the waveform and this erroneous step will be reflected in the spectral information obtained. These spectral errors are commonly referred to as "leakage" errors.

There are a number of ways to modify the time domain waveform data in order to avoid this problem. The one chosen for this application is based on eq. (4-13). In effect, the acquired 64-point averaged waveform is inverted and added to the end of itself. Thus, a 128-point waveform results with equal end points. As long as the actual waveform acquired came from a linear system, this algorithm is physically valid. In addition to solving the end point problem, however, the particular method solves another problem.

As was discussed in Chapter 4, the DFT of a square pulse whose width is exactly half the time window generates only odd harmonics. All the even harmonics are forced to zero. Generally, for the sin x/x form of the integral Fourier transform of an ideal square pulse, the sin x term is forced to unity for odd harmonic terms and to zero for even

harmonic terms. In fact, the sin x term will be eliminated in this manner for any time domain waveform having 1/2 wave symmetry

$$f(t) = -f(t + T/2) \tag{7-1}$$

where T is the time window. The windowing algorithm used in this program will always modify the acquired time domain waveform such that the resulting waveform exactly satisfies eq. (7-1).

Thus, the algorithm not only ensures that the beginning and end points of the acquired waveform will match but also ensures that the sin x term in the waveform transform will be either unity or zero. Therefore, after throwing out the even harmonic terms in the spectrum amplitude of the transformed waveform, the remainder are odd harmonic terms that are independent of the sin x terms. Consequently, distorted spectra such as those shown in figures 4-13, 4-14, and 4-15 are always avoided.

Once modified, the time domain waveform is again displayed on the monitor oscilloscope for operator verification. Statements 620 through 670 perform this task.

4. Statements 680 through 1180 contain the FFT instructions. The subroutine in statements 1340 through 1410 is also a part of the FFT. This FFT routine is virtually identical to that described previously. It performs the FFT of the 128-point modified waveform and then computes the spectrum amplitude.
5. Statements 1190 through 1330 are for frequency domain averaging. If more than one frequency domain average is requested by the operator then the program stores into upper memory the spectrum amplitude just computed and returns to acquire and process another averaged time domain waveform. The succeeding calculated spectrum amplitude will be added to the first in upper memory. When all of the requested number of spectrum amplitudes have been added together the final result is returned to BASIC and stored into array C. This, then is just simple additive averaging of each spectral point. Since this final waveform spectrum shall ultimately be divided by another (that of the output waveform) then there is no need to normalize either one.
6. Once a frequency domain averaged spectrum amplitude for the reference waveform has been calculated and stored into array C, the program asks the operator the questions contained in statements 1540 through 1600 followed by the questions in statements 140 through 200. The program than repeats the entire process of acquiring the second waveform, computing the spectrum amplitude and storing the result. This time, however, the resulting spectrum is stored in array A. Statements

1660 through 1690 then compute the transfer function of the unknown device by computing, for each frequency point,

$$IL_n = 20 \log_{10} \frac{(V_{out})_n}{(V_{in})_n} \qquad (7\text{-}2)$$

The resulting 32-point transfer function in dB versus frequency is then printed out on the teletypewriter and displayed in the monitor oscilloscope. Statements 1760 through 1840 are used to scale the transfer function data for display purposes only. This scaling is controlled by the operators response to the questions contained in statements 1570 through 1600.

Runtime of this program, excluding output printing on the teletypewriter, is approximately five minutes.

7.3.3 1024-Point Transfer Function

A listing of this program is contained in Appendix A-3. Except for the fact that this program utilizes a 1024-point called assembly language FFT subroutine, it is practically identical to the previously described 128-point transfer function program. The major differences are described as follows:

1. This program causes the acquisition of 512-point waveforms instead of 64-point waveforms. The same averaging and windowing schemes are used but the point A(0) is defined as

$$A(0) = \frac{1}{6} \sum_{i=1}^{6} A(i) \qquad . \qquad (7\text{-}3)$$

rather than as the linear extension used in the 128-point program. (Note that this method of correcting A(0) is only valid if the slope of the measured waveform is zero.)

2. The first 256 points of the acquired waveform are put into array A and the second 256 points into array B. The other 512 points resulting from the windowing algorithm are put into arrays C and D sequentially. Then all four arrays are converted to binary and stored in upper memory. Statement number 660 then calls the assembly language FFT to operate on the real 1024 point array stored in upper memory starting at octal location 50000. The FFT routine will be described in the next section. Statements 670 through 700 then return the resulting spectral points into BASIC floating point arrays A, B, C and D. A and B contain the first 512 spectral real parts while C and D are the first 512 spectral imaginary parts. The spectrum amplitude is then calculated as previously described.
3. Statement 1000 prints out the value of the variable S on the teletypewriter. This variable is the number of times the spectral array was

right-shifted, or divided by two, in the FFT computation. More will be said in the section describing the assembly language FFT routine. It is sufficient at this point to note that the larger this number the lower the resolution of the resulting spectral points.

4. Statements 1010 through 1040 cause a logarithmic display of the computed spectrum amplitude on the monitor oscilloscope for each waveform transformed.

In contrast to the 128-point transfer function program this program runs faster and generates 256 spectral points instead of 32. The actual FFT routine runtime is only about one or two seconds. Since this FFT only operates on single-precision binary numbers, however, and since an FFT algorithm contains a large number of additions and multiplications, in general, then the expense incurred with the program is extremely poor spectral amplitude resolution. Consequently, this program was used for FFT experimentation only; all measurements on actual microwave devices were accomplished with the 128-point transfer function program.

7.4 Assembly Language Program Descriptions

All of the programs described in this section were written in assembly language and absolutely assembled. Each subroutine is called from BASIC with an instruction of the form

$$n_1 \text{ CALL } n_2, X_1, X_2, X_3, \ldots, X_8$$

where n_1 is the BASIC instruction number, n_2 is the called subroutine number and the X's are variables to be transferred either from BASIC to the subroutine or vice versa. Up to eight variables may be transferred in this manner.

With the exception of the FFT subroutine all of the programs are thoroughly commented in the listings. Therefore, only brief descriptions of each routine are presented.

7.4.1 Subroutine Table (Appendix B-1)

In order to use the called subroutine feature of BASIC a subroutine table must be written. This table performs a number of functions. First, it serves as an index of all assembly language user-written subroutines. When a CALL instruction is encountered in a BASIC program, the computer jumps through location 10 to the starting address of the subroutine table (40000 in this case). It then searches through the index for the starting address of the subroutine called and jumps to that location. Second, the table is used to tell BASIC, by means of a code word, how many input and output parameters are associated with the subroutine and in what order they

appear in the CALL statement. Thus, in the listing in appendix B-1, the lines

```
40007      000003          3
40010      040400          DATOP
40011      130000          130000
```

all refer to subroutine number 3. The five digit octal number in the left column is the absolute memory location of that line, while the six digit octal number in the next column is the contents of that location. In memory location 40007 there is a 000003 which is the subroutine number. In location 40010 there is a 040400 which is the starting address of subroutine number three and in location 40011 there is a 130000 which is the parameter code word mentioned above. In the right hand column are the programming statements that caused the program assembler to generate the first two columns. DATOP is the particular subroutine's label used for referencing the program.

All subroutines are listed in the table in this manner. In addition, an interrupt-handling subroutine must be the first subroutine listed. In this case, the interrupt routine is labeled INTRP and its starting address is contained in location 40000. Whenever an interrupt occurs the computer will jump to the user's interrupt routine to see if the interrupt was caused by a user-programmed device. Even, as is the case here, if no interrupts are used an interrupt routine must be provided. At the bottom of the table listing is the interrupt routine used in the system. It merely turns off the A/D converter interrupt capability and returns to the BASIC interrupt routine starting in location 521.

After all subroutines have been listed in the table the list must be terminated with a -1. In this case location 40050 is the end of the table and contains a 177777 which is the machine representation for a -1.

Finally, the table is used to define global labels and devices. .FIX and .FLOT are the floating point to binary and binary to floating point conversion routines located in BASIC locations 130 and 132 respectively. The two statements in the table allow reference to these routines from any user-written assembly language program. The next two .DUSR instructions simply define the mnemonics ADCV and DACV as device numbers 21 and 23. Thereafter, the mnemonics may be used to reference the A/D and D/A converters, respectively.

This table must be located right above the BASIC users area in memory. When a program is executed in BASIC all memory locations above BASIC and below the table are erased. Referring to figure 7-1, any assembly language programs or binary data stored in the memory block labeled BASIC Program and Data Storage will be lost at runtime. Thus, the subroutine table also tells BASIC the upper limits of BASIC's operating area.

7.4.2 Memory Clear Routine (Appendix B-2)

The starting address for this routine is location 40100. It is designed to set the contents of locations 50000 through 53777 (octal) to zero. These 2048 (decimal) locations are used to store the acquired time domain waveforms. Before acquisition of a waveform begins, this routine is called from BASIC to reset the contents of the binary array memory locations to zero. The BASIC instruction used to call this routine is n_1 CALL 1 where n_1 is the BASIC instruction number.

7.4.3 Data Acquisition Routine (Appendix B-3)

Absolute location 40200 is the starting address for this routine. It is used to generate the x-axis sweep for the sampling oscilloscope and to acquire a time-averaged time domain waveform. The form of the BASIC instruction used to call this routine is n_1 CALL 2, N1, N3 where n_1 is the BASIC instruction number, N1 is the number of waveforms to be averaged and N3 is the x-axis spacing between sample points. As waveform acquisition takes place the D/A is set to i times N3 for the ith x sample point. The sampling oscilloscope is instructed to take a y-axis sample and the A/D converter is instructed to convert the sample from analog to binary. This sample is then added to the sum of the previous samples taken at that x-location and this new sum is returned to the appropriate memory location. Upon completion, the sum of the N1 acquired waveforms, each consisting of 2^{14}/N3 sample points is stored sequentially in memory locations 50000 through 53777. Each sample point occupies 2 16-bit word locations so the maximum number of sample points allowable for each waveform is 4000/2 (octal) or 1024 (decimal) points.

7.4.4 Data Binary to BASIC Routine (Appendix B-4)

Once the time-averaged waveform has been acquired and stored this subroutine is called in order to transfer the waveform from upper memory binary form to a BASIC floating point array. The BASIC instruction format is n_1 CALL 3, N, A where n_1 is the BASIC instruction number, N is the multiple of 256 data points and A is the destination BASIC array variable. Since BASIC limits a single array dimension to 256 then a 1024-point waveform must be put into four different 256-point arrays. Thus, this subroutine must be called four times in order to transfer the complete waveform into BASIC. The instructions to transfer a 1024 point waveform into BASIC arrays A, B, C and D, sequentially would be

n_1 CALL 3, 0, A

n_2 CALL 3, 256, B

n_3 CALL 3, 512, C

n_4 CALL 3, 768, D

The absolute starting address of this routine is 40400. It operates on data stored only in locations 50000 through 53777 and assumes each data point occupies 2 16-bit words.

7.4.5 Data BASIC to Binary Routine (Appendix B-5)

This subroutine, starting in location 40500, is essentially the reverse of the routine just described in 7.4.4. It is designed to transfer floating point BASIC arrays to upper memory binary putting the 16-bit binary numbers sequentially into locations 50000 through 53777. The one difference is that the binary numbers produced by this program are 16-bit single precision numbers while the binary numbers operated upon by the previously described program are 32-bit double precision numbers.

This program is designed to return spectrum amplitude data to binary form for monitor oscilloscope display purposes. Therefore, double precision number representation is unnecessary. The calling format for this routine is the same as for the previous subroutine except that CALL 3 is replaced with CALL 4.

7.4.6 Data Display Routine (Appendix B-6)

The absolute starting address of this subroutine is 40600. It is designed to display the data stored in locations 50000 through 53777 on the monitor oscilloscope. As was the case with the previously described data acquisition routine, this program operates the x-axis sweep and sends this x information to the monitor oscilloscope via D/A #2. D/A #4 is used to send the y value of data associated with the current value of x to the monitor oscilloscope. When both the x and y values have been loaded into the two D/A converters, a z-axis intensifier pulse is sent out causing the display of one point on the screen.

This routine will display one full sweep and return to BASIC. For a continuous display of data the program must be repeatedly called from BASIC. For example, for a display of 500 sweeps the BASIC instructions would be

n_1 FOR I = 1 TO 500

n_2 CALL 5, N3

n_3 NEXT I

where n_1, n_2 and n_3 are BASIC instruction numbers and N3 is the spacing between x-axis points in parts of 2^{14}. (NOTE-2^{14} corresponds to full-scale deflection for all D/A and A/D converters. However, D/A #2 and D/A #4 are 10 bit devices and only utilize the 10 most significant bits.)

7.4.7 X-Y Recorder Zero and Full Scale Set Routine (Appendix B-7)

X-Y recordings of data in locations 50000 through 53777 may be obtained by means of this program and the next (section 7.4.8). This routine, starting in location 40700 allows the operator to adjust the X-Y recorder for calibrated full scale and zero settings with respect to the X and Y D/A converter outputs. Actually, this listing contains two separate subroutines, one for full scale set and one for zero set. Thus a CALL 6 will cause the X and Y axis D/A converters to output full scale signals while a CALL 7 instruction will cause the D/A's to output a zero signal.

7.4.8 X-Y Record Subroutine (Appendix B-8)

Once the X-Y recorder has been calibrated, this routine, starting in location 40750, is called to record sequentially the data contained in locations 50000 through 53777. The variable DELA is the pen speed factor and may be changed via the computer front panel switches prior to execution in order to speed up or slow down the x-axis recording speed. This program will generate one 1024-point X-Y recording and then return to BASIC. The variable CT6 must be changed via the computer front panel switches in order to change the number of data points in the recording.

7.4.9 Data Binary to BASIC Routine (Appendix B-9)

Whereas the binary-to-BASIC routine described in 7.4.4 is designed to convert double precision positive binary numbers to BASIC floating point, this routine is designed to convert single precision positive or negative binary numbers to BASIC floating point. Otherwise, this routine is virtually identical to that described in 7.4.4. The reason two different routines are necessary is that while the data acquisition routine generates a binary array of double-precision positive numbers, the assembly language FFT routine generates a binary array of single precision numbers that may be either positive or negative. Thus, this program is used to transfer the result of the assembly language FFT into BASIC while the previous program is used to transfer the results of the time-domain waveform acquisition into BASIC. The starting address for this routine is 41020.

7.4.10 Assembly Language FFT Routine (Appendix B-10)

This program was obtained from a minicomputer user's group and was modified to work in a CALL BASIC environment [37]. It will compute the forward or inverse DFT of a complex or real input time series consisting of 2^M points, M an integer less than or equal to 10. This corresponds to a maximum transform length of 1024 points.

The program is designed to operate on a binary time series stored in location 50000 through 53777 (octal). The time series must be arranged so that location 50000 through 51777 contain the real part of the time-sequential input series and locations 52000 through 53777 contain the imaginary part of that series. The BASIC instruction used to call the routine is of the form

n_1 CALL 10, N0, N2, S

where n_1 is the BASIC instruction number, N0 is a +1 for an inverse transform and a 0 for a forward transform, N2 is the transform length (number of sample points), and S is the number of times the data is scaled during FFT computation.

Upon completion of FFT computation, the spectral data is returned to locations 50000 through 53777 such that the real part of the frequency-sequential spectral series is in locations 50000 through 51777 and the imaginary part is in locations 52000 through 53777. Each spectral coefficient is a single-precision binary integer that may be positive or negative.

This program is very fast (< 2 sec. execution time) but has a severe limitation. The input time series must contain no number larger than 2^{14} (decimal) or an overflow will occur. Also, as computation progresses, if any number in an array exceeds 13,107 (decimal), then that array is divided by 2. The variable S mentioned above is the number of times that this array division has taken place. Typically, for a 1024-point transform, the arrays are scaled down by a factor of two from 7 to 9 times. The result of this scaling is extremely poor resolution of spectral values. A high order harmonic may have a spectral amplitude of either zero or one or two, for example, and there could easily be an error in the first significant digit.

Consequently, this routine was considered unusable for quantitative analysis of waveforms; its use was restricted to qualitative FFT experimentation only. The starting address for this routine is location 41747.

7.4.11 Spectral Memory Clear Routine (Appendix B-11)

This routine performs the same function as the memory clear routine described in section 7.4.2 except that it clears a different block of memory. Once the spectrum amplitude of a time-averaged waveform has been computed in BASIC, it is returned to binary form in upper memory for frequency domain averaging and monitor oscilloscope display purposes. This program zeroes absolute memory locations 45000 through 45777 (512 points) in preparation for additive storage of spectral arrays. This routine's starting address is 42500, and is called by an instruction of the form n_1 CALL 11.

7.4.12 Spectral Data BASIC to Binary Routine (Appendix B-12)

This routine is similar to that described in section 7.4.5. The difference, again, is that this program operates on a different upper memory block. In the same manner as the previously described routine, this program transfers a BASIC floating-point array to upper memory double precision binary form. The instruction form is n_1 CALL 12, A where A is the BASIC array name. 42600 is the starting address for this routine.

7.4.13 Spectral Data Binary to BASIC Routine (Appendix B-13)

After the desired number of 256-point spectral arrays have been additively stored in locations 45000 through 45777, this routine is called to return the frequency-domain averaged spectrum to BASIC. Except for the memory block difference, this program is the same as that described in section 7.4.4. The instruction format is n_1 CALL 13, A where A, again, is the BASIC array name. This last subroutine's starting address is 42700 and it ends at location 42731. 42731, then, is also the last location of the assembly language subroutine package.

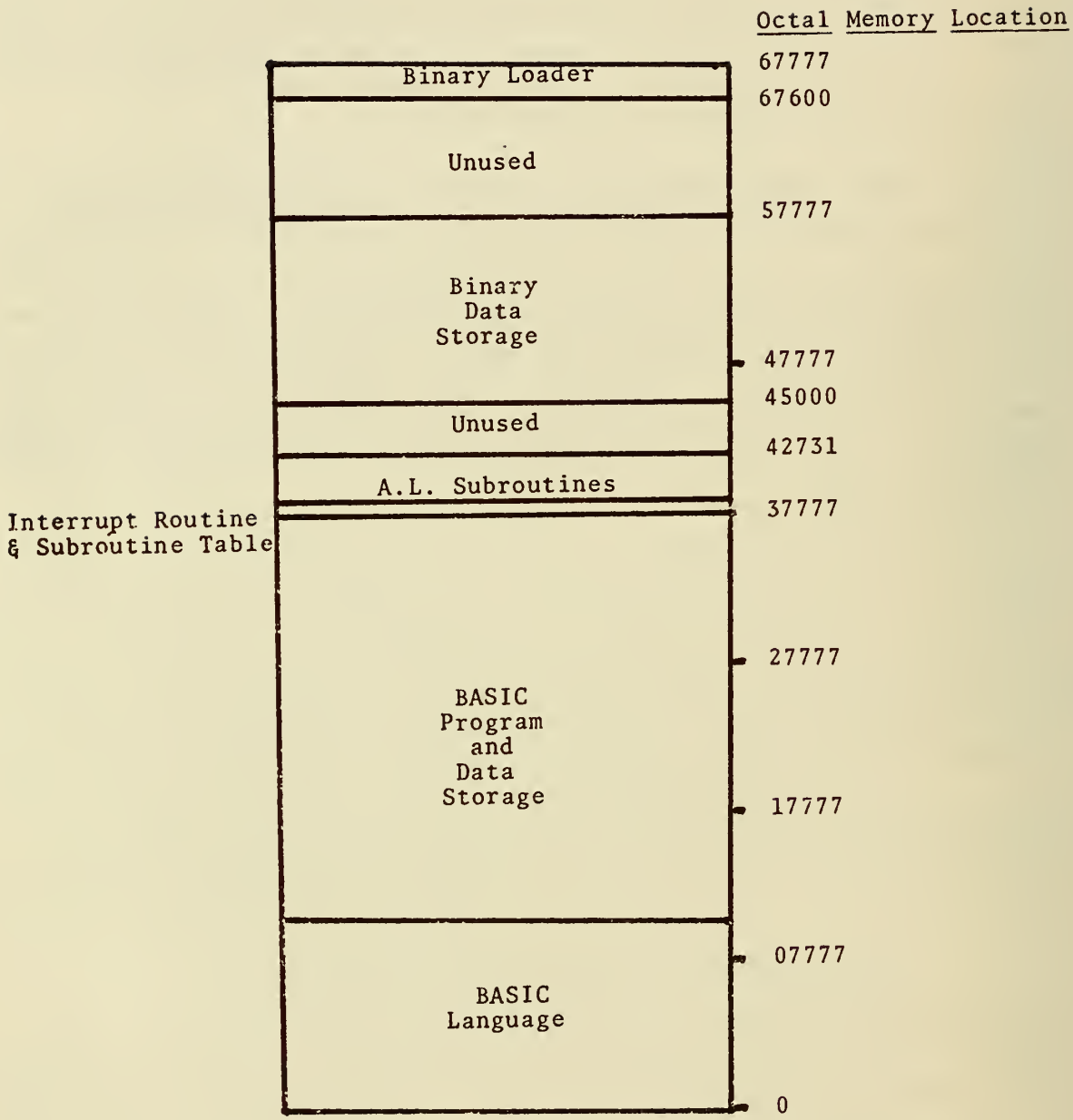

Figure 7.1. Minicomputer System Memory Map (28K Core).

8. EXPERIMENTAL RESULTS

8.1 Introduction

To determine the agreement of measured insertion loss between the time domain measurement system (TDANA) and equivalent frequency domain systems, a number of experimental comparative measurements were made. The insertion losses of three wideband coaxial attenuators, nominally 10, 20 and 40 dB, were measured at discrete frequency points over a band from 0.5 to 12.5 GHz. Three systems were used to perform these measurements; the TDANA system, the NBS automatic network analyzer system (ANA), and the NBS fixed frequency 30 MHz IF substitution system (NBS system). For purposes of this report, and because both the TDANA and the ANA systems are still experimental, the measured insertion loss values obtained with the NBS system were considered to be the "correct" values. These measurements should not be considered an exhaustive analysis of the comparative measurement capabilities of the three systems, but rather, a first order or rough system comparison.

8.2 NBS System Measurements

The 30 MHz IF substitution system is the NBS, Boulder Labs working standard for calibrations of wideband coaxial attenuators. The heart of this system is a precision 30 MHz waveguide below cut-off standard attenuator. Beatty [38] has written a comprehensive analysis of this method of attenuation measurement as well as an excellent list of additional references on the subject. References [39] and [40] are also pertinent.

Due to cost and time limitations the three coaxial attenuator's insertion losses were measured on this system at only a few different frequencies. The resulting measurement data from this system as well as that for the TDANA and ANA systems are tabulated and displayed graphically in Tables 8-1 through 8-3 and figures 8-1 through 8-3. Conclusions drawn from these data are deferred to section 8.5.

8.3 ANA System Measurements

The NBS automatic network analyzer is essentially a commercially available computer-controlled microwave network analyzer that is in the process of being extensively modified. Using computer controlled swept frequency CW generators, the system measures such parameters as reflection coefficient magnitude and phase, insertion loss, and VSWR for both coaxial and waveguide microwave components over the bands 100 MHz to 2 GHz and 2 to 18 GHz. The goal of these modifications is to extend the range of operating frequencies and to upgrade the measurement accuracy and precision to achieve a new NBS automated working standard for calibration. At present, the measurement

uncertainty is essentially that quoted by the analyzer manufacturer [41]. Beatty [42] again, has written an overview of ANA's as well as a list of almost 50 additional references on the subject.

A set of five separate insertion loss measurements was performed on this system for each of the three attenuators. Again, the results are tabulated and graphically displayed in the tables and figures mentioned previously.

8.4 TDANA System Measurements

The circuit models for the insertion loss measurements made with the TDANA system are shown in figures 2-4 and 2-5. A time window of 1 ns was chosen for waveform acquisition, each waveform consisting of 64 time sample points. The precision coaxial air lines, represented in the figures as ℓ_1 and ℓ_2, were chosen long enough to introduce no secondary reflections in the 1 ns time window. For this measurement ℓ_1 and ℓ_2 were each 30 cm long. Time-averaged sampled data representations of the waveform $v_{d1}(t)$ and $v_{d2}(t)$ were obtained using an ultra-fast tunnel diode pulse generator as a source ($v_{d1} \simeq 250$ mV). These two waveforms were then Fourier transformed using an FFT on the system minicomputer and the insertion loss of the test attenuator was computed to be

$$IL(f_n) = 20 \log_{10} \frac{S_n(OUT)}{S_n(IN)}, \qquad n = 1,3,5,\cdots,\frac{N}{2}-1 \qquad (8\text{-}1)$$

where $IL(f_n)$ = insertion loss at n^{th} harmonic in dB,
S_n = computed spectral amplitude of the n^{th} harmonic, see eq. (2-7),
N = number of samples in the transformed time series (128 points in this case).

Because the windowing algorithm used in this system effectively doubles the time window length (to 2 ns for this measurement) and because this same algorithm causes all even spectral harmonics to be zero, then the actual frequencies at which the insertion loss is measured are

$$\frac{1}{2ns}, \frac{3}{2ns}, \frac{5}{2ns}, \cdots, \frac{\frac{N}{2}-1}{2ns}$$

or, at .5 GHz, 1.5 GHz, 2.5 GHz, ···, 31.5 GHz. Of these, only the insertion losses at frequencies out to 12.5 GHz were tabulated.

8.5 Experimental Conclusions

Tables 8-1, 8-2, and 8-3 contain a summary of all measurement data for the 10, 20 and 40 dB attenuators respectively. In each table, column (1) lists the frequencies at which insertion loss measurements were performed.

Columns (2) through (4) summarize the data from measurements on the TDANA. Column (2) lists the mean insertion losses computed from a set of ten independent measurements. Column (3) is a list of the estimated standard deviations computed from the formula,

$$\hat{\sigma} = \left[\frac{1}{n-1} \sum_{j=1}^{n} (x_j - \bar{x})^2 \right]^{1/2} \qquad (8\text{-}2)$$

where n is the number of measurements (10), x_j is the j^{th} measured value, and $\bar{x}$ is the mean value of the n measured values. Column (4) is the deviation, in percent, of the mean insertion loss measured on the TDANA system compared to that obtained on the NBS system.

Columns (5) through (7) are summaries of the data from measurements performed on the ANA. In this case, five independent measurements were made. Otherwise, columns (5) through (7) are exactly analogous to columns (2) through (4), respectively, that is, mean, estimated standard deviations and percent deviation from the NBS system.

Columns (8) and (9) summarize the data obtained from the NBS fixed frequency 30 MHz IF substitution system. The mean value of several insertion loss measurements is reported in column (8). Column (9) contains the estimated maximum total uncertainty.

Figures 8-1 through 8-3 are graphs of the measured mean values of insertion loss versus frequency for the 10, 20 and 40 dB attenuators, respectively.

The salient features of these results are as follows. 1) The mean values of insertion loss measured on the TDANA appear to be consistently less than those measured on the NBS system. 2) There appears to be a measurement agreement of within 1.5% between the TDANA and the NBS systems out to 12.5 GHz. 3) The estimated standard deviations of the TDANA measurements are within ± 1% of nominal attenuation for the 10 and 20 dB pads but approach ± 2.5% for the 40 dB pad. Also, the estimated standard deviations for each attenuator increase with increasing frequency. This is to be expected because the standard deviations are all proportional to the system signal-to-noise ratio which, because of the 1/f decay of available spectral power in the driving source pulse, becomes smaller with increasing frequency.

Table 8-1. Measured Insertion Loss Data Summary for 10 dB Coaxial Attenuator.

(1)	(2)	(3)	(4)	(5)	(6)	(7)	(8)	(9)
	TDANA System			ANA System			NBS System	
Freq. (GHz)	Insertion Loss (dB)	Standard Deviation (dB)	Percent Deviation (%)	Insertion Loss (dB)	Standard Deviation (dB)	Percent Deviation (%)	Insertion Loss (dB)	Total Uncertainty (dB)
.5	9.87	.02	-1.1	9.99	.02	+.03	9.987	.04
1.5	9.91	.03	-1.0	10.09	.01	+.80	10.010	.05
2.5	9.93	.03	- .98	10.00	.01	+.23	10.028	.05
3.5	9.92	.03		10.13	.02			
4.5	9.93	.04	- .80	10.01	.03	0	10.010	.05
5.5	9.96	.05		10.02	.05			
6.5	9.99	.07		10.20	.06			
7.5	9.93	.09		10.16	.06			
8.5	9.86	.09	-1.4	9.99	.04	-.12	10.002	.12
9.5	9.84	.07		10.17	.03			
10.5	9.95	.09		10.14	.02			
11.5	9.85	.09	-1.4	9.97	.02	-.19	9.989	.08
12.5	9.73	.09		10.05	.02			

Table 8.2. Measured Insertion Loss Data Summary for 20 dB Coaxial Attenuator.

(1)	(2)	(3)	(4)	(5)	(6)	(7)	(8)	(9)
	TDANA System			ANA System			NBS System	
Freq. (GHz)	Insertion Loss (dB)	Standard Deviation (dB)	Percent Deviation (%)	Insertion Loss (dB)	Standard Deviation (dB)	Percent Deviation (%)	Insertion Loss (dB)	Total Uncertainty (dB)
.5	20.13	.08	-.42	20.27	.06	+.28	20.214	.06
1.5	20.23	.07		20.42	.05			
2.5	20.28	.08	-.37	20.34	.01	-.07	20.355	.07
3.5	20.34	.07		20.52	.01			
4.5	20.42	.08		20.44	.01			
5.5	20.47	.10		20.49	.01			
6.5	20.53	.07		20.68	.02			
7.5	20.55	.12		20.70	.01			
8.5	20.64	.14	0	20.64	.03	0	20.639	.12
9.5	20.66	.15		20.91	.02			
10.5	20.73	.09		20.95	.03			
11.5	20.66	.14	-.95	20.82	.04	-.18	20.858	.13
12.5	20.60	.17		20.96	.05			

Table 8-3. Measured Insertion Loss Data Summary for 40 dB Coaxial Attenuator.

(1)	(2)	(3)	(4)	(5)	(6)	(7)	(8)	(9)
	TDANA System			ANA System			NBS System	
Freq. (GHz)	Insertion Loss (dB)	Standard Deviation (dB)	Percent Deviation (%)	Insertion Loss (dB)	Standard Deviation (dB)	Percent Deviation (%)	Insertion Loss (dB)	Total Uncertainty (dB)
.5	39.95	.27	-.11	40.10	.07	+.27	39.993	.22
1.5	40.07	.21		40.18	.01			
2.5	39.99	.33	-.09	40.21	.03	+.45	40.028	.19
3.5	40.01	.40		40.20	.04			
4.5	40.16	.48		40.04	.06			
5.5	40.21	.40		40.04	.10			
6.5	40.15	.42		40.06	.02			
7.5	40.01	.41		40.12	.03			
8.5	39.51	.56	-.69	39.87	.04	+.21	39.786	.29
9.5	39.58	.51		40.01	.04			
10.5	39.61	.60		39.93	.02			
11.5	39.79	.97	+.52	39.68	.09	+.24	39.585	.27
12.5	39.36	.95		39.87	.07			

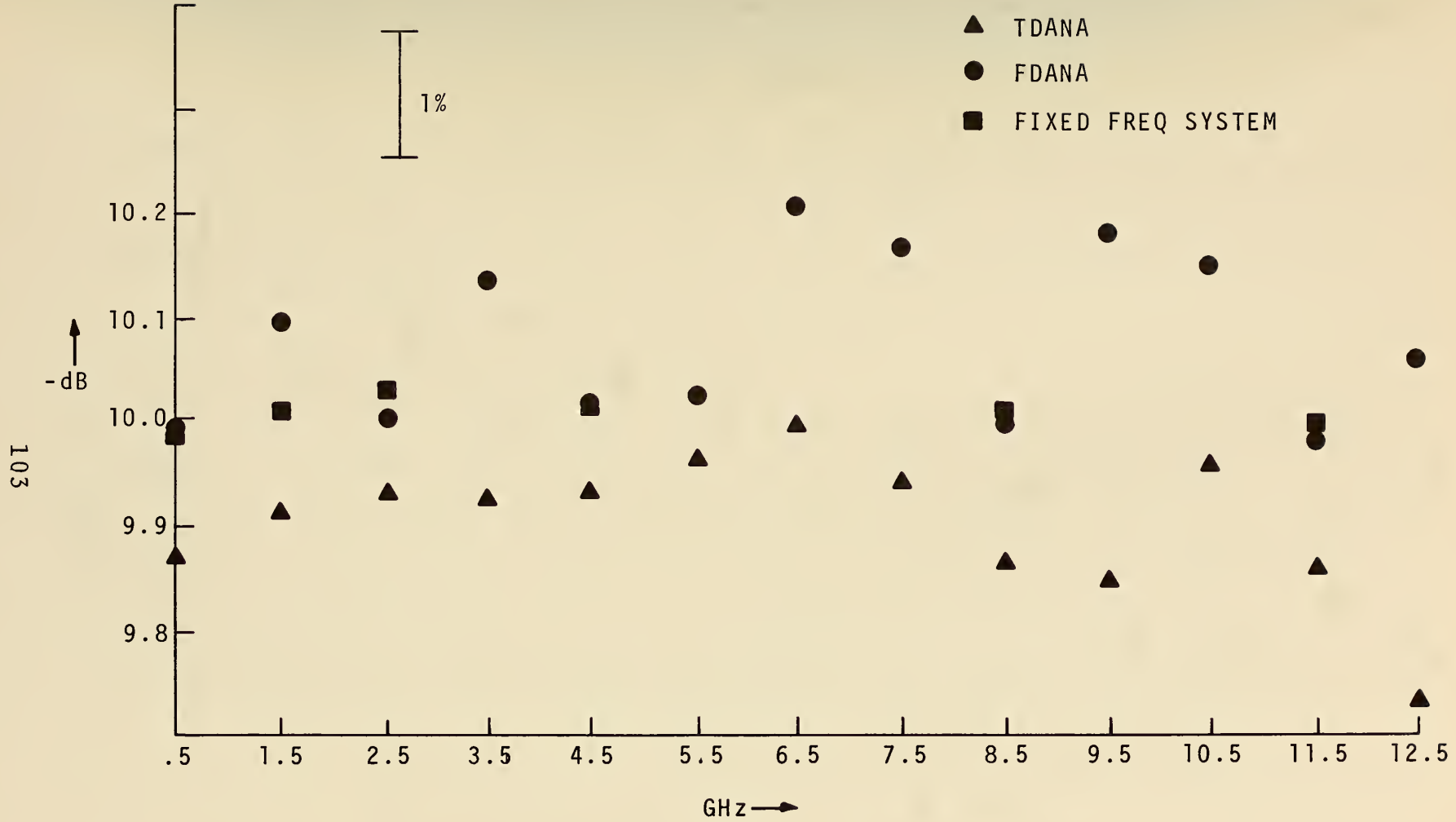

Figure 8-1. Comparative Plot of Insertion Loss Versus Frequency for 10 dB Pad.

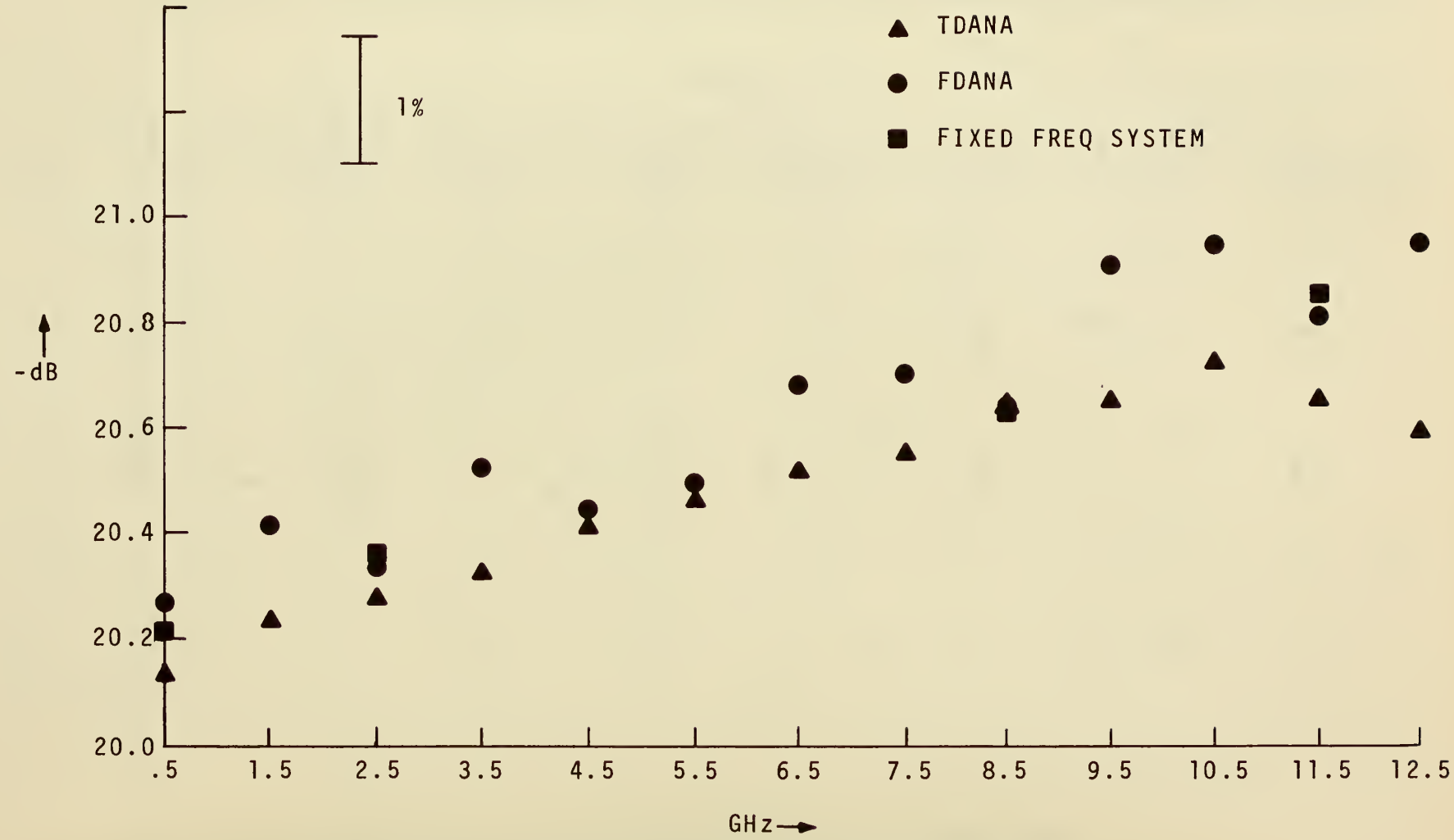

Figure 8-2. Comparative Plot of Insertion Loss Versus Frequency for 20 dB Pad.

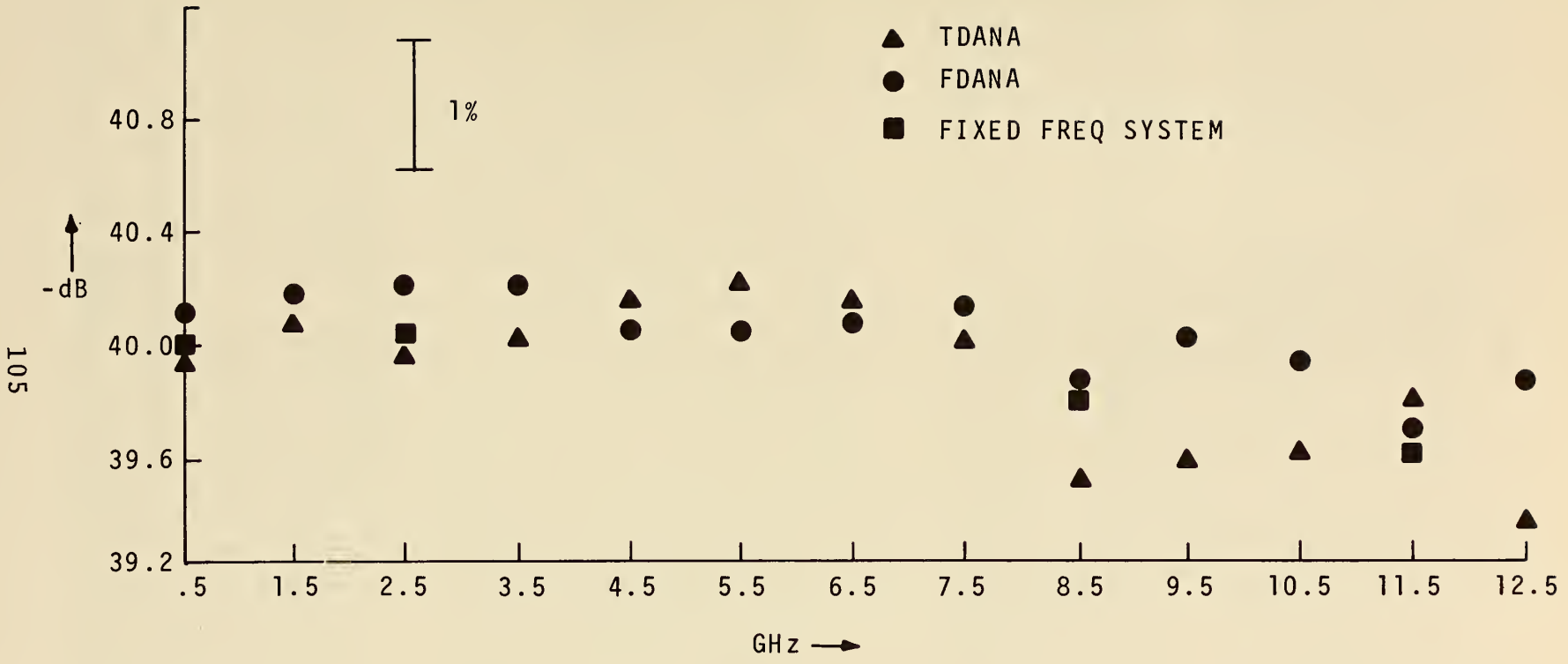

Figure 8-3. Comparative Plot of Insertion Loss Versus Frequency for 40 dB Pad.

9. SYSTEM ERROR ANALYSIS

9.1 Introduction

This chapter is concerned with a discussion of errors in the TDANA system, both systematic and random. At present, the system should be considered experimental in that an exhaustive effort to analyze and reduce system errors has yet to be done. This analysis, as well as efforts to extend the system measurement ranges for both frequency and insertion loss, remain as planned future work.

Some system error analysis experiments have been conducted, however, and some sources of error have been observed and noted in a qualitative sense. The results of these experiments are summarized in this chapter. Also, a discussion of suspected sources of error and their relative magnitudes is presented.

Some prior work has been accomplished pertaining to errors in sampling oscilloscope systems similar to the TDANA. Efforts at Sperry Rand Research [43] and at IBM Watson Research Center [44], in particular, have been fruitful.

9.2 Systematic Errors

As opposed to random errors, systematic errors may be thought of as errors that introduce a fixed bias into the measurement process. As reported in Chapter 8, the comparative insertion loss measurements conducted on three coaxial attenuators indicate a tendency for the values of insertion loss measured on the TDANA to be consistently less than those measured on the other two systems. In all probability, this lack of agreement is caused for the most part by systematic errors in one or more of the three systems used. The results of the attenuation experiments, themselves, say nothing about which system or systems are the ones in error, but experience indicates that the fixed frequency 30 MHz IF substitution system is the most accurate and precise of the three.

9.2.1 Impedance Matching Errors

The theoretical development presented in Chapter 2 shows that, were the system perfect in all other respects, the insertion loss measurement accuracy of the TDANA would be entirely dependent on the accuracy of the values of Z_0 for the lines ℓ_1 and ℓ_2 shown in figures 2-4 and 2-5. That is, the fundamental limitation of system accuracy for insertion loss measurements is solely dependent upon how close the impedances of lines ℓ_1 and ℓ_2 are to an ideal 50.0 Ω over the frequency band of interest. The lines ℓ_1 and ℓ_2, then, may be thought of as the system standards which will dictate the

absolute measurement accuracy of the system. It should be noted that the connector pair used between the precision air lines and the reference insertion plane is the major physical obstacle to achieving a perfect Z_0 transmission line over the time window of interest. This error in Z_0 may be considered analagous to the problem of trying to achieve a perfectly reflectionless line when looking from the insertion plane towards both the load and generator in a frequency domain measurement system.

9.2.2 System Nonlinearities

Several distinct sources of systematic error have been lumped into the category of system nonlinearities. The first of these are errors caused by the nonlinearities associated with the oscilloscope sampling head. The dynamic voltage range of the sampling head is specified as ± 1 V by the manufacturer. A plot of displayed voltage on the CRT versus input voltage demonstrated a definite nonlinearity with severe compression above 800 mV [45]. Thus this must be considered a source of systematic error in the range 0.8 to 1 V.

Closely related to the sampling head nonlinearities as a source of error are the nonlinearities associated with the sampling oscilloscope vertical channel circuitry. In addition, any nonlinearities of the 14 bit A/D converter must be considered. It is very likely that the trend of smaller values of insertion loss measured on the TDANA compared with the frequency domain systems' results is caused, in part, by some combination of these three systematic error sources. In particular, if these nonlinearities caused a compression of the initial waveform voltage while faithfully acquiring an accurate representation of the smaller attenuator response waveform, the resulting measured values of insertion loss computed by the system would indeed be less than their true values. Once these errors are modeled, it should be possible to provide corrections by means of the system minicomputer.

It should be noted that for simple waveform spectral analysis, as opposed to insertion loss measurements, the error associated with the absolute calibration of the entire vertical channel must be taken into account. For amplitude-independent absolute vertical channel errors, their cancellation is ensured by the insertion loss computation (see section 2-3).

Horizontal nonlinearities are also present, primarily in the sampling oscilloscope horizontal trigger and sweep circuitry and the horizontal sweep-controlling 14 bit D/A. Because application of the discrete Fourier transform assumes system linearity and equally-spaced time samples, any variation in sampling point time spacing will cause errors in the resulting computed waveform spectrum. The errors caused by these horizontal nonlinearities result essentially in an uncertainty in frequency associated with each computed spectral point.

9.2.3 Computational Errors

For machine computation purposes, errors may be thought of as being inherent errors, truncation errors, or roundoff errors [46]. Inherent errors in data are errors introduced into the data before it reaches the computer. These data errors may be caused by such things as systematic and random measurement errors, measurement recording errors, and data input errors (caused by a faulty paper tape reader, for example). Truncation errors are caused by the necessity of truncating an infinite series representation of a function for computational purposes. For example, calculation of the sine of x from the series,

$$\sin x = x - \frac{x^3}{3!} + \frac{x^5}{5!} - \frac{x^7}{7!} + \ldots \qquad (9\text{-}1)$$

leads to truncation errors because an exact answer can be obtained only by computing the values of an infinite number of terms.

Roundoff errors are caused by memory limitation in the computer. Depending on the machine design, only so much memory is allocated for storage of a number. Also, arithmetic processors are limited in the size of numbers upon which they can operate. Thus, only an approximation for such irrational numbers as π and e may be stored and used in a computer. The TDANA system minicomputer, operating in BASIC, is capable of storing and operating upon numbers up to seven decimal digits in length. Remaining least significant digits are simply discarded.

It is known that both truncation and roundoff errors are generated by an FFT computation but an exhaustive attempt to establish bounds on these errors remains for necessary future work.

Another source of computational error that must be considered is the error introduced by the FFT algorithm. Use of this algorithm not only generates errors of truncation and roundoff, as mentioned above, but also errors due to aliasing and windowing may be introduced.

As discussed in Chapter 4 aliasing errors occur whenever the frequency content of the acquired time domain waveform exceeds $1/2\Delta t$ where Δt is the time sampling interval. For the most part, these errors may be effectively eliminated by use of bandpass or low pass filters, either analog or digital, that remove any frequency components of the time domain waveform at or above the Nyquist frequency.

Errors introduced by windowing are more difficult to resolve. The problem faced is that leakage errors will occur in the FFT computation if the time domain waveform to be transformed does not start and stop at exactly the same value of amplitude. Physically, it is considered impractical to either build or modify the system pulse driving sources to exhibit this characteristic. Rather, an algorithm was devised that operates on the

acquired waveform in such a manner that the equal-amplitude requirement is always met (see section 4.4 for description). This algorithm works quite well for the pulse sources used in the TDANA but it should be kept in mind that a blind application of this rule may lead to disaster. At present, a mathematical study is in progress to determine the types of time domain functions suitable for reduction by means of this algorithm. Preliminary results indicate that time domain waveforms whose beginning and end point slopes are zero may be operated on by the algorithm with error-free results. Conclusive results of this analytical study will be published at a later date.

9.3 Random Errors

For purposes of random error source identification and error evaluation, the random errors associated with data acquisition have been categorized as being either X-axis or Y-axis errors, and further, as either short term or long term in nature. What follows is a discussion of these different errors along with the results of a number of experiments performed in an effort to quantify some of these errors.

9.3.1 Y-Axis Random Errors -- Short Term

A set of experiments was performed to determine experimentally the shape of the probability density function for the overall Y-channel short term noise. Figure 9-1 shows a typical noisy sweep of 1024 points obtained on the TDANA with a sampling oscilloscope vertical deflection factor of 10 mV/cm and with no input signal to the sampler. In order to show that additive time-domain waveform averaging is a valid data processing operation for removing Y-channel noise, it is more that sufficient to show that the Y-channel density function is symmetrical about the mean and that the Y-channel noise is serially uncorrelated. That is, at each X sampling location, if the voltage probability density function is an even function about the mean then

$$\lim_{N\to\infty} v(x) = \lim_{N\to\infty} \left\{ \frac{1}{N} \sum_{j=1}^{N} [v_s(x) + v_j(x)] \right\} = v_s(x) \qquad (9\text{-}2)$$

where N = number of voltage samples taken at location X

$v(x)$ = value of voltage obtained at location x after additively averaging N voltage samples

$v_s(x)$ = actual signal voltage at location x

$v_j(x)$ = random noise voltage added to j^{th} voltage sample taken at location x.

Equation (9-2) will be satisfied, that is, the actual signal voltage may be separated from the noise, if the voltage probability density function for $v_j(x)$ is symmetrical, has a zero mean, and the v_j's are uncorrelated.

The experimental technique used to determine the Y-channel short term probability density function follows. Using the system minicomputer, sequences of 2048 Y-channel sample voltages were obtained and recorded for various fixed locations of X and Y on the CRT screen. The sampling rate was approximately 10 kHz. For each location (X,Y) that was tested on the sampling oscilloscope, the 2048 voltage points obtained were sorted such that the points were listed in order from smallest to largest in voltage magnitude. Every eighth point was then plotted on a specially scaled normal probability graph. The graph is so scaled that a linear plot of data indicates a normal (Gaussian) density function for that data.

Figure 9-2 is a plot of a set of 2048 points taken at center screen on the sampling oscilloscope display. The horizontal axis of this graph is calibrated in units of millivolts and the vertical axis is calibrated in both percentage of points below a value v (left scale), and in units of standard deviation (right scale). The vertical scale is linear in σ (standard deviation) for a normal probability density function. Thus, one would expect a constant-slope plot to result from data that is normally distributed. It is observed from this plot that the Y-channel data obtained from the TDANA center screen display appears to behave in an essentially Gaussian manner. Results of the same experiment performed at different CRT locations yielded virtually the same results. Additional preliminary experiments, to be reported at a later date, appear to indicate that the Y-channel noise is essentially uncorrelated. Experimentally, then, it appears that additive voltage waveform averaging is a valid technique to remove the short term Y-channel noise voltage from the desired signal voltage. Figure 9-3 is an example of 100 averages of a 25 mV pulse. A dramatic improvement is quite apparent.

9.3.2 X-Axis Random Errors -- Short Term

In addition to the vertical noise described above, another major source of random errors is time base (X axis) jitter. Elliott gave some consideration to the effects of X-axis drift and jitter in a paper published in November, 1970 [47]. The derivations and experimental results reported in this section are an extension and mathematical justification for Elliott's assumption that stationary X-axis jitter has the effect of a low-pass filter in a sampling system.

Experiments similar to those used to determine the Y-channel noise characteristics were performed to determine the X-channel noise characteristics (short term). A more circumspective approach was taken, however, in order to obtain X-channel noise data that most nearly resembled that observed in normal TDANA operation.

Figure 9-4 is a 1024 point single-sweep representation of a tunnel diode pulse acquired on the TDANA. The vertical deflection factor was 50 mV/cm and the horizontal time scale was 10 ps/cm. By positioning the 50% point of this waveform as close as possible to center-screen, and by acquiring a set of 2048 vertical voltage samples with X fixed at center screen, it was possible to obtain a reasonable estimate for the X-channel noise characteristics as described below.

The 2048 points obtained may be considered realizations of a random variable Z where

$$Z = X \tan \theta + Y \tag{9-3}$$

The following assumptions are made (see figure 9-5): (1) Y, the random variable corresponding to Y-channel noise is small compared to X, the X-channel noise random variable; (2) X and Y are independent random variables; (3) the rising portion of the tunnel diode pulse is linear near the 50% point; and (4) the rising portion of the pulse crosses the X axis at an angle θ at the 50% point.

Then X may be obtained from eq. (9-3),

$$X = (Z-Y)\cot \theta \tag{9-4}$$

and the standard deviation for X becomes (for X and Y independent)

$$\sigma_x = [(\sigma_z^2-\sigma_y^2)\cot^2 \theta]^{\frac{1}{2}} \tag{9-5}$$

Note that for eqs. (9-3) through (9-5), the units of X, Y, and Z are centimeters. Appropriate CRT deflection factors must be used to convert these variables to units of either time or voltage.

For the case of a tunnel diode pulse, θ was measured to be approximately 65° and σ_x was computed from eq. (9-5) to be 3 ps using a 10 ps/cm conversion factor. Figure 9-6 is a normal probability plot of the data obtained as realizations of Z. A separate measurement on the 50 mV/cm vertical scale, similar to those performed in section 9.3.1, was made to determine σ_y. It was found that σ_z was approximately equal to 0.61 cm while σ_y was approximately equal to 0.05 cm. Thus, since $\sigma_z >> \sigma_y$, figure 9-6 may be considered essentially a plot of the density function of X and has been scaled in units of picoseconds. It will be noted that the plotted data is not quite linear. The most probable explanation for this nonlinearity (deviation from Gaussian distribution) is that the rising portion of the displayed tunnel diode pulse deviated substantially from the assumed linearity.

Summarizing up to this point, a reasonable estimate for $p_x(x)$ has been experimentally measured to the extent that assumptions (1) through (4), above, have been satisfied. The question that remains is what are the effects of this X-axis short-term jitter with respect to the time domain response of the sampling system and the computed frequency domain values. An intuitive answer to this question may be obtained by studying figure 9-7. Notice that the idealized waveforms appear to become filtered by some equivalent low-pass filter when subjected to voltage additive time domain averaging in the presence of X-axis jitter. What are the characteristics of this equivalent filter?

To answer this question analytically, consider an idealized sampling system, with a perfectly impulsive sampling gate, such that an exact representation of any measured voltage waveform, f(t), will be acquired and displayed. Next, allow this "perfect" sampler one flaw; assume that for each X-axis sampling location the delay between the sampling trigger and the time at which a voltage sample is actually taken consists of the proper delay time plus a stationary random noise delay component. For the i^{th} X location and the j^{th} sample taken at that location,

$$\tau = T + t_{ij} \tag{9-6}$$

where τ, a random variable, is the actual trigger to sample delay time, T is the correct delay time, and t_{ij} is the random added error delay time caused by the assumed X-axis stationary noise. (t_{ij} may be either positive or negative.) Also, assume that the statistics of τ are not functions of i.

Next, assume an idealized pulse source that generates an exactly (jitter-free) periodic train of unity-amplitude rectangular pulses each of width Δt. Then, for conventional time-sequential sampling of the assumed rectangular waveform one would expect samples of zero volts to be acquired and displayed except when τ falls in the interval

$$\hat{T} < \tau \leq \hat{T} + \Delta t \tag{9-7}$$

where $\hat{T}$ is the delay time between the sampling trigger and the rectangular pulse (see figure 9-8). Whenever τ does fall in the above interval, a unity volts sample will be acquired and displayed.

If this idealized sampling system is allowed to acquire N complete sweeps each consisting of K equally spaced samples separated by Δt, and if these acquired waveforms are stored in memory such that

$$V_i = \frac{1}{N} \sum_{j=1}^{N} v_{ij} \qquad i = 1,2,3,\ldots,K \tag{9-8}$$

where V_i is the sum of all voltage samples taken at the i^{th} X location and the v_{ij} are the individual voltage samples taken at the i^{th} X location, then the

resulting waveform, in the limit as $N \to \infty$, will simply be the discrete probability density function of τ (see figure 9-9). In addition, this waveform will be the time-domain averaged impulse response of the sampling system if the rectangular pulse width and the sampling period are simultaneously allowed to approach a zero limit ($\Delta t \to 0$).

Now, realizing that the density function for τ is really identical to the previously defined density function $p_x(x)$ for X-axis stationary jitter, then the effect of this jitter may be calculated, in both the time domain and frequency domain, from the <u>measured</u> $p_x(x)$!

As an aside, recalling eq. (9-3),

$$Z = X \tan \theta + Y \tag{9-3}$$

it will be noted that, for an arbitrary deterministic input waveform, as opposed to the constant-slope model waveform of figure 9-5, tan θ will not be constant. Rather, it will be the slope or first derivative of the input waveform at the (unknown) actual sampling location in time. Fortunately, the results of the idealized sampler model theory eliminate the need for attempting to solve eq. (9-3) for an arbitrary input waveform.

Assume, for simplicity only, that the time domain averaged waveform acquired from the idealized sampler model (and thus $p_x(x)$) is a Gaussian waveform of the form

$$g(t)_{AVG} = Ae^{-\frac{1}{2}\left(\frac{t}{t_1}\right)^2} \tag{9-9}$$

where A is a constant and the standard deviation $\sigma_t = t_1$. Then the frequency domain effects of this assumed Gaussian time jitter may be obtained by taking the Fourier transform of eq. (9-9) to yield

$$G(f) = Be^{-\frac{1}{2}\left(\frac{f}{f_1}\right)^2} \tag{9-10}$$

where

$$B = At_1\sqrt{2\pi} \tag{9-11}$$

and where f_1 is the frequency domain standard deviation, related to the time domain standard deviation by,

$$\sigma_f = f_1 = \frac{1}{2\pi t_1} \tag{9-12}$$

To summarize, it has been shown that a stationary Gaussian time jitter in a sampling oscilloscope system may be thought of as having the same effect as a Gaussian roll-off low-pass filter introduced into the Y-axis channel, when additive time domain signal averaging is employed. Furthermore, it

has been shown that a measurable density function, $p_x(x)$, may be used to calculate the effective cutoff frequency of a sampling system as well as its time domain impulse response due to time axis jitter.

Thus, for the TDANA sampling on the 10 ps/cm scale in a free-running trigger mode with Gaussian time jitter present,

$$f_1 \simeq \frac{1}{2\pi(3\text{ ps})} = 53\text{ GHz} \tag{9-13}$$

That is, the standard deviation cutoff frequency of the sampling system due only to stationary time jitter, is approximately 53 GHz. Or, in terms of voltage decibels, the 3 dB cutoff frequency may be calculated from the equation

$$-3\text{ dB} = 20\log_{10} e^{-\frac{1}{2}\left(\frac{f}{53\text{ GHz}}\right)^2} \tag{9-14}$$

to yield a 3 dB cutoff frequency of approximately 44 GHz.

It should be noted here that, in practice, the density function $p_x(x)$ must be measured for each sampling sweep speed setting on the TDANA. It is not valid to assume that the same σ of 3 ps would be measured on, say, the 100 ps/cm or the 1 ns/cm sweep ranges. Measurements on all other sweep ranges remain to be done as future work.

With the above derivation for X-axis jitter, a TDANA system transfer function may be stated for the case where sufficient additive time domain averaging is utilized.

$$R(f) = G(f)I(f)P_f(f) \tag{9-15}$$

where $R(f)$ = system response in frequency domain
$G(f)$ = unknown input waveform in frequency domain
$I(f)$ = system transfer function due to all deterministic causes (non-ideal sampling gate for example)
$P_f(f)$ = X-axis density function in frequency domain.

In the time domain, eq. (9-15) becomes a convolution as follows,

$$r(t) = g(t) * i(t) * p_t(t) \tag{9-16}$$

in the limit as $\Delta t \to 0$ where Δt is the sampling period (see figure 9-10).

Equations (9-15) and (9-16) do not account for any non-stationary random processes that may exist in the TDANA system. These sources of error are discussed in the next section.

It also should be noted that some prior work has been done in an effort to identify I(f) and/or i(t). In particular, Nahman's and Jickling's work [48], using innovative frequency domain techniques to characterize broadband

sampling heads, is very promising. Considerable future work remains, however, in order to achieve a suitably accurate estimate of I(f) or i(t) for the TDANA. Nahman, Chipman and Lennon are continuing this work at the University of Toledo.

9.3.3 X- and Y- Channel Errors -- Long Term

Up to this point the errors discussed have been either systematic errors that cause a fixed error bias in the system or random errors assumed to have only time-invariant statistics. The remaining class of errors to be discussed are those errors, either of a random or systematic nature, that exhibit some time-varying statistics. Of these, by far the most detrimental are "drift" and "hopping" errors.

Drift errors are particularly troublesome to deal with. Experiments may be conducted (yet to be done) which will yield an estimate of the characteristics of any X- or Y-channel drift, but even with this knowledge, it is very difficult to remove the effects to an adequate degree of precision through software. It is felt that hardware waveform stabilization techniques offer the most promise as a means of controlling drift. Elliott, in particular, has devoted a sizeable amount of work to this problem [49]. In addition, Nicolson and Cronson, et al., at Sperry Rand Research, have developed a three-point sampling technique designed to detect and correct drift errors in certain classes of waveforms [50]. It remains as a large future effort, however, to find a suitable solution to drift errors.

Hopping errors are defined as waveform acquisition errors caused by an abrupt shift of the waveform during acquisition. Probable causes of these errors are hardware problems such as intermittent switch contacts, faulty circuits, and intermittent or faulty connectors (as well as miscellaneous gremlins and spooks). The relatively straightforward solution to problems of this sort involves utilization of careful hardware assembly and maintenance practices.

The last error source in this category that bears discussion is electromagnetic interference (EMI). This includes RFI, computer noise, power supply fluctuations, ground loops, etc. In terms of general system development, where the TDANA may be utilized in any of a number of non-laboratory (ideal) environments, more care would be expected to be necessary to ensure that these errors did not creep into the system.

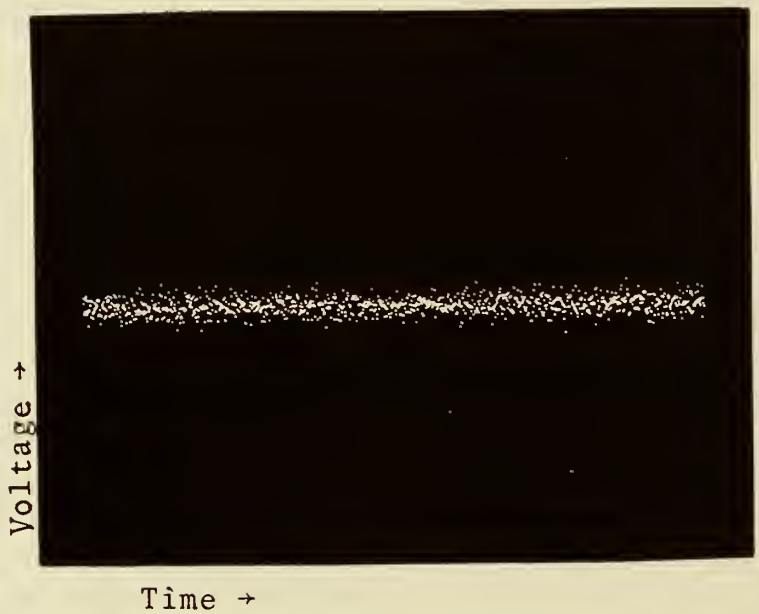

Figure 9-1. Typical 1024-Point Noisy Display on the Monitor CRT With the Sampling Oscilloscope Deflection Factor Set at 10 mV/cm and With No Signal Input.

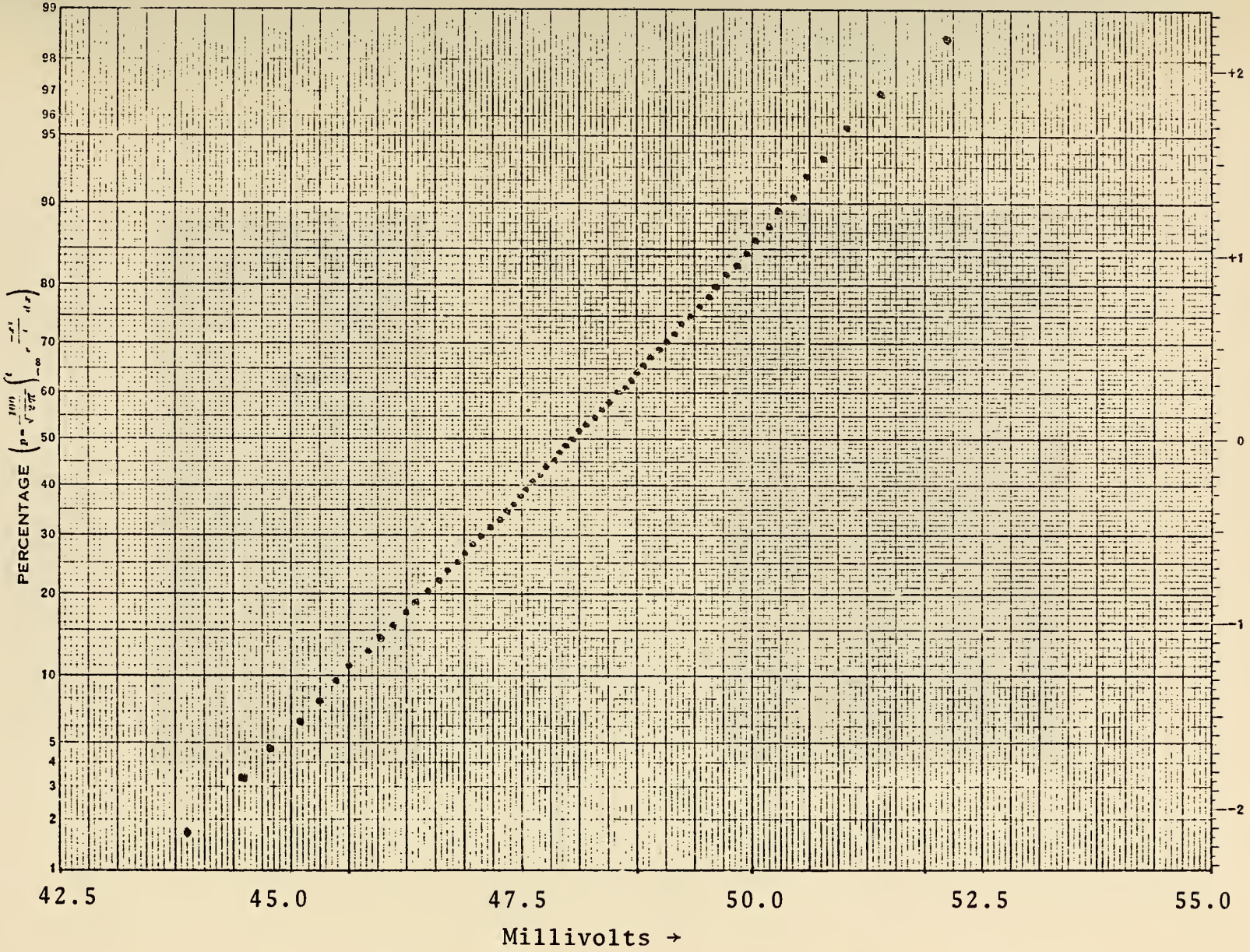

Figure 9-2. Y-Channel Center-Screen Short Term Noise Plot.

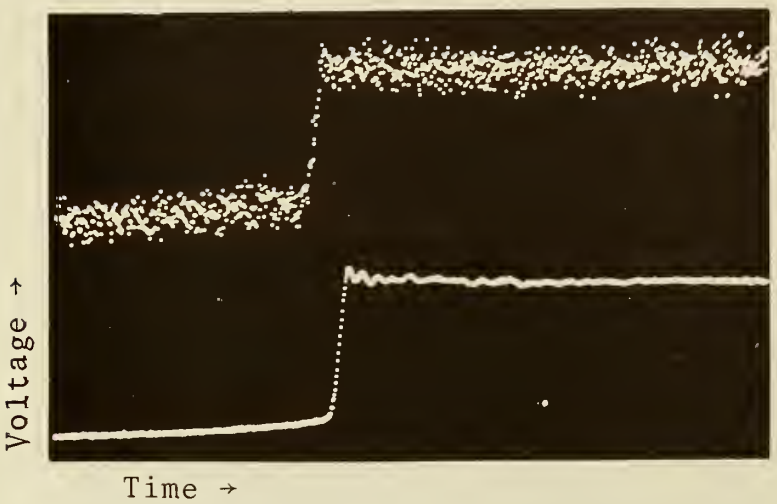

Figure 9-3. Example of Additive Time Domain Signal Averaging. The Signal is a 25 mV Pulse Displayed in a 2 ns Window. The Top Trace is a Single Sweep While the Bottom Trace is the Result of 100 Averages.

Figure 9-4. 1024-Point Single-Waveform Representation of a Tunnel Diode Pulse Acquired on the TDANA. Oscilloscope Settings Were 50 mV/cm and 10 ps/cm.

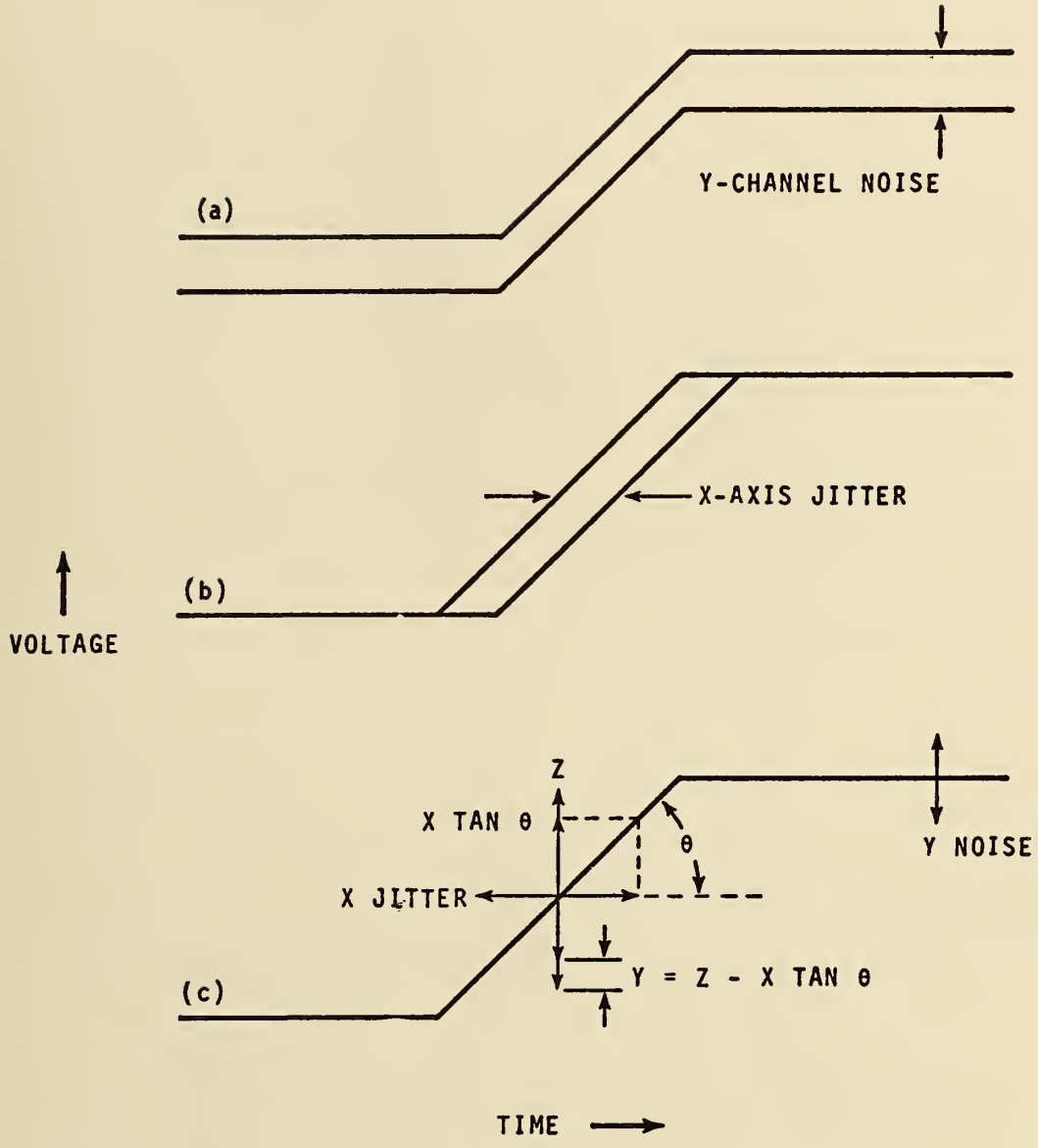

Figure 9-5. Waveform Models Used for X-Axis Noise Analysis.

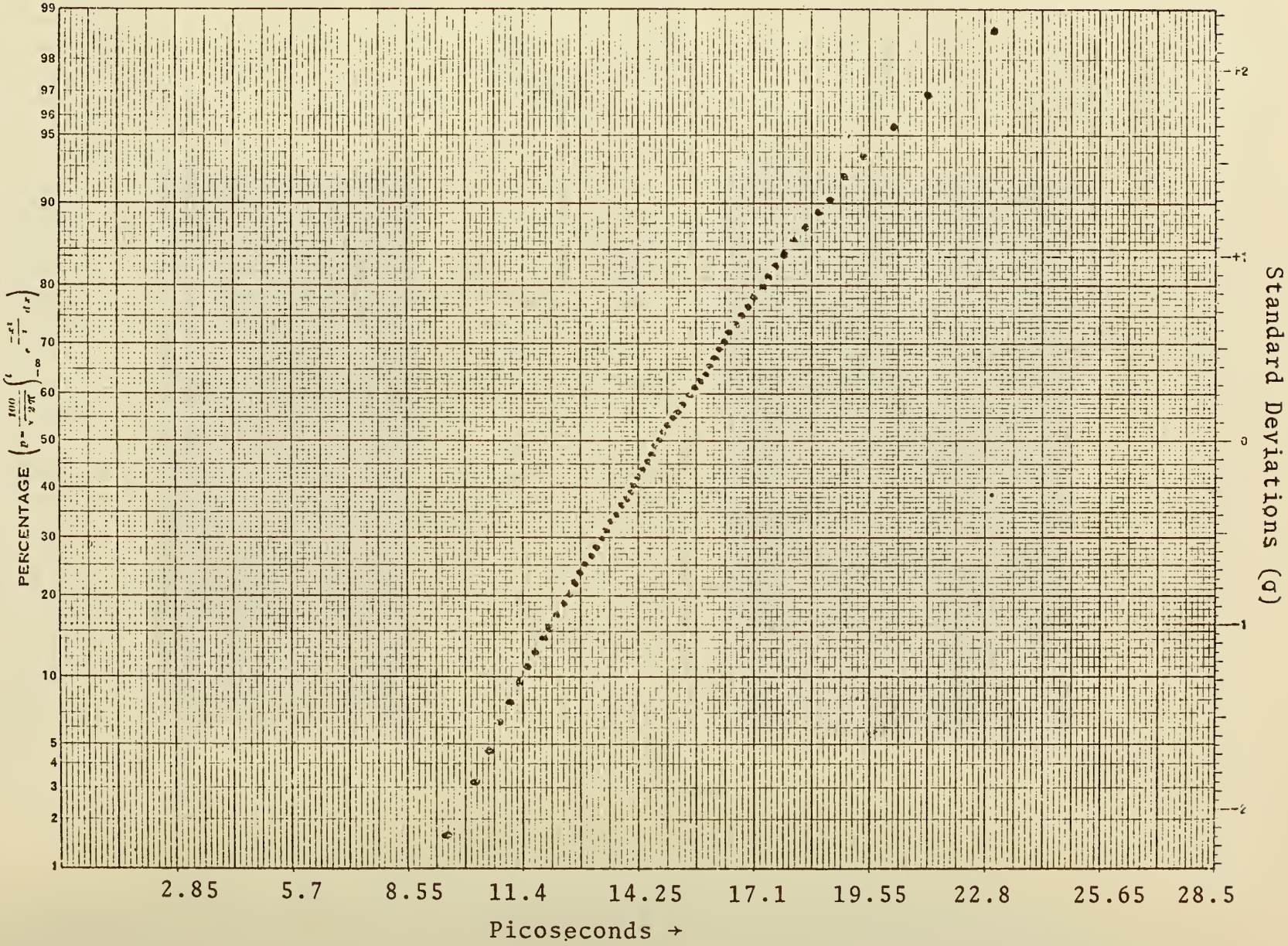

Figure 9-6. Normal Probability Plot of X-Channel Noise (Time Jitter).

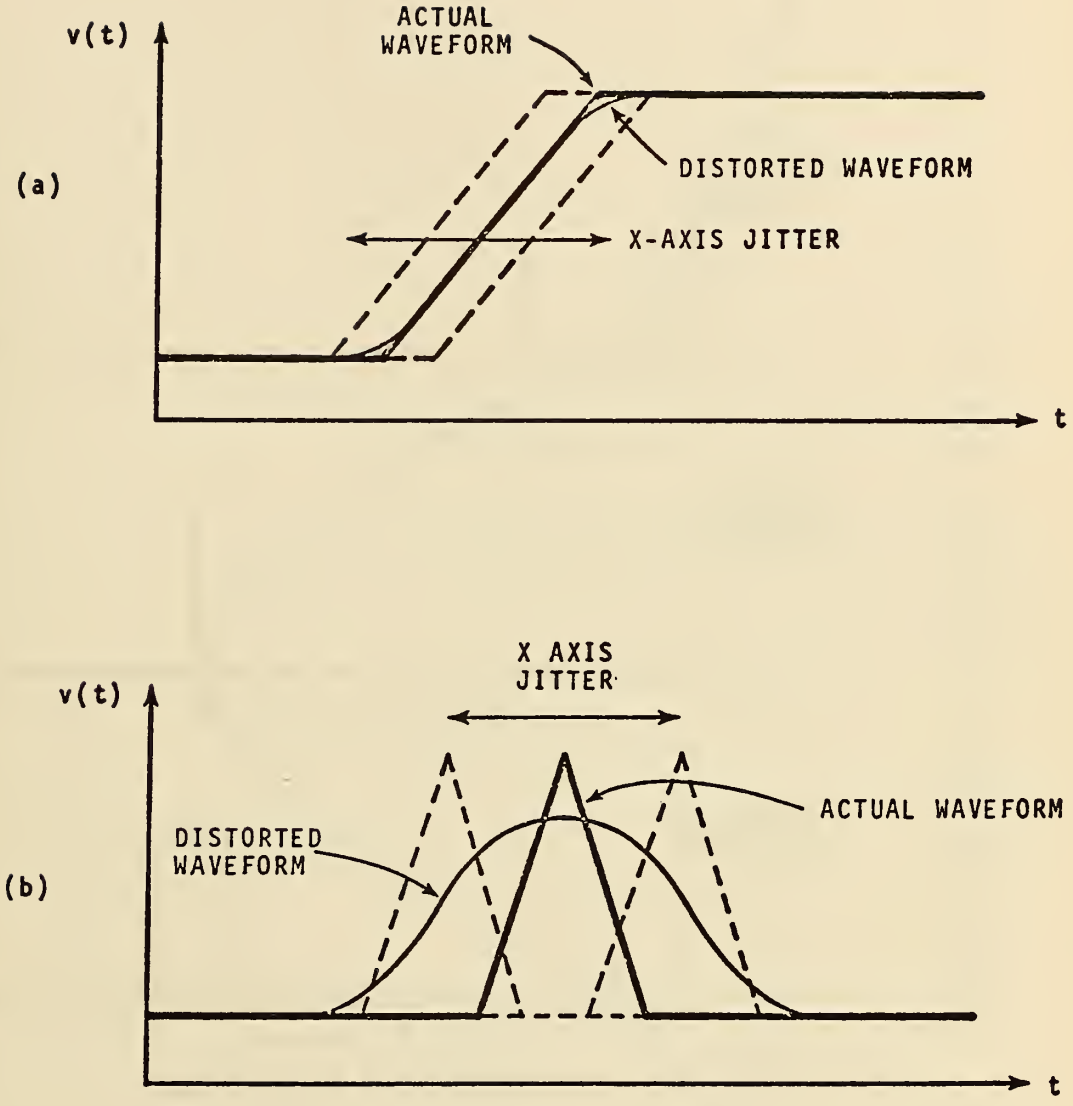

Figure 9-7. Plots of an Ideal Ramp Waveform (a) and an Ideal Triangular Waveform (b) Showing the Filtering Effects Caused By X-Axis Time Jitter.

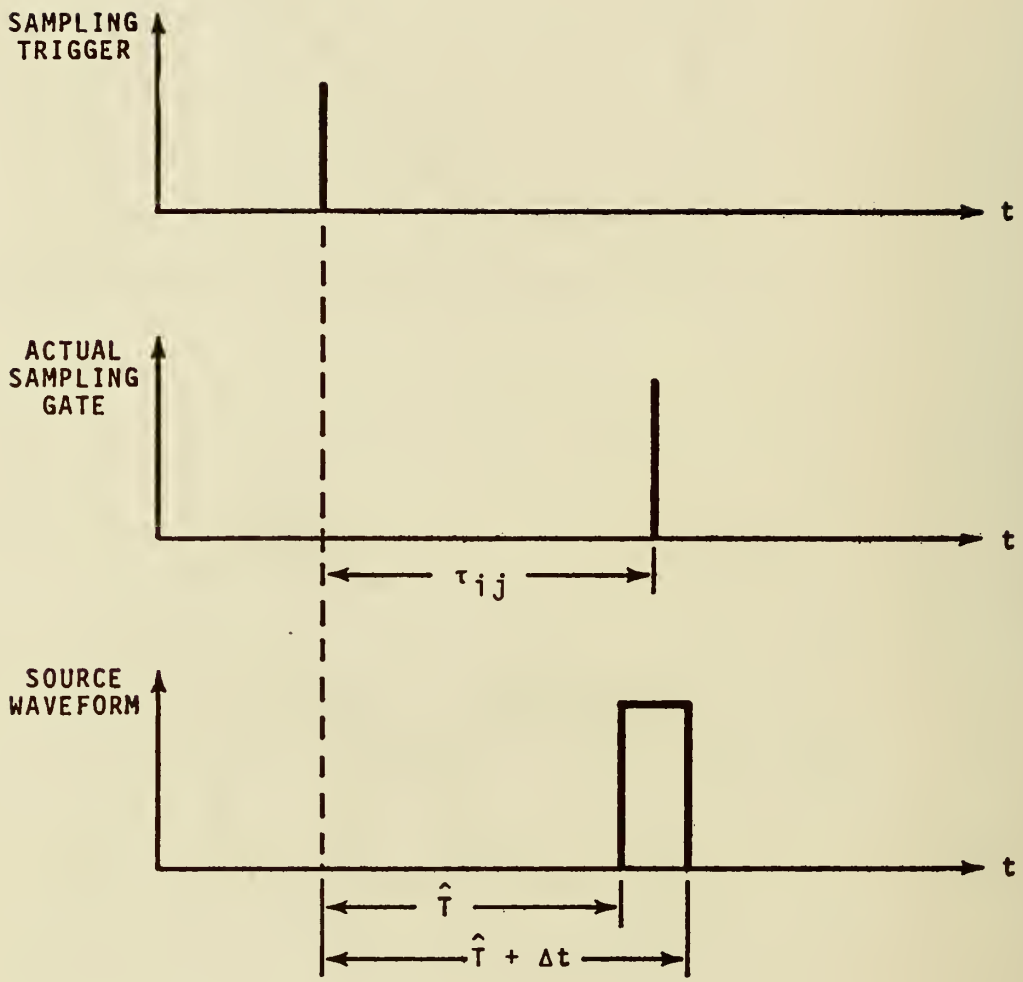

Figure 9-8. Typical Time Relationship of the Sampling Trigger, Actual Sampling Gate and Source Waveform in the Presence of X-Axis Time Jitter.

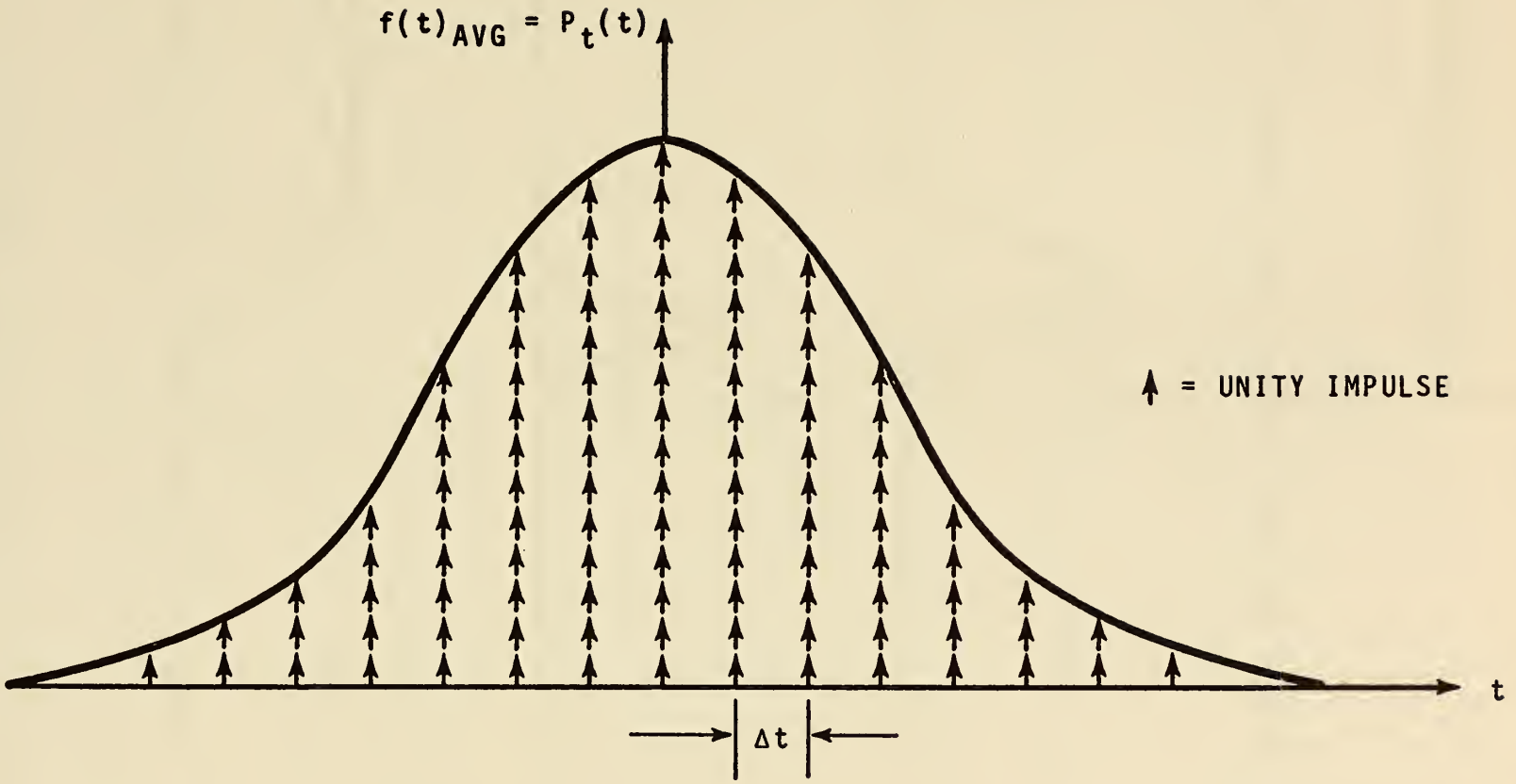

Figure 9-9. Probability Density Function, $P_t(t)$, Acquired From Idealized Sampler Model as N Approaches Infinity.

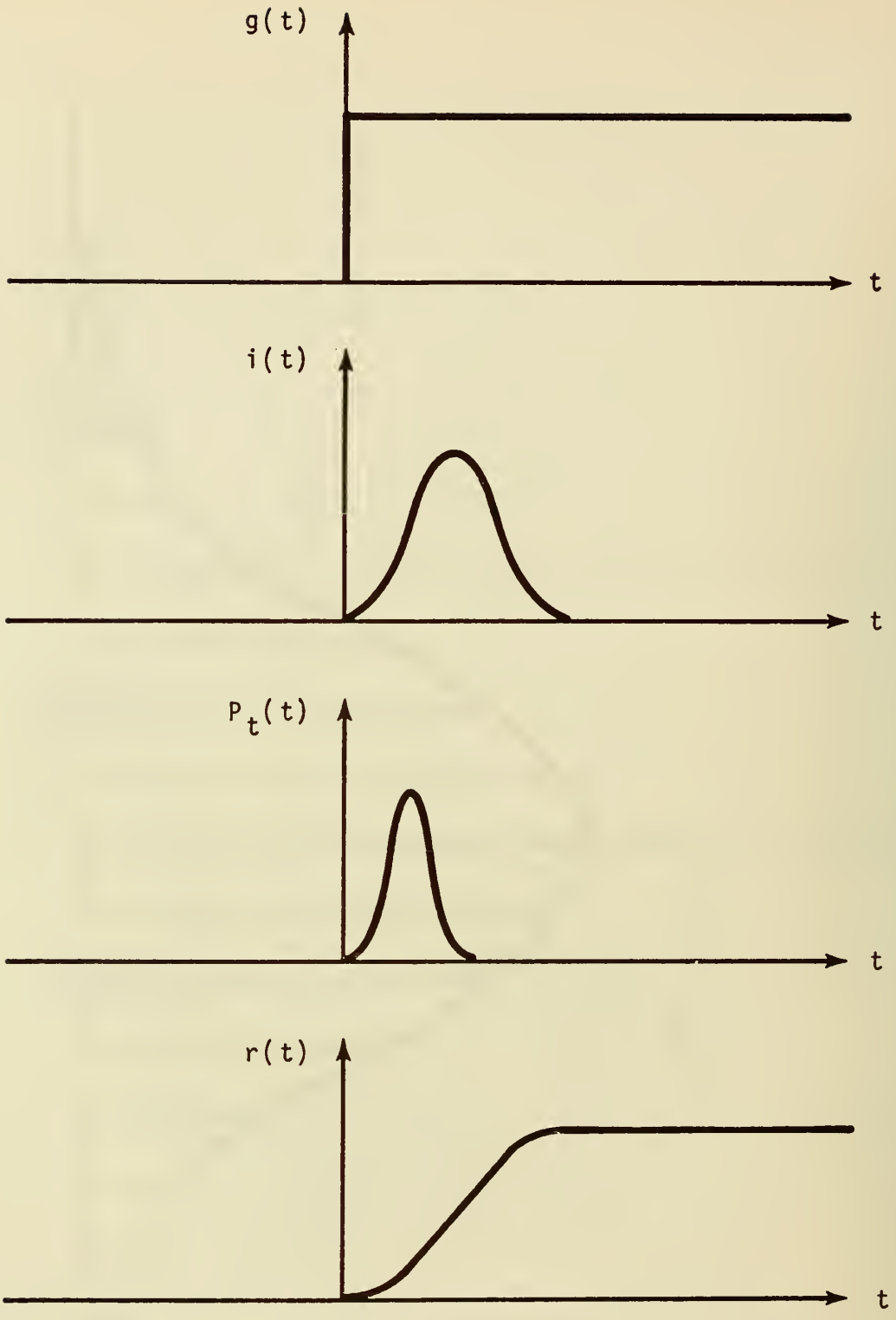

Figure 9-10. Plots of Typical Shapes of i(t), $P_t(t)$ and r(t) For an Assumed Unit Step Waveform For g(t).

10. SUMMARY AND CONCLUSIONS

10.1 Introduction

This final chapter is composed of two sections. First, a brief chapter-by-chapter summary is presented emphasizing key conclusions drawn from work accomplished to date. The second section is devoted to a future work plan along with suggested priorities.

10.2 Report Summary

The introductory chapter presented an overview of the report along with a brief history of prior time domain metrology work done both at NBS and at other laboratories.

Chapter 2 was devoted to a theoretical development and justification for using time domain techniques to measure insertion loss and scattering parameters of microwave devices. In particular, it was shown that accurate measurements can be achieved over a certain time window regardless of the generator and load impedance match and the oscilloscope transfer function.

In Chapter 3 the interrelationships of the Fourier integral transform, Fourier series, discrete Fourier transform and fast Fourier transform were discussed. Terminology and units were stressed in order to avoid confusion.

The next chapter consisted of a set of actual discrete Fourier transforms of ideal rectangular pulses performed on the system minicomputer. The pulses and their resulting spectrum amplitudes were chosen to point out some of the pitfalls and problems associated with applying the FFT to time domain measurements.

Chapter 5 contains a description of the TDANA system. The three major parts of the system, pulse generator, sampling oscilloscope and minicomputer, are discussed in detail with an emphasis on design criteria and available state-of-the-art components. Chapter 6 provides a detailed description of the complete sampling oscilloscope/minicomputer interface. This interface was the most formidable hardware obstacle to overcome in the development of the TDANA.

The system software package was presented in Chapter 7. At this stage of system development it should be noted that the software is in a continual state of change. Additional comments on future software goals are presented in the next section. This chapter also contains a description of a new windowing algorithm that, for certain classes of time domain waveforms, yields transform magnitude spectra essentially free of leakage errors and free of ambiguity between spectral zeros caused by the measured waveform and those caused by the necessarily finite time window.

Chapter 8 contains the results of some wideband coaxial attenuator insertion loss measurements. The measurements were performed on the TDANA and two frequency domain systems with a resulting ± 1.5% system agreement over a 40 dB range and a band of frequencies from 500 MHz to 12.4 GHz.

Chapter 9 contains a partial system error analysis as pertains primarily to insertion loss measurements. Particular emphasis in this work was placed on an analysis of Y and X channel short term noise and jitter. The effects of X-axis jitter were shown to behave as a low pass filter when additive time domain signal averaging is employed and a method for measuring the characteristics of this equivalent filter was presented.

In summary, this technical note is a report of work accomplished to date at NBS toward the development of an automated time domain measurement system. In comparison to frequency domain measurement technology, the art and science of time domain metrology is considered to be in its infancy. A great deal of future work remains.

10.3 Future Work

As presently envisioned there will be several major areas of future work. Most of these will be undertaken in parallel. The first of these is concerned with the automation of the APMS for pulse parameter measurements such as rise time, delay time, distortion, and spectrum amplitude among others. One of the long range goals of this work will be to establish standards of terminology and of measurable parameters for pulses geared to the end user and his application needs.

The second area of major effort will be that of system measurement error analysis. Further work will be done relative to modeling, measurement and reduction of system errors, both systematic and random. Closely related, further work is planned in the area of hardware modeling of system elements such as samplers and pulse generators.

The third major work topic will be software development. In the immediate future, the flexible disk mass memory storage unit will be incorporated into the system to facilitate an on-line operating system built around FORTRAN with called assembly language subroutines. The software system will be file oriented with macro command capability and will eliminate the necessity for paper tape operations almost entirely. In addition, incorporation of hardware floating point array processing is planned to increase both speed and accuracy of the system.

The fourth major effort will be in the area of hardware development. Included in this area will be hardware reduction of sampling system time base drift, development of improved pulse generators and samplers, and construction of microwave hardware assemblies for dedicated use in the measurement of microwave scattering parameters.

The last area of major effort will be an investigation of other possible applications of the APMS system in general. Measurement of broadband antenna characteristics, for example, utilizing time domain techniques appears promising. Investigations will also be conducted into the feasibility of using pseudo-random binary sequence noise generators with the APMS to measure certain parameters of data communication systems over a wide range of frequencies.

REFERENCES

[1] Elliott, B.J., Private communication (Nov. 1974).

[2] Hines, M.E. and H.E. Stinehelfer, Jr., "Time-domain oscillographic microwave network analysis using frequency-domain data," IEEE Trans. MT&T, MTT-22, No. 3, 276-282 (March 1974).

[3] Reeve, G.R., "Calibration of impulse noise generators," NBSIR 73-343, National Bureau of Standards, Boulder, Colorado (Oct. 1973).

[4] Simpson, P.A., "Broadband pulsed/cw calibration signal standard for field intensity meter (FIM) receivers," NBSIR 74-371, National Bureau of Standards, Boulder, Colorado (June 1974).

[5] Nicolson, A.M., "Broadband microwave transmission characteristics from a single measurement of the transient response," IEEE Trans. I&M, IM-17, No. 4, 395-402 (Dec. 1968).

[6] Ross, G.F. and A.M. Nicolson, "The measurement of the intrinsic properties of materials by time domain techniques," IEEE Trans. I&M, IM-19, No. 4, 377-382 (Nov. 1970).

[7] Nicolson, A.M., et al., "Applications of time domain metrology to the automation of broadband microwave measurement," IEEE Trans. PGMTT, MTT-20, No. 1, 3-9 (Jan. 1972).

[8] Cronson, H.M. and G.F. Ross, "Current status of time domain metrology in material and distributed network research," IEEE Trans. I&M, IM-19, No. 4, 495-500 (Nov. 1972).

[9] Cronson, H.M. and P.G. Mitchell, "Time domain measurements of microwave components," IEEE Trans. I&M, IM-20, No. 4, 320-325 (Nov. 1973).

[10] Cronson, H.M., et al., "Extensions of time domain metrology above 10 GHz to materials measurements," IEEE Trans. I&M, IM-21, No. 4 (Dec. 1974).

[11] Stuckert, P., "Computer augmented oscilloscope system," IEEE Trans. I&M, IM-18, No. 4, 299-306 (Dec. 1969).

[12] Norris, N. and R. Hanst, "Picosecond beam monitors and data-acquisition system," IEEE Trans. Nuc. Sci., NS-16, No. 3, 927-931 (June 1969).

[13] Bancroft, J. and R. Johnston, "Microwave measurements by Fourier analysis of network pulse response," Proc. of IEEE, 61, No. 4, 472-473 (April 1973).

[14] Hannaford, D., "The application of picosecond pulses in time domain metrology," Proceedings of the 1972 Joint Measurement Conference, NBS, Gaithersburg, Md. (Nov. 12-14, 1974) (in print).

[15] Gans, W.L, and N. Nahman, "Fast Fourier transform implementation for the calculation of network frequency domain transfer functions from time domain waveforms," NBSIR 73-303, National Bureau of Standards, Boulder, Colorado (Dec. 1972).

[16] Reference Data for Radio Engineers, 5th Ed., Chapter 42 (Howard W. Sams & Co., New York, 1968).

[17] Arthur, M.G., "Impulse spectral intensity -- What is it?," NBSIR 74-365, National Bureau of Standards, Boulder, Colorado (May 1974).

[18] IEEE Standard Dictionary of Electrical and Electronics Terms, IEEE Std. 100-1972, p. 549 (Wiley Interscience, New York, 1972).

[19] Arthur, M.G., op. cit. [17].

[20] Bunze, Vic, "Probing in perspective," AN-152, Hewlett Packard, Colorado Springs, Colorado (1972).

[21] Weber, J., Oscilloscope Probe Circuits (Tektronix, Beaverton, Oregon, 1969).

[22] Wigington, R.L. and N.S. Nahman, "Transient analysis of coaxial cables considering skin effect," Proc. IRE, 45, 166-174 (Feb. 1957).

[23] Atwater, H.A., Introduction to Microwave Theory, pp. 103-107 (McGraw-Hill, New York, 1962).

[24] Campbell, G. and R. Foster, Fourier Integrals for Practical Applications (Van Nostrand Co., New York, 1948).

[25] Gardner, M.F. and J.L. Barnes, Transients in Linear Systems, Vol. 1 (J. Wiley & Sons, New York, 1942).

[26] Bergland, G.D., "A guided tour of the fast Fourier transform," IEEE Spectrum, 41-52 (July 1969). See also other articles in the same issue.

[27] Ibid.

[28] Brigham, E.O., The Fast Fourier Transform (Prentice-Hall, Englewood Cliffs, N.J., 1974).

[29] Cooley, J.W. and J.W. Tukey, "An algorithm for the machine calculation of complex Fourier series," Mat. Comput., 19, 297-301 (April 1965).

[30] Bergland, G.D., op. cit. [26].

[31] Gans, W.L., op. cit. [15].

[32] Brigham, E.O., op. cit. [28].

[33] Shannon, C.E., "Communication in the presence of noise," Proc. IRE, 37 10 (1949).

[34] Bergland, G.D., op. cit. [26].

[35] Nahman, N.S. and R.M. Jickling, "Frequency domain measurement of base-band instrumentation," NBSIR 73-330, National Bureau of Standards, Boulder, Colorado, 28 (July 1973).

[36] Elliott, B.J., "System for precise observation of repetitive picosecond pulse waveforms, IEEE Trans. I&M, IM-19, No. 4, 391-395 (Nov. 1970).

[37] Cox, Charles S. and Ronald Stutheit, "Fast Fourier transform and inverse," Stripps Institute of Oceanography, University of California, San Diego, California (1970).

[38] Beatty, Robert W., Microwave Attenuation Measurements and Standards (National Bureau of Standards Monograph 97, April 1967).

[39] IEEE Standard Specifications and Test Methods for Fixed and Variable Attenuators, DC to 40 GHz, IEEE STD 474-1973 (The Institute of Electrical and Electronics Engineers, Inc., 1973).

[40] Russell, D. and W. Larson, "RF attenuation," Proc. of IEEE, 55, No. 6, 942-959 (June 1967).

[41] Wilson, A.C., Private communication (Nov. 1974).

[42] Beatty, Robert W., "Methods for automatically measuring network parameters," Microwave Journal, 17, 45-49, 63 (April 1974).

[43] Nicolson, A.M., op. cit. [5].

[44] Elliott, B.J., op. cit. [36].

[45] Nahman, N.S., op. cit. [35].

[46] McCracken, Daniel D. and William S. Dorn, Numerical Methods and Fortran Programming, pp. 46-49 (John Wiley & Sons, Inc., New York, 1970).

[47] Elliott, B.J., op. cit. [36].

[48] Nahman, N.S., op. cit. [35].

[49] Elliott, B.J., op. cit. [1].

[50] Ross, G.F., op. cit. [6].

[51] Cooper, G.R. and C.D. McGillen, "Methods of signal and system analysis," Holt, Rinehart & Winston, Inc. (1967).

APPENDIX A-1

```
10  DIM A[255],B[255],C[129],D[129]
100  LET N3=128
110  LET N1=1
120  CALL 1
130  CALL 2,N1,N3
140  PRINT
150  PRINT "TIME SCALE IN NSEC/CM?"
160  INPUT N5
170  PRINT
180  LET F1=(1/N5)*100
190  LET N2=128
200  LET N3=128
210  FOR I= 0 TO 255
220    LET A[I]= 0
230    LET B[I]= 0
240  NEXT I
250  REM    INSERT TEST WAVEFORM HERE
430  REM   FFT STARTS HERE
440  LET G=7
450  LET N=128
460  LET P=8* ATN (1)/N
470  FOR L= 0 TO G-1
480    LET G1= INT (2↑(G-L-1)+.001)
490    LET M= 0
500    LET I9= INT (2↑L+.001)
510    FOR I=1 TO I9
520      LET K1= INT (M/G1)
530      GOSUB  920
540      LET B1= COS (P*K2)
550      LET B2=- SIN (P*K2)
560      FOR J=1 TO G1
570        LET B3=A[M+G1+1]*B1-B[M+G1+1]*B2
580        LET B4=A[M+G1+1]*B2+B[M+G1+1]*B1
 590        LET A[M+G1+1]=A[M+1]-B3
600        LET B[M+G1+1]=B[M+1]-B4
610        LET A[M+1]=A[M+1]+B3
620        LET B[M+1]=B[M+1]+B4
630        LET M=M+1
640      NEXT J
650      LET M=M+G1
660    NEXT I
670  NEXT L
680  FOR I= 0 TO N-1
690    LET K1=I
700    GOSUB  920
710    IF K2>=I GOTO  780
720    LET K3=A[I+1]
730    LET A[I+1]=A[K2+1]
740    LET A[K2+1]=K3
```

```
750    LET K3=B[I+1]
760    LET B[I+1]=B[K2+1]
770    LET B[K2+1]=K3
780  NEXT I
790  FOR I= 0 TO N-1
800    IF A[I+1]>.000001 GOTO  830
810    IF A[I+1]<-.000001 GOTO  830
820    LET A[I+1]= 0
830    IF B[I+1]>.000001 GOTO  860
840    IF B[I+1]<-.000001 GOTO  860
850    LET B[I+1]= 0
860    LET A[I+1]=A[I+1]*A[I+1]
870    LET B[I+1]=B[I+1]*B[I+1]
880    LET A[I+1]=A[I+1]+B[I+1]
890    LET A[I+1]= SQR (A[I+1])
900  NEXT I
910  GOTO  1010
920  LET K2= 0
930  FOR K=1 TO G
940    LET K3=K1-2* INT (K1/2)
950    LET K1= INT (K1/2)
960    IF K3= 0 GOTO  980
970    LET K2=K2+ INT (2↑(G-K)+.001)
980  NEXT K
990  RETURN
1010  FOR I=1 TO 128
1020    LET C[I]=A[I]
1030    LET D[I]=(I-1)*F1
1040  NEXT I
1050  FOR I=1 TO 32
1060    PRINT I,D[I];"MHZ",C[I]
1070  NEXT I
1080  FOR I=1 TO 128
1090    LET A[I-1]=A[I]
1100  NEXT I
1110  LET N3=256
1120  CALL 1
1130  CALL 4, 0,A
1140  CALL 5,N3
1150  GOTO  1140
1160  END
```

```
10  DIM A[255],B[255],C[129],D[129]
100  PRINT "REF. WAVEFORM ACQ. READY? (TYPE 0)"
110  INPUT H1
120  LET N4= 0
130  PRINT
140  PRINT "# OF TIME DOMAIN AVERAGES?"
150  INPUT N1
160  PRINT
170  PRINT "# OF FREQ. DOMAIN AVERAGES?"
180  INPUT N7
190  PRINT
200  PRINT "TIME SCALE IN NSEC/CM?"
210  INPUT N5
220  PRINT
230  CALL 11
240  LET F1=(1/N5)*50
250  FOR H=1 TO N7
260    LET N2=128
270    LET N3=128
280    FOR I= 0 TO 128
290      LET A[I]= 0
300      LET B[I]= 0
310    NEXT I
320    CALL 1
330    LET N6=400
340    CALL 2,N6,N3
350    CALL 1
360    LET N3=256
370    CALL 2,N1,N3
380    CALL 3, 0,A
390    FOR I= 0 TO 127
400      LET A[I]=A[I]/N1
410    NEXT I
420    LET W1=A[3]-A[2]
430    LET W2=A[4]-A[3]
440    LET W3=A[5]-A[4]
450    LET W4=(W1+W2+W3)/3
460    LET A[1]=A[2]-W4
470    LET A[ 0]=A[1]-W4
480    LET M1=A[ 0]
490    CALL 1
500    CALL 4, 0,A
510    FOR I=1 TO 500
520      CALL 5,N3
530    NEXT I
540    LET M2= 0
550    FOR I=60 TO 63
560      LET M2=M2+A[I]
570    NEXT I
```

```
580     LET R=M2/4-M1
590     FOR I= 0 TO 63
600       LET A[I+64]=2*M2/4-A[I]-R
610     NEXT I
620     LET N3=128
630     CALL 1
640     CALL 4, 0,A
650     FOR I=1 TO 500
660       CALL 5,N3
670     NEXT I
680     REM   FFT STARTS HERE
690     LET G=7
700     LET N=128
710     LET P=8* ATN (1)/N
720     FOR I= 0 TO 127
730       LET A[128-I]=A[127-I]
740     NEXT I
750     FOR L= 0 TO G-1
760       LET G1= INT (2↑(G-L-1)+.001)
770       LET M= 0
780       LET I9= INT (2↑L+.001)
790       FOR I=1 TO I9
800         LET K1= INT (M/G1)
810         GOSUB  1340
820         LET B1= COS (P*K2)
830         LET B2=- SIN (P*K2)
840         FOR J=1 TO G1
850           LET B3=A[M+G1+1]*B1-B[M+G1+1]*B2
860           LET B4=A[M+G1+1]*B2+B[M+G1+1]*B1
870           LET A[M+G1+1]=A[M+1]-B3
880           LET B[M+G1+1]=B[M+1]-B4
890           LET A[M+1]=A[M+1]+B3
900           LET B[M+1]=B[M+1]+B4
910           LET M=M+1
920         NEXT J
930         LET M=M+G1
940       NEXT I
950     NEXT L
960     FOR I= 0 TO N-1
970       LET K1=I
980       GOSUB  1340
990       IF K2>=I GOTO  1060
1000       LET K3=A[I+1]
1010       LET A[I+1]=A[K2+1]
1020       LET A[K2+1]=K3
1030       LET K3=B[I+1]
1040       LET B[I+1]=B[K2+1]
1050       LET B[K2+1]=K3
1060     NEXT I
1070     FOR I= 0 TO N-1
```

```
1080      IF A[I+1]>.000001 GOTO  1110
1090      IF A[I+1]<-.000001 GOTO  1110
1100      LET A[I+1]= 0
1110      IF B[I+1]>.000001 GOTO  1140
1120      IF B[I+1]<-.000001 GOTO  1140
1130      LET B[I+1]= 0
1140      LET A[I+1]=A[I+1]*A[I+1]
1150      LET B[I+1]=B[I+1]*B[I+1]
1160      LET A[I+1]=A[I+1]+B[I+1]
1170      LET A[I+1]= SQR (A[I+1])
1180    NEXT I
1190    PRINT
1200    PRINT H
1210    FOR I= 0 TO 31
1220      LET B[I]=10*A[2*I+2]
1230    NEXT I
1240    FOR I=32 TO 255
1250      LET B[I]=10
1260    NEXT I
1270    CALL 12,B
1280    LET X1= 0
1290  NEXT H
1300  LET X1= 0
1310  CALL 13,A
1320  LET X1= 0
1330  GOTO  1420
1340  LET K2= 0
1350  FOR K=1 TO G
1360    LET K3=K1-2* INT (K1/2)
1370    LET K1= INT (K1/2)
1380    IF K3= 0 GOTO  1400
1390    LET K2=K2+ INT (2↑(G-K)+.001)
1400  NEXT K
1410  RETURN
1420  IF N4=1 GOTO  1630
1430  FOR I= 0 TO 31
1440    LET C[I]=A[I]
1450    LET D[I]=(2*I+1)*F1
1460  NEXT I
1470  FOR I= 0 TO 31
1480    PRINT I,D[I];"MHZ",C[I]
1490  NEXT I
1500  LET N4=1
1510  LET N1= 0
1520  LET N5= 0
1530  PRINT
1540  PRINT "UNKNOWN DEVICE WAVEFORM ACQ. READY? (TYPE 0)"
1550   INPUT H2
1560  PRINT
1570  PRINT "NOMINAL INSERTION LOSS IN DB?"
```

```
1580  INPUT Z1
1590  PRINT
1600  PRINT "FULL SCALE INSERTION LOSS IN DB?"
1610  INPUT Z2
1620  GOTO  130
1630  FOR I= 0 TO 31
1640    PRINT I,D[I];"MHZ",A[I]
1650  NEXT I
1660  FOR I= 0 TO 31
1670    LET A[I]=A[I]/C[I]
1680    LET A[I]=20*( LOG (A[I])/ LOG (10))
1690  NEXT I
1700  PRINT
1710  FOR I= 0 TO 31
1720    PRINT I,D[I];"MHZ",A[I];"DB"
1730  NEXT I
1740  LET N3=512
1750  CALL 1
1760  FOR I= 0 TO 31
1770    IF A[I]>-(Z2+Z1) GOTO  1800
1780    LET A[I]= 0
1790    GOTO  1840
1800    LET Z3=9000/Z2
1810    LET A[I]=10000+Z3*A[I]+Z3*Z1
1820    IF A[I]<16383 GOTO  1840
1830    LET A[I]=16383
1840  NEXT I
1850  CALL 4, 0,A
1860  CALL 5,N3
1870  GOTO  1860
1880  END
```

```
10  DIM A[255],B[255],C[255],D[255],E[255]
100  PRINT "REF. WAVEFORM ACQ. READY? (TYPE 0)"
110  INPUT H1
120  LET N4= 0
130  PRINT
140  PRINT "# OF TIME DOMAIN AVERAGES?"
150  INPUT N1
160  PRINT
170  PRINT "# OF FREQ. DOMAIN AVERAGES?"
180  INPUT N7
190  PRINT
200  PRINT "TIME SCALE IN NSEC/CM?"
210  INPUT N5
220  PRINT
230  LET F1=(1/N5)*50
240  CALL 11
250  FOR K=1 TO N7
260    LET N6=1000
270    LET N3=64
280    CALL 1
290    CALL 2,N6,N3
300    LET N2=512
310    LET N3=16384/N2
320    CALL 1
330    CALL 2,N1,N3
340    CALL 3, 0,A
350    CALL 3,256,B
360    FOR I= 0 TO 255
370      LET A[I]=A[I]/N1
380      LET B[I]=B[I]/N1
390    NEXT I
400    LET M1= 0
410    FOR I=1 TO 6
420      LET M1=M1+A[I]
430    NEXT I
440    LET M1=M1/6
450    LET A[ 0]=M1
460    LET M2= 0
470    FOR I=250 TO 255
480      LET M2=M2+B[I]
490    NEXT I
500    LET R=M2/6-M1
510    FOR I= 0 TO 255
520      LET C[I]=2*M2/6-A[I]-R
530      LET D[I]=2*M2/6-B[I]-R
540    NEXT I
550    CALL 1
560    CALL 4, 0,A
570    CALL 4,256,B
```

```
580     CALL 4,512,C
590     CALL 4,768,D
600     LET N3=16
610     FOR I=1 TO 200
620       CALL 5,N3
630     NEXT I
640     LET N0= 0
650     LET N2=2*N2
660     CALL 10,N0,N2,S
670     CALL 9, 0,A
680     CALL 9,256,B
690     CALL 9,1024,C
700     CALL 9,1280,D
710     FOR I= 0 TO 255
720       IF A[I]>.000001 GOTO  750
730       IF A[I]<-.000001 GOTO  750
740       LET A[I]= 0
750       IF B[I]>.000001 GOTO  780
760       IF B[I]<-.000001 GOTO  780
770       LET B[I]= 0
780       IF C[I]>.000001 GOTO  810
790       IF C[I]<-.000001 GOTO  810
800       LET C[I]= 0
810       IF D[I]>.000001 GOTO  840
820       IF D[I]<-.000001 GOTO  840
830       LET D[I]= 0
840       LET A[I]=A[I]*A[I]
850       LET B[I]=B[I]*B[I]
860       LET C[I]=C[I]*C[I]
870       LET D[I]=D[I]*D[I]
880       LET A[I]=A[I]+C[I]
890       LET B[I]=B[I]+D[I]
900       LET A[I]= SQR (A[I])
910       LET B[I]= SQR (B[I])
920       LET C[I]=A[I]
930       LET D[I]=B[I]
940       IF C[I]>1 GOTO  960
950       LET C[I]=1
960       IF D[I]>1 GOTO  980
970       LET D[I]=1
980     NEXT I
990     PRINT
1000     PRINT S
1010     FOR I= 0 TO 255
1020       LET C[I]=2↑(S-10)*6400*( LOG (C[I])/ LOG (10))
1030       LET D[I]=2↑(S-10)*6400*( LOG (D[I])/ LOG (10))
1040     NEXT I
1050     CALL 1
1060     LET N3=32
```

```
1070    CALL 4, 0,C
1080    CALL 4,256,D
1090    FOR I=1 TO 300
1100      CALL 5,N3
1110    NEXT I
1120    FOR I= 0 TO 127
1130      LET A[I]=A[2*I+1]
1140    NEXT I
1150    FOR I= 0 TO 127
1160      LET A[I+128]=B[2*I+1]
1170    NEXT I
1180    FOR I= 0 TO 255
1190      LET A[I]=2↑(S-8)*A[I]
1200    NEXT I
1210    CALL 12,A
1220    LET X1= 0
1230  NEXT K
1240  LET X1= 0
1250  CALL 13,A
1260  LET X1= 0
1270  CALL 4, 0,A
1280  LET N3=64
1290  FOR I=1 TO 300
1300    CALL 5,N3
1310  NEXT I
1320  IF N4=1 GOTO  1470
1330  FOR I= 0 TO 255
1340    LET E[I]=A[I]
1350  NEXT I
1360  LET N4=1
1370  PRINT
1380  PRINT "TEST DEVICE WAVEFORM ACQ. READY? (TYPE 0)"
1390  INPUT H2
1400  PRINT
1410  PRINT "NOMINAL INSERTION LOSS IN DB?"
1420  INPUT Z1
1430  PRINT
1440  PRINT "FULL SCALE INSERTION LOSS IN DB?"
1450  INPUT Z2
1460  GOTO  130
1470  FOR I= 0 TO 255
1480    IF A[I]>.00001 GOTO  1500
1490    LET A[I]=.00001
1500    IF E[I]>.00001 GOTO  1520
1510    LET E[I]=.00001
1520    LET A[I]=A[I]/E[I]
1530    LET A[I]=20*( LOG (A[I])/ LOG (10))
1540  NEXT I
1550  PRINT
```

```
1560  FOR I= 0 TO 100
1570    LET C[I]=(2*I+1)*F1
1580    PRINT I,C[I];"MHZ",A[I];"DB"
1590  NEXT I
1600  CALL 1
1610  FOR I= 0 TO 255
1620    IF A[I]>-(Z2+Z1) GOTO  1650
1630    LET A[I]= 0
1640    GOTO  1690
1650    LET Z3=6000/Z2
1660    LET A[I]=10000+Z3*(A[I]+Z1)
1670    IF A[I]<16383 GOTO  1690
1680    LET A[I]=16383
1690  NEXT I
1700  CALL 4, 0,A
1710  LET N3=64
1720  CALL 5,N3
1730  GOTO  1720
1740  END
```

APPENDIX B-1

```
      000010            .LOC     10        ;SUBROUTINE START ADDRESS
00010 040000            SBTB
      040000            .LOC     40000
40000 040051 SBTB:      INTRP              ;INTERRUPT ROUTINE SA
40001 000001            1                  ;SUBROUTINE CALL NUMBER
40002 040100            MEMC               ;MEMORY CLEAR ROUTINE
40003 000000            000000             ;VARIABLE CODE
40004 000002            2
40005 040200            DATAQ              ;DATA ACQUISITION ROUTINE
40006 120000            120000             ;CALL 2,N1,N3
40007 000003            3
40010 040400            DATOP              ;DATA OPERATE ROUTINE
40011 130000            130000             ;CALL 3,256,B  ETC.
40012 000004            4
40013 040500            DATRT              ;DATA RETURN ROUTINE
40014 130000            130000             ;CALL 4,512,C  ETC.
40015 000005            5
40016 040600            DISPL              ;DATA DISPLAY ROUTINE
40017 100000            100000             ;CALL 5,N3
40020 000006            6
40021 040700            FULSC              ;X-Y RECORD FULL SCALE SET
40022 000000            000000             ;CALL 6
40023 000007            7
40024 040730            ZERO               ;X-Y RECORD ZERO SET
40025 000000            000000             ;CALL 7
40026 000010            10
40027 040750            RECOR              ;X-Y RECORD
40030 000000            000000             ;CALL 8
40031 000011            11
40032 041020            DATD2              ;DATA RTN ROUTINE-SINGLE SPACE
40033 130000            130000             ;CALL 9,0,A  ETC.
40034 000012            12
40035 041747            FFTST              ;FAST FOURIER TRANSFORM
40036 126000            126000             ;CALL 10,N0,N2,S
40037 000013            13
40040 042500            MEMC2              ;SPECTRAL MEMORY CLEAR
40041 000000            000000             ;CALL 11
40042 000014            14
40043 042600            SPECB              ;SPECTRAL DATA TO BINARY
40044 140000            140000             ;CALL 12,A
40045 000015            15
40046 042700            SPECF              ;SPECTRAL DATA TO BASIC
40047 140000            140000             ;CALL 13,A
40050 177777            -1                 ;END OF SUBROUTINE TABLE
                ;          BASIC LINKAGES
      000130 .FIX=      130
      000132 .FLOT=     132
                ;          A/D-D/A LINKAGES
      000021            .DUSR    ADCV=21   ;A/D DEVICE CODE
      000023            .DUSR    DACV=23   ;D/A DEVICE CODE
                ;          INTERRUPT ROUTINE
40051 020404 INTRP:     LDA      0,ADM     ;PUT A/D MASK BIT IN AC(0)
40052 062077            MSKO     0         ;DISABLE A/D INTERRUPT
40053 002401            JMP      0.+1      ;GO TO BASIC INTERRUPT
40054 000521             521               ;IN LOCATION 521
40055 000200 ADM:       200      ;A/D MASK INTERRUPT WORD
                        .EOT
```

APPENDIX B-2

```
                        MEMORY CLEAR ROUTINE
      040100            .LOC    40100     ;ABS. SA
40100 054422 MEMC:      STA     3,RTN1    ;RETURN ADDRESS
40101 030416            LDA     2,CST1    ;2K OF MEMORY RESERVED
40102 050416            STA     2,CNT1    ;COUNTER
40103 020416            LDA     0,A0      ;ZERO
40104 034020            LDA     3,20      ;SAVE LOCATION 20
40105 054416            STA     3,SV20    ;  "
40106 034410            LDA     3,ST1     ;CLEARED MEMORY SA
40107 054020            STA     3,20      ;INITIALIZE AUTOINCREMENT
40110 042020 CLEAR:     STA     0,@20     ;PUT ZERO IN 50000 ETC.
40111 014407            DSZ     CNT1      ;FINISHED?
40112 000776            JMP     CLEAR     ;NO--RETURN
40113 034410            LDA     3,SV20    ;YES--RESTORE LOCATION 20
40114 054020            STA     3,20      ;  "
40115 002405            JMP     @RTN1     ;RETURN TO BASIC
40116 047777 ST1:       47777   ;CLEARED MEMORY SA MINUS 1
40117 004000 CST1:      4000    ;NUMBER OF CLEARED LOCATIONS
40120 000000 CNT1:      0       ;COUNTER FOR CST1
40121 000000 A0:        0       ;CONSTANT 0
40122 000000 RTN1:      0       ;BASIC RETURN ADDRESS
40123 000000 SV20:      0       ;CONTENTS OF LOC 20
                        .EOT
```

APPENDIX B-3

DATA ACQUISITION ROUTINE

```
        040200          .LOC    40200   ;ABS. SA
40200 031400 DATA0:     LDA     2,0,3   ;N1 ADDRESS IN AC(2)
40201 021000            LDA     0,0,2   ;1ST HALF OF N1, IN AC(0)
40202 025001            LDA     1,1,2   ;2ND HALF OF N1 IN AC(1)
40203 054472            STA     3,RTN2  ;RETURN ADDRESS IN RTN2
40204 006130            JSR     @.FIX   ;CONVERT N1 TO BINARY
40205 044464            STA     1,CST2  ;BINARY N1 TO CST2
40206 034467            LDA     3,RTN2  ;RETURN ADDRESS IN AC(3)
40207 031401            LDA     2,1,3   ;N3 ADDRESS IN AC(2)
40210 021000            LDA     0,0,2   ;1ST HALF OF N3 IN AC(0)
40211 025001            LDA     1,1,2   ;2ND HALF OF N3 IN AC(1)
40212 006130            JSR     @.FIX   ;CONVERT N3 TO BINARY
40213 044460            STA     1,CST3  ;BINARY N3 TO CST3
40214 020020            LDA     0,20    ;SAVE LOC 20
40215 040463            STA     0,S20   ;  "
40216 020021            LDA     0,21    ;SAVE LOC 21
40217 040462            STA     0,S21   ;  "
40220 030451            LDA     2,CST2  ;# OF WAVEFORMS IN AC(2)
40221 151400            INC     2,2     ;ADD 1 TO AC(2)
40222 050450            STA     2,CNT2  ;RESULT IN CNT2
40223 034452 SWP1:      LDA     3,RTN2  ;RETURN ADDRESS
40224 014446            DSZ     CNT2    ;# OF WAVEFORMS YET?
40225 000406            JMP     REPT    ;NO--RETURN
40226 020452            LDA     0,S20   ;YES--RESTORE LOC 20
40227 040020            STA     0,20    ;  "
40230 020451            LDA     0,S21   ;RESTORE LOC 21
40231 040021            STA     0,21    ;  "
40232 001402            JMP     2,3     ;RETURN TO BASIC
40233 020444 REPT:      LDA     0,BGN   ;SA FOR STORAGE
40234 040020            STA     0,20    ;AUTOINCREMENT LOC
40235 040021            STA     0,21    ;  "
40236 034440            LDA     3,ADD   ;ZERO IN AC(3)
40237 054435            STA     3,CNT3  ;ZERO POINT COUNTER
40240 030434 PT1:       LDA     2,CNT3  ;POINT COUNTER IN AC(2)
40241 020435            LDA     0,ADD   ;ZERO IN AC(0)
40242 061023            DOA     0,DACV  ;ADDRESS D/A #0
40243 072023            DOB     2,DACV  ;OUTPUT X LOCATION
40244 061121            DOAS    0,ADCV  ;START A/D #0
40245 063621            SKPDN   ADCV    ;CONVERSION FINISHED?
40246 000777            JMP     .-1     ;NO--RETURN
40247 076421            DIC     3,ADCV  ;YES--PUT NUMBER IN AC(3)
40250 177120            ADDZL   3,3     ;REMOVE LEADING SIGN BITS
40251 175220            MOVZR   3,3     ;  "
40252 175220            MOVZR   3,3     ;  "
40253 026020            LDA     1,@20   ;LARGE HALF OF # IN AC(1)
40254 022020            LDA     0,@20   ;SMALL HALF OF # IN AC(0)
40255 163022            ADDZ    3,0,SEC ;ADD TWO SMALL NUMBERS
40256 125400            INC     1,1     ;OVERFLOW, ADD 1 TO AC(1)
40257 046021            STA     1,@21   ;RETURN SUM TO MEMORY
40260 042021            STA     0,@21   ;  "
40261 024412            LDA     1,CST3  ;BITE SIZE IN AC(1)
40262 133000            ADD     1,2     ;INCREMENT POINT COUNTER
40263 050411            STA     2,CNT3  ;NEW COUNT IN CNT3
40264 034404            LDA     3,PEAC  ;TOTAL # OF POINTS IN AC(3)
40265 156414            SUB#    2,3,SZR ;WAVEFORM FINISHED?
40266 000752            JMP     PT1     ;NO--RETURN
40267 000734            JMP     SWP1    ;YES GET NEW WAVEFORM?
40270 040000 PEAC:      40000   ;MAX # OF POINTS (2↑14)
40271 000000 CST2:      0       ;# OF WAVEFORMS
```

```
40272 000000 CNT2:    0         ;WAVEFORM COUNTER
40273 000000 CST3:    0         ;BITE SIZE
40274 000000 CNT3:    0         ;POINT COUNTER
40275 000000 RTN2:    0         ;BASIC RETURN ADDRESS
40276 000000 AD0:     0         ;CONSTANT 0
40277 047777 BGN:     47777     ;SA MINUS 1 FOR DATA STORAGE
40300 000000 S20:     0         ;CONTENTS OF LOC 20
40301 000000 S21:     0         ;CONTENTS OF LOC 21
                      .EOT
```

APPENDIX B-4

```
                                SEND DATA TO BASIC SUBROUTINE
      040400                    .LOC    40400       ;ABS. SA
40400 031400 DATOP:             LDA     2,0,3       ;DATA ARRAY ADR. IN AC(2)
40401 021000                    LDA     0,0,2       ;1ST HALF IN AC(0)
40402 025001                    LDA     1,1,2       ;2ND HALF IN AC(1)
40403 054432                    STA     3,RTN3      ;RETURN ADDRESS TO RTN3
 40404 006130                    JSR     @.FIX       ;CONVERT TO BINARY
 40405 020433                    LDA     0,CST5      ;DATA STORAGE SA IN CST5
40406 125120                    MOVZL   1,1         ;DOUBLE ARRAY NUMBER
 40407 107000                    ADD     0,1         ;ADD SA TO ARRAY NUMBER
40410 020426                    LDA     0,CST4      ;256 POINTS IN ARRAY
40411 040426                    STA     0,CNT4      ;POINT COUNTER
40412 044427                    STA     1,ADBN      ;BINARY ADDRESS
40413 034422                    LDA     3,RTN3      ;RETURN ADDRESS TO AC(3)
40414 035401                    LDA     3,1,3       ;ARRAY SA TO AC(3)
40415 054425                    STA     3,ADFP      ;ARRAY SA TO ADFP
 40416 030423 LOOP:              LDA     2,ADBN      ;BINARY ADDRESS TO AC(2)
40417 021000                    LDA     0,0,2       ;1ST HALF OF # IN AC(0)
40420 025001                    LDA     1,1,2       ;2ND HALF OF # IN AC(1)
40421 151400                    INC     2,2         ;INCREMENT BINARY ADDRESS
40422 151400                    INC     2,2         ;  "
40423 050416                    STA     2,ADBN      ;NEW BINARY ADDRESS TO ADBN
40424 006132                    JSR     @.FLOT      ;CONVERT TO FLOATING POINT
40425 042415                    STA     0,@ADFP     ;1ST HALF TO BASIC ARRAY
40426 010414                    ISZ     ADFP        ;INCREMENT FP ADDRESS
40427 046413                    STA     1,@ADFP     ;2ND HALF TO BASIC ARRAY
40430 010412                    ISZ     ADFP        ;INCREMENT FP ADDRESS
40431 014406                    DSZ     CNT4        ;FINISHED?
40432 000764                    JMP     LOOP        ;NO--RETURN
40433 034402                    LDA     3,RTN3      ;YES--LOAD RETURN ADDRESS
40434 001402                    JMP     2,3         ;RETURN TO BASIC
40435 000000 RTN3:              0                   ;BASIC RETURN ADDRESS
40436 000400 CST4:              400                 ;256-POINT ARRAY
40437 000000 CNT4:              0                   ;POINT COUNTER
40440 050000 CST5:              50000               ;BINARY STORAGE SA
40441 000000 ADBN:              0                   ;CURRENT BINARY ADDRESS
40442 000000 ADFP:              0                   ;CURRENT FLOATING POINT ADDRESS
                                .EOT
```

APPENDIX B-5

```
                                RETURN DATA FROM BASIC ROUTINE
      040500                .LOC    40500    ;ABS. SA
40500 031400 DATRT:         LDA      2,0,3   ;ARRAY ADDRESS IN AC(2)
40501 021000                LDA      0,0,2   ;1ST HALF IN AC(0)
40502 025001                LDA      1,1,2   ;2ND HALF IN AC(1)
40503 054430                STA      3,RTN4  ;RETURN ADDRESS TO RTN4
40504 006130                JSR      @.FIX   ;CONVERT TO BINARY
40505 020427                LDA      0,CST6  ;DATA STORAGE SA TO CST6
40506 107000                ADD      0,1     ;ADD SA TO ARRAY NUMBER
40507 044430                STA      1,BNAD  ;BINARY ADDRESS
40510 020425                LDA      0,CST7  ;256 POINTS IN ARRAY
40511 040425                STA      0,CNT7  ;POINT COUNTER
40512 034421                LDA      3,RTN4  ;RETURN ADDRESS TO AC(3)
40513 035401                LDA      3,1,3   ;ARRAY SA TO AC(3)
40514 054424                STA      3,FPAD  ;ARRAY SA TO FPAD
40515 022423 LUPE:          LDA      0,@FPAD ;1ST HALF TO AC(0)
40516 010422                ISZ      FPAD    ;INCREMENT FP ADDRESS
 40517 026421                LDA      1,@FPAD ;2ND HALF TO AC(1)
 40520 010420                ISZ      FPAD    ;INCREMENT FP ADDRESS
40521 006130                JSR      @.FIX   ;CONVERT TO BINARY
40522 030415                LDA      2,BNAD  ;NEW BINARY ADDRESS TO AC(2)
40523 020416                LDA      0,ZER   ;PUT ZERO IN AC(0)
 40524 045000                STA      1,0,2   ;DATA IN DATA STORAGE
40525 151400                INC      2,2     ;INCREMENT BINARY ADDRESS
40526 050411                STA      2,BNAD  ;NEW BINARY ADDRESS TO BNAD
40527 014407                DSZ      CNT7    ;FINISHED?
40530 000765                JMP      LUPE    ;NO--RETURN
40531 034402                LDA      3,RTN4  ;YES--LOAD RETURN ADDRESS
40532 001402                JMP      2,3     ;RETURN TO BASIC
40533 000000 RTN4:          0        ;BASIC RETURN ADDRESS
40534 050000 CST6:          50000    ;BINARY STORAGE SA
40535 000400 CST7:          400      ;256 POINT ARRAY
40536 000000 CNT7:          0        ;POINT COUNTER
40537 000000 BNAD:          0        ;CURRENT BINARY ADDRESS
40540 000000 FPAD:          0        ;CURRENT FP ADDRESS
40541 000000 ZER:           0        ;CONSTANT 0
                            .EOT
```

APPENDIX B-6

```
                ;              DATA DISPLAY ROUTINE
        040600          .LOC    40600     ;ABS. SA
40600 031400 DISPL:     LDA     2,0,3     ;N3 ADDRESS TO AC(2)
40601 021000            LDA     0,0,2     ;1ST HALF TO AC(0)
40602 025001            LDA     1,1,2     ;2ND HALF TO AC(1)
40603 054431            STA     3,RTN5    ;RETURN ADDRESS TO RTN5
40604 006130            JSR     @.FIX     ;CONVERT N3 TO BINARY
40605 044430            STA     1,CST8    ;BITE SIZE TO CST8
40606 030433            LDA     2,B0      ;ZERO TO AC(2)
40607 020427            LDA     0,CST9    ;DATA STORAGE SA TO AC(0)
40610 040427            STA     0,CNT9    ;DATA ADDRESS COUNTER
40611 020431 POINT:     LDA     0,AD2     ;TWO TO AC(0)
40612 061023            DOA     0,DACV    ;ADDRESS D/A #2
40613 072023            DOB     2,DACV    ;OUTPUT X VALUE TO D/A #2
40614 026423            LDA     1,@CNT9   ;DATA TO AC(1)
40615 020426            LDA     0,AD4     ;FOUR TO AC(0)
40616 061023            DOA     0,DACV    ;ADDRESS D/A #4
40617 066023            DOB     1,DACV    ;OUTPUT Y VALUE TO D/A #4
40620 010417            ISZ     CNT9      ;INCREMENT ADDRESS COUNTER
40621 126400            SUB     1,1       ;DELAY DUMMY INSTRUCTION
40622 126400            SUB     1,1       ;  "
40623 060477            DIA     0,CPU     ;SW 15, 0=STORE, 1=NONSTORE
40624 063123            DOCS    0,DACV    ;SEND Z INTENSIFY PULSE
40625 034413            LDA     3,PEKE    ;MAX # OF POINTS
40626 024407            LDA     1,CST8    ;BITE SIZE TO AC(1)
40627 133000            ADD     1,2       ;INCREMENT X POINT
40630 156414            SUB#    2,3,SZR   ;X SWEEP FINISHED?
 40631 000760            JMP     POINT    ;NO--RETURN
40632 034402            LDA     3,RTN5    ;YES--LOAD RETURN ADDRESS
40633 001401            JMP     1,3       ;RETURN TO BASIC
40634 000000 RTN5:      0                 ;BASIC RETURN ADDRESS
40635 000000 CST8:      0                 ;BITE SIZE
40636 050000 CST9:      50000             ;BINARY STORAGE SA
40637 000000 CNT9:      0                 ;DATA ADDRESS COUNTER
40640 040000 PEKE:      40000             ;MAX NUMBER OF POINTS
40641 000000 B0:        0                 ;CONSTANT 0
40642 000002 AD2:       2                 ;CONSTANT 2
40643 000004 AD4:       4                 ;CONSTANT 4
                        .EOT
```

APPENDIX B-7

```
                ;           X-Y RECORD--FULL SCALE SET
        040700              .LOC    40700   ;ABS. SA
40700 054414 FULSC:         STA     3,RTN6  ;RETURN ADDRESS TO RTN6
40701 020410                LDA     0,D2    ;TWO TO AC(0)
40702 030411                LDA     2,FS    ;FS VALUE TO AC(2)
40703 061023                DOA     0,DACV  ;ADDRESS D/A #2
40704 072023                DOB     2,DACV  ;FS VALUE TO D/A #2
40705 020405                LDA     0,D4    ;FOUR TO AC(0)
40706 061023                DOA     0,DACV  ;ADDRESS D/A #4
40707 072023                DOB     2,DACV  ;FS VALUE TO D/A #4
40710 002404                JMP     @RTN6   ;RETURN TO BASIC
40711 000002 D2:            2               ;CONSTANT 2
40712 000004 D4:            4               ;CONSTANT 4
40713 037777 FS:            37777           ;FULL SCALE VALUE FOR D/A'S
40714 000000 RTN6:          0               ;BASIC RETURN ADDRESS
                ;           X-Y RECORD--ZERO SET
        040730              .LOC    40730   ;ABS. SA
40730 054414 ZERO:          STA     3,RTN7  ;RETURN ADDRESS TO RTN7
40731 020410                LDA     0,DA2   ;TWO TO AC(0)
40732 030411                LDA     2,ZE    ;ZERO TO AC(2)
40733 061023                DOA     0,DACV  ;ADDRESS D/A #2
40734 072023                DOB     2,DACV  ;ZERO VALUE TO D/A #2
40735 020405                LDA     0,DA4   ;ADDRESS D/A #4
40736 061023                DOA     0,DACV  ;  "
40737 072023                DOB     2,DACV  ;ZERO VALUE TO D/A #4
40740 002404                JMP     @RTN7   ;RETURN TO BASIC
40741 000002 DA2:           2               ;CONSTANT 2
40742 000004 DA4:           4               ;CONSTANT 4
40743 000000 ZE:            0               ;ZERO VALUE FOR D/A'S
40744 000000 RTN7:          0               ;BASIC RETURN ADDRESS
                            .EOT
```

APPENDIX B-8

```
                ;                X-Y RECORD SUBROUTINE
        040750          .LOC    40750       ;ABS. SA
40750 054426 RECOR:     STA     3,RTN8  ;RETURN ADDRESS TO RTN8
40751 030426            LDA     2,CT0   ;ZERO TO AC(2)
40752 020430            LDA     0,CT5   ;DATA STORAGE SA TO AC(0)
40753 040430            STA     0,CN5   ;DATA ADDRESS COUNTER
 40754 020430 POYNT:     LDA     0,DELA  ;PEN SPEED FACTOR TO AC(0)
40755 040430            STA     0,DELAY ;PEN SPEED FACTOR TO DELAY
40756 020422            LDA     0,CT2   ;TWO TO AC(0)
40757 061023            DOA     0,DACV  ;ADDRESS D/A #2
40760 072023            DOB     2,DACV  ;X VALUE TO D/A #2
40761 026422            LDA     1,@CN5  ;DATA TO AC(1)
40762 020417            LDA     0,CT4   ;ZERO TO AC(0)
40763 061023            DOA     0,DACV  ;ADDRESS D/A #4
40764 066023            DOB     1,DACV  ;Y VALUE TO D/A #4
40765 010416            ISZ     CN5     ;INCREMENT DATA ADDRESS
40766 014417            DSZ     DELAY   ;PEN SPEED SLOW ENOUGH?
40767 000777            JMP     .-1     ;NO--RETURN
40770 034417            LDA     3,CT7   ;YES--MAX # OF POINTS TO AC(3)
40771 024415            LDA     1,CT6   ;BITE SIZE TO AC(1)
40772 133000            ADD     1,2     ;INCREMENT X POINT
40773 156414            SUB#    2,3,SZR ;X SWEEP FINISHED?
40774 000760            JMP     POYNT   ;NO--RETURN
40775 002401            JMP     @RTN8   ;YES--RETURN TO BASIC
40776 000000 RTN8:      0       ;BASIC RETURN ADDRESS
40777 000000 CT0:       0       ;CONSTANT 0
41000 000002 CT2:       2       ;CONSTANT 2
41001 000004 CT4:       4       ;CONSTANT 4
41002 050000 CT5:       50000   ;DATA STORAGE SA
41003 000000 CN5:       0       ;DATA ADDRESS COUNTER
41004 004400 DELA:      4400    ;PEN SPEED FACTOR
41005 000000 DELAY:     0       ;PEN SPEED COUNTER
41006 000020 CT6:       20      ;BITE SIZE FOR 1024-PT RECORDING
41007 040000 CT7:       40000   ;MAX # OF POINTS
                        .EOT
```

APPENDIX B-9

```
                ;               SEND DATA TO BASIC SUBROUTINE
      041020            .LOC    41020    ;ABS. SA
41020 031400 DAT02:     LDA     2,0,3    ;DATA ARRAY ADR. TO AC(2)
41021 021000            LDA     0,0,2    ;1ST HALF TO AC(0)
41022 025001            LDA     1,1,2    ;2ND HALF TO AC(1)
41023 054432            STA     3,RTN31  ;RETURN ADDRESS TO RTN31
41024 006130            JSR     @.FIX    ;CONVERT TO BINARY
41025 020433            LDA     0,CST51  ;DATA STORAGE SA TO CST51
41026 107000            ADD     0,1      ;ADD SA TO ARRAY NUMBER
41027 020427            LDA     0,CST41  ;256 POINTS IN ARRAY
 41030 040427            STA     0,CNT41  ;POINT COUNTER
41031 044430            STA     1,ADBN1  ;BINARY ADDRESS
41032 034423            LDA     3,RTN31  ;RETURN ADDRESS TO AC(3)
41033 035401            LDA     3,1,3    ;ARRAY SA TO AC(3)
 41034 054426            STA     3,ADFP1  ;ARRAY SA TO ADFP1
 41035 030424 LOOPE:     LDA     2,ADBN1  ;BINARY ADDRESS TO AC(2)
 41036 020425            LDA     0,ZERO1  ;1ST HALF OF # TO AC(0)
41037 025000            LDA     1,0,2    ;2ND HALF OF # TO AC(1)
41040 125112            MOVL#   1,1,SZC  ;IS NUMBER NEGATIVE?
41041 102000            ADC     0,0      ;YES--PUT ONES IN AC(0)
41042 151400            INC     2,2      ;INCREMENT BINARY ADDRESS
41043 050416            STA     2,ADBN1  ;NEW BINARY ADDRESS TO ADBN1
41044 006132            JSR     @.FLOT   ;CONVERT TO FLOATING POINT
41045 042415            STA     0,@ADFP1 ;1ST HALF TO BASIC ARRAY
41046 010414            ISZ     ADFP1    ;INCREMENT FP ADDRESS
 41047 046413            STA     1,@ADFP1 ;2ND HALF TO BASIC ARRAY
41050 010412            ISZ     ADFP1    ;INCREMENT FP ADDRESS
41051 014406            DSZ     CNT41    ;FINISHED?
41052 000763            JMP     LOOPE    ;NO--RETURN
41053 034402            LDA     3,RTN31  ;YES--LOAD RETURN ADDRESS
41054 001402            JMP     2,3      ;RETURN TO BASIC
41055 000000 RTN31:     0        ;BASIC RETURN ADDRESS
41056 000400 CST41:     400      ;256-POINT ARRAY
41057 000000 CNT41:     0        ;POINT COUNTER
41060 050000 CST51:     50000    ;BINARY STORAGE SA
41061 000000 ADBN1:     0        ;CURRENT BINARY ADDRESS
 41062 000000 ADFP1:     0        ;CURRENT FLOATING POINT ADDRESS
41063 000000 ZERO1:     0        ;CONSTANT 0
                        .EOT
```

```
        041600          .LOC    41600
        000002 NUM=     2
        000003 ALPHA=   3
        000004 M=       4
        000005 FLAG=    5
        000006 NUM4=    6
        000007 SCNT=    7
41600 020462 FFTRA:  LDA     0,SPF
41601 101235         MOVZR#  0,0,SNR
41602 000402         JMP     OUT2
41603 000436         JMP     OUT1
41604 102440 OUT2:   SUBO    0,0
41605 024007         LDA     1,SCNT
41606 006132         JSR     @.FLOT
41607 034537         LDA     3,RTN9
41610 031402         LDA     2,2,3
41611 041000         STA     0,0,2
41612 045001         STA     1,1,2
41613 030520         LDA     2,SA2
41614 050002         STA     2,2
41615 030517         LDA     2,SA3
41616 050003         STA     2,3
41617 030516         LDA     2,SA4
41620 050004         STA     2,4
41621 030515         LDA     2,SA5
41622 050005         STA     2,5
41623 030514         LDA     2,SA6
41624 050006         STA     2,6
41625 030513         LDA     2,SA7
41626 050007         STA     2,7
41627 030512         LDA     2,SA20
41630 050020         STA     2,20
41631 030511         LDA     2,SA21
41632 050021         STA     2,21
41633 030510         LDA     2,SA30
41634 050030         STA     2,30
41635 030507         LDA     2,SA31
41636 050031         STA     2,31
41637 034507         LDA     3,RTN9
41640 001402         JMP     2,3
41641 030565 OUT1:   LDA     2,BETA
41642 034417         LDA     3,MAX4
41643 024006         LDA     1,NUM4
41644 133000         ADD     1,2
41645 151400         INC     2,2
41646 024414         LDA     1,SPF
41647 050030         STA     2,30
41650 050031         STA     2,31
41651 021400         LDA     0,0,3
41652 032030         LDA     2,@30
41653 042031         STA     0,@31
41654 051400         STA     2,0,3
41655 136400         SUB     1,3
41656 014006         DSE     NUM4
41657 000772         JMP     .-6
41660 000724         JMP     OUT2
41661 041577 MAX4:   FFTRA-1
41662 000000 SPF:    0
41663 042304 GFFTN:  FFTNC
41664 054407 GETDA:  STA     3,BACK
```

```
41665 133000           ADD      1,2
41666 052020           STA      2,@20
41667 021000           LDA      0,0,2
41670 004537           JSR      FFTSC
41671 042021           STA      0,@21
41672 002401           JMP      @BACK
41673 000000 BACK:     0
41674 101132 TEST:     MOVZL#   0,0,SZC
41675 101241           MOVOR    0,0,SKP
41676 101220           MOVZR    0,0
41677 001400           JMP      0,3
41700 034526 FFTCC:    LDA      3,BETA
41701 054020           STA      3,20
41702 054021           STA      3,21
41703 020426           LDA      0,MM
41704 024004           LDA      1,M
41705 123000           ADD      1,0
41706 126520           SUBZL    1,1
41707 101404           INC      0,0,SZR
41710 125121           MOVZL    1,1,SKP
41711 101001           MOV      0,0,SKP
41712 000775           JMP      .-3
41713 044747           STA      1,SPF
41714 020002           LDA      0,NUM
41715 101220           MOVZR    0,0
41716 101220           MOVZR    0,0
41717 040006           STA      0,NUM4
41720 040753           STA      0,BACK
41721 137000           ADD      1,3
41722 021400           LDA      0,0,3
41723 032020           LDA      2,@20
41724 042021           STA      0,@21
41725 051400           STA      2,0,3
41726 014745           DSZ      BACK
41727 000772           JMP      .-6
41730 002733           JMP      @GFFTN
41731 177765 MM:       -13
41732 063077 FACPT:    HALT
41733 000000 SA2:      0
41734 000000 SA3:      0
41735 000000 SA4:      0
41736 000000 SA5:      0
41737 000000 SA6:      0
41740 000000 SA7:      0
41741 000000 SA20:     0
41742 000000 SA21:     0
41743 000000 SA30:     0
41744 000000 SA31:     0
41745 050000 CK50:     50000
41746 000000 RTN9:     0
41747 024002 FFTST:    LDA      1,2
41750 044763           STA      1,SA2
41751 024003           LDA      1,3
41752 044762           STA      1,SA3
41753 024004           LDA      1,4
41754 044761           STA      1,SA4
41755 024005           LDA      1,5
41756 044760           STA      1,SA5
41757 024006           LDA      1,6
41760 044757           STA      1,SA6
```

```
41761 024007           LDA     1,7
41762 044756           STA     1,SA7
41763 024020           LDA     1,20
41764 044755           STA     1,SA20
41765 024021           LDA     1,21,
41766 044754           STA     1,SA21
41767 024030           LDA     1,30
41770 044753           STA     1,SA30
41771 024031           LDA     1,31
41772 044752           STA     1,SA31
41773 031400           LDA     2,0,3
41774 021000           LDA     0,0,2
41775 025001           LDA     1,1,2
41776 054750           STA     3,RTN9
41777 006130           JSR     @.FIX
42000 044005           STA     1,FLAG
42001 034745           LDA     3,RTN9
42002 031401           LDA     2,1,3
42003 021000           LDA     0,0,2
42004 025001           LDA     1,1,2
42005 006130           JSR     @.FIX
42006 044002           STA     1,NUM
42007 024736           LDA     1,CK50
42010 044003           STA     1,ALPHA
42011 020002           LDA     0,NUM
42012 126440           SUBO    1,1
42013 101223           MOVZR   0,0,SNC
42014 125401           INC     1,1,SKP
42015 000402           JMP     .+2
42016 000775           JMP     .-3
42017 044004           STA     1,M
42020 126400           SUB     1,1
42021 044536           STA     1,ATF
42022 044536           STA     1,ATF+1
42023 044007           STA     1,SCNT
42024 044636           STA     1,SPF
42025 000653           JMP     FFTCC
42026 041177 BETA:     FFTRA-401
42027 024531 FFTSC:    LDA     1,ATF+1
42030 125014           MOV#    1,1,SZR
42031 000643           JMP     TEST
42032 001400           JMP     0,3
42033 063077           HALT
42034 054522 CALC:     STA     3,RETN
42035 024575           LDA     1,N
42036 004530           JSR     FFTAG
42037 030512           LDA     2,SAP
42040 050020           STA     2,20
42041 030520           LDA     2,TAM
42042 050021           STA     2,21
42043 030003           LDA     2,ALPHA
42044 024566           LDA     1,N
42045 004617           JSR     GETDA
42046 024002           LDA     1,NUM
42047 004615           JSR     GETDA
42050 024563           LDA     1,A
42051 004613           JSR     GETDA
42052 024002           LDA     1,NUM
42053 124400           NEG     1,1
42054 004610           JSR     GETDA
```

```
42055 024472          LDA     1,COS
42056 004556          JSR     FFTNT
42057 131000          MOV     1,2
42060 024505          LDA     1,TEMP3
42061 004553          JSR     FFTNT
42062 004560          JSR     MULT
42063 042472          STA     0,@SAV3
42064 024464          LDA     1,SIN
42065 004547          JSR     FFTNT
42066 131000          MOV     1,2
42067 024475          LDA     1,TEMP4
42070 004544          JSR     FFTNT
42071 004551          JSR     MULT
42072 032463          LDA     2,@SAV3
42073 113000          ADD     0,2
42074 024466          LDA     1,TEMP1
42075 140400          NEG     2,0
42076 133000          ADD     1,2
42077 123000          ADD     1,0
42100 052452          STA     2,@SAV1
42101 042454          STA     0,@SAV3
42102 004564          JSR     FFTAT
42103 010454          ISZ     ATF
42104 101000          MOV     0,0
42105 111000          MOV     0,2
42106 004560          JSR     FFTAT
42107 010450          ISZ     ATF
42110 101000          MOV     0,0
42111 024436          LDA     1,COS
42112 004522          JSR     FFTNT
42113 131000          MOV     1,2
42114 024450          LDA     1,TEMP4
42115 004517          JSR     FFTNT
42116 004524          JSR     MULT
42117 042435          STA     0,@SAV4
42120 024430          LDA     1,SIN
42121 124400          NEG     1,1
42122 004512          JSR     FFTNT
42123 131000          MOV     1,2
42124 024441          LDA     1,TEMP3
42125 004507          JSR     FFTNT
42126 004514          JSR     MULT
42127 032425          LDA     2,@SAV4
42130 113000          ADD     0,2
42131 140400          NEG     2,0
42132 024431          LDA     1,TEMP2
42133 133000          ADD     1,2
42134 123000          ADD     1,0
42135 052416          STA     2,@SAV2
42136 042416          STA     0,@SAV4
42137 004527          JSR     FFTAT
42140 010417          ISZ     ATF
42141 101000          MOV     0,0
42142 111000          MOV     0,2
42143 004523          JSR     FFTAT
42144 010413          ISZ     ATF
42145 101000          MOV     0,0
42146 002410          JMP     @RETN
42147 000000 COS:     0
42150 000000 SIN:     0
```

```
42151 042151 SAP:     SAP
42152 000000 SAV1:    0
42153 000000 SAV2:    0
42154 000000 SAV4:    0
42155 000000 SAV3:    0
42156 000000 RETN:    0
42157 000000 ATF:     0
42160 000000 ATFC:    0
42161 042161 TAM:     TAM
42162 000000 TEMP1:   0
42163 000000 TEMP2:   0
42164 000000 TEMP4:   0
42165 000000 TEMP3:   0
42166 054476 FFTAG:   STA       3,MSAV
42167 020573          LDA       0,I
42170 030004          LDA       2,M
42171 142405          SUB       2,0,SNR
42172 000404          JMP       MID
42173 125220          MOVZR     1,1
42174 101404          INC       0,0,SZR
42175 000776          JMP       .-2
42176 004565 MID:     JSR       FFTRV
42177 020006          LDA       0,NUM4
42200 111000          MOV       0,2
42201 122422          SUBZ      1,0,SZC
42202 000407          JMP       .+7
42203 143000          ADD       2,0
42204 030622          LDA       2,BETA
42205 113000          ADD       0,2
42206 021000          LDA       0,0,2
42207 100400          NEG       0,0
42210 000404          JMP       .+4
42211 030615          LDA       2,BETA
42212 133000          ADD       1,2
42213 021000          LDA       0,0,2
42214 040733          STA       0,COS
42215 020006          LDA       0,NUM4
42216 122032          ADCZ#     1,0,SZC
42217 122401          SUB       1,0,SKP
42220 106401          SUB       0,1,SKP
42221 105000          MOV       0,1
42222 030604          LDA       2,BETA
42223 133000          ADD       1,2
42224 021000          LDA       0,0,2
42225 030005          LDA       2,FLAG
42226 151232          MOVZR#    2,2,SZC
42227 100400          NEG       0,0
42230 040720          STA       0,SIN
42231 002433          JMP       @MSAV
42232 000000 N:       0
42233 000000 A:       0
42234 125133 FFTNT:   MOVZL#    1,1,SNC
42235 001400          JMP       0,3
42236 124400          NEG       1,1
42237 010402          ISZ       ASF
42240 001400          JMP       0,3
42241 000000 ASF:     0
42242 102460 MULT:    SUBC      0,0
42243 054421          STA       3,MSAV
42244 034421          LDA       3,M20
```

```
42245 125203 MLOOP:  MOVR     1,1,SNC
42246 101201         MOVR     0,0,SKP
42247 143220         ADDZR    2,0
42250 175404         INC      3,3,SZR
42251 000774         JMP      MLOOP
42252 101160         MOVCL    0,0
42253 125120         MOVZL    1,1
42254 101100         MOVL     0,0
42255 024764         LDA      1,ASF
42256 125233         MOVZR#   1,1,SNC
42257 002405         JMP      @MSAV
42260 100400         NEG      0,0
42261 126400         SUB      1,1
42262 044757         STA      1,ASF
42263 002401         JMP      @MSAV
42264 000000 MSAV:   0
42265 177760 M20:    -20
42266 014671 FFTAT:  DSZ      ATF
42267 010670         ISZ      ATF
42270 001400         JMP      0,3
42271 024412         LDA      1,CUTO
42272 151132         MOVZL#   2,2,SZC
42273 000404         JMP      NEGA
42274 132032         ADCZ#    1,2,SZC
42275 001400         JMP      0,3
42276 001401         JMP      1,3
42277 124400 NEGA:   NEG      1,1
42300 132032         ADCZ#    1,2,SZC
42301 001401         JMP      1,3
42302 001400         JMP      0,3
42303 031463 CUTO:   31463
42304 024004 FFINC:  LDA      1,M
42305 044452         STA      1,ACNT
42306 102520         SUBZL    0,0
42307 040453         STA      0,I
42310 126400 NODS:   SUB      1,1
42311 044721         STA      1,N
42312 020450 AGET:   LDA      0,I
42313 030002         LDA      2,NUM
42314 100400           NEG      0,0
42315 151220         MOVZR    2,2
42316 101404         INC      0,0,SZR
42317 000776         JMP      .-2
42320 050713         STA      2,A
42321 050437         STA      2,NCNT
42322 006437 ROAD:   JSR      @GCALC
42323 014435         DSZ      NCNT
42324 000427         JMP      NIND
42325 010705         ISZ      N
42326 030705         LDA      2,A
42327 050431         STA      2,NCNT
42330 024702         LDA      1,N
42331 147000         ADD      2,1
42332 044700         STA      1,N
42333 030002         LDA      2,NUM
42334 132404         SUB      1,2,SZR
42335 000765         JMP      ROAD
42336 014421         DSZ      ACNT
42337 000416         JMP      AIND
42340 000434         JMP      OUT
```

```
42341 020616 STSR:   LDA      0,ATF
42342 101134         MOVZL#   0,0,SZR
42343 000403         JMP      SCALE
42344 040614         STA      0,ATF+1
42345 000743         JMP      NODS
42346 010612 SCALE:  ISZ      ATF+1
42347 010007         ISZ      SCNT
42350 102400         SUB      0,0
42351 040606         STA      0,ATF
42352 000736         JMP      NODS
42353 010657 NIND:   ISZ      N
42354 000746         JMP      ROAD
42355 010405 AIND:   ISZ      I
42356 000763         JMP      STSR
42357 000000 ACNT:   0
42360 000000 NCNT:   0
42361 042034 GCALC:  CALC
42362 000000 I:      0
42363 030004 FFTRV:  LDA      2,M
42364 121000         MOV      1,0
42365 126400         SUB      1,1
42366 150400         NEG      2,2
42367 101220         MOVZR    0,0
42370 125100         MOVL     1,1
42371 151404         INC      2,2,SZR
42372 000775         JMP      .-3
42373 001400         JMP      0,3
42374 024437 OUT:    LDA      1,PHASE
42375 044020         STA      1,20
42376 024003         LDA      1,ALPHA
42377 044433         STA      1,ALPHB
42400 101001         MOV      0,0,SKP
42401 002433         JMP      @GFFRA
42402 126400         SUB      1,1
42403 044627         STA      1,N
42404 024002         LDA      1,NUM
42405 044753         STA      1,NCNT
42406 024624 CYCLE:  LDA      1,N
42407 004754         JSR      FFTRV
42410 030422         LDA      2,ALPHB
42411 034621         LDA      3,N
42412 136432         SUBZ#    1,3,SZC
42413 000407         JMP      EQUAL
42414 157000         ADD      2,3
42415 133000         ADD      1,2
42416 025000         LDA      1,0,2
42417 021400         LDA      0,0,3
42420 041000         STA      0,0,2
42421 045400         STA      1,0,3
42422 010610 EQUAL:  ISZ      N
42423 014735         DSZ      NCNT
42424 000762         JMP      CYCLE
42425 030405         LDA      2,ALPHB
42426 024002         LDA      1,NUM
42427 133000         ADD      1,2
42430 050402         STA      2,ALPHB
42431 002020         JMP      @20
42432 000000 ALPHB:  0
42433 042377 PHASE:  OUT+3
42434 041600 GFFRA:  FFTRA
```

```
        041177          .LOC    FFTRA-491
41177 040000            040000
41200 040000            040000
41201 037777            037777
41202 037775            037775
41203 037773            037773
41204 037770            037770
41205 037765            037765
41206 037761            037761
41207 037754            037754
41210 037747            037747
41211 037741            037741
41212 037733            037733
41213 037724            037724
41214 037714            037714
41215 037704            037704
41216 037673            037673
41217 037661            037661
41220 037647            037647
41221 037634            037634
41222 037621            037621
41223 037605            037605
41224 037570            037570
41225 037553            037553
41226 037535            037535
41227 037517            037517
41230 037500            037500
41231 037460            037460
41232 037440            037440
41233 037417            037417
41234 037375            037375
41235 037353            037353
41236 037330            037330
41237 037305            037305
41240 037261            037261
41241 037235            037235
41242 037210            037210
41243 037162            037162
41244 037134            037134
41245 037105            037105
41246 037055            037055
41247 037025            037025
41250 036774            036774
41251 036743            036743
41252 036711            036711
41253 036657            036657
41254 036623            036623
41255 036570            036570
41256 036533            036533
41257 036477            036477
41260 036441            036441
41261 036403            036403
41262 036344            036344
41263 036305            036305
41264 036245            036245
41265 036205            036205
41266 036144            036144
41267 036102            036102
41270 036040            036040
41271 035775            035775
```

41272	035732	035732
41273	035666	035666
41274	035622	035622
41275	035555	035555
41276	035507	035507
41277	035441	035441
41300	035372	035372
41301	035323	035323
41302	035253	035253
41303	035202	035202
41304	035131	035131
41305	035060	035060
41306	035006	035006
41307	034733	034733
41310	034660	034660
41311	034604	034604
41312	034530	034530
41313	034453	034453
41314	034375	034375
41315	034317	034317
41316	034241	034241
41317	034161	034161
41320	034102	034102
41321	034022	034022
41322	033741	033741
41323	033660	033660
41324	033576	033576
41325	033513	033513
41326	033430	033430
41327	033345	033345
41330	033261	033261
41331	033175	033175
41332	033110	033110
41333	033022	033022
41334	032734	032734
41335	032645	032645
41336	032556	032556
41337	032467	032467
41340	032377	032377
41341	032306	032306
41342	032215	032215
41343	032123	032123
41344	032031	032031
41345	031737	031737
41346	031643	031643
41347	031550	031550
41350	031454	031454
41351	031357	031357
41352	031262	031262
41353	031164	031164
41354	031066	031066
41355	030770	030770
41356	030671	030671
41357	030571	030571
41360	030471	030471
41361	030371	030371
41362	030270	030270
41363	030166	030166
41364	030064	030064
41365	027762	027762

41366	027657	027657
41367	027554	027554
41370	027450	027450
41371	027344	027344
41372	027237	027237
41373	027132	027132
41374	027025	027025
41375	026717	026717
41376	026610	026610
41377	026501	026501
41400	026372	026372
41401	026262	026262
41402	026152	026152
41403	026041	026041
41404	025730	025730
41405	025617	025617
41406	025505	025505
41407	025373	025373
41410	025260	025260
41411	025145	025145
41412	025032	025032
41413	024716	024716
41414	024601	024601
41415	024465	024465
41416	024347	024347
41417	024232	024232
41420	024114	024114
41421	023776	023776
41422	023657	023657
41423	023540	023540
41424	023421	023421
41425	023301	023301
41426	023161	023161
41427	023040	023040
41430	022717	022717
41431	022576	022576
41432	022454	022454
41433	022332	022332
41434	022210	022210
41435	022065	022065
41436	021742	021742
41437	021616	021616
41440	021473	021473
41441	021347	021347
41442	021222	021222
41443	021075	021075
41444	020750	020750
41445	020623	020623
41446	020475	020475
41447	020347	020347
41450	020221	020221
41451	020072	020072
41452	017743	017743
41453	017614	017614
41454	017464	017464
41455	017334	017334
41456	017204	017204
41457	017053	017053
41460	016723	016723
41461	016571	016571

41462	016440	016440
41463	016306	016306
41464	016154	016154
41465	016022	016022
41466	015670	015670
41467	015535	015535
41470	015402	015402
41471	015247	015247
41472	015113	015113
41473	014757	014757
41474	014623	014623
41475	014467	014467
41476	014333	014333
41477	014176	014176
41500	014041	014041
41501	013704	013704
41502	013546	013546
41503	013411	013411
41504	013253	013253
41505	013114	013114
41506	012756	012756
41507	012620	012620
41510	012461	012461
41511	012322	012322
41512	012163	012163
41513	012023	012023
41514	011664	011664
41515	011524	011524
41516	011364	011364
41517	011224	011224
41520	011064	011064
41521	010723	010723
41522	010563	010563
41523	010422	010422
41524	010261	010261
41525	010120	010120
41526	007756	007756
41527	007615	007615
41530	007453	007453
41531	007312	007312
41532	007150	007150
41533	007006	007006
41534	006644	006644
41535	006501	006501
41536	006337	006337
41537	006174	006174
41540	006032	006032
41541	005667	005667
41542	005524	005524
41543	005361	005361
41544	005216	005216
41545	005053	005053
41546	004707	004707
41547	004544	004544
41550	004401	004401
41551	004235	004235
41552	004071	004071
41553	003726	003726
41554	003562	003562
41555	003416	003416

```
41556 003252          003252
41557 003106          003106
41560 002742          002742
41561 002576          002576
41562 002432          002432
41563 002265          002265
41564 002121          002121
41565 001755          001755
41566 001610          001610
41567 001444          001444
41570 001300          001300
41571 001133          001133
41572 000767          000767
41573 000622          000622
41574 000456          000456
41575 000311          000311
41576 000145          000145
41577 000000          000000
                      .EOT
```

APPENDIX B-11

```
                ;          SPECTRAL MEMORY CLEAR SUBROUTINE
      042500               .LOC     42500    ;ABS. SA
42500 054422 MEMC2:  STA     3,RTN10 ;RETURN ADDRESS
42501 030415         LDA     2,CST10 ;1/2K OF MEMORY RESERVED
42502 050417         STA     2,CNT10 ;COUNTER
42503 020414         LDA     0,B1    ;ZERO
42504 034020         LDA     3,20    ;SAVE LOCATION 20
42505 054416         STA     3,SB20  ;   "
42506 034412         LDA     3,ST2   ;CLEARED MEMORY SA
42507 054020         STA     3,20    ;INITIALIZE AUTOINCREMENT
42510 042020 CLEER:  STA     0,@20   ;PUT 0 IN 45000 ETC.
42511 014410         DSZ     CNT10   ;FINISHED?
42512 000776         JMP     CLEER   ;NO--RETURN
42513 034410         LDA     3,SB20  ;YES--RESTORE LOCATION 20
42514 054020         STA     3,20    ;   "
42515 002405         JMP     @RTN10  ;RETURN TO BASIC
42516 001000 CST10:  1000    ;NUMBER OF CLEARED LOCATIONS
42517 000000 B1:     0       ;CONSTANT 0
42520 044777 ST2:    44777   ;CLEARED MEMORY SA MINUS 1
42521 000000 CNT10:  0       ;COUNTER FOR CST10
42522 000000 RTN10:  0       ;BASIC RETURN ADDRESS
42523 000000 SB20:   0       ;CONTENTS OF LOCATION 20
                     .EOT
```

APPENDIX B-12

```
                ;         SPECTRAL DATA TO BINARY SUBROUTINE
        042600            .LOC    42600    ;ABS. SA
42600 031400 SPECB:       LDA     2,0,3    ;FP ADDRESS TO AC(2)
42601 050433              STA     2,FAD    ;FP ADDRESS TO FAD
 42602 054433              STA     3,RTN11 ;RETURN ADDRESS TO RTN11
42603 034433              LDA     3,BAD    ;BINARY SA TO BAD
42604 054433              STA     3,BND1   ;COUNTER
42605 054433              STA     3,BND2   ;   "
42606 020434              LDA     0,CST11  ;256 POINT ARRAY
42607 040432              STA     0,CNT11  ;COUNTER
42610 022424 SPEC:        LDA     0,@FAD   ;1ST HALF OF # TO AC(0)
42611 010423              ISZ     FAD      ;INCREMENT FP ADDRESS
42612 026422              LDA     1,@FAD   ;2ND HALF OF # TO AC(1)
42613 010421              ISZ     FAD      ;INCREMENT FP ADDRESS
42614 006130              JSR     @.FIX    ;CONVERT TO BINARY
42615 036422              LDA     3,@BND1  ;LARGE HALF OF # TO AC(3)
42616 010421              ISZ     BND1     ;INCREMENT BINARY ADDRESS
42617 032420              LDA     2,@BND1  ;SMALL HALF OF # TO AC(2)
42620 010417              ISZ     BND1     ;INCREMENT BINARY ADDRESS
42621 133022              ADDZ    1,2,SZC  ;ADD NEW AND OLD NUMBERS
42622 101400              INC     0,0      ;OVERFLOW--ADD 1 TO AC(0)
42623 163000              ADD     3,0      ;ADD NEW AND OLD NUMBERS
42624 042414              STA     0,@BND2  ;RETURN LARGE HALF TO MEMORY
42625 010413              ISZ     BND2     ;INCREMENT BINARY ADDRESS
42626 052412              STA     2,@BND2  ;RETURN SMALL HALF TO MEMORY
42627 010411              ISZ     BND2     ;INCREMENT BINARY ADDRESS
42630 014411              DSZ     CNT11    ;FINISHED?
42631 000757              JMP     SPEC     ;NO--RETURN
42632 034403              LDA     3,RTN11  ;YES--LOAD RETURN ADDRESS
42633 001401              JMP     1,3      ;RETURN TO BASIC
42634 000000 FAD:         0        ;FLOATING POINT SA
42635 000000 RTN11:       0        ;BASIC RETURN ADDRESS
42636 045000 BAD:         45000    ;BINARY SA
42637 000000 BND1:        0        ;BINARY ADDRESS COUNTER
42640 000000 BND2:        0        ;   "
42641 000000 CNT11:       0        ;256 POINT ARRAY COUNTER
42642 000400 CST11:       400      ;256 POINT ARRAY
                          .EOT
```

APPENDIX B-13

```
                ;         SPECTRAL DATA TO BASIC SUBROUTINE
        042700            .LOC    42700   ;ABS. SA
42700 031400 SPECF:  LDA     2,0,3   ;FP ADDRESS TO AC(2)
42701 050423         STA     2,FAD1  ;FP ADDRESS TO FAD1
42702 054423         STA     3,RTN12 ;RETURN ADDRESS TO RTN12
42703 034423         LDA     3,BAD1  ;BINARY SA TO AC(3)
42704 054423         STA     3,BND3  ;BINARY SA TO BND3
42705 020424         LDA     0,CST12 ;256 POINT ARRAY
42706 040422         STA     0,CNT12 ;COUNTER
42707 022420 SPEC1:  LDA     0,@BND3 ;1ST HALF OF # TO AC(0)
42710 010417         ISZ     BND3    ;INCREMENT BINARY ADDRESS
42711 026416         LDA     1,@BND3 ;2ND HALF OF # TO AC(1)
42712 010415         ISZ     BND3    ;INCREMENT BINARY ADDRESS
42713 006132         JSR     0,FLOT  ;CONVERT TO FP
42714 042410         STA     0,@FAD1 ;1ST HALF TO BASIC ARRAY
42715 010407         ISZ     FAD1    ;INCREMENT FP ADDRESS
42716 046406         STA     1,@FAD1 ;2ND HALF TO BASIC ARRAY
42717 010405         ISZ     FAD1    ;INCREMENT FP ADDRESS
42720 014410         DSZ     CNT12   ;FINISHED?
42721 000766         JMP     SPEC1   ;NO--RETURN
42722 034403         LDA     3,RTN12 ;YES--LOAD RETURN ADDRESS
42723 001401         JMP     1,3     ;RETURN TO BASIC
42724 000000 FAD1:   0       ;FLOATING POINT ARRAY SA
42725 000000 RTN12:  0       ;BASIC RETURN ADDRESS
42726 045000 BAD1:   45000   ;BINARY SA
42727 000000 BND3:   0       ;BINARY ADDRESS COUNTER
42730 000000 CNT12:  0       ;256 POINT ARRAY COUNTER
42731 000400 CST12:  400     ;256 POINT ARRAY
                     .END
```

NBS-114A (REV. 7-73)

U.S. DEPT. OF COMM. BIBLIOGRAPHIC DATA SHEET	1. PUBLICATION OR REPORT NO. NBS Technical Note 672	2. Gov't Accession No.	3. Recipient's Accession No.

4. TITLE AND SUBTITLE

Time Domain Automatic Network Analyzer for Measurement of RF and Microwave Components

5. Publication Date: September 1975

6. Performing Organization Code: NBS 276.50

7. AUTHOR(S)
William L. Gans and James R. Andrews

8. Performing Organ. Report No. NBS TN-672

9. PERFORMING ORGANIZATION NAME AND ADDRESS

NATIONAL BUREAU OF STANDARDS
DEPARTMENT OF COMMERCE
WASHINGTON, D.C. 20234

10. Project/Task/Work Unit No. FY-74 2725390

11. Contract/Grant No. CCG 72-68

12. Sponsoring Organization Name and Complete Address *(Street, City, State, ZIP)*
Department of Defense
Calibration Coordination Group
c/o Mr. R. Y. Bailey
Chairman, MTCG-METCAL/CCG

13. Type of Report & Period Covered
Final Report
FY 73-74

14. Sponsoring Agency Code

15. SUPPLEMENTARY NOTES
Aerospace Guidance and Metrology Center
Newark AFS
Newark, Ohio 43055

16. ABSTRACT *(A 200-word or less factual summary of most significant information. If document includes a significant bibliography or literature survey, mention it here.)*

This technical note describes in detail a new NBS instrument for the measurement of the scattering parameters (S_{ij}) of RF and microwave components. The instrument is the Time Domain Automatic Network Analyzer (TDANA). It utilizes time domain pulse measurements to obtain frequency domain parameters. The frequency range is dc to 18 GHz with a lower upper limit for large values of attenuation. The instrument consists of three major components: an ultra-fast pulse generator, a broadband sampling oscilloscope, and a digital minicomputer.

17. KEY WORDS *(six to twelve entries; alphabetical order; capitalize only the first letter of the first key word unless a proper name; separated by semicolons)*

Attenuation; discrete Fourier transform; fast Fourier transform; insertion loss; jitter; microwave measurement; mismatch; network analyzer; noise; pulse generator; pulse measurement; sampling oscilloscope; scattering parameters; spectral analysis; time domain analysis.

18. AVAILABILITY

[X] Unlimited

[ ] For Official Distribution. Do Not Release to NTIS

[X] Order From Sup. of Doc., U.S. Government Printing Office Washington, D.C. 20402, SD Cat. No. C13.46:672

[ ] Order From National Technical Information Service (NTIS) Springfield, Virginia 22151

19. SECURITY CLASS (THIS REPORT): UNCLASSIFIED

21. NO. OF PAGES: 176

20. SECURITY CLASS (THIS PAGE): UNCLASSIFIED

22. Price: $2.40

USCOMM-DC 29042-P74

☆ U. S. GOVERNMENT PRINTING OFFICE 1975 - 677-347/1216 Reg. 8

NBS TECHNICAL PUBLICATIONS

PERIODICALS

JOURNAL OF RESEARCH reports National Bureau of Standards research and development in physics, mathematics, and chemistry. It is published in two sections, available separately:

• **Physics and Chemistry (Section A)**

Papers of interest primarily to scientists working in these fields. This section covers a broad range of physical and chemical research, with major emphasis on standards of physical measurement, fundamental constants, and properties of matter. Issued six times a year. Annual subscription: Domestic, $17.00; Foreign, $21.25.

• **Mathematical Sciences (Section B)**

Studies and compilations designed mainly for the mathematician and theoretical physicist. Topics in mathematical statistics, theory of experiment design, numerical analysis, theoretical physics and chemistry, logical design and programming of computers and computer systems. Short numerical tables. Issued quarterly. Annual subscription: Domestic, $9.00; Foreign, $11.25.

DIMENSIONS/NBS (formerly Technical News Bulletin)—This monthly magazine is published to inform scientists, engineers, businessmen, industry, teachers, students, and consumers of the latest advances in science and technology, with primary emphasis on the work at NBS. The magazine highlights and reviews such issues as energy research, fire protection, building technology, metric conversion, pollution abatement, health and safety, and consumer product performance. In addition, it reports the results of Bureau programs in measurement standards and techniques, properties of matter and materials, engineering standards and services, instrumentation, and automatic data processing.

Annual subscription: Domestic, $9.45; Foreign, $11.85.

NONPERIODICALS

Monographs—Major contributions to the technical literature on various subjects related to the Bureau's scientific and technical activities.

Handbooks—Recommended codes of engineering and industrial practice (including safety codes) developed in cooperation with interested industries, professional organizations, and regulatory bodies.

Special Publications—Include proceedings of conferences sponsored by NBS, NBS annual reports, and other special publications appropriate to this grouping such as wall charts, pocket cards, and bibliographies.

Applied Mathematics Series—Mathematical tables, manuals, and studies of special interest to physicists, engineers, chemists, biologists, mathematicians, computer programmers, and others engaged in scientific and technical work.

National Standard Reference Data Series—Provides quantitative data on the physical and chemical properties of materials, compiled from the world's literature and critically evaluated. Developed under a world-wide program coordinated by NBS. Program under authority of National Standard Data Act (Public Law 90-396).

NOTE: At present the principal publication outlet for these data is the Journal of Physical and Chemical Reference Data (JPCRD) published quarterly for NBS by the American Chemical Society (ACS) and the American Institute of Physics (AIP). Subscriptions, reprints, and supplements available from ACS, 1155 Sixteenth St. N. W., Wash. D. C. 20056.

Building Science Series—Disseminates technical information developed at the Bureau on building materials, components, systems, and whole structures. The series presents research results, test methods, and performance criteria related to the structural and environmental functions and the durability and safety characteristics of building elements and systems.

Technical Notes—Studies or reports which are complete in themselves but restrictive in their treatment of a subject. Analogous to monographs but not so comprehensive in scope or definitive in treatment of the subject area. Often serve as a vehicle for final reports of work performed at NBS under the sponsorship of other government agencies.

Voluntary Product Standards—Developed under procedures published by the Department of Commerce in Part 10, Title 15, of the Code of Federal Regulations. The purpose of the standards is to establish nationally recognized requirements for products, and to provide all concerned interests with a basis for common understanding of the characteristics of the products. NBS administers this program as a supplement to the activities of the private sector standardizing organizations.

Federal Information Processing Standards Publications (FIPS PUBS)—Publications in this series collectively constitute the Federal Information Processing Standards Register. Register serves as the official source of information in the Federal Government regarding standards issued by NBS pursuant to the Federal Property and Administrative Services Act of 1949 as amended, Public Law 89-306 (79 Stat. 1127), and as implemented by Executive Order 11717 (38 FR 12315, dated May 11, 1973) and Part 6 of Title 15 CFR (Code of Federal Regulations).

Consumer Information Series—Practical information, based on NBS research and experience, covering areas of interest to the consumer. Easily understandable language and illustrations provide useful background knowledge for shopping in today's technological marketplace.

NBS Interagency Reports (NBSIR)—A special series of interim or final reports on work performed by NBS for outside sponsors (both government and non-government). In general, initial distribution is handled by the sponsor; public distribution is by the National Technical Information Service (Springfield, Va. 22161) in paper copy or microfiche form.

Order NBS publications (except NBSIR's and Bibliographic Subscription Services) from: Superintendent of Documents, Government Printing Office, Washington, D.C. 20402.

BIBLIOGRAPHIC SUBSCRIPTION SERVICES

The following current-awareness and literature-survey bibliographies are issued periodically by the Bureau:

Cryogenic Data Center Current Awareness Service

A literature survey issued biweekly. Annual subscription: Domestic, $20.00; foreign, $25.00.

Liquefied Natural Gas. A literature survey issued quarterly. Annual subscription: $20.00.

Superconducting Devices and Materials. A literature survey issued quarterly. Annual subscription: $20.00. Send subscription orders and remittances for the preceding bibliographic services to National Technical Information Service, Springfield, Va. 22161.

Electromagnetic Metrology Current Awareness Service Issued monthly. Annual subscription: $100.00 (Special rates for multi-subscriptions). Send subscription order and remittance to Electromagnetics Division, National Bureau of Standards, Boulder, Colo. 80302.

U.S. DEPARTMENT OF COMMERCE
National Bureau of Standards
Washington, D.C. 20234

OFFICIAL BUSINESS

Penalty for Private Use, $300

POSTAGE AND FEES PAID
U.S. DEPARTMENT OF COMMERCE
COM-215

FOURTH CLASS MAIL

U.S.MAIL